2007

The Structure Function Relationship of Silica Polyamine Composites

Mark Anthony Hughes
The University of Montana

THE STRUCTURE FUNCTION RELATIONSHIP

OF SILICA POLYAMINE COMPOSITES

By

Mark Anthony Hughes

B.Eng. Mechanical, Queens University of Belfast, N. Ireland, 2001
M.Sci. Polymer Engineering, Queens University of Belfast, N.Ireland, 2003

Thesis

presented in partial fulfillment of the requirements
for the degree of

Doctor of Philosophy
in Chemistry, Inorganic

The University of Montana
Missoula, MT

Summer 2007

Approved by:

Dr. David A. Strobel, Dean
Graduate School

Dr. Edward Rosenberg, Committee Chairperson
Department of Chemistry

Dr. Mike De Grandpre, Committee Member
Department of Chemistry

Dr. Alexander Ross, Committee Member
Department of Chemistry

Dr. John Gerdes, Committee Member
Department of Biomedical and Pharmaceutical Science

Dr. Jesse Johnson, Committee Member
Department of Computer Science

Hughes, Mark A., Ph.D., Summer 2007 Chemistry

The Structure Function Relationship of Silica Polyamine Composites

Chairperson: Dr. Edward Rosenberg, Department of Chemistry

The goals of this thesis were to improve the performance of silica polyamine composites by manipulating the surface structure and to understand the relationship between, polymer structure and ligand modification of the grafted polyamine. Improvements in silica polyamine composite performance resulted from modifying silica gel with methyltrichlorosilane (MTCS) substituted for a molar fraction of reagent chloropropyltrichlorosilane (CPTCS), which has been traditionally employed. MTCS does not possess a terminal chloride group thus preventing the subsequent attachment of a polyamine to this moiety. MTCS has a smaller molecular volume than CPTCS and as a consequence greater coverage of the silica gel surface by silanes was determined by elemental analysis and NMR. An increase in the fraction of amines not attached to the surface (free amines) allowed improved mass transfer kinetics and in some cases improvements in metal ion sorption capacities of the polymer modified materials. Further, MTCS is cheaper than CPTCS thus allowing a more economically sound synthesis. As a result of an increase in free amines, silica gel polyamine composites were modified with sodium chloroacetate and other metal selective ligands in higher yield, resulting in a material with substantially improved copper ion capacities.

Silica polyamine composites have also been modified with a novel series of amino acid chelating ligands for the purpose of selective extraction of heavy metals from aqueous media. The presence of the functional groups was confirmed by ^{13}C NMR and elemental analysis. The adsorption properties of modified composites have been determined for divalent and trivalent metal ions. Cycle testing was performed to measure longevity. Selective extraction and recovery of a single metal ion from media containing multiple metal ions has been demonstrated. The structure of the polyamine used has been shown to have a significant impact on the specific selectivity of modified silica polyamine composites even when modified with the same ligand. Potential areas of application have been tested and appear promising. These include an acid mine drainage polluted stream near Helena, MT, as well as synthetic high pressure leach laterite solutions.

ACKNOWLEDGEMENTS

I will always look back with fondness on my time at the University of Montana, Missoula, Montana, USA. I would like to give my sincerest thanks to all those during my time at UM who helped make my graduate school years enjoyable and memorable. The UM Chemistry Department has served as wonderful host for my studies and the Rosenberg research group has made my time particularly fulfilling. I appreciate the assistance and guidance of those who came before me in the Rosenberg group and in particular I would like to thank Bob Fischer, Carolyn Hart, Fabrizio Spada, Dhalia Rhoksana, Paul Miranda and Dan Nielsen. I would like to acknowledge the contributions of undergraduate research students most notably Jessica Wood, Brianne Cross, Yuen Onn Wong and Chauncey Means. I sincerely appreciate the help, support and encouragement of my mentor Professor Edward Rosenberg. For Professor Rosenberg I have the utmost respect and will strive to represent the Rosenberg group to the best of my ability for the entirety of my professional career. Throughout my time at UM my family in Belfast, Northern Ireland, as well as my family in Great Falls, MT, USA, have given me unconditional support and kept me in a positive frame of mind. I will love them always and I will constantly endeavor to make them proud. Finally, I wish to express my deepest love to my beautiful wife Tiffany, without whom this thesis would not be possible.

TABLE OF CONTENTS

LIST OF FIGURES

LIST OF TABLES

CHAPTER 1: Background

1.1 Introduction

The importance of metals to modern society can not be overestimated. Metals are found naturally in the earth's crust. The metallic elements are the most abundant of all the known elements and they are of central importance to both contemporary academic research and industry alike. There are 86 known metals. In general metals have high electrical and thermal conductivity. Metals are malleable, ductile and are reflective. Metals possess high structural strength per unit mass. Most metals have high energies of vaporization. However metals such as Hg, Ba, Na and Cs do not. Metals readily form useful compounds with many other elements. These properties and many other useful traits make metals useful for a wide variety of applications. A broad and expanding array of industries make use of metals which include transportation, aerospace, computers, decoration,[1] communications, construction, biomedical applications, energy production, food production,[2] and household appliances. Ongoing research continually identifies further uses for metals and a growing world population consumes metals and their related products in ever greater amounts. As a result of the great significance of metals to modern society, a large amount of resources have been, and continue to be, invested in the extraction of metals from the earth's crust.[3] Depletion of the earth's limited supply of metals is a growing concern. It is estimated that ~25% of the earth's copper is now lost in aqueous wastes.[4] The extraction of metals from the earth and the use of metals for industrial applications raise two very important socio-economic issues. The first issue is the pollution of natural waters with potentially toxic amounts of heavy metal ions

generated through the extensive use of metals in many industries.[5] The second issue of great concern is the environmental impact of the separation and recovery of metal ions from the complex mixtures of other metallic and non-metallic species typically found in ores extracted from the earth's surface.[6] Section 1.2 describes these key issues in greater detail.

1.2. Motivation for the research

1.2.1 Industrial Wastewaters. Industrial processes have long been associated with wastes which can adversely affect the health of the environment.[7] Since the onset of the industrial revolution, between 1760 and 1830, inland waters have experienced elevated levels of pollutants from manufacturing effluent. In particular, increased concentrations of metal ions are commonly found in waters emanating from tanneries, agricultural wastes, steel pickling plants, metal plating factories,[8] pigments industries, municipal landfills, food industries,[9] wastewater treatment facilities, nuclear weapons production facilities, nuclear power generators[10] as well as natural resource mining projects.[11] Heavy metal ions from manufacturing sources can compromise the integrity of various ecological cycles as well as negatively impacting the health of humans through contamination of drinking water supplies and the food chain. Increased levels of well known poisonous metals such as arsenic, lead, and mercury have been frequently detected in aqueous waste waters.[7;12;13] Other hazardous heavy metal ions including cadmium, barium, copper, nickel, selenium and chromium are also found at alarming concentrations.[14-16] Heavy metals can cause acute and chronic illnesses in humans and

other animals.[17] There are approximately 70 trace element metals that are necessary for human life.[18] However heavy metals such as mercury, lead, and cadmium have no natural function in the human body and can be highly toxic. These metals are directly antagonistic to essential trace elements. Toxic heavy metals compete with nutrient elements for binding sites on transport and storage proteins, metalloenzymes and receptors. For example, it is known that the Hg^{2+} ion forms a strong bond with selenium. Through forming this bond Hg^{2+} removes selenium from its critical role as a constituent of the tetrameric glycoprotein, glutathione peroxidase, which is a vital protection against oxidative damage.[19] Selenium is also toxic at levels higher than 400 micrograms per day.[20] The prevention of toxic metal ions entering natural waters is a necessity.

1.2.2 Acid Mine Drainage. Refuse from natural resource mining is of particular importance. This source of toxic heavy metal pollutants is termed acid mine drainage (AMD).[21] The introduction of air and water to mine sites can cause the oxidation of metal sulfides located in the mines rock structures. During normal operation water is pumped out of the mine. However, in many cases when the mine is non-operational, a build-up of water below the water table will occur. Equations (1.1) through (1.5) illustrate some of the major contributors to AMD.[22]

Chalcocite

$$Cu_2S_{(s)} + 2.5O_{2(g)} + 2H^+_{(aq)} \rightarrow 2Cu^+_{(aq)} + SO_4^{2-}{}_{(aq)} + H_2O_{(l)} \quad (1.1)$$

Pyrrhotite

$$FeS_{(s)} + 2O_{2(g)} \rightarrow Fe^{2+}_{(aq)} + 2SO_4^{2-}{}_{(aq)} \quad (1.2)$$

Arsenopyrite

$$FeAsS_{(s)} + 5SO_{2\,(g)} + 3H_2O_{(l)} \rightarrow 2As(OH)_{3\,(s)} + 2SO_4^{2-}{}_{(aq)} + Fe^{2+}{}_{(aq)} \quad (1.3)$$

Pyrite

$$2FeS_{2\,(s)} + 7O_{2\,(g)} + 2H_2O_{(l)} \rightarrow 2Fe^{2+}{}_{(aq)} + 4SO_4^{2-}{}_{(aq)} + 4H^{+}{}_{(aq)} \quad (1.4)$$

Iron Oxidation

$$2Fe^{2+}{}_{(aq)} + 0.5O_{2\,(g)} + 5H_2O_{(l)} \rightarrow 2Fe(OH)_{3\,(s)} + 4H^{+}{}_{(aq)} \quad (1.5)$$

Abandoned copper mines are a common source of AMD. Decomposition over time of sulfide ores assisted by rain water and runoff leads to the build up of metal laden water. Chalcocite, pyrrhotite, arsenopyrite and pyrite are some of the major contributors to AMD.[23] The production and subsequent oxidation of ferrous iron to ferric iron (Fe^{2+} to Fe^{3+} (Eqn. 1.5) produces a significant amount of H^+ hence the pH decreases. Although the reaction is exothermic (ΔH = -349 kcal/mole), the oxidation process is relatively slow.[22] However, as the oxidation reaction proceeds and pH decreases below 3.5, extremophiles dubbed acidophiles such as *Acidithiobacillus ferrooxidans* can catalyze the oxidation by a factor of up to 10^3.[24] As a result, water temperatures have been reported to reach 50°C and the solution pH has been reported to decrease to less than pH 0.[25] Very low pH values are often an outcome of the evaporation of water leading to the concentration of H^+. AMD is an especially important problem in the Western United States and no where more so than in Western Montana. Although there are many AMD sites around the world the Berkeley Pit copper mine in Butte, Montana, USA, is one of the largest and most contaminated superfund sites.[22] The pit was first mined in 1955. Since then one billion tons of earth have been removed creating a vast void. The pit is

approximately 900 ft deep, one mile wide in places, and now contains roughly 37 billion gallons of water. Due to groundwater, the pit is filling with water at a rate of 2.55 million gallons per day. Table 1.1 depicts the array of metals that have built up in this non-operational mine site since its year of abandonment in 1982. The water is heavily contaminated and has a pH of approximately 2.5.[26]

Table 1.1. The composition (mg/L) of Berkeley Pit Water (Butte, Montana, USA) with depth as analyzed in February 2002.

Depth (ft)	SO_4	Fe	Zn	Mg	Ca	Al	Mn	Cu	Cd	As
0	6345	270	378	430	512	195	179	87	1.84	0.22
50	8994	892	578	538	494	281	212	145	2.39	0.34
500	9105	986	580	536	494	281	209	177	2.43	0.78

The copper concentration has elevated in the pit to the point that the water has been considered as a potential commercial source for the metal. The water is a major environmental concern and must be treated before the toxic cocktail of metals enters the drinking water supply. Metal leaching from mine tailings can contaminate waters many miles from its origin as well as the regional aquifer. Precipitation and subsequent leaching can permit metals access to surface and subsurface waters. The cleanup of these highly polluted waters is of prime importance to the survival of the surrounding aquifer and local ecosystems. Several methods of cleanup have been used to tackle the polluted water resulting from AMD.[27-29;29;30] These include carbonate neutralization (limestone), constructed wetlands, active treatment with aeration and precipitation of metal sulfides. However, none of these techniques can separate those metals with economic value from toxic or less valuable metals. Furthermore, issues such as the expense of the disposal of

resulting precipitates, as well as the construction and maintenance of large areas of wetlands,[31] are some of the significant disadvantages of these methods.

1.2.3 Nuclear Waste Processing. An additional source of metal pollutants is from the nuclear industry.[32] Allowing long-lived radioactive metal ions to interact with natural waters and potentially infiltrate the environment would be disastrous. For example, exposure to drinking water containing uranium can have toxic consequences for the liver. Chronic exposure to drinking water containing radionuclides in excess of the maximum contamination level (MCL) can lead to cancer.[33] Long-lived radionuclides are a consequence of nuclear power and nuclear weapon generation. Forty years of weapons grade plutonium production has afforded the US government with a taxing cleanup predicament.[34] At the Hanford site in Benton County, south-central Washington State, USA, more than 151 million m^3 of radionuclide contaminated water has been poured directly onto the soil. High level nuclear waste (HLW) poses a difficult remediation problem.[35] For instance, the half-life of plutonium is 24,100 years, thus a decay of ten half-lives is required to make a sample safe. As a result, a central research focus is the selective removal of radionuclides from complex waste mixtures. [35]This would permit the separated waste to be treated much more inexpensively as low level waste (LLW). In order to neutralize radionuclides, they must undergo transmutation into short-lived isotopes by irradiation with neutrons. Partitioning of the minor actinides (cerium, americium, neptunium) is a prerequisite for their conversion to their less toxic derivatives.[36-41] Secure and effective separation of the minor actinides is a must. This is an area of active and intense research that may serve to ameliorate nuclear waste disposal

and may lead to comprehensive advances in the recovery of f-element metals from aqueous solution.[42]

1.2.4 Processing of Mining Solutions. The third issue is the processing of mining solutions. Many active mining projects implement a leaching process in which acid is employed to extract metals from ore. Consequently, the majority of aqueous mine process solutions include high concentrations of several metal ions at low pH (< 3).[43] In general only one or two metals are targeted for removal. For example, leach solutions from laterite ores can contain a significant amount of several main group metal ions and transition metal ions.[42;44;45] Laterite ores are formed in hot tropical areas enriched with iron and aluminum. Rainfall dissolves the more soluble metals such as sodium, potassium, and silicon leaving the less soluble metals behind. Usually it is the abnormally large concentrations of Ni^{2+} and small amounts of Co^{2+} that are targeted for extraction.[45;46] Currently there is an unprecedented increase in the demand for technologies for the extraction of Ni^{2+} and Co^{2+} from sulfide ores. Laterite ores found in Australia contain 1% to 2% nickel by weight. In fact approximately 70% of the world's nickel reserves are found in laterite ores. In contrast only 30% of the worlds nickel production comes from mining these ores. This is primarily a result of the absence of viable technologies for processing laterite leach solutions.

Contemporary pyrometallurgical and hydrometallurgical processes are energy intensive and economically demanding. Pyrometallurgical processing consists of a thermal treatment of metallurgical ores to produce physical and chemical transformations that will allow the recovery of valuable metals. Pyrometallurgy includes roasting,

smelting, and refining. Hydrometallurgy is the use of aqueous chemistry for the recovery of metals from metallurgical ores. Leaching is an example of a hydrometallurgical technique. The two prevalent methods for processing laterite ores include the Nicaro (Caron) process in which nickel and cobalt oxides are reduced to a metallic form in a roasting stage and the metals are then leached in ammonia solution. The second process is a Sherritt (Moa Bay) process in which the oxides are subjected to a high pressure acid leach (HPAL) followed by a selective sulfide precipitation.[47;48] The HPAL process has much higher Ni and Co recoveries (95% and 93% respectively) in comparison to the Nicaro process (70% and 50% respectively).[49] Although there are now three major projects underway in Australia in which the upstream HPAL process is used, the downstream separation of the impurity metals in the resulting leach solution is quite different.

To separate Co^{2+} and Ni^{2+} from impurities, an ammonia leach from a hydroxide precipitation after iron neutralization can be used to yield a product solution high in nickel and cobalt. A direct solvent extraction-electrowinning (SX-EW) method has also been employed after iron neutralization, as well as a selective sulfide precipitation technique. Electrowinning is the electrodeposition of metals from their dissolved or liquefied metallurgical ores. Upon the recovery of a solution containing primarily nickel and cobalt, the cobalt can then be removed from nickel by way of solvent extraction using a cobalt selective Cyanex 272 extractant.[50] Unfortunately, precipitation methods, re-leaching, and solid-liquid separation techniques are cost intensive. A consequence has been the continued development of a stepwise process in which laterite leach impurities

could be removed by solvent extraction only. Extensive research is also underway with regards to the use of cross-linked polystyrene ion exchange (IX) resins.[51]

1.3 Literature Review

1.3.1. Overview. For some time now, there has been extensive research regarding the development of techniques for the removal of metal ions from aqueous solution. Continuing areas of research include sorption onto solid surfaces, solvent extraction[52], ion exchange[53], membrane filtration[54], bio-sorption[55], flotation techniques, chemical precipitations, turbidity removal, sorption onto nano-particles, wet-land construction, bio-magnetic separations, and solid-liquid separations. There is much that can be learned from other extraction technologies. A survey of the relevant literature identified the requisite criteria for an advanced metal ion removal method. These include:

- A high metal ion sorption capacity
- Selective removal of one metal ion from a mixture of metal ions in high purity
- Operational across a range of pH values
- Reduction of metal ion concentrations to very low levels
- Mechanical and chemical integrity for an extended lifetime
- Favorable mass transfer kinetics to allow high throughputs
- Economically viable

Although several techniques exist for the removal of metal ions from water, three of the most commonly used methods are solvent extraction (SX), ion exchange (IX), and polymer filtration (PF).[43;51;52;54;56-58] SX is one of the most frequently utilized techniques for commercial metal ion separations. SX was initially developed for the purification of uranium for the construction of nuclear devices in the 1950's and 1960's.[59] SE is now used for many metals including copper, nickel, cobalt, zinc, tungsten and vanadium.[60;61]

For example, an acid leach – solvent extraction – electrowinning (AL-SX-EW) process has become an important method for copper recovery. Of all the target metals that SX has been used for, copper is traditionally the least valuable.[43;59] Copper recovery has been traditionally conducted through cementation on scrap iron.[62] The fundamental chemistry of the cementation process can be found in equation 1.6. However, the ferrous produced can oxidize to ferric which results in redissolving copper to form copper sulfate (Equation 1.7)

$$Fe_{(s)} + CuSO_{4\,(aq)} \rightarrow Cu_{(s)} + FeSO4_{(aq)} \quad (1.6)$$

$$Cu_{(s)} + Fe_2(SO_4)_{3\,(aq)} \rightarrow CuSO_{4\,(aq)} + 2FeSO4_{(aq)} \quad (1.7)$$

The commercial practice of AL-SX-EW in the copper industry began in March 1968 when the Bluebird Mine in Miami, Arizona, USA, commenced their operations.[63] World production of AL-SX-EW copper in 1998 was approximately 2.0 Mt, compared with a total world copper mining production of 11.5 Mt. Al-SX-EW is now regarded as a mature, low technical risk technology by the copper industry as a whole. Although SX technology remains prevalent, there has been sustained growth in the use of chelating ion exchangers for both environmental and hydrometallurgical applications.[64] Ion exchange (IX) materials have many advantages over SX that have resulted in the use of IX materials for AMD remediation, wastewater treatment, and for the processing of mining solutions such as HPAL laterite solutions. The DOW polystyrene based IX resin M-4195[65] is used to separate Ni from Co in cobalt refining facilities at INCO in Port Colbourne, Ontario, Canada, as well as at the Chambishi Metals Plc., cobalt refinery in Zambia, Africa. Chambishi produces between 2,000 and 4,000 tons of cobalt and more than 5,000 tons of copper a year from slag dumps using IX. Recently, ultrafiltration used

in conjunction with soluble polymers, has demonstrated promise as a technique for metal ion extraction.[54;65] This technology, which has come to be known as polymer filtration (PF), was originally conceived in 1968 and has found applications in industrial wastewater treatment, analytical techniques and radionuclide separations. Advantages of PF include rapid attainment of equilibrium, avoidance of organic solvents and zero mixed wastes.[66] Furthermore, selectivity for specific metal ions can be enhanced by using polymer blends. SX, IX and PF are closely related. Each of the three metal ion extraction techniques attempts to form a complex with a metal ion that facilitates its removal from aqueous solution. The following sections provide a summary of these techniques. Advantages and disadvantages of each have been identified.

1.3.2. Solvent Extraction (SX). SX, also known as liquid-liquid extraction (LLE), is a method for the separation of molecules based on their preference for each of two immiscible liquids. It is essentially ion exchange in the liquid phase.[67] In general the two liquids are water and an organic solvent (commonly kerosene). For the sequestration of metal ions, the organic solvent contains an extractant (typically a chelating agent) that can form a coordination complex with a desired metal ion. A complete solvent extraction process is typically comprised of four steps:

1. *Extraction* – Transfer of the metal ion from aqueous phase into the organic phase by chemical reaction with an extractant during mixing of solvents.
2. *Scrubbing* – Removal of co-extracted materials for the purpose of increased purity.

3. *Stripping* – Transfer of metal back into a pure aqueous phase for further processing.
4. *Make-up* – Purification by treatment with a third aqueous phase, replenishment of lost solvent and/or extractant and removal of crud build up.

Modifiers are used to enhance coalescence of the emulsion and increase the solubility of metal complexes formed in the solvent.[67] This serves to suppress the formation of solids which may lead to a total collapse of the process by clogging. Modifiers such as isodecanol and tridecanol have been used to increase the solubility of tertiary amine-uranium complexes in hydrocarbons. This alleviates the problem of the formation of a third phase that can settle between the organic and aqueous phase preventing circulation. During thorough mixing of the two immiscible liquids, an extractant that is much more soluble in the organic phase than the aqueous phase forms a complex with the metal to be removed. This is termed a reactive extraction as it involves a chemical reaction. In SX, an ion exchange reaction is exploited if the extractant forms a strong water insoluble complex with the target metal ion.

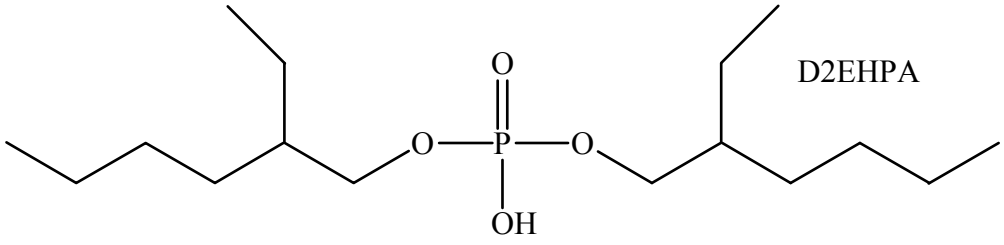

Figure 1.1. Di-2-ethylhexyl phosphoric acid (D2EHPA) SX extractant.

A common extractant is Di-2-ethylhexyl phosphoric (D2EHPA).[68] This extractant has been used to remove transition metals from acidic solutions (Figure 1.1.). The phosphoric

acid portion of the molecule engages in coordination and the hydrocarbon portion ensures solubility in an organic solvent.

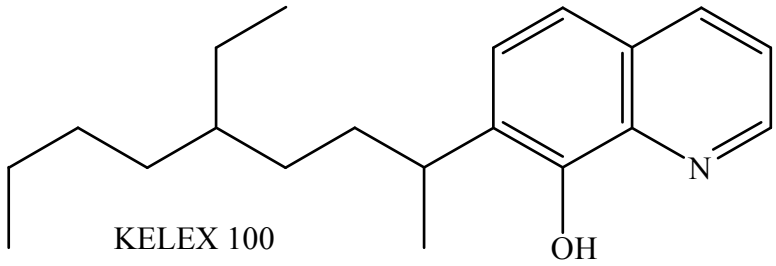

Figure 1.2. 7-(4-Ethyl-1-methylocty)-8-hydroxyquinoline (KELEX 100) SX extractant.

A second example is the frequently employed extractant KELEX 100 (Figure 1.2.) which is used to selectively separate gallium from highly alkaline solutions also containing large amounts of aluminum (BAYER solution).[69] Similar to D2EHPA the hydrocarbon chain is to promote solubility in the organic medium and the oxine functional group is the gallium complexing agent. The process of copper extraction by D2EHPA can be summarized by equation 1.8.

$$Cu^{2+}{}_{(aq)} + 2(D2EHPA)H_{(oil)} \rightarrow 2H^{+}{}_{(aq)} + (2(D2EHPA))Cu^{2+}{}_{(oil)} \qquad (1.8)$$

As a result of this process, Cu^{2+} is transferred from an aqueous phase into an organic phase.[70] To complete the process and maintain charge balance, two equivalents of H^{+} transfer from the organic based extractant to the water. If the constant for this chemical reaction is greater than one, the extraction of copper to the organic phase is favorable. Therefore in SX one typically utilizes the extractant with the highest equilibrium constant for the purpose of increasing efficiency. In general the equilibrium is characterized by a distribution coefficient (λ) which is defined as the ratio of the concentration of metal ion in the organic phase to the concentration of metal ion in the aqueous phase (Equation 1.9). The ratio λ is dependent on initial concentrations. It

is independent of phase flow conditions and somewhat characteristic for a given system. As mixing continues mass transfer between the two phases reaches an equilibrium.

$$\lambda = \frac{C_{org}}{C_{aq}} \tag{1.9}$$

The time to reach equilibrium for a given technically relevant system is typically between several seconds and a few hours. Time to equilibrium is a function of the mass transfer coefficient (k_t) and the interface area/liquid volume (a). Equilibrium is never fully reached, 90% to 99% is considered to be sufficient. In the operation of a SX refining process, in which the solution contains more than one metal ion, it is apparent that the extraction of species other than the desired metal value must be minimized. For the separation of two metal ions, A and B, the equilibrium constant for the formation of the complex generated by metal ion A with the extractant must be sufficiently greater than the equilibrium constant for metal ion B with the same extractant. As a result, metal ion A will be preferentially extracted into the organic layer. To increase the efficiency of the separation process, the aqueous phase is passed through a counter-current sequence of mixer-settlers to produce an organic extract containing almost all of the target metal A. It is a well known separation science concept that a series of smaller equilibriums is substantially more efficient than a single large equilibrium. In the case of a solution containing several metal ions, a process can be established in which each metal ion is removed sequentially by the correct selection of extractant and appropriate process conditions at each stage.

SX has many established advantages over the previously prevalent precipitation dissolution method such as reduced overall process time, improved primary yields, flexibility and versatility, increased process control, simplicity and detailed

understanding of concept. SX can have a high degree of metal ion selectivity as a result of tailored extractants. However, there are also many disadvantages of SX that have led to a growing interest in other technologies.[43] These disadvantages include a finite solubility of extractants and modifiers in the aqueous layer, evaporation of volatile, flammable and often toxic organics, build-up of solid crud at the solid liquid interface, the difficulty of recovering the extracted ion from the organic solvent and the inability of solvent extraction to practically reduce metal ion content in the aqueous phase to negligible levels.[71]

1.3.3. Polymer Filtration (PF). Polymer filtration (membrane filtration) is a second example of using water soluble chelating complexing agents to selectively extract metal ions from aqueous solution.[54] The key to membrane filtration is the semi-permeable membrane.[72;73] Certain elements of an aqueous solution will pass through the membrane, which becomes the permeate, leaving a portion behind which forms the retentate. The factors that determine the composition of the permeate and the retentate include solution composition, pH, temperature, membrane material, pore size and more. However, the most important variable is the size of the dissolved species. In an ideal separation, the target species would be located in high yield in the retentate and the non-target species will be found in high yield in the permeate. If the target and the non-target components do not differ substantially in size, then there will be a low degree of separation of target from the other species. In order to improve the separation, the target species can be bound to a macromolecule so that it now differs substantially in size and molecular weight from the non-target species. Thus, for PF, polymers are designed to form an ionic interaction

or a coordination complex with a target metal ion. The polymer must be water soluble and must have an affinity for the target metal ion in the appropriate aqueous solution.[66] The polymer agent must also have a high molecular weight, chemical and mechanical stability, low cost, low toxicity and it must be possible to strip and reuse the macromolecule for continued use. One of the most common polymers used in polymer filtration is polyethyleneimine (PEI).[74] PEI is a water soluble polyamine with a large degree of amine groups. Amine groups can be used as donor atoms in complex formation or as sites for further functionalization with ligands which provide a greater degree of selectivity as a result of the specificity of complex formation. PEI is considered toxic, and can not be used in water treatment applications.[66] Other polymers that show promise include polyacrylic acid and polyvinyl sulfonic acid.[75] These acidic polymers are non-toxic and are relatively cheap. Unfortunately, they display low selectivity for target metal ions relative to the polyamines. Several novel polymers have been synthesized for use in polymer filtration. These polymers are much more expensive and little is known with regard to their toxicity and mechanical and chemical stability.[76] There are several disadvantages associated with polymer filtration such as polymer sorption into the pores of the membrane which negatively impacts permeate flux. In addition, the sensitivity of macromolecules to colloidal particles can lead to the polymer acting as a flocculent.[66] Degradation of soluble polymers can occur by hydrolysis or mechanical shearing by the pumps, especially polymers of large molecular weight. In order to positively impact the thermodynamics of the process, a low molecular weight complexing agent such as succinic acid is often needed to yield a polymer – target species – complexing agent complex with increased stability relative to the polymer – target species complex. PF is

an innovative and rapidly developing technology but it is IX that has emerged as the most promising alternative to SE for selective removal of metal ions from aqueous solution.

1.3.4. Polymeric Ion Exchange (IX) Materials. An IX material permits the exchange of ions onto and off of a polymeric material (organic ion exchangers) or a crystalline material (inorganic ion exchanger). At no point in the dissociation or association of ions does the ion exchanger dissolve. It is the heterogeneous nature of ion exchange materials that can be exploited to yield flexible and versatile metal removal processes with many advantages. Definitions of ion exchange materials include:

1. Insoluble materials carrying reversible fixed ions that can be reversibly exchanged for other ions of the same sign
2. A phase containing osmotically inactive insoluble carrier of electrical charge
3. An insoluble material that permits the exchange of ions between two or more ionized species located in different phases (one of which is the ion exchanger)

Ion exchange resembles sorption. In both ion exchange and sorption a solid extracts a dissolved species. The difference between ion exchange and sorption is the stoichiometric nature of ion exchange. Sorption removes species from solution but does not replace that species by donating to the solution. In contrast, ion exchange must satisfy balance of charge by the stoichiometric transfer of a species back into solution. Typically IX materials posess a functional group immobilized on a solid support. The solid support or matrix may be organic or inorganic in nature. The most commonly used IX materials

are organic IX materials.[77] Organic IX matrixes are comprised of a three dimensional crosslinked polymeric structure onto which functional groups can be attached.[78]

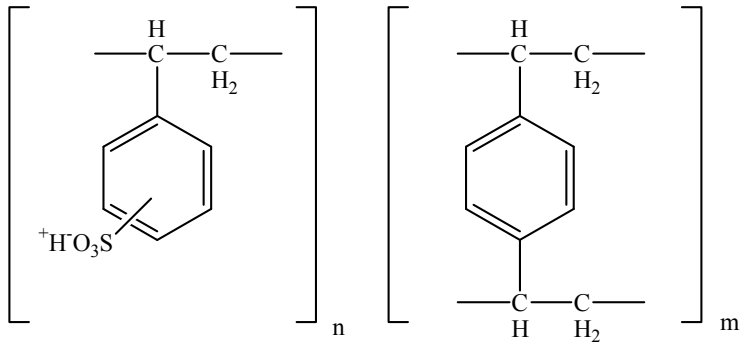

Figure 1.3. A typical example of ion exchange resin is sulfonated polystyrene cross-linked with divinylbenzene.

Styrene-divinylbenzene is the most common matrix because of chemical and mechanical stability (Figure 1.3).[79] Other polymers used include a copolymer of phenol and formaldehyde as well as polyacrylic or polymethacrylic acid with divinylbenzene. Divinylbenzene is an example of a crosslinker. A crosslinker provides strength and stability to the matrix. The density of crosslinks between the polymeric chains is the degree of crosslinking. The degree of crosslinking affects the structure, elasticity, swelling ability and diffusion characteristics with the material. There is a balance between the stability gained by increased crosslinking and the improved mass transfer kinetics incurred as a result of lower crosslinking. In general crosslinking for commercial ion exchangers ranges from 1% to 8 %. Non-crosslinked polymeric IX materials are also of interest. These materials are held together by hydrogen bonding and London forces. There has not been wide spread use of this technology, though, because of stability concerns. There are several types of polymeric IX materials, which include *cation*

exchangers (e.g. equation 1.10) if they possess negatively charged functional groups, *anion exchangers* (e.g. equation 1.11) if they include fixed positive charges, *amphoteric IX material* if the fixed groups have both positive and negative charges, and *chelating IX material* if the group can form a chelate with a metal ion.

$$2P^{-}H^{+}_{(IX)} + Ca^{2+}(Cl^{-})_{2\,(aq)} \rightarrow (P^{-})_2Ca^{2+}_{(IX)} + 2H^{+}Cl^{-}_{(aq)} \quad (1.10)$$

$$2P^{+}Cl^{-}_{(IX)} + H_2SO_{4\,(aq)} \rightarrow 2P^{+}(SO_4)^{2-}_{(IX)} + 2H^{+}Cl^{-}_{(aq)} \quad (1.11)$$

P in equations 1.10 and 1.11 represents the immobilized ionic group of the IX material. Functional groups are attached to the polymeric resin to allow for ion exchange reactions. The functional group can be tailored to provide a range of materials, each with a different specific metal ion selectivity profile. Polystyrene resins can be easily converted to their chloro-methyl and amino-methyl derivatives which provide a reactive group for further functionalization.[80] This permits a range of chemistry that has allowed for the attachment of a range of functional groups. The presence of pendant groups with the ability to act as a ligand has resulted in some particularly useful chelating IX resins.[77;80] It should be noted that the chelating nature of some IX materials has resulted in some scientists not considering chelating materials as IX materials. However, it is possible for these materials to act precisely in the manner of an IX material without demonstrating any evidence of chelation. Chelating IX materials demonstrate non-classical IX behavior. Chelating IX materials can form coordination compounds when electron donor atoms such as nitrogen, sulfur, and oxygen are present. The number of coordination bonds is the *coordination number* of the metal ion. When more than one atom from an individual ligand donates an electron pair to the same central ion, a chelate is formed. The formation of a chelated structure provides a high degree of selectivity due

to the high specificity required for complex formation. Therefore, depending on the nature of the functional group chelating IX materials can have a significant and practical preference for one type of metal ion over another. This is quite similar to the action of an extractant in SX systems. In IX materials, geometrical constraints imposed by immobilization affect the nature of the coordination compound formed. In SX systems, the dissolved extractants have the freedom of mobility in solution to satisfy the coordination sphere of the target ion. For IX materials the immobilization of a ligand does not permit the same degree of freedom this thus the coordination sphere is often satisfied by non-selective ligands such as H_2O, Cl^- or SO_4^{2-}. As a consequence of the geometrical constraints arising from solid phase immobilization, the specific selectivity of a ligand can be significantly different to the specific selectivity of the ligand when used for SX.

Polymeric chelating IX materials can be used repeatedly without the solvent and extractant losses symptomatic to SX.[77] Polymeric chelating IX materials can be readily functionalized with a wide range of ligands.[51] For example, the well known and extensively researched DOWEX crosslinked polystyrene resin M-4195 (Figure 1.4) has been functionalized with a bis-picolylamine functional group to the extent of 0.65 mmol/mL.[65] The regularly used Amberlite IRC-748 resin (Figure 1.4) has been functionalized with an iminodiacetic acid chelating group to the extent of 4.4 mmol/g.[81] Chelating groups such as these allow the resins to extract large amounts of metal ion at low pH.

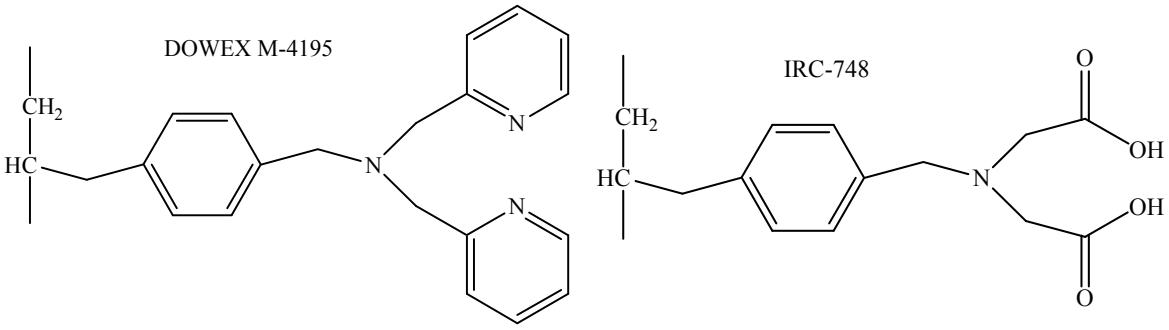

Figure 1.4. (left) DOWEX crosslinked polystyrene resin M-4195 contains a bis-picolylamine ligand. (right) Amberlite IRC-748 crosslinked polystyrene resin from Rohm and Haas contains iminodiacetic acid functional groups.

Research by the Rosenberg Group at the University of Montana, (Missoula, Montana, USA) has shown that the M-4195 polystyrene resin removes approximately 0.9 mmol/g Cu^{2+} per gram of resin, as received, at pH 1, from a solution with an initial Cu^{2+} concentration of 1.5 g/L.[82] Similarly, IRC-748 will remove 0.71 mmol of Fe^{3+} per gram of resin from a solution of 1.5 g/L.[82] The polystyrene matrix will withstand temperatures of 60°C to 80°C and operate across all pH values including very basic pH. There are several drawbacks to using crosslinked polystyrene chelating IX materials. One disadvantage of the crosslinked polymeric structure is shrinking and swelling. Shrinking and swelling imposes limitations on column processes, as the volume of the resin is subject to large variations.[66] Swelling is a result of an osmotic pressure difference between the interior and exterior of the material. It is also a result of repulsion of ionized functional groups within the matrix and the repulsion of water by the hydrophobic polystyrene matrix. Undesirable swelling may build up pressure that may damage the structure of the material. Water wet IX resins shrink or swell when they change from one ionic form to another. For instance shrinking occurs when polymeric IX materials are in

contact with acids and non-polar solvents. Increasing the crosslinking reduces the ability of the material to swell. Swelling is also decreased when the functional group loading per mL of material is minimized. Increasing crosslinking negatively impacts the diffusion of ions through the matrix. Decreasing the functional group loading decreases the materials metal ion sorption capacity. In general, the mass transfer kinetics (i.e. the rate of metal ion capture) of polymeric resins is poor. This is a result of factors that negatively impact the diffusion of the metal ions deep into the matrix. Hydrophobic interactions between matrix and aqueous solution, degree of crosslinking, particle size and the concentration of functional groups all contribute. To summarize, the major disadvantages of polymeric organic chelating IX materials include shrink/swell properties, poor mass transfer kinetics, and instability at elevated temperatures. In order to address these issues the Rosenberg Research Group at the University of Montana, (Missoula, Montana, USA) has for some time now been engaged in the preparation of a new class of inorganic-organic hybrid chelating IX materials. [66;83]

1.4 Silica Polyamine Composites (SPCs)

1.4.1. Overview. An alternative to SX, PF and IX resins based on organic polymers are amorphous silica gel polyamine composites (SPCs), as developed and patented by the Rosenberg Group at the University of Montana (UM) in cooperation with Purity Systems Inc. (PSI), (Missoula, Montana, USA).[84] SPC materials have exhibited promising heavy metal ion extraction characteristics from aqueous media. SPCs possess all the advantages that polymeric IX resins have over SX and PF.[85] Direct comparisons have also demonstrated several advantages of using SPC IX materials relative to organic polymeric IX resins.[82] These advantages include improved mechanical stability, chemical stability in acid, higher operational temperatures, the absence of shrink/swell behavior and significant improvements in mass transfer kinetics.[77;85] SPCs are composed of a polyamine attached through a functionalized silane layer to an amorphous silica gel support.

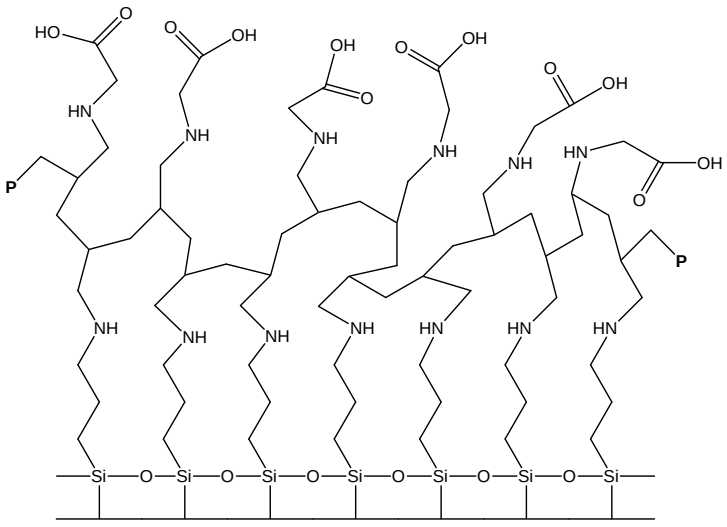

Figure 1.5. An idealized representation of a portion of the surface of an amino-acetate modified PAA SPC.

The polyamine can be further functionalized with metal selective ligands to yield a novel organic/inorganic hybrid chelating IX material.[86] It is through this strategy that an IX material has been prepared that has both the advantages of organic based IX materials as well as those of an inorganic based IX material as shown in Figure 1.5.

1.4.2 Silica Gel Support. Depending on the method of production, the silica gel particles can have irregular or spherical shape. The silica used for SPC production have included amorphous gels which have had particle sizes ranging from 30 μm – 1000 μm, average pore diameters of 8 nm – 30 nm, pore volumes of 0.8 mL – 1.5 mL/g and surface areas of 250 m^2/g - 400 m^2/g (Table 1.2) For IX materials, particle size causes a trade off between mass transfer kinetics and backpressure during column operations. Decreased particle size promotes improved mass transfer kinetics which allows increased flow rates during column processes. However, a consequence of smaller particles is greater pressure drops across the column. Large pressure drops across the column can cause problems when IX resins are employed commercially.

Table 1.2. Physical characteristics of silica gels used to date in the production of SPCs.

Silica Gel	Diameter (um)	Pore Diameter	Pore Volume (mL/g)	Porosity (%)	Surface Area (m^2/g)
Crosfield	90-105	267	2.82	84.7	422
Qingdao Haiyang	150-250	194	2.39	85.0	493
Qingdao Meigao	180-250	378	2.86	85.3	303
Nanjing	180-250	164	2.30	85.8	561
Nanjing Tianyi	80-250	150	2.28	85.6	526

Increased particle size has been shown to reduce the metal ion uptake capacity per gram of material as a result of increases in the interstitial space between particles. A SPC

material prepared from raw amorphous silica in the range of 150 μm to 250 μm diameter has been found to be a reasonable compromise. In contrast, polymeric IX resins are typically in range 250 μm to 800 μm for diameter. Typical flow rates for SPC column operations are in the range 0.1 CV/min (column volume per minute) to 1.0 CV/min. In contrast polymeric IX resins often require flow rates <0.2 CV/min.[45;65;86]

***1.4.3. Synthesis of* SPCs.** For the preparation of SPCs, the initial steps include the sieving (typically 150 microns to 250 microns) and cleaning with acid (1 M HCl) of the amorphous silica gel. The silica gel is then hydrated uniformly with a monolayer of water. At this point the weight of the SPC has increased by 6% of the original weight. Previous reports on the development of HPLC columns have identified that a humidifying step promotes lateral polymerization of a silanizing agent which in turn produces a more fully silanized surface of great uniformity.[87] Thus, for the preparation of SPC materials, the hydration step is used to facilitate the addition of chloropropyltrichlorosilane (CPTCS). CPTCS is a trifunctional silane that reacts with readily available surface silanol sites producing a polymeric -O-Si((CH)$_3$Cl)-O- layer. [88]

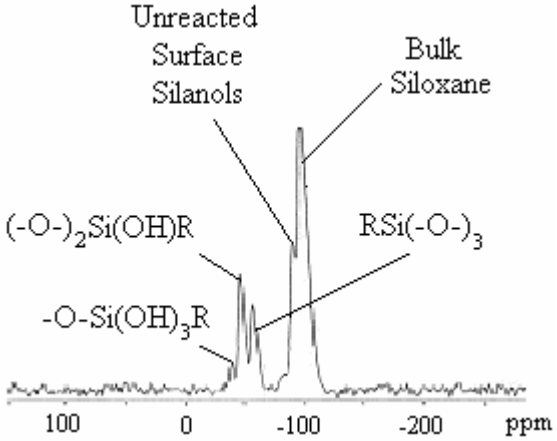

Figure 1.6. CP/MAS ^{29}Si NMR spectrum of amorphous silica gel after reaction with CPTCS at 99.5MHz.

Ideally three equivalents of HCl are released for each CPTCS that reacts. After the attachment of the trifunctional silane, the weight of the SPC has increased approximately 15% over the weight prior to silanization. The ^{29}Si cross polarization magic angle spinning (CP/MAS) spectrum of amorphous silica gel after treatment with CPTCS only is shown in Figure 1.6. The assignments shown are based on the prior work of Wirth *et al*.[87] All the species expected on the surface of the silanized gel are resolved: 1) the bulk siloxane; 2) the unreacted surface silanols; 3) the reagent geminal silanols ((-O-)$Si(OH)_2R$); 4) the reagent silanols ((-O-)$_2Si(OH)R$; 5) the reagent siloxane ((-O-)$_3SiR$).

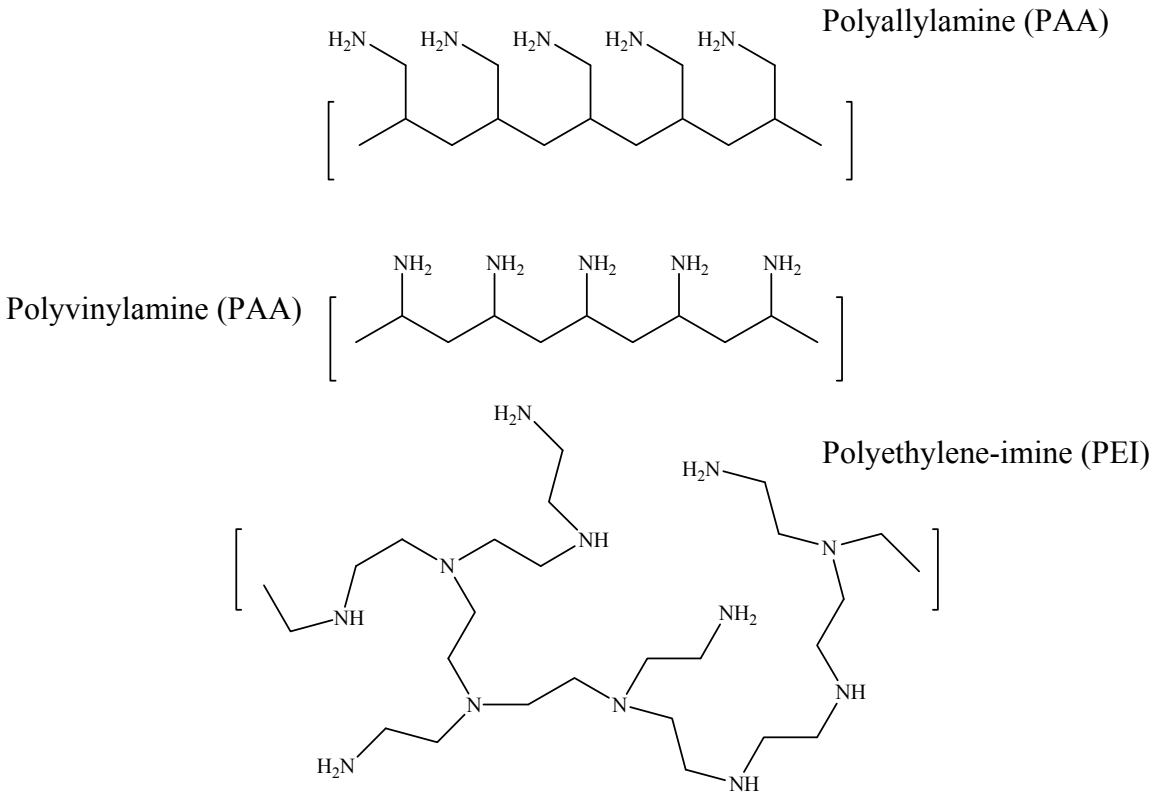

Figure 1.7. The three water soluble polyamines typically used in the preparation of SPC materials. (Top) Polyallylamine (PAA) MW = 15,000. (Middle) Polyvinylamine (PVA) MW = 1000 and 50,000. (Bottom) Polyethylene-imine (PEI) MW = 1200 and 25,000.

The ^{29}Si NMR of CP-Gel clearly illustrates the non-ideal nature of the silanization process. The presence of unreacted silanols indicates incomplete functionalization.[87] Also the presence of reagent silanols and geminal silanols are a sign of significant imperfections in the surface polymerizatrion. Despite these flaws, chloropropyl functionalized amorphous silica gel (CP-Gel) typically has surface silane coverage of approximately 1.5 mmol silanes per gram of functionalized silica gel and the resultant SPCs show excellent stability characteristics when compared to other IX materials.[88]

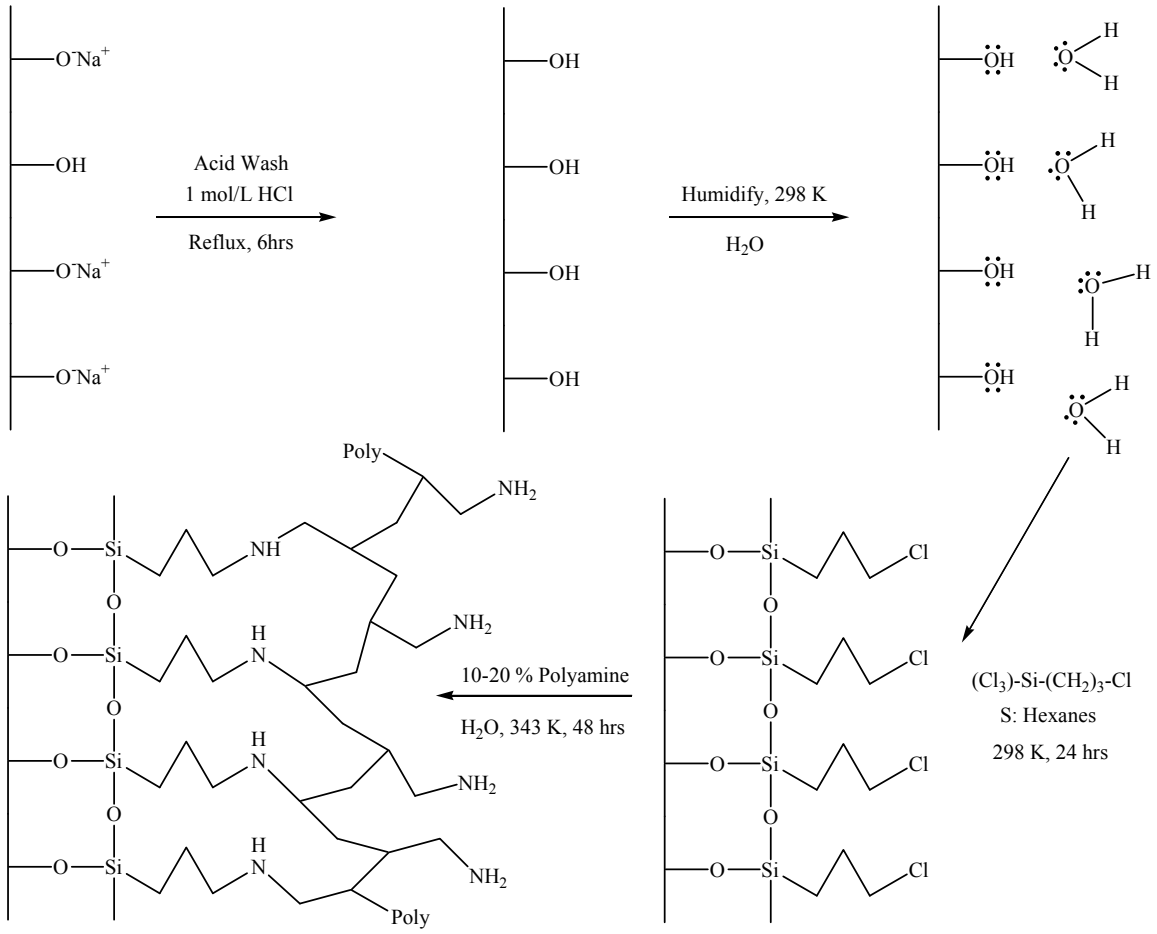

Figure 1.8. The patented synthetic pathway used for the production of SPCs.

The pendant chloropropyl groups then undergo nucleophilic attack by amino groups of a polyamine such as those illustrated in Figure 1.7. These polymers have included polyallyamine, polyvinylamine and polyethyleneimine. The resultant materials have been arbitrarily named BP-1, VP-1 and WP-1 respectively. This produces a robust C-N attachment of a polyamine to the amorphous silica gel and releases HCl as a side product, hence acidifying the reaction mixture. Thus, the progress of the reaction can be monitored by pH. The basic structure of a SPC is then complete (Figure 1.8) and the weight increase ranges from 10% to 20% of the initial weight of silica gel depending on the polyamine grafted, the silica gel used, and reaction conditions employed. The resulting SPC always has a density greater than the raw amorphous silica gel. Greater than 95% of the surface area of amorphous silica gel is contained within the pores. The additional layers have been shown to reduce the pore volume and surface area. Depending on the silica gel type, the polyamine, and the pendant functional group, the density of SPC IX materials is typically in the range of 0.5 g/mL to 0.7 g/mL.[89] SPCs are not the first attempt at using polymers in conjunction with a silica gel support. In fact there have been several reports of similar endeavors in the areas of chromatography and metal sequestering.[90] There have been attempts at physical sorption as well as various synthetic procedures in which the polymer was chemically bound. Physical sorption has the drawback of polymer leaching over time. Many of the chemical procedures resulted in low yields. Reasons include a combination of the absence of the humidifying step, the use of trialkoxysilanes as opposed to trihalosilanes, choice of solvents, and order of steps in the synthetic pathway.[91] The patented pathway used to create SPC IX materials

provides a material with metal sequestering characteristics (metal ion capacity) that surpass previously reported silica-polymer IX materials.[92]

1.4.4. Functionalization of SPCs. Amine groups when deprotonated have the ability to donate an electron pair to a Lewis acid. Therefore the polyamine can act as a chelating agent for a range of metal ions. Target solutions for remediation and processing are more often than not pH < 3. In such solutions, the amine groups will be almost completely protonated. Base regeneration is used to remove the proton and allow the amine to engage in metal coordination. SPC materials containing only the polyamine can extract a range of transition metals from low pH aqueous solutions. SPCs in this form have been used to selectively remove Pd and Pt from solutions containing Cu and Ni.[92;93] However, with the exception of this example, base regenerated SPCs are generally not efficient at the task of removing one metal ion from a solution containing many metal ions.

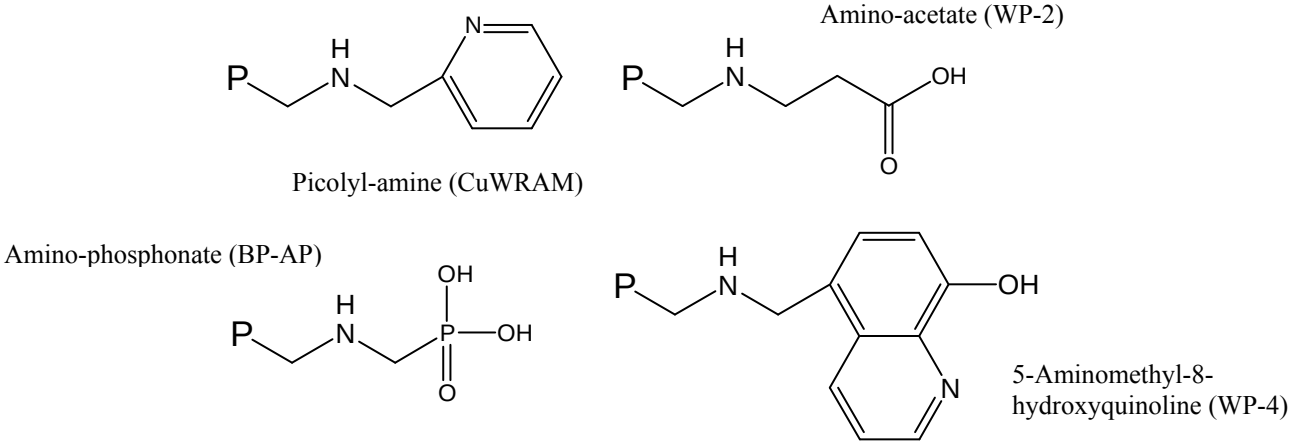

Figure 1.9. SPCs modified with four chelating ligands. P represents the polyamine grafted to the silanized amorphous silica gel. (Top left) CuWRAM. (Top right) WP-2. (Bottom right) WP-4. (Bottom left) BP-AP.

To invoke selectivity and to gain a competitive advantage, producers of organic crosslinked polymeric IX materials have incorporated metal ion selective ligands.[94] SPC

materials have great potential in this area due to the extensive chemistry available for modifying the amine functionality. A series of functionalized SPCs have been created by covalent binding of selective ligands to the polyamine (Figure 1.9).[71]

An example of a functionalization is the reaction of polyallylamine grafted to the silica surface (BP-1) with 2-picolylchloride, which yields a copper selective ligand dubbed CuWRAM. This pyridinyl SPC has been very effective at the selective extraction of Cu^{2+} in the presence of high quantities of Fe^{3+}, and other divalent ions, at low pH (0.5 to 2.0). The CuWRAM composite material is a close analogue of a crosslinked polystyrene resin produced by DOW (DOWEX 43084).[95] In side by side comparisons, CuWRAM exhibits advantages over the DOW resin such as better Cu^{2+} capacity at low pH. This may be due to greater ligand loading. The use of the Mannich condensation reaction has facilitated the synthesis of composites bearing a phosphonic acid and 8-hydroxyquinoline functional groups.[71] In a one pot reaction, BP-1 is modified with phosphorous acid to yield BP-AP.[66] BP-AP selectively removes trivalent lanthanide metal ions in the presence of divalent transition metal ions at low pH. In a two step synthesis, BP-1 is modified with 8-hydroxyquinoline to produce WP-4. This composite selects gallium or ferric iron in favor of aluminum, zinc and ferrous in the pH range 1.5 to 3.0. The modification of polyethyleneimine grafted onto a silica gel surface (WP-1) by sodium chloroacetate yields the composite WP-2. This composite captures divalent 1st row transition metals at low pH, without the need for base regeneration.[71]

SPCs have demonstrated great promise for tackling the environmental and industrial issues raised earlier in this chapter.[66;82;83;86] The early progress in the development of SPCs has seen the refinement of the synthetic pathway. This was

followed by the functionalization of SPCs with ligands similar to those found in the literature for other IX matrixes to invoke selectivity. The uses for SPCs are being expanded outside of cation removal to include anion removal, bacteria elimination, as well as catalysis of organic reactions. Recently these materials were used for sulfide sorption and oxidation.[96] There still remains much to be understood with regards to the structure function relationship in SPCs. The intricacies of the silane layer and the consequences of the nature of the attachment of the polyamine to the silica surface remain relatively unclear. Further, although SPCs are able to selectively remove several important metals selectively, Ni^{2+} has received only passing attention. The DOW resin DOWEX M-4195 remains the only commercially available IX material for selective nickel extraction.[65;66;82;83;86] However, this material not only has the disadvantages discussed previously for organic polymeric IX resins but also has only a modest Ni^{2+} capacity at low pH. With much of the worlds nickel reserves tied up in laterite ores, it is imperative that improved technologies for nickel removal are developed. A significant difference between polymeric chelating IX resins and SPC chelating materials is the location and density of functional groups. In general, the characteristics of the polymeric resins allow the attachment of functional groups throughout the entirety of the particle. In contrast, the functional groups of SPC materials are located only on the surface of the material as the interior of an SPC is bulk silica.[65;66] As a result of the more efficient use of material volume, polymeric resins are typically modified with functional groups to a greater extent per unit mass of material when compared to SPCs. For example, the iminodiacetic acid modified crosslinked polystyrene chelating IX material IRC-748 is reported to contain an estimated 4.4 mmol of ligand per gram of resin.[65;81] A similar SPC

modified with aminoacetate groups possesses approximately 2.8 mmole of aminoacetate per gram. An obvious consequence of greater ligand loading is a subsequent increase in metal ion capacity per unit mass of material making SPCs somewhat less attractive. To ensure the competitiveness of SPCs, it is necessary to substantially improve the ligand loading hence the metal ion capacity. Following functionalization, the quantity of metal selective functional groups per gram of SPC loaded is dependent on the number of polymer amines available for functionalization per unit volume of SPC. In this case, increasing the number of amines should lead to an increase in degree of ligand loading. The following describes initial attempts to increase metal ion capacity.

Several methods for increasing the number of amines attached to the SPC per unit mass were proposed. Increasing polymer molecular weight appeared to be the logical approach for increasing the amine density on SPCs. However, it was demonstrated in previous work that the metal ion capacity of SPCs was not dependent on polymer MW for a given polyamine. These studies were conducted by preparing a series of SPCs (particle size 90 μm to 105 μm) using selected polyvinylamines of MW = 5000, 23,000 and 40,000. The metal uptake characteristics of each SPC were then studied in column tests with the polyamine in the deprotonated form. The resulting Cu^{2+} uptake capacity for the three SPCs were 0.89 ± 0.03, 0.86 ± 0.05 and 0.88 ± 0.06 mmol/g respectively. Therefore, there could not have been a significant change in the quantity of amines per unit mass of SPC using higher molecular weight polyamines. It must be the case that larger polyamine chains (higher MW polymer) attach and conform on the silica gel surface in a manner that consumes an equal molecular volume, as do several smaller chains (lower MW polymer), so that the overall quantity of monomers per unit mass of

SPC has not changed. This also infers that a substantial portion of the polymer chain is proximal to or attached to the surface.

Modifying the SPC polyamine with more amines may also appear to be a logical path to larger capacities. Previous research increased the quantity of amine groups by functionalizing the existing SPC amine groups with chloropropylamine by way of base assisted nucleophilic attack.[65;81] It was hypothesized that the tethering amines away from the polymer would improve mass transfer kinetics. The result was the attachment of one or more propylamine groups to the SPC amines, thus increasing the overall quantity of amines. The resulting product was then modified with 8-HQ to produce the WP-4 SPC and tested for metal ion capacity characteristics. There was a modest increase in Ga^{3+} capacity (~14%) per unit mass and an improvement in mass transfer kinetics (~20%).[65;81;84] As a result of only a modest improvement and because of the potential for polymerization of the reagent this was not deemed a viable pathway. In conclusion initial attempts were only moderately successful at improving metal ion sorption capacity for SPCs.

1.5. Research Goals.

1.5.1. Overall Goals:

1. To investigate the impact of the partial substitution of the reagent chloropropyltrichlorosilane with methyltrichlorosilane on surface coverage, mass transfer kinetics, metal ion sorption capacity and chemical stability.
2. To assess differences in SPCs modified with an amino acid ligand using two different polyamines. Variations in ligand loading, specific selectivity, mass transfer kinetics, sorption equilibrium and dynamic separations are to be investigated.
3. Synthesis and characterization of a series of novel amido-amino acid modified SPCs. Differences in performance characteristics as a function of ligand structure, size and denticity will be assessed.
4. Novel SPC materials will be used in conjunction with existing SPC materials to separate Ni^{2+} from synthetic Laterite solutions as well as to remediate highly contaminated AMD solutions from western Montana.

Chapter 2 – Structural Investigations.

2.1. Introduction.

The modification of amorphous silica surfaces with functional silane moieties has much precedent.[87] Silanes are typically used to impart a degree of either hydrophobicity or hydrophilicity on a solid surface. Trifunctional silanes such as chloropropyltrichlorosilane (CPTCS) are commonly used for surface modification.[97-99] Many labile groups can be utilized, and each varies in relative reactivity with a surface in the order $Si\text{-}NR_2 > Si\text{-}Cl > Si\text{-}NH\text{-}Si > Si\text{-}O_2CCH_3 > Si\text{-}OCH_3 > Si\text{-}OCH_2CH_3$.

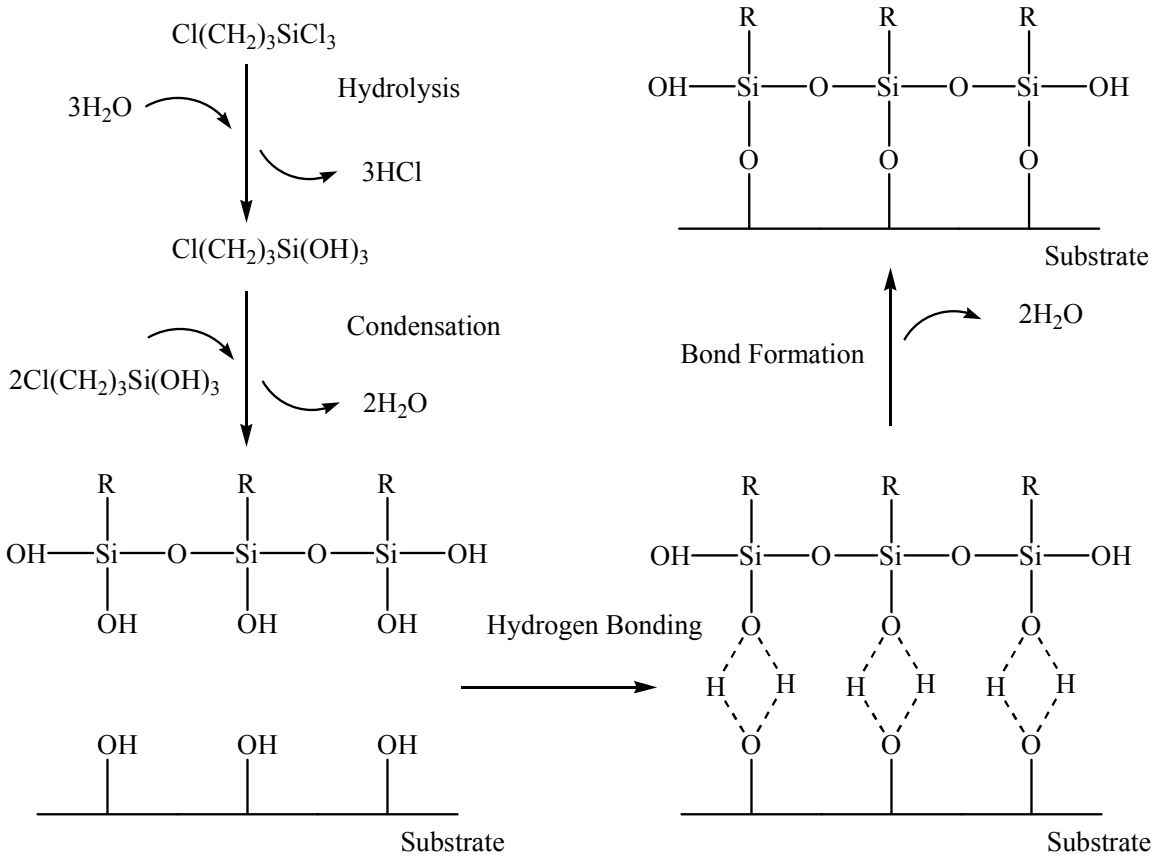

Figure 2.1. An example of the hydrolytic silanization of a silica gel surface using a trifunctional silane. In this case the trifunctional silane is of the form R-trichlorosilane.

The advantage of using less reactive silanes can be greater control, as well as creating less toxic or hazardous byproducts. However, the more reactive silanes give, in general, superior surface silane coverage (mmol of silane per m^2 of silica gel). For the production of SPC materials, it is important that surface coverage is maximized in order to protect the surface from chemical degradation.[71;99]

The initial step in the reaction of a trifunctional silane with a silica gel surface is the hydrolysis of the labile groups by water (Scheme 2.1). This is followed by condensation to oligomers that create hydrogen bonds with the surface silanols. A covalent linkage is then formed with the concomitant loss of water. At the interface between silane and surface usually only one bond is formed between each silane molecule and the surface. Ideally, the remaining two sites engage in the horizontal polymerization of the silanes over the surface. The degree of polymerization is dependent on the quantity of water present on the silica gel surface. It has been demonstrated previously that a monolayer of water on the amorphous silica gel surface promotes a more uniform polymerized layer of functional silane.[87] For the preparation of SPCs a monolayer is applied by passing hydrated air through a column containing silica. Previous work has confirmed the formation of a hydrogen bonded monolayer on the surface. [71] Traditionally, SPCs have been prepared using CPTCS. However, silica gel surfaces can be modified using a wide array of trifunctionalalkylsilanes. In a previous attempt to understand how the nature of the silane alkyl group influences the surface silane coverage and the percent composition of each reagent silane species, amorphous Quingdoa Haiyang (QH) type silica gel was treated with CPTCS only, a 1:1 molar ratio mixture of CPTCS, and methyltrichlorosilane (MTCS) and with MTCS only.[100] MTCS

occupies a smaller molecular volume than CPTCS. It was hypothesized that the addition of MTCS to the reagent silane mixture may promote greater surface silane coverage, thus resulting in a more stable material. Using elemental analysis and ^{29}Si NMR experiments with spectral deconvolution techniques it was possible to estimate the extent of surface silane coverage (mmol/g).[100] Surface coverage was converted to μmol/m^2 through the use of the surface area of the raw silica gel (493 m^2/g) and a correction factor based upon the density increase after surface modification. In comparison to the CPTCS only product, the MTCS only product had greater surface silane coverage (~30% increase). The MTCS only product had surface silane coverage of 6.6 μmol/m^2 ± 0.7 μmol/m^2 (3.2 mmol/g ± 0.3 mmol/g). Interestingly, the physicohemical constant[101] (Kiselev-Zhuravlev constant) for surface silanol concentration is 8 μmol/m^2 ± 1 μmol/m^2 (4.6 OH groups per nm^{-2}) indicating that the majority of silanols have been reacted. ^{29}Si NMR indicated that the percent reagent siloxane also increases, while the percent geminal (two hydroxyl groups per Si) reagent silanol significantly decreases. For the 1:1 MTCS:CPTCS mixture surface silane coverage (μmol/m^2) was also improved relative to the CPTCS only composite, however not to the same extent as the MTCS only silica gel (~12% increase compared to ~30%).[100]

2.2 Impact of Mixed Silanes on Surface Coverage.

Preliminary work demonstrated the positive consequences of incorporating MTCS into the reagent silane mixture. Therefore, a more thorough study of the impact of silanizing amorphous silica gel with molar silane ratios of MTCS:CPTCS of 1:1 to 12.5:1 for INEOS type silica gel was undertaken. This study was conducted in order to examine

in greater detail the relationship between the reagent MTCS:CPTCS ratio and the surface silane coverage. It also provided an opportunity to investigate the incorporation of MTCS into the reagent mixture for a second silica gel. In total 7 silanized silica gels were prepared. Each silica gel underwent elemental analysis for carbon, hydrogen and nitrogen content.

Table 2.1. Elemental analysis of INEOS silica gel modified with CPTCS only, MTCS only, and a series of molar MTCS:CPTCS ratios. There is <0.3 % absolute error in carbon elemental analysis. There is a relative percent error of <3% in chlorine analysis by the ion selective electrode method.

SAMPLE	%Carbon	%Chlorine
'CPTCS only'	4.94	4.69
1:1	4.54	3.05
2.5:1	4.31	1.67
5:1	3.94	1.37
7.5:1	3.50	0.98
10:1	3.38	0.74
12.5:1	3.74	0.63

INEOS amorphous silica gel has a large average pore diameter (25.0 nm) and high surface area (320 m^2/g). A large pore diameter allows efficient diffusion into the pores whilst a large surface area allows greater functionalization per gram of silica gel. Elemental analysis indicates a decrease in chlorine content as the fraction of MTCS in the reagent mixture increases (Table 2.1). The carbon content also decreases, which is due to the replacement of chloropropyl by methyl (3 carbons replaced by 1) groups. From elemental analysis an array of useful data can be derived. Equations 2.1 through 2.4 demonstrate how elemental analysis data can be converted to mmol of a particular surface moiety per gram of functionalized silica gel. Cl represents surface chlorine, Cp

represents surface chloropropyl groups, C_{tot} represents the total amount of surface carbon, and M represents surface methyl groups.

$$\frac{\%\,\mathrm{Cl}}{35.4\ \mathrm{g\,mol^{-1}}} \times 1000\ \frac{\mathrm{mmol}}{\mathrm{mol}} \times \frac{1}{100\%} = \mathrm{Cl\ mmol\,g^{-1}} \tag{2.1}$$

$$\mathrm{Cl\,mmol\,g^{-1}} \equiv \mathrm{Cp\ mmol\,g^{-1}} \tag{2.2}$$

$$\frac{\%\,\mathrm{C}}{12.0\ \mathrm{g\,mol^{-1}}} \times 1000\ \frac{\mathrm{mmol}}{\mathrm{mol}} \times \frac{1}{100\,\%} = \mathrm{C_{tot}\ mmol\,g^{-1}} \tag{2.3}$$

$$\mathrm{C_{tot}} - \left(3 \times \mathrm{Cp\ mmol\,g^{-1}}\right) = \mathrm{M\ mmol\,g^{-1}} \tag{2.4}$$

Equations 2.5 and 2.6 show how the elemental data can be further manipulated to provide surface coverage information. S_c represents surface silane coverage and A_s is total surface area.

$$\mathrm{S_C\ mmol\,g^{-1}} = \mathrm{Cp\ mmol\,g^{-1}} + \mathrm{M\ mmol\,g^{-1}} \tag{2.5}$$

$$\mathrm{S_C\ mmol\,m^{-2}} = \frac{\mathrm{S_C\ mmol\,g^{-1}}}{\mathrm{A_S\ m^2\ g^{-1}}} \times \mathrm{d_f} \tag{2.6}$$

Table 2.2. Elemental analysis of INEOS amorphous silica gels modified with CPTCS only and a series of reagent molar MTCS:CPTCS ratios. There is < 0.3 % absolute error in carbon elemental analysis. There is a relative percent error of < 3.0 % in chlorine analysis by the ion selective electrode method.

MOLAR SILANE RATIO INTENDED R_i	MOLAR SILANE RATIO FOUND R_f	CHLOROPROPYL GROUPS Cp	SURFACE SILANE COVERAGE S_c	
mol MTCS / mol CPTCS	mol MTCS / mol CPTCS (± 8 to 10 %)	mmol/g (± 3 %)	μmol/m^2 (± 1.1)	mmol/g (± 0.28)
0.0	0.1	1.32	5.7	1.47
1.0	1.4	0.86	8.1	2.07
2.5	4.6	0.47	10.4	2.65
5.0	5.5	0.39	9.8	2.51
7.5	7.6	0.28	9.1	2.36
10.0	10.5	0.21	9.2	2.40
12.5	14.6	0.18	10.8	2.76

As the molar fraction of MTCS in the reagent silane mixture increases there is therefore a significant decrease in alkyl halide groups (Table 2.2 3rd column from left). This confirms that fewer CPTCS molecules are incorporated onto the surface as the mole fraction of MTCS increase. Table 2.2 also shows the actual MTCS:CPTCS silane ratio found (R_f) on the modified silica gel, based on elemental analysis (Equation 2.8) compared with the actual reagent molar MTCS:CPTCS ratio used (R_i). That $R_f > R_i$ indicates that the less bulky (lower molecular volume) MTCS reagent reacts more rapidly than CPTCS. For all INEOS silica gels modified with a MTCS:CPTCS mixture, the silane surface coverage was greater than the INEOS 'CPTCS only' case.

$$R_f = \frac{\mathrm{M}}{\mathrm{Cp}} \tag{2.8}$$

Table 2.2 shows surface silane coverage as a function of the MTCS:CPTCS silane ratio for the INEOS silica gel based on elemental analysis (see Table 1). Surface coverage was converted to μmol/m^2 through the use of the specific surface area of the raw silica gel (A_S = 320 m^2 g^{-1}) and a correction factor based upon the density (d_f) change after surface modification. A technique that has been previously applied to silica surfaces to determine the surface silanol coverage involves the modification of a silica gel surface with chlorotrimethylsilane (CTMS). It has been established that the coverage of CTMS on the surface is roughly half that of the surface density of silanols. Modifying amorphous INEOS silica gel with CTMS provides an estimate of the mmol silanol groups per gram.[102] The value obtained from elemental analysis of the CTMS modified INEOS silica was 2.4 mmol/g ± 0.3 mmol/g. The percent carbon (C) from elemental analysis of the resulting material can be converted to mmol of surface CTMS (C_{CTMS}) carbon using equation 2.9. Dividing C_{CTMS} by three (Equation 2.10) allows the determination of mmols

CTMS surface groups per gram functionalized silica (*CTMS*). Thus multiplying this value by two yields an estimate of the number of surface silanol groups α_{OH}.

$$\frac{\%\,C}{g\,mol^{-1}} \times 1000\,\frac{mmol}{mol} \times \frac{1}{100\,\%} = C_{CTMS}\,mmol\,g^{-1} \tag{2.9}$$

$$\frac{C_{CTMS}\,mmol\,g^{-1}}{3} = CTMS\,mmol\,g^{-1} \tag{2.10}$$

$$\left(CTMS\,mmol\,g^{-1}\right) \times 2 \approx \alpha_{OH}\,mmol\,g^{-1} \tag{2.11}$$

Through inserting the CTMS derived value into the Zhuravlev equation (Equation 2.12) the specific surface area (A_S) can be estimated.

$$A_s = K \times \frac{\delta_{OH}}{\alpha_{OH}} \tag{2.12}$$

Where K is a known constant (602.2), δ_{OH} is the mmol silanol per gram and α_{OH} is the Kiselev-Zhuravlev constant (4.6 OH groups per nm^2).[103] The specific surface area arrived at of 310 $m^2\ g^{-1}$ is very close to the specific surface area (320 $m^2\ g^{-1}$) arrived at by the mercury porosimetry method thus validating the mmol per gram silanol value of ~2.4 mmol/g. The average concentration of surface silanes for MTCS:CPTCS ratios ≥2.5:1 is 2.5 mmol/g ± 0.3 mmol/g (9.9 μmol/m^2 ± 1 μmol/m^2), which is within the error of the CTMS derived estimate and the error of the Kiselev-Zhuravlev constant. The surface coverage calculated for ratios above and including 2.5:1 is generally higher than the CTMS derived estimate and the Kiselev-Zhuravlev constant. This could be due in part to non-ideal vertical polymerization of the small and volatile MTCS groups.[87] Any polymerization in a direction perpendicular and away from the surface may result in surface silane coverage somewhat greater than the theoretical constant for uniform horizontal silanization. More importantly, this data infers that, with the exception of the

1:1 MTCS:CPTCS (most likely hindered by the large fraction of CPTCS) and 'CPTCS only' modified silica gels, silanization utilizes the vast majority of INEOS silica gel surface silanols for MTCS:CPTCS ratios greater than or equal to 2.5:1. A surface silane coverage similar to the other mixed silane materials for the 1:1 MTCS:CPTCS mixture is most likely hindered by the large fraction of CPTCS. A large fraction of the bulkier CPTCS may remove the spatial volume required for large amounts of MTCS to react with the surface. Utilizing more potentially reactive silanol groups and increasing the coverage of the INEOS silica surface should ultimately add to the stability of the resulting composites.

In a second similar but independent study the effect of incorporating a different trifunctional silane propyltrichlorosilane (PTCS) was assessed. PTCS has a propyl chain as opposed to the methyl group of MTCS and therefore should occupy a more similar molecular volume relative to CPTCS. Therefore if the above descriptions of improved surface coverage using MTCS are valid then the use of PTCS should not lead to similar improvements in surface coverage. Also a larger particle size of 150 μm – 250 μm was investigated. To investigate PTCS and compare with MTCS the functionalized silica gels listed in Table 2.3 were prepared and underwent C, H, N and Cl elemental analysis. From elemental analysis data much can be determined regarding the nature of the silane layer and surface coverage. Carbon and chlorine content can be converted to mmol/g using equations 2.1 and 2.3 as done previously. The quantity of chloropropyl groups is equated to the amount of chlorine (Equation 2.2). The quantity of propyl groups (P) can be calculated using equation 2.14.

$$C_{tot} - \left(3 \times Cp \text{ mmol g}^{-1}\right) = P \text{ mmol g}^{-1} \qquad (2.14)$$

The ratio of M to Cp and P to Cp can be used to determine the actual surface ratio of MTCS to CPTCS and PTCS to CPTCS on the functionalized silica (Table 2.3 last column). The total quantity of silane attached to the surface can be determined by the sum of M and Cp or the sum of P and Cp, such as that shown in equation 2.5.

Table 2.3. Composition of mixed silane functionalized silica gels (particle size 150-250 μm) as derived from elemental analysis of a series of CPTCS:MTCS modified silica gels and from a series of CPTCS:PTCS modified silica gels.

CPTCS %	MTCS %	Carbon (mmol/g)	Hydrogen (mmol/g)	Chlorine (mmol/g)	C/Cl	Surface Ratio (% MTCS)
0	100	2.92	10.4	0.00	-	100
10	90	2.85	7.90	0.17	16.8	93
25	75	3.83	11.6	0.57	6.72	79
50	50	4.62	1.29	1.08	4.28	56
75	25	5.08	1.32	1.43	3.55	36
100	0	5.95	1.38	1.88	3.16	0
CPTCS %	PTCS %					(%PTCS)
0	100	5.14	14.4	0.00	-	100
10	90	5.56	13.1	0.28	19.9	85
25	75	5.81	15.4	0.67	8.67	65
50	50	5.73	14.5	1.14	5.02	40
75	25	5.57	13.4	1.47	3.79	21
100	0	5.95	13.8	1.88	3.16	0

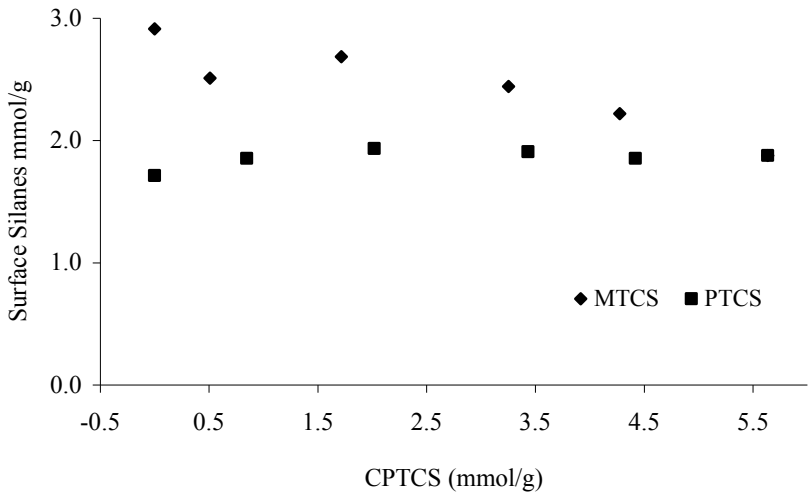

Figure 2.2. Graph of surface silane coverage versus quantity of CPTCS attached to the silica gel surface per gram of silica gel when CPTCS is mixed MTCS in various molar ratios and when CPTCS is mixed with PTCS in various molar ratios.

As expected the chlorine content decreases rapidly upon the introduction of either MTCS or PTCS for 150 μm - 250 μm silica gel. As a consequence of the increased carbon content for PTCS, which is the same as for CPTCS, there is no significant variation in the carbon content for the range of PTCS functionalized silica gels. In contrast the carbon content increases for increasing amounts of CPTCS in the MTCS:CPTCS functionalized silica gels. As a result silica gels modified with a large fraction of MTCS relative to the total reagent silanes should show less hydrophobic character than one with a smaller relative fraction of MTCS. The C/Cl ratio is higher throughout for PTCS which is again a result of the increased carbon content of the two silanes. It was possible to calculate surface silane coverage. It is then possible to determine the ratio of the silanes employed once reacted and attached to the surface. The surface ratios for the MTCS:CPTCS materials indicate that a greater fraction of MTCS reacted with the surface than expected from the reagent ratio. In contrast, the surface

ratios for the PTCS:CPTCS materials are in favor of the CPTCS. Also the quantity of total silanes covalently attached to the surface was graphed against the amount of CPTCS on the surface (Figure 2.2). The graph demonstrates clearly for the PTCS mixtures that there is no significant variation in total silane coverage as the amount of CPTCS attached to the surface varies. In the case of MTCS the surface coverage increases as expected. To explain these results, it must be the case that CPTCS and PTCS occupy a similar volume on the surface. Also MTCS due to its size must be more reactive than PTCS. In conclusion, incorporating MTCS improves overall surface silane coverage. In contrast, PTCS appears to have little effect on surface silane coverage when used in various ratios with CPTCS.

2.2 Investigating Polyamine Structure

Traditionally SPCs have been prepared by the covalent attachment of a polyamine to a silica gel functionalized with CPTCS only.[93] Thus, it was necessary to investigate the consequences of the incorporation of MTCS with regards to polyamine attachment. However, it was necessary to first understand the nature and consequences of polyamine attachment to the CPTCS only functionalized silica gel before incorporating MTCS. This will provide a benchmark with which to evaluate any modifications. Figure 1.7 displays each of the three polyamines used in the preparation of SPCs. SPCs can be prepared using polyethyleneimine (PEI).[85] The resulting SPC has been termed WP-1. PEI is a branched chain, and water soluble polyamine. PEI contains a high density of amine groups and is cheap and readily available. PEI contains carbon and nitrogen only in a 2:1 ratio. PEI possesses primary, secondary and tertiary amines in the ratio of 35:35:30.

Polyallylamine (PAA) and polyvinylamine (PVA) can also been employed for SPC synthesis. The resulting SPCs have been termed BP-1 and VP-1 resultively. These polyamines are also water soluble polymers. However, PAA and PVA are linear polyamines and have C/N ratios of 3 and 2, respectively. In a previous study, it was established that the metal ion extraction capacity of the resultant SPC was independent of polyamine molecular weight.[84] However, there are substantial differences in the metal ion extraction selectivity of the resulting SPCs prepared from each of the three polyamines. Differences in performance must be due to differences in the structures of each the polyamines investigated. Thus, further study was required to investigate the implications of the differences between each of the three polyamines.

Table 2.4. Composition of amorphous silica gel functionalized with CPTCS only followed by the attachment of three distinct polyamines.

SPC	Polyamine	Carbon (mmol/g)	Nitrogen (mmol/g)	Poly C/N	Cu(II) Capacity (mmol/g)	N/Cu(II)
WP-1	PEI branched	11.4	3.9	2	1.25	3.2
VP-1	PVA	12.7	3.4	2	0.92	3.7
BP-1	PAA	11.7	2.4	3	1.85	1.3

SPCs were prepared from each of the three polyamines listed in table 2.4. Each of the three SPC materials was sent for C, H and N elemental analysis. Elemental analysis has an absolute error of ± 0.3%. It is immediately evident that branched PEI (WP-1) contains the largest quantity of amines per gram of SPC. In contrast linear PAA (BP-1) has the lowest density of amine groups. From the data in Table 2.2 it can be seen that a greater amine density is favored when the polyamine C/N ratio is smaller. WP-1 contains the largest quantity of amines per gram most likely as a result of the presence of a large

fraction of both secondary and tertiary amines. The attachment of polymer molecules must lead to a complex and crowded environment on the sililca gel. It therefore appears logical to assume that secondary and tertiary amines are less likely to react with the surface as a result of greater steric hindrance relative to primary amines. The linear polyamines contain only primary amines, which are much less sterically hindered. As a result a single linear polyamine molecule can react many times with the surface. Thus if only a small fraction of PEI amine groups can react per each polymer molecule more chloropropyl sites remain available to react with further PEI molecules. In contrast less chloropropyl groups remain when a linear polyamine molecule reacts with the surface. The consequence of this is a relatively large quantity of PEI molecules covalently bound to the functionalized silica gel, hence a greater number of amines. In the case of the linear polyamines there will be a lower relative amount of polymer molecules attached to each gram of silica gel, hence less amines when compared to PEI. This theory can be validated by assessing, from elemental analysis, the percentage of amines that attach to the surface. For BP-1 over half (54.1%) of the polymer amines are attached to the surface. For WP-1 (PEI) approximately one third (33.5 %) of the polymer amines are attached to the surface. It should be noted that approximately one third of PEI amines are primary amines.

It is noteworthy that the number of amine groups does not correlate at all with the Cu^{2+} capacity of the material. BP-1 (PAA), with the lowest quantity of amines, has the highest Cu^{2+} extraction capacity (mmol/g). There are some possible explanations for this phenomenon. It may be that those amines attached to the surface are prevented from engaging in metal ion capture by a crowded local environment. Also, in the case of WP-1 tertiary amines, which constitute 30% of all amines, may not have the conformational

freedom required to engage in complex formation. PVA is used for the synthesis of VP-1. PVA is prepared from the hydrolysis of the corresponding polyformamide thus incomplete hydrolysis leaves a significant quantity of amide groups in the VP-1 material. PAA is prepared from the polymerization of allylamine and would therefore not suffer from such a problem. A second reason may be in relation to the C/N ratio of the polyamines. For the materials with lower polyamine C/N ratios amine groups are relatively proximal. As a result a chelate is more likely to develop between two or more amines and a metal center. For example two amine groups in WP-1 are separated by one $(CH_2)_2$ moiety. As a result a thermodynamically favored five member chelate ring can occur. However, in the case of BP-1 the amines are separated by a five carbon chain making the chelate structure less stable and thus less likely. As a result, the number of polymer amines per captured Cu^{2+} is higher in the SPC with the higher polymer C/N ratios. In conclusion the structure of the polyamine heavily impacts not only the number of polymer molecules appended to the surface but also the resulting metal ion capacity. BP-1 (PAA) provides the highest per gram Cu^{2+} capacity. However, it is WP-1 (PEI) that provides the greatest quantity of amines per gram SPC. It will be shown later that the choice of polymer can significantly impact metal ion sorption characteristics.

2.4. Impact of Mixed Silanes on Amine Density

2.4.1. Initial Studies. Through elemental analysis of SPC materials it has been shown that almost all of the surface alkyl halide groups undergo nucleophilic attack by polymer amines (Table 2.5). This is based upon the reasonable assumption that hydrolysis of a

chloropropyl group is less favored under the reaction conditions utilized than is nucleophilic substitution. Therefore, it is reasonable to argue that the quantity of polymer amines attached (N_s) to the surface is primarily governed by the number of alkyl halide groups. Elemental analysis has demonstrated that PAA (polyallylamine) reacts with CP-Gel (silica functionalized with chloropropyltrichlorosilane only) to yield approximately 54% of all amines attached to the surface. Therefore, in the case of PAA with a molecular weight of 15,000 and a monomer molecular mass of 58, on average, there are approximately 100 polymer amines (out of a total of 260) attached to the surface per individual polymer chain. This number must be considered to have a wide distribution range since the distribution of surface silanols on a silica gel surface is not uniform and therefore the surface silanes may not be distributed evenly. However, with such a large number of amines attached to the surface it should be possible to decrease N_s without sacrificing total polymer loaded and without diminishing the remarkable stability of SPCs, which is attributable to multipoint anchoring.

Table 2.5. C, H, N and Cl elemental analysis of polyamine modified amorphous silica gel indicating that upon the reaction of the CPTCS modified silica gel with PAA and PEI the residual Cl is negligible.

SPC	Particle Size	% Carbon	% Hydrogen	% Nitrogen	% Chlorine
BP-1	90-105	11.23	27.2	2.86	0.07
BP-1	150-250	9.63	23.6	2.33	0.05
WP-1	150-250	10.38	30.3	5.29	0.03

A reduction in the quantity of alkyl halide groups should provide a decrease in the fraction of polymer amines attached to the surface. Translating this to a single polymer chain it appears logical that a reduction in the amount of attached sites should produce an increase in free amines (Figure 2.3). A greater quantity of free amines (those amines not

attached to the surface), N_f, should increase the number of sites available for modification by a metal selective ligand. This is based on the assumption that the addition of a metal selective ligand is more likely for a free amine relative to a surface attached amine. If an increased fraction of free amines can be achieved without a substantial decline in the overall number of polymer chains appended, it may be possible to create a silica polyamine composite of improved performance.

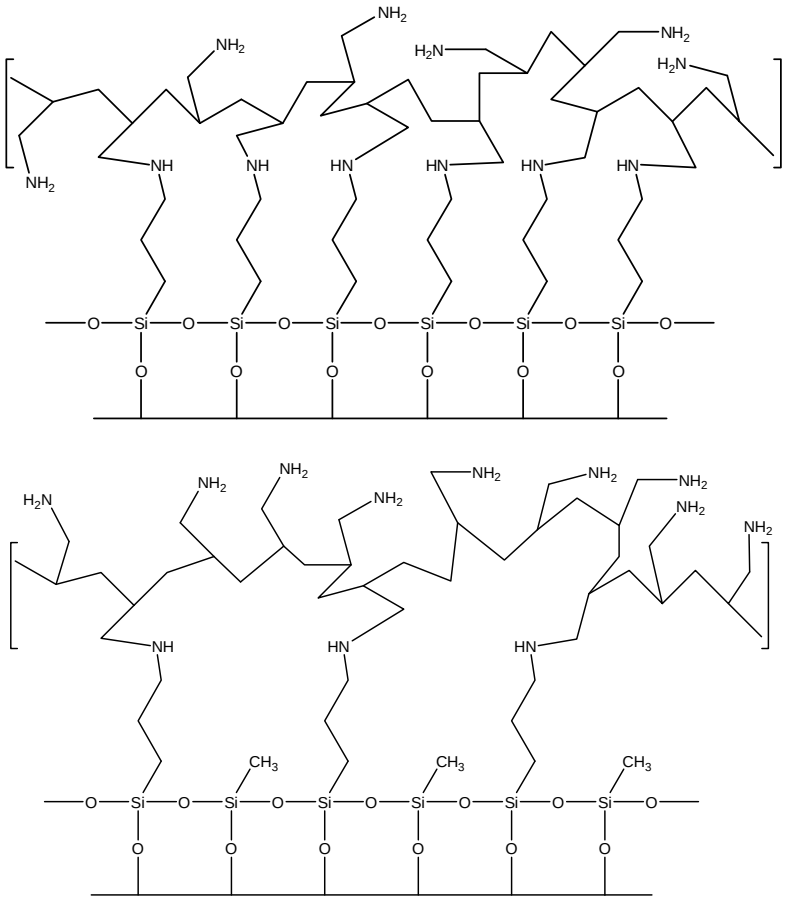

Figure 2.3. Top: A 2D idealized cross-section of a BP-1 composite material produced from CPTCS only. Bottom: A 2D idealized cross-section of a BP-1 structure for a 1:1 MTCS (Methyltrichlorosilane) / CPTCS (Chloropropyltrichlorosilane) silane ratio.

It has been clearly demonstrated that it is possible to control the number of alkyl halide attachments within the silanized surface layer through the incorporation of silanes with the alkyl halide functionality absent. It has also been shown to this point that the result is an increase in surface silane coverage. The quantity of alkyl halide anchors can be dictated by reacting chloropropyltrichlorosilane (CPTCS) and its methyl counterpart, methyltrichlorosilane (MTCS), simultaneously with a hydrated silica gel surface. Silica gel modified in this manner should still have the polymeric silane layer vital for polyamine support and product integrity, but with a reduced amount of chloropropyl group per gram silica gel. The chloropropyl and methyl modified silica gels (CP/M Gels) can then be further modified with the three polyamines discussed above. Thus the effect of reducing the number of polymer attachment points can be scrutinized. It may be possible to determine an optimum MTCS:CPTCS ratio for which the surface coverage is maximized and where the number of attachments of the polymer to the surface is sufficient to maintain composite integrity. If increasing the number of free amines per gram SPC improves SPC performance (i.e. metal ion capacity and mass transfer kinetics) it should follow that the subsequent reaction with modifying groups such as 2-picolyl chloride, 8-hydroxy-quinoline and phosphorous acid would yield improvements in modified SPCs also.

To test the polymer modified materials synthesized using MTCS and CPTCS an appropriate metal ion solution was required. SPCs show affinity for divalent transition metal ions, the order of which is in accordance with the Irving-Williams series. Using the series, it was clear that the polyamine modified materials will show greatest affinity for Cu^{2+} from aqueous solution, relative to other 1^{st} row divalent transition metals. As a

result, Cu^{2+} was chosen as the metal ion to be used for analyzing the mixed silane SPC investigations. As a consequence of the weakly basic nature of the polyamines, metal sequestration is heavily dependent on pH. Therefore, it was necessary to determine how the pH of a Cu^{2+} challenge solution impacts the metal ion extraction performance of SPCs before proceeding further with investigations. As the pH of the initial challenge solution increases, the quantity of metal ion extracted per gram of SPC should also increase. At high pH there is less H^+ in solution, thus the left hand side of the equilibrium expressed in Equation 2.13 will be favored. The equation assumes a coordination number of 2 and only considers coordination by primary amines. R represents the hydrocarbyl portion of a polyamine monomer.

$$2RNH_3^+(OH^-) + Cu^{2+}(SO_4^{2-}) \rightleftharpoons (RNH_2)_2Cu^{2+}(SO_4^{2-}) + 2H_2O \qquad (2.13)$$

50 mmol/L $CuSO_4$ challenge solutions at pH 2, 3 and 4 were prepared and breakthrough tests were conducted using VP-1 (polyvinylamine SPC) prepared from silica gel functionalized with CPTCS only. A description of the breakthrough process is necessary at this point. A column process is used to more accurately demonstrate material performance under commercially applicable conditions relative to batch testing. A batch test involves the addition of 10 mL of challenge solution to 0.1 g of SPC. The IX reaction then proceeds to equilibrium. However, it is impossible that at equilibrium all of the metal ions present in solution will have been removed by the SPC. The column technique attempts to ensure the completion of the IX reaction. Column studies resemble carrying out an infinite number of successive batch operations in series. As a result of carrying out many batch tests sequentially the metal ion levels in solution can be brought to negligible levels. A plot of the concentration variation at the column outlet versus the volume of

solution treated at each point is termed a *breakthrough curve*. The breakthrough curve is dependent not only on material characteristics but is also heavily dependent on processing conditions. Therefore, for a fair comparison the flow rates and initial concentrations of column experiments must remain constant. In a column process the *breakthrough capacity* (Q_b) is the mmol quantity of metal ion B^+ removed per gram of SPC prior to the presence of B^+ is the effluent. The *full breakthrough capacity* (Q_{tot}) is the mmol quantity of metal ion B^+ removed per gram of SPC when the concentration of B^+ in the effluent is equal to the concentration of B^+ in the feed solution. Q_{tot} is the total IX capacity of the column. SPC material was packed into a 5 mL or 10 mL column and all subsequent operations are carried out in the bed. The full breakthrough capacity data was collected from column breakthrough testing using the formula shown in equation 2.14.

$$Q_{tot}\ \text{mmol}\,\text{ml}^{-1} = \frac{\left(C_o \cdot V_{tot}\right) - \sum_0^n \left(C_n \cdot V_c\right)}{V_c} \tag{2.14}$$

C_o is the initial copper concentration (50 mmol/L), V_{tot} is the total volume processed, n is the number of column volumes processed, V_c is the volume of the column (5mL) and C_n is the concentration of Cu^{2+} in each 5 mL volume of effluent collected. Through column testing it was found that Q_{tot} increased from 0.76 mmol/g to 1.04 mmol/g as the pH climbed from 2 to 4 for VP-1 (polymer MW = 50,000 BASF Lupamin 5095). Figure 2.4 illustrates the breakthrough profile for VP-1 showing the increase in the effluent Cu^{2+} concentration from the start of breakthrough, Q_b, until full breakthrough at $C_n = C_o$, Q_{tot}. For all three pH values the effluent contains negligible Cu^{2+} initially. As the experiment continues Cu^{2+} is detected in the effluent in the order pH 2<pH 3<pH 4. The *degree of bed utilization* (*U*), which is the ratio of the amount of Cu^{2+} adsorbed before

breakthrough (Q_b) to the Cu^{2+} adsorbed in total (Q_{tot}), is a useful measure of how efficient the break through process was. This is an important consideration because industrial column operations rarely go much past the point of breakthrough, Q_b.

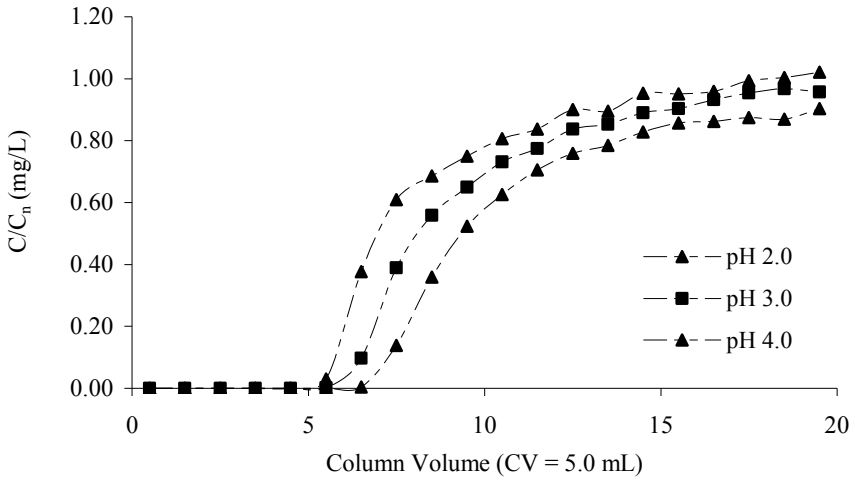

Figure 2.4. Column extraction of Cu^{2+} from aqueous solution by VP-1. VP-1 is prepared with Lupamin 5095 polyvinylamine (PVA) MW = 50,000. Comparison of breakthrough profiles at pH 2, 3 and 4.0.

Beyond Q_b the column utilization becomes increasingly less efficient. For VP-1 at pH 2, 3 and 4 the degree of utilization is 0.76, 0.78 and 0.76 respectively. Therefore increasing the pH allows increases in capacity without any significant change in the efficiency, *U*. In order to facilitate metal ion extraction the SPC material is washed with ammonium hydroxide, followed by rinse water, prior to each experiment. The purpose of the base is to deprotonate the polymer amine groups. Base regeneration enhances metal ion extraction properties relative to the polyamine in the acid form. However, when SPC materials are base regenerated (30 mL of 4 mol/L NH_4OH followed by 30 mL DI water) entrained base introduces the possibility of the precipitation of hydroxides. 6 column volumes of DI water is used to remove excess base. Precipitation can also be combated by using a challenge solution of a low pH. Although precipitation was not an issue during

these tests, it was deemed prudent to conduct Cu^{2+} capture tests from solutions at pH 3 to ensure high metal ion extraction capacity while avoiding precipitation. A further factor is that the full breakthrough was not reached after 20 column volumes of feed when tested with the Cu^{2+} solution at pH 4. In contrast the pH 3 profile had reached a C_n/C_o value of 1 at 20 column volumes.

2.4.2. Low Molecular Weight Polyamines. WP-1 and VP-1 can be prepared using polyamines of various molecular weights. Two of the lower molecular weight polyamines include PEI MW = 1200 (WP-1) and PVA MW = 1000 (VP-1). Several of the CP/M Gels prepared previously were reacted with each of these two polyamines. The VP-1 and WP-1 products then underwent elemental analysis, the results of which are presented in Table 2.6. The carbon and nitrogen content in mmol/g was calculated using equations 2.3 and 2.15 respectively. C/N is the ratio of carbon in mmol/g to nitrogen mmol/g. N_s the number of surface attached amines (mmol/g).

$$\frac{\%\,\mathrm{N}}{14.0\ \mathrm{g\,mol^{-1}}} \times 1000\ \frac{\mathrm{mmol}}{\mathrm{mol}} \times \frac{1}{100\,\%} = \mathrm{N_{tot}\ mmol\,g^{-1}} \tag{2.15}$$

$$\mathrm{N_f\ mmol\,g^{-1}} = \mathrm{N_{tot}\ mmol\,g^{-1}} - \mathrm{N_s\ mmol\,g^{-1}} \tag{2.16}$$

N_s is equivalent to the number of chloropropyl groups (mmol/g). The assumption that all chloropropyl groups react individually with a single polymer amine group is used. N_f is the number of amines not attached to the surface (Equation 2.16). N_{tot} is the total number of amines. Q_{tot} is the full breakthrough capacity for the sorption of the divalent Cu^{2+} ion from sulfate solution at pH 3. N/Cu^{2+} is the ratio of amine groups to copper ions. N/Cu^{2+} is useful measure of how efficient the SPC is at Cu^{2+} sorption. It is clear that the

incorporation of MTCS into silane mixture resulted in a VP-1 material with much lower carbon content and nitrogen content than the same SPC derived from the CPTCS only gel. This indicates a substantial loss in overall polyvinylamine.

Table 2.6. Data derived from elemental analysis for various CP/M gels modified with PVA MW = 1000 (VP-1).

M:CP Gel	Carbon (mmol/g)	Nitrogen (mmol/g)	C/N	N_s (mmol/g)	N_f (mmol/g)	$Cu^{2+}Q_{tot}$ (mmol/g)	N/Cu^{2+}
0:1	11.43	3.36	3.40	1.32	2.04	0.85	3.95
2.5:1	7.13	1.90	3.75	0.47	1.43	0.80	2.38
5:1	7.12	2.05	3.47	0.39	1.66	0.63	3.25
7.5:1	6.28	1.79	3.51	0.29	1.52	0.55	3.25
10:1	7.12	2.01	3.54	0.21	1.80	0.61	3.30

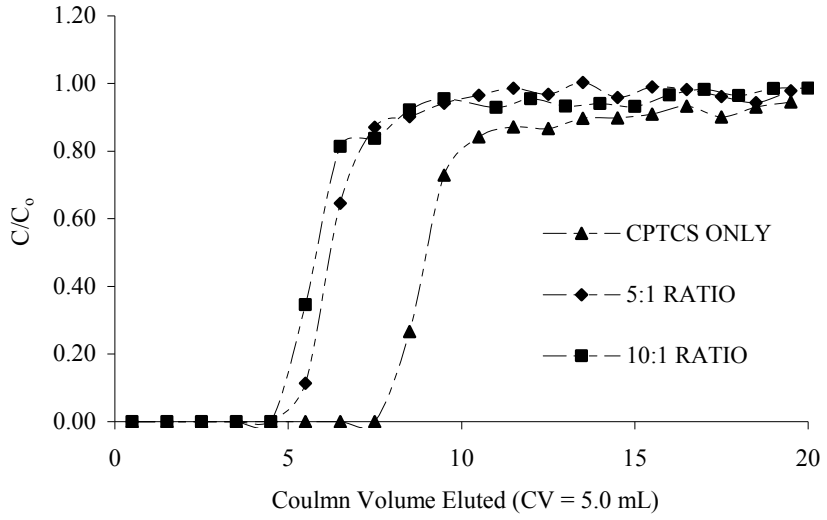

Figure 2.5. Breakthrough profiles for VP-1 (PVA SPC) prepared without MTCS, with MTCS and CPTCS in the ratio of 5:1 and in the ratio 10:1.

Also, the quantity of free amines (those not reacted with the surface) appears to have decreased due to the presence of MTCS. To further investigate each material the

Cu^{2+} full breakthrough capacity was determined through column experiments. At the MTCS:CPTCS silane ratio of 7.5:1, VP-1 prepared from low molecular weight PVA (MW = 1000) exhibited approximately a 30% decrease in Cu^{2+} Q_{tot} breakthrough capacity relative to the CPTCS only VP-1. Finally the number of amines required to adsorb one equivalent of Cu^{2+} decreases upon the introduction of MTCS. Figure 2.5 shows the breakthrough profiles for two of the VP-1 materials made from CP/M gels in comparison to the VP-1 made from CP-Gel. It is clear that a substantial decrease in Cu^{2+} breakthrough capacity results from the introduction of MTCS. The degree of utilization does not vary significantly from 0.75 to 0.80 throughout, thus there was no significant impact on the already efficient mass transfer kinetics.

Table 2.7. Data derived from elemental analysis for various CP/M gels modified with PEI MW = 1200 (WP-1).

M:CP Gel	Carbon (mmol/g)	Nitrogen (mmol/g)	C/N	N_s (mmol/g)	N_f (mmol/g)	Cu^{2+} Q_{tot} (mmol/g)	N/Cu^{2+}
0:1	11.94	4.34	2.75	1.32	3.02	1.26	3.44
2.5:1	6.92	2.11	3.28	0.47	1.64	0.68	3.09
5:1	6.33	1.89	3.35	0.39	1.50	0.55	3.44

A similar study was conducted for WP-1 prepared using low molecular weight PEI (MW = 1200). Three WP-1 SPC materials were prepared. Two of the materials were prepared using a large fraction of MTCS relative to CPTCS (2.5:1 and 5.0:1). One material was prepared with CPTCS only. The resulting materials underwent elemental analysis and were subjected to column tests for Cu^{2+} uptake. A summary of the results can be found in Table 2.7. The data was derived using the equations employed for low molecular weight VP-1 analysis. The amine content decreases substantially when MTCS

is introduced to the synthetic procedure. For WP-1 the drop off in Cu^{2+} breakthrough capacity was equally severe. The 2.5:1 MTCS:CPTCS WP-1 had a breakthrough capacity approximately 46% that of the 'CPTCS only' WP-1 and the 5:1 MTCS:CPTCS WP-1 breakthrough capacity was approximately 56% that of the 'CPTCS only'WP-1. The breakthrough profiles presented in Figure 2.6 show a similar trend to that found for VP-1 composites. The *U* value for the CPTCS only, the 2.5:1 and the 5.0:1 materials are 0.80, 0.76 and 0.71 respectively. This indicates a small decrease in efficiency as the fraction of MTCS increases. The low Cu^{2+} extraction capacities obtained for MTCS:CPTCS composites prepared using lower molecular weight polyamines ruled them out as good candidates for the inclusion of MTCS in the silane layer. No further studies of low molecular weight polyamines were conducted.

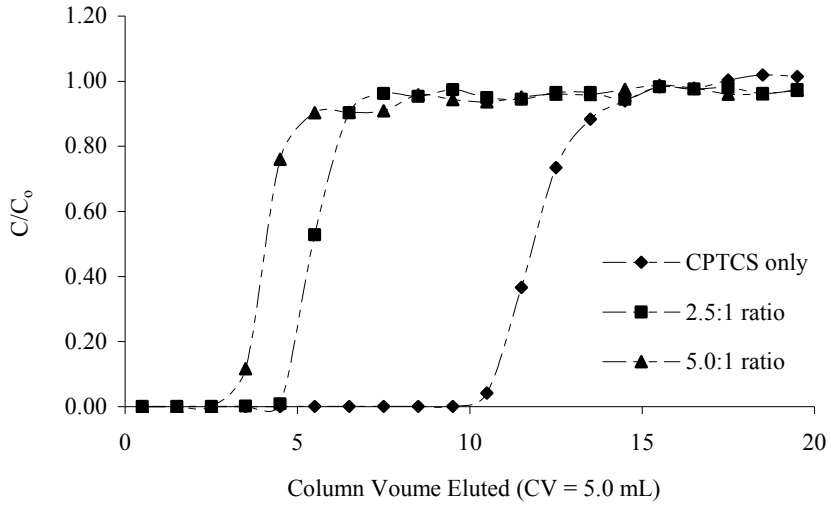

Figure 2.6. Breakthrough profiles for WP-1 (PEI SPC) prepared without MTCS, with MTCS and CPTCS in the ratio of 2.5:1 and in the ratio 5.0:1.

2.4.3. High Molecular Weight Polyamines. High molecular weight PVA, PAA and PEI were grafted onto the MTCS:CPTCS modified INEOS (90 μm to105 μm particle size)

amorphous silica gels prepared previously for the surface coverage study discussed in section 2.4.1. The presence of the MTCS and CPTCS on the surface of these silica gel polyamine composites is confirmed in the ^{13}C NMR spectra of 50,000 MW PVA grafted onto a 7.5:1 MTCS:CPTCS modified INEOS silica gel surface. A methyl resonance is observed at -5.6 ppm in addition to the n-propyl resonances at 45.7, 26.9 and 10.50 ppm (Figure 2.7). A series of resonances at 150 ppm to 165 ppm of significant intensity indicates unhydrolyzed formamide in the PVA (PVA is prepared by the hydrolysis of polyvinyl formamide).

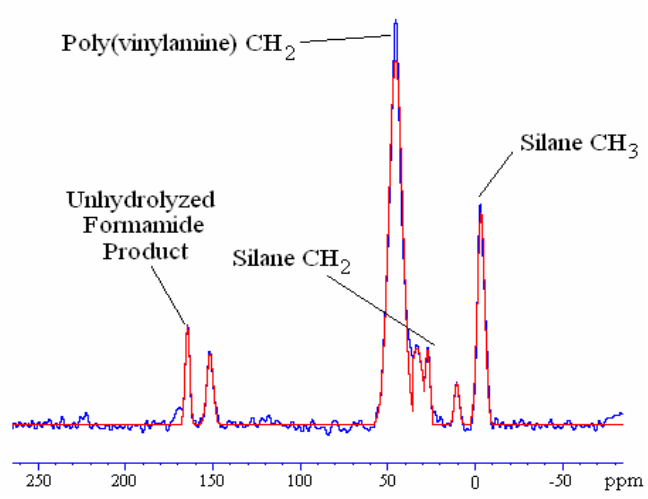

Figure 2.7. CP/MAS ^{13}C NMR at 125 MHz of VP-1 (PVA MW = 50,000) silica composite 7.5:1 MTCS:CPTCS with deconvolution overlay.

Table 2.8. Data derived from elemental analysis for various CP/M gels modified with PVA MW = 50,000

M:CP Gel	Carbon (mmol/g)	Nitrogen (mmol/g)	C/N	N_s	N_f	Cu^{2+} Q_{tot} (mmol/g)	N/Cu^{2+}
0:1	15.26	4.76	3.21	1.32	2.08	0.93	3.66
2.5:1	11.33	3.97	2.85	0.47	2.36	0.98	2.91
5:1	12.71	4.77	2.66	0.39	3.02	1.05	3.23
7.5:1	11.77	4.33	2.72	0.28	2.81	1.09	2.85
10:1	11.31	4.13	2.74	0.21	2.74	1.01	2.93
12.5:1	7.18	2.25	3.19	0.18	1.43	0.52	3.09

Elemental analysis for high molecular weight VP-1 modified with MW = 50,000 PVA is presented in Table 2.8. The data has been converted to this form using equations 2.3, 2.15 and 2.16. There is no linear trend in this data. This is a result of the playoff between polymer loading and the decrease in carbon content due to the increase in the MTCS:CPTCS ratio. For all three polyamines, N_f increases substantially with increases in MTCS:CPTCS reagent silane ratio. Reducing the quantity of chloropropyl groups per gram of functionalized silica gel results in increases in N_f when the polymer is reacted with the functionalized surface, relative to the case of CPTCS only. This is in contrast to the analogous low molecular weight VP-1, for which N_f decreases substantially.

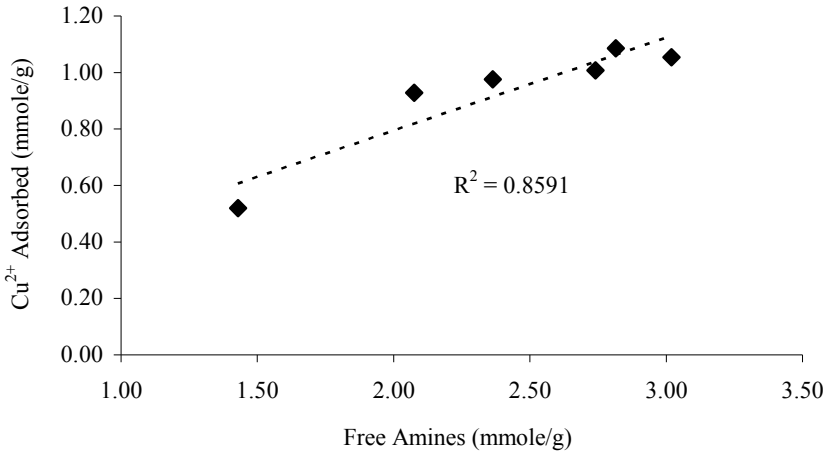

Figure 2.8 Cu^{2+} sorption as a function of free amines for VP-1 (PVA SPC).

The maximum percent increase in free amines over the CPTCS only modified SPC found through elemental analysis of the resultant composites was approximately 48% for VP-1 at a MTCS:CPTCS ratio of 5:1. Therefore N_f must be heavily dependent on the

polyvinylamine molecular weight. When fewer surface attachments are available the effect is not a reduction in overall polymer relative to CPTCS only. Instead each polyamine molecule must attach to the surface at fewer points i.e. fewer monomers react with the surface. At higher ratios the quantity of free amines (mmol/g) decreases. This indicates that there are not enough chloropropyl sites on the functionalized amorphous silica gel at high MTCS:CPTCS ratios to prevent decreased polyvinylamine loading.

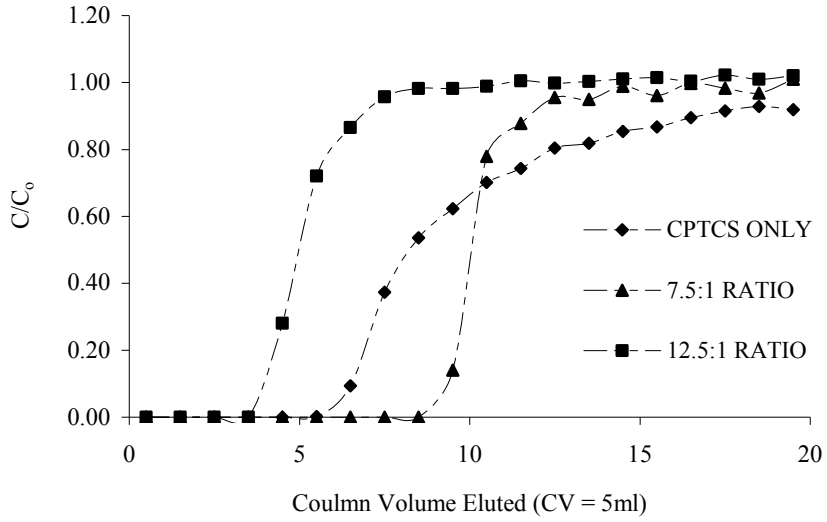

Figure 2.9 A comparison of the Cu^{2+} breakthrough profiles for VP-1 (PVA SPC) for increasing ratios of MTCS:CPTCS

The results of column testing the high molecular weight VP-1 polyamine composites listed in the left most column of Table 2.8 with a pH 3, 50 mmol/L Cu^{2+} feed solution are displayed in Figure 2.7 and Figure 2.9. In Figure 2.6 Cu^{2+} adsorbed (mmol/g) is plotted as a function of N_f. N_f was calculated from elemental analysis using equations 2.15 and 2.16. The data suggests a reasonable correlation between N_f and Cu^{2+} adsorbed. An increase in N_f by the incorporation of MTCS results in an increase in Cu^{2+} adsorbed (mmol/g) for PVA. However, in contrast to the increase in free amines, the effect on Cu^{2+}

adsorbed (mmol/g) was relatively small. For high molecular weight VP-1 the optimum value (highest Cu^{2+} adsorbed) for the ratio of MTCS:CPTCS exists at 7.5:1. This corresponds to a 17% increase in Cu^{2+} capacity relative to the CPTCS only high molecular weight VP-1, but an increase of approximately 1 mmol/g for N_f. Higher ratios (> 7.5:1) of MTCS:CPTCS result in decreased Cu^{2+} sorption (mmol/g) most likely due to a decrease in total polymer grafted to the silica surface. The N/Cu^{2+} ratio is higher for the CPTCS only VP-1 in comparison to the materials which incorporate MTCS. This indicates a small coordination number when MTCS is used. A smaller coordination number may indicate that amine groups are further apart due to a more flexible surface layer. A second interpretation could be the involvement of more amines in the sorption process due to less steric hindrance as a result of a more flexible polyvinylamine layer. In either case the result is a more flexible polyvinylamine layer as a result of the use of MTCS. This is validated by the breakthrough curves presented in Figure 2.9. Mass transfer kinetics, which can be quantitatively described by the degree of utilization *U* (given that all process parameters are held constant), are an important aspect of overall ion exchange performance. A material with superior mass transfer kinetics will result in a breakthrough profile which will display a quick transition from negligible metal ion in the eluent to a concentration of metal ion in the eluent equal to the feed metal ion concentration. This will be reflected in a high value for *U*. A value of unity indicates an ideal process. For practical applications it is advantageous for a composite to possess chelating sites that are all equally accessible to an aqueous metal solution and that form stable complexes with the target metal. Previous work has shown that composite divalent metal capacities are independent of polyamine molecular weight. One disadvantage of

high molecular weight polyvinylamine is inferior mass transfer kinetics in comparison to low molecular weight polyvinylamine, most likely due to obstruction of pores and/or slow diffusion through the large polymer (MW = 50,000). The MTCS:CPTCS high molecular weight SPCs exhibit significantly improved mass transfer kinetics over the CPTCS only polyamine composites. Figure 2.9 displays a comparison of breakthrough profiles for three composites: VP-1 prepared from CPTCS only silica gel and VP-1 grafted onto the 7.5:1 and 12.5:1 MTCS:CPTCS composites. The U values for each of the SPC materials are 0.52, 0.83 and 0.67 respectively. At a MTCS:CPTCS ratio of 7.5:1 VP-1 has a degree of utilization as high as any low molecular weight VP-1 studied. A significant improvement in *U* indicates that the mass transfer kinetics for the 7.5:1 VP-1 material must have improved relative to the CPTCS only VP-1. Improvements in mass transfer indicate improved diffusion into the SPC surface layer as a result of increased flexibility. Due to the inefficiency of allowing a composite to go to full capacity, it is prudent to terminate the process once the effluent is at 10 % of the feed solution concentration. This is particularly useful in industrial applications where separation efficiency is paramount. Improved mass transfer kinetics will have a substantial impact on the 10% breakthrough capacity. The 10% breakthrough capacity for the CPTCS only VP-1 is 37 mg/g whereas for the 7.5:1 MTCS:CPTCS VP-1, the 10% breakthrough capacity is 65 mg/g (~76% improvement).

Table 2.9. Data derived from elemental analysis for various CP/M gels modified with PEI MW = 25,000 (WP-1).

M:CP Gel	Carbon (mmol/g)	Nitrogen (mmol/g)	C/N	N_s	N_f	Cu^{2+} Q_{tot} (mmol/g)	N_{tot}/Cu^{2+}
0:1	11.43	3.94	2.91	1.32	1.69	1.24	3.17
2.5:1	9.80	3.41	2.87	0.47	2.21	1.07	3.19
5:1	9.52	3.43	2.78	0.39	2.26	1.12	3.06
12.5:1	9.83	3.50	2.81	0.18	2.39	1.01	3.47

Elemental analysis for MTCS and CPTCS functionalized silica gel modified with MW = 25,000 PEI to yield WP-1 is presented in Table 2.9. The data has been converted to this form using equations 2.3, 2.15 and 2.16. Similar to VP-1, N_f increases substantially (~59% increase relative to CPTCS only WP-1) over the range of MTCS:CPTCS ratios studied. The maximum value in the range studied was 2.39 mmol/g, which corresponds to a MTCS:CPTCS ratio of 12.5:1. Again, this is in contrast to the low molecular weight WP-1 study in which N_f decreased substantially as MTCS was introduced. Therefore N_f must be a function of the MTCS:CPTCS ratio as well as PEI molecular weight. The explanation provided above for VP-1 must therefore apply for PEI also. A notable difference between WP-1 and VP-1 is the continued increase in N_f at higher MTCS:CPTCS ratios for WP-1. This indicates that at high MTCS:CPTCS ratios there is no significant loss of PEI whereas at the same ratio there is a loss in PVA relative to the smaller MTCS:CPTCS ratios. This suggests that the PEI polymer used for the preparation of WP-1 can tolerate a lower fraction of amines attached (N_s/N_{tot}) to the surface than can PVA. At 12.5:1 MTCS:CPTCS N_s/N_{tot} = 0.05 for WP-1 whereas, for VP-1 at the same ratio, N_s/N_{tot} = 0.11.

Improvements in Cu^{2+} adsorbed are not found for composites made from branched PEI (MW = 25,000). Cu^{2+} adsorbed by the WP-1 materials decrease slightly to a lowest value at the 12.5:1 MTCS:CPTCS ratio (~18% decrease across the range analyzed). This is opposite to the trend found for VP-1, in which gains in Cu^{2+} sorption were found. This indicates that for WP-1 it is N_{tot} that governs the quantity of Cu^{2+} adsorbed. Whereas in the case of VP-1 a correlation exists between N_f and Cu^{2+} adsorbed, this is not the case for WP-1. This suggests that in the case of WP-1 all amines, including surface attached amines engage in coordination of Cu^{2+}. However, for VP-1 the linear trend in Figure 2.8 indicates that it is primarily the free amines that govern Cu^{2+} coordination.

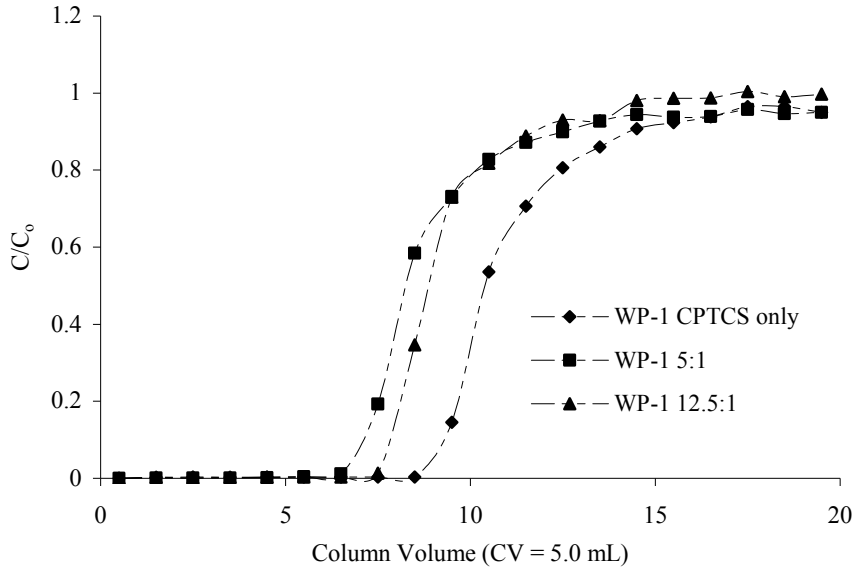

Figure 2.10. comparison of the Cu^{2+} breakthrough profiles for WP-1 (PEI SPC) for increasing ratios of MTCS: CPTCS

Thus the conformation adopted by PVA when attached to the surface must prevent those amines attached to the surface from participating in metal coordination.

Conversely the conformation adopted by the PEI polymer when grafted to the surface must promote the engagement of surface attached amines in coordination. Figure 2.10 illustrates the Cu^{2+} breakthrough profiles for WP-1 SPC materials. The degree of utilization, *U*, for CPTCS only WP-1, for WP-1 5:1 and for WP-1 12.5:1 are 0.76, 0.70 and 0.81 respectively. The *U* value for the low molecular weight (MW = 1200) CPTCS only WP-1 is 0.80 which is only marginally improved relative to the high molecular weight CPTCS only WP-1. There was no substantial improvement in U value upon the incorporation of MTCS. Elemental analysis for high molecular weight BP-1 (PAA, MW = 15,000) is presented in Table 2.10.

Table 2.10. Data derived from elemental analysis for BP-1 prepared from various CP/M gels. CP/M gels modified with PAA MW = 15,000.

M:CP Gel	Carbon (mmol/g)	Nitrogen (mmol/g)	C/N	N_s	N_f	Cu^{2+} Q_{tot} (mmol/g)	N/Cu^{2+}
CPTCS only	11.68	2.44	4.78	1.32	1.12	1.86	1.32
2.5:1	11.05	2.43	4.55	0.47	1.57	1.40	1.73
5:1	10.10	2.28	4.43	0.39	1.81	1.56	1.46
7.5:1	11.51	2.81	4.09	0.28	2.43	1.75	1.61
12.5:1	9.18	2.15	4.27	0.21	1.97	1.38	1.55

The data has been converted to this form using equations 2.3, 2.15 and 2.16. In general the C/N ratio decreases as the fraction of MTCS is increased. N_f increases to an optimum at a MTCS:CPTCS ratio of 7.5:1. The increase in N_f over the CPTCS only BP-1 was approximately 1.31 mmol/g, which is an increase of greater than 100%. Figure 2.11 demonstrates that there is a general increase in free amines relative to the fraction of MTCS in the reagent silane mixture. This is a similar trend to that observed for N_f for VP-1.

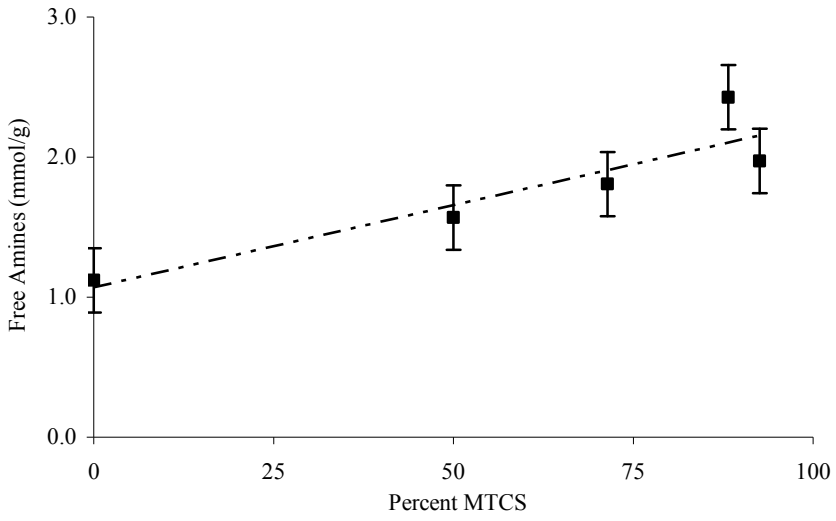

Figure 2.11. BP-1 (PAA SPC) free amines as a function of percent MTCS.

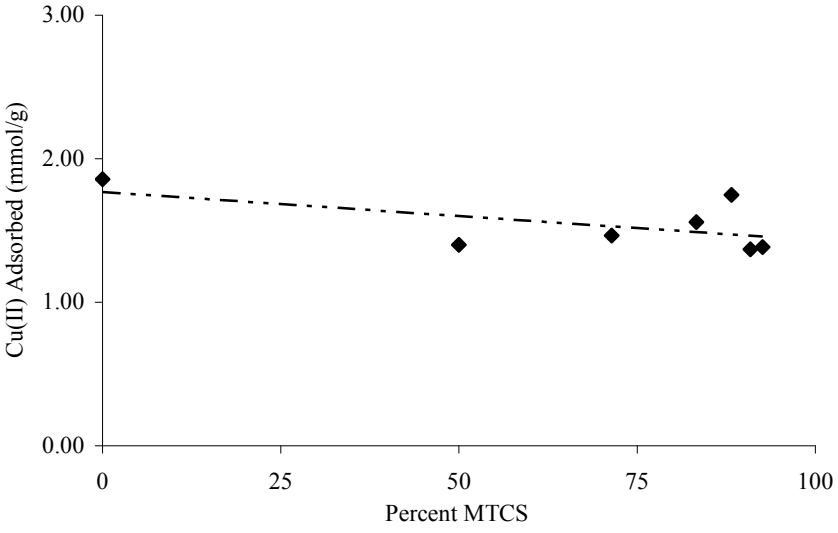

Figure 2.12. BP-1 (PAA SPC) Cu^{2+} sorption as a function of percent MTCS.

However, Cu^{2+} sorption is greatest for the CPTCS only BP-1. Cu^{2+} sorption decreases approximately 25% for the 2.5:1 MTCS:CPTCS BP-1, then gradually increases until it is within approximately 6% of the value for the CPTCS only BP-1, reaching a maximum at a MTCS:CPTCS silane ratio of 7.5:1 and then gradually decreasing at higher ratios in a similar fashion to VP-1. Figure 2.12 shows the Cu^{2+} sorption data

graphically. It is clear that although 7.5:1 may represent a maximum that in general increasing the percentage of MTCS leads to a decrease in Cu^{2+} sorption. However, because of the complexity of the system it should be noted that it is unlikely that this trend is linear. There is no trend in the N/Cu^{2+} data relative to the fraction of MTCS except for the fact that all of the BP-1 materials prepared using MTCS have greater N/Cu^{2+} values compared to the CPTCS only BP-1. This infers that a larger number of amines are engaging, on average, in coordination of each Cu^{2+} ion. As the conformational freedom of the bound polymer increases, less amines will be hindered from participating in coordination. To test whether or not surface amines engage in coordination for BP-1, the coordination number using only free amines can be calculated ($CN = N_f/Cu^{2+}$). This assumes that all free amines are coordinating copper. For BP-1 the values for free amine only *CN* range from 0.6 to 1.4 across the range of BP-1 SPCs studied. The highest *CN* occurs at the point of highest free amines (7.5:1). A *CN* value of less than unity for BP-1 is nonsensical, because at least one amine is required for each one Cu^{2+} captured. Therefore, surface attached amines must also participate in Cu^{2+} coordination. This is in contrast to VP-1 for which the data suggests that free amines govern Cu^{2+} sorption. As a consequence of one less CH_2 on each PVA monomer, relative to a PAA monomer a greater degree of conformation freedom must be available to BP-1 compared to VP-1. A less rigid polymer environment may favor the participation of more BP-1 amine groups in coordination.

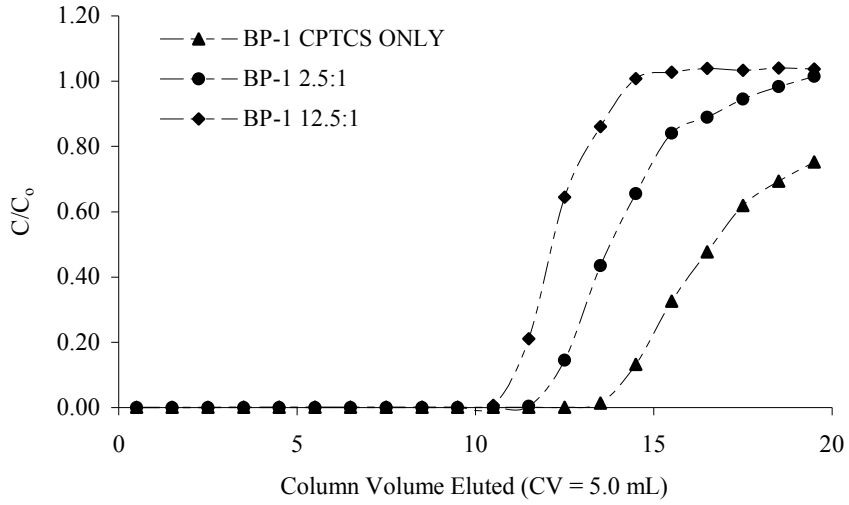

Figure 2.13. A comparison of the Cu^{2+} breakthrough profiles for BP-1 (PAA SPC) for increasing ratios of MTCS: CPTCS.

Figure 2.13 displays the results of column tests for BP-1 SPCs prepared from CPTCS only, 2.5:1 MTCS:CPTCS and 12.5:1 MTCS:CPTCS functionalized silica gel. It is apparent that the mass transfer kinetics for the CPTCS only BP-1 are relatively poor. As a result the CPTCS only BP-1 does not reach full breakthrough. Through extrapolation of the curve the *U* value for CPTCS only BP-1 is 0.79. However the U value for 2.5:1 BP-1 and 12.5:1 BP-1 are both 0.89, which is a substantial improvement. This validates the hypothesis that increasing the fraction of MTCS in the reagent silane mixture yields SPC materials with improvements in mass transfer kinetics. Such improvements must be due to more favorable diffusion into the polymer layer which must be a result of great conformational freedom in the polyamine.

2.5 Impact of Mixed Silanes on Ligand Functionalized SPCs.

Elemental analyses of WP-1 SPCs clearly indicate a substantial increase in N_f for those composites incorporating MTCS in the silane layer. Of the WP-1 SPCs tested 12.5:1 MTCS:CPTCS had the greatest N_f increase (~41 %). Thus the next task was to investigate the relationship between increased free amines, as a consequence of MTCS introduction, and the metal sequestration performance of the resulting composite when modified further with selective ligands. A detailed comparison was conducted of a 12.5:1 MTCS:CPTCS WP-1 composite modified with sodium chloroacetate and the CPTCS only WP-1 composite modified similarly. The resulting materials are dubbed WP-2 (Figure 2.14). Six five gram samples of hydrated INEOS silica gel were modified, three with a 12.5:1 MTCS:CPTCS silane mixture and three with CPTCS only.

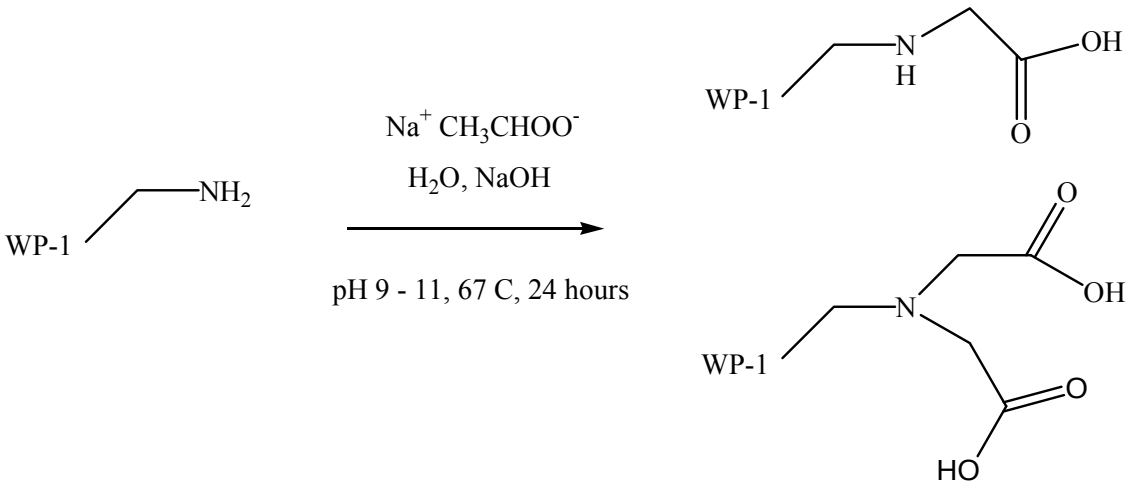

Figure 2.14. Synthetic pathway from WP-1 to WP-2. Mono- di- and tri- functionalization of a WP-1 primary amine are theoretically possible. Showing primary amine only.

PEI (MW = 25,000) was then grafted to each of the six samples and the resultant composites were modified with sodium chloroacetate according to previously reported procedures. As a result six WP-2 materials were prepared. It has been previously reported

that CPTCS only WP-2 SPC (MW = 1200) can effectively adsorb Cu^{2+} at from solutions of lower pH than can the unmodified WP-1 SPC. The results of column breakthrough testing of the CPTCS only WP-2 (MW = 25,000) composite and the 12.5:1 MTCS:CPTCS WP-2 SPC using 25 mmol/L Cu^{2+} are displayed in Figure 2.15. For clarity two trials are shown for each of the two types materials although a total of three materials were prepared and tested for each. Testing revealed an improvement in performance (as measured by improvements in Cu^{2+} breakthrough capacity) for the 12.5:1 MTCS:CPTCS acetate modified SPC over the CPTCS only acetate modified PEI composite. Table 2.11 provides the actual Cu^{2+} full breakthrough capacities for the six experiments. Further the results demonstrate the excellent reproducibility of the synthetic procedures for each WP-2 material. Increases in Cu^{2+} capacities were found for the three 12.5:1 MTCS:CPTCS composites (0.62 mmol/g) over the CPTCS only WP-2 materials (0.44 mmol/g) of approximately 41% on average.

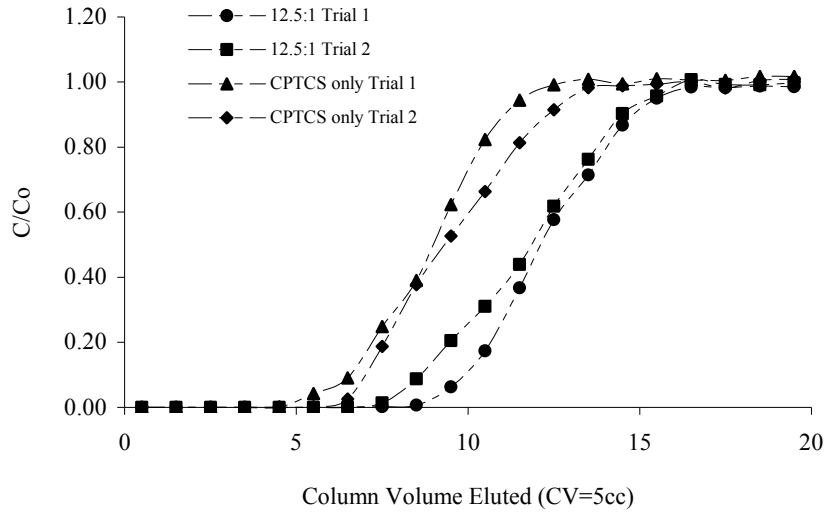

Figure 2.15. A comparison of the Cu^{2+} breakthrough profiles for WP-2 prepared from CPTCS only silica gel and from MTCS:CPTCS (12.5:1) silica gel. 2 trials illustrated each from a total of 3 each.

This increase in Cu^{2+} sorption capacity is indicative of increased ligand loading. Calculations based on the elemental analysis of CPTCS WP-2 and 12.5:1 MTCS:CPTCS WP-2 show that approximately 60% and 71% of all amines on each composite have been modified (1.78 mmol/g and 2.08 mmol/g) with the acetate functionality respectively.

Table 2.11. Data defining the Cu^{2+} sorption for WP-2 prepared from CPTCS only silica gel and from MTCS : CPTCS (12.5:1) silica gel. Data for three separate trials and average provided.

	Metal ion adsorbed (mmol/g)	
	CPTCS Only WP-2	12.5:1 MTCS:CPTCS WP-2
Load Trial 1	0.46	0.61
Load Trial 2	0.40	0.56
Load Trial 3	0.45	0.66
Average	0.44	0.62

Since approximately 30% of PEI amines are tertiary, which are likely unavailable for modification, it must be assumed that either the majority of primary and secondary amines have been modified or each primary amine has been modified with more than one acetate group forming a di- or tri- acetate ligands. Although there is an approximate 14% increase in ligand loading, this does not account for a 41% increase in Cu^{2+} breakthrough capacity. Thus more acetate groups may be available for Cu^{2+} capture as a result of a more flexible polymer matrix. A less rigid polyamine matrix may lead to decreased conformational strain in the coordination complex thus stabilizing and promoting chelation. An SPC with both a more flexible polymer matrix and a greater quantity of free amines might also lead to situations in which unmodified amines are involved in coordination. Although amines are generally protonated in acidic media, when Cu^{2+} coordination initiates at acetate functionalities a proximal amine may also engage in

coordination. Polydentate coordination of this fashion may lead to greater stability of the Cu^{2+} complex hence increased Cu^{2+} capacities.

Stripping of Cu^{2+} was accomplished with 2 mol/L H_2SO_4. The CPTCS only WP-2 retained a light blue color whereas the 12.5:1 MTCS:CPTCS WP-2 did not. Therefore, although both composites stripped similarly (100% mass balance for the 12.5:1 MTCS:CPTCS WP-2 and 97% mass balance for CPTCS only WP-2) the residual color suggests that a small amount of Cu^{2+} (3% of the capacity) remains in the CPTCS only composite after the initial load strip cycle, which is removed in the case of 12.5:1 MTCS:CPTCS WP-2. Previous studies have shown that there is a negligible negative impact on the long term capacity of these materials by repeated exposure to acid.[88] The absence of retained Cu^{2+} can be explained by an increase in the flexibility of the PEI polyamine in the 12.5:1 MTCS:CPTCS composites which may allow the acid strip solution greater access to the chelating sites in the polymer matrix.

Table 2.12. Data defining the metal sorptions for ligand modified SPCs prepared from CPTCS only silica gel and from MTCS : CPTCS (7.5:1) silica gel.

SPC	Metal Ion	pH	Metal ion adsorbed (mmol/g)		
			CPTCS Only	7.5:1 MTCS:CPTCS	% Difference
BP-2	Cu^{2+}	2.0	0.54	0.75	+ 25 %
BP-AP	Eu^{3+}	2.0	0.36	0.37	+ 3 %
CuWRAM	Cu^{2+}	3.0	0.47	0.61	+ 23 %
WP-4	Fe^{3+}	1.5	0.35	0.52	+ 33 %

As a result of the large improvement in sorption capacity for WP-2 when prepared with a large fraction of MTCS in the reagent silane layer, it was then useful to investigate possible improvements for PAA and other ligands. Thus BP-1 7.5:1 MTCS:CPTCS was

also modified with sodium chloroacetate (BP-2) as well as with phosphorous acid (BP-AP), picolyl chloride (CuWRAM) and 8-hydroxyquinoline (WP-4) according to previously reported experimental procedures.[96] Table 2.12 displays the resulting SPC material, the metal ion for which it was analyzed under batch conditions and the initial pH of the feed solution. The metal ion adsorbed per gram of SPC for the CPTCS only and the 7.5:1 MTCS:CPTCS products are provided. It is clear that, with the exception of BP-AP, substantial improvements in metal sorption result from the introduction of a large quantity of MTCS to the reagent silane mixture. Previous work has shown that the loading of phosphorous acid by way of the Mannich condensation reaction is greater than 100% of the total amines.[71] Increasing the fraction of MTCS, hence increasing N_f does not lead to an increase in ligand loading. Furthermore, the ratio of phosphorous ligand to metal ion is approximately 2 to 1 for large metal ions such as Eu^{3+}. As a result, a highly stable complex is formed between the two ligands and one metal ion. The stability of the complex formed with large trivalent metals is such that the metal can not be stripped from the BP-AP with conventional mineral acids. Increasing the conformational freedom of the polyamine layer should not impact the thermodynamic stability of metal ion coordination because any energy change associated with the conformational change must be small in comparison to the energy of complex formation. Improvements in the Cu^{2+} sorption batch capacity for BP-2, CuWRAM and for Fe^{3+} with WP-4 must are most likely a result of improvements in ligand loading as well improved conformational freedom for the polyamine.

2.5 Stability of SPCs modified with CPTCS and MTCS. It has been clearly demonstrated that the use of MTCS as a large fraction of the reagent silane mixture increases the surface silane coverage per gram of functionalized silica gel by approximately 1 mmole/g. The use of MTCS also facilitates an increase in the quantity of free amines depending on the polyamine. This allows an increase in the degree of functionalization with metal selective ligands and improvements in metal ion sorption mass transfer kinetics both on and off the functionalized SPCs. These conclusions have been clearly laid out in the preceding sections. Figure 2.1 illustrates the manner of silane addition to an amorphous silica surface. The surface silanol groups facilitate the functionalization of the silica gel surface through hydrogen bonding followed by the release of water. As a result, increased surface silane coverage should utilize more of the surface silanols, thus covering and protecting more of the surface. The dissolution of silica involves a chemical reaction or hydrolysis in an excess of water at neutral pH (Equation 2.17).[104]

$$SiO_2 + 2\ H_2O \rightleftharpoons Si(OH)_4 \rightleftharpoons Si(OH)_3O^- + H^+ \qquad (2.17)$$

The dissolution and deposition of silica at high pH involves hydrolysis reactions, which are promoted in more basic conditions.

$$(SiO_2)_x + 2\ OH^- \rightleftharpoons (SiO_2)_{x-1} + Si(OH)_3^{2-} + H_2O \qquad (2.18)$$

This is a result of the formation of silicate ion in addition to the monomer which is in equilibrium with the solid phase (Equation 2.18). The silicate ion is instantly converted to the monomer under acid conditions. Thus at low pH any silicate ions present immediately become part of the equilibrium in equation 2.17. However, above pH 10.7 the concentration of $Si(OH)_4$ is lowered by conversion to the readily soluble anion. As a

result of removing the product from the equilibrium the solid readily converts to the monomer and remains in solution.[104]

Therefore it is reasonable to argue that an increase in surface silane coverage will lead to an increase in the resulting materials chemical stability. In order to test this hypothesis, samples of CPTCS only functionalized INEOS silica gel and samples of MTCS and CPTCS functionalized INEOS silica gel were tested for silica leaching over time and over a range of initial solution pH. This data was contrasted with similar data obtained for raw silica gel. Table 2.13 identifies the Si concentration in 10 mL of H_2O at each pH listed after 48 hours of contact with 0.1 g of SPC material. There is an obvious increase in the amount of Si in solution with increasing pH, as to be expected for a silica gel which is subject to base hydrolysis. It should be noted that the operational range of SPCs is typically pH 0 to pH 10.[71]

Table 2.13. Data defining Si leaching as a function of pH for raw silica, CPTCS only silica gel, CPTCS:MPTCS silica gel, BP-1 CPTCS only and BP-1 7.5:1 MTCS:CPTCS..

pH	Raw silica Si (mg/L)	CPTCS only silica Si (mg/L)	CPTCS and MTCS silica Si (mg/L)	BP-1 Si (mg/L)	BP1 7.5:1 Si (mg/L)
-0.6	4.83	0.593	7.00	5.58	7.46
0	13.3	0.704	20.1	10.0	16.1
2	2.47	0.278	3.57	23.9	43.1
4	32.3	0.365	2.64	21.0	44.1
6	33.5	0.241	2.61	22.0	43.7
8	32.1	0.207	2.47	21.1	40.3
10	33.0	1.08	3.77	22.6	43.3
12	401	88.3	389	128	194
14	4330	3290	3360	2830	2900

In this range the amount of Si that has dissolved is less than 0.35% of the 0.1 g of raw silica gel used in the control experiment. Above pH 10 the quantity of raw silica gel dissolved quickly approaches significant levels. At pH 14 approximately 43% of the 0.1 g of raw silica gel has now dissolved. This pH trend is in agreement with the discussion of the dissolution of silica gel found above. The pH trend found for raw silica gel is repeated for silica gel modified with CPTCS only and for silica gel modified with CPTCS and MTCS. Both modified materials show decreased amounts of dissolved Si when compared with raw silica gel. This can be attributed to the protection of the silica surface by the silanized layer and the incorporation of a hydrophobic group onto the surface which may make the interaction between the solution and silica gel less favorable. Hydrophobic behavior is generally observed on surfaces with critical surface tensions of less than 35 dynes/cm. Surfaces modified with methyl silane groups have critical surface tensions of approximately 20 dynes – 23 dynes whilst surfaces modified with chloropropyl groups have critical surface tensions of approximately 40 dynes/cm. Significantly, the CPTCS only modified silica gel has less dissolved Si in general when compared to the MTCS and CPTCS modified silica gel in the range pH 2 to pH 10. It was assumed that a greater functionalization density would improve stability, but the data suggests that it is the larger CPTCS trifunctional silane that improves chemical stability. Therefore the hydrophobic nature of the surface must not be the overriding influence on Si leaching from the substrate. The critical surface tension is a measure of the wettability of the surface. However, in these experiments the materials have been fully submerged for 48 hours, hence allowing water adequate time to saturate the amorphous material. Degradation of the amorphous silica gel is a function of the steric barrier to the diffusion

of hydroxide ions through the hydrocarbyl layer to the silica surface. The carbon content of the CPTCS only modified surface equals 4.4 mmol/g. In contrast there are approximately 3 mmol/g of carbon on the surface of the 7.5:1 MTCS:CPTCS modified silica gel. CPTCS only modified SPC has approximately 1.2 mmoles of chlorine per gram of modified material, whereas CPTCS:MTCS modified silica gel contains only 0.3 mmoles of chlorine per gram. It therefore follows that it is the substantially larger molecular volume of the CPTCS only modified layer in comparison to the MTCS:CPTCS 7.5:1 modified silica gel that prevents degradation of the amorphous silica substrate.

Table 2.13 also shows the polyamine modified materials, BP-1, CPTCS only and BP-1, MTCS/CPTCS. After the covalent attachment of the polyamine it is clear that within the range of pH 2 to pH 10 there is an increase in dissolved Si when compared to the dissolved Si for the precursors. However, in the pH range greater than 10 the dissolved Si was found to be lower than that of the precursors. The attachment of the polyamine will undoubtedly increase the thickness of the surface layer thus hindering the interaction of surface and solvent. As shown above, basic conditions facilitate the degradation of silica gel, and at high pH there is sufficient hydroxide present to cause significant dissolution of silica. The polymer and silane layer act to sterically protect the substrate from dissolution. The high pH data reflects this trend. As the surface layer increases the amount of dissolved Si found in the supernatant decreases. In contrast, at lower pH the opposite trend was found. At a lower pH there is much less hydroxide ion present. Therefore, there must be a second factor that influences the dissolution of silica. The polyamine is an organic base. When contacted with a solution of pH less than the pKa of PAA (~10) the polymer amines will be at least partially. The ammonium ion will

then promote the dissolution of silica by the formation of the silicate salt. Thus, in the lower pH regime, the protection of the surface by the polyamine is counteracted by the formation of silicate salts with the protonated amines. This explains the increased Si in solution upon the attachment of the polymer.

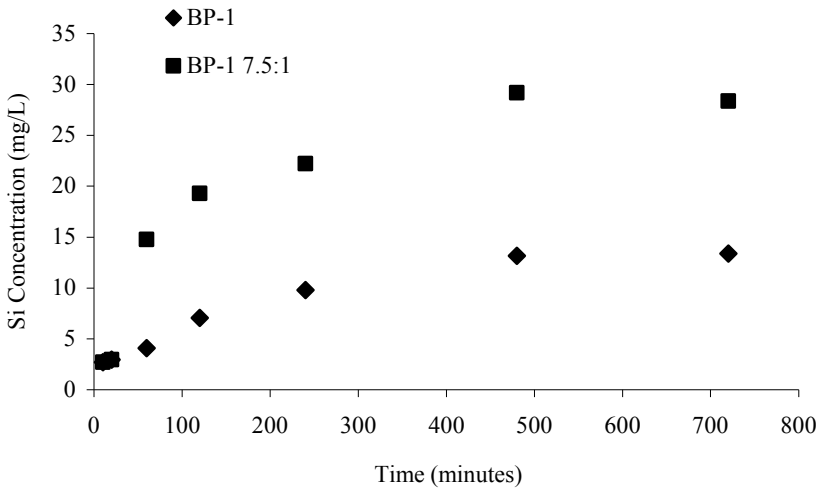

Figure 2.16. Si leaching (mg/L) as a function of time for two polyallylamine modified SPCs.

Figure 2.16 illustrates the kinetic profile for silica dissolution for BP-1 CPTCS only and BP-1 7.5:1 MTCS:CPTCS. It is clear in both cases that equilibrium is approached after approximately 500 minutes. It is also evident that the CPTCS only BP-1 allows a significantly smaller amount of dissolved Si when compared with the BP-1 prepared from the MTCS and CPTCS modified silica gel. This is a similar finding to the relative silica dissolution of the precursors. It has been clearly demonstrated in the preceding sections that the incorporation of MTCS into the preparation of SPCs yields increases in metal ion extraction capacity, improvements in both loading and stripping mass transfer kinetics and reduces the cost of the resulting material. These improvements are a result of a more flexible polyamine layer covalently attached to the surface at a

reduced number of sites per polymer chain. However, this increased flexibility also allows increased silica dissolution relative to the CPTCS only BP-1. Increased flexibility diminishes the polymers ability to act as a tightly bound layer protecting the amorphous silica from dissolution due to increased steric hindrance. The increased fraction of free amines with greater relative freedom may also promote the formation of silicate salts resulting in a more favorable interaction between the silica surface and the protonated polymer amines. Despite this, the amount of silica dissolved upon contact with solutions at a pH within the operational range of SPC materials is negligible. For BP-1 MTCS:CPTCS (7.5:1) at pH 4 the percent silica dissolved is approximately 0.43 % of the 0.1 g of material treated after 48 hours of constant exposure.

CHAPTER 3 – Acetate Modified SPCs

3.1 Introduction

The benefits of incorporating a large fraction of MTCS into the preparation of SPC materials have been clearly illustrated in Chapter 2.[86] Improvements in sorption capacity (mmol/g) and mass transfer kinetics have been verified for SPC materials modified with a selection of functional groups (Section 2.4) In addition, MTCS is a considerably cheaper reagent than CPTCS. As a result MTCS is now a key ingredient in the commercial production of SPC materials. However, there remain many metal ion combinations that cannot be tackled using the presently available assortment of SPCs. For example, in order to separate metal ions contained in complex solutions such as laterite (HPAL) high pressure acid leach solutions or (AMD) acid mine drainage solutions, SPC materials are required with a specific selectivity for nickel and cobalt.[44] In this chapter a series of novel tailored amino acid SPC materials have been synthesized and characterized. In particular, the variation in specific metal selectivity of amino acid SPC materials prepared using two different polyamines has been investigated. Differences in specific selectivity due to structural changes in the pendant ligand have also been examined. These materials may be useful for the selective removal of Ni^{2+} from other transition metals.

3.2 BP-2 and WP-2

3.2.1 Results. Modification of the polyallylamine SPC (BP-1) and polyethyleneimine SPC (WP-1) with sodium chloroacetate yields BP-2 and WP-2 respectively (Figure 2.12). BP-2 and WP-2 were prepared by the reaction of 7.5:1 BP-1 and 12.5:1 WP-1 with sodium chloroacetate under basic (NaOH) conditions. These specific MTCS:CPTCS ratios were determined, from the work presented in chapter 2, to be the optimal reagent silane ratios for each SPC material.

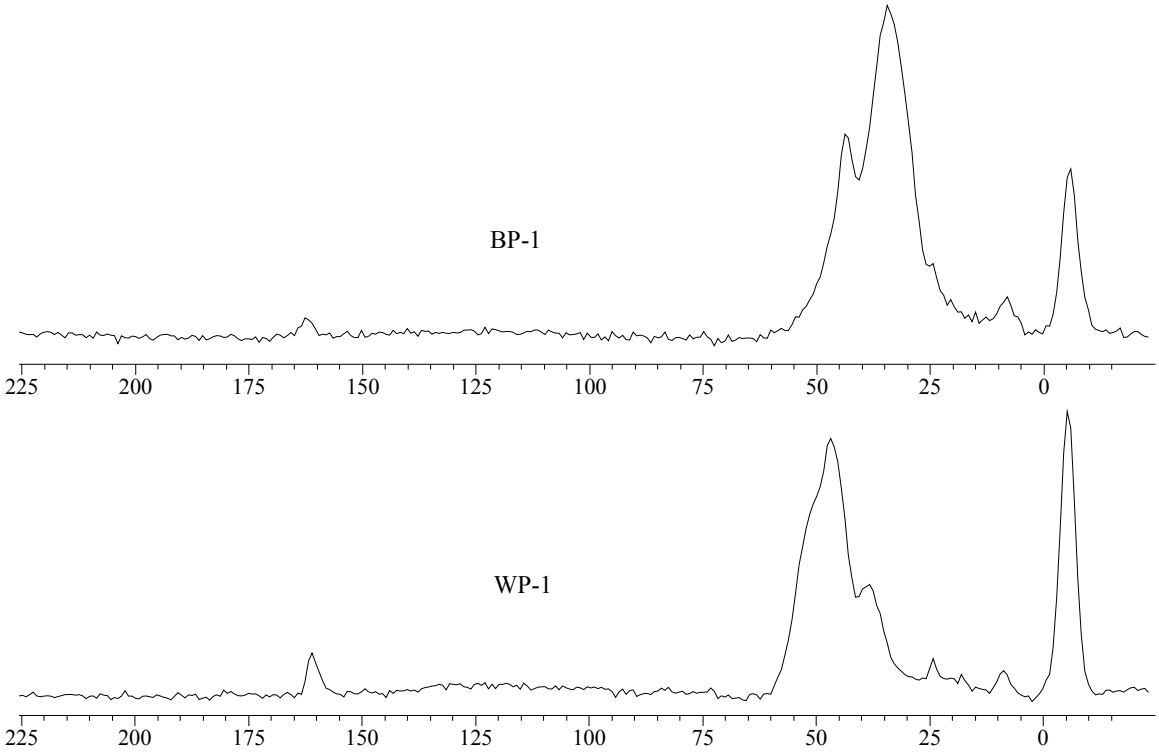

Figure 3.1. Both spectra in ppm. (Top) CP/MAS ^{13}C NMR at 126 MHz of BP-1 (7.5:1 MTCS:CPTCS). (Bottom) CP/MAS ^{13}C NMR at 126 MHz of WP-1 (12.5:1 MTCS:CPTCS).

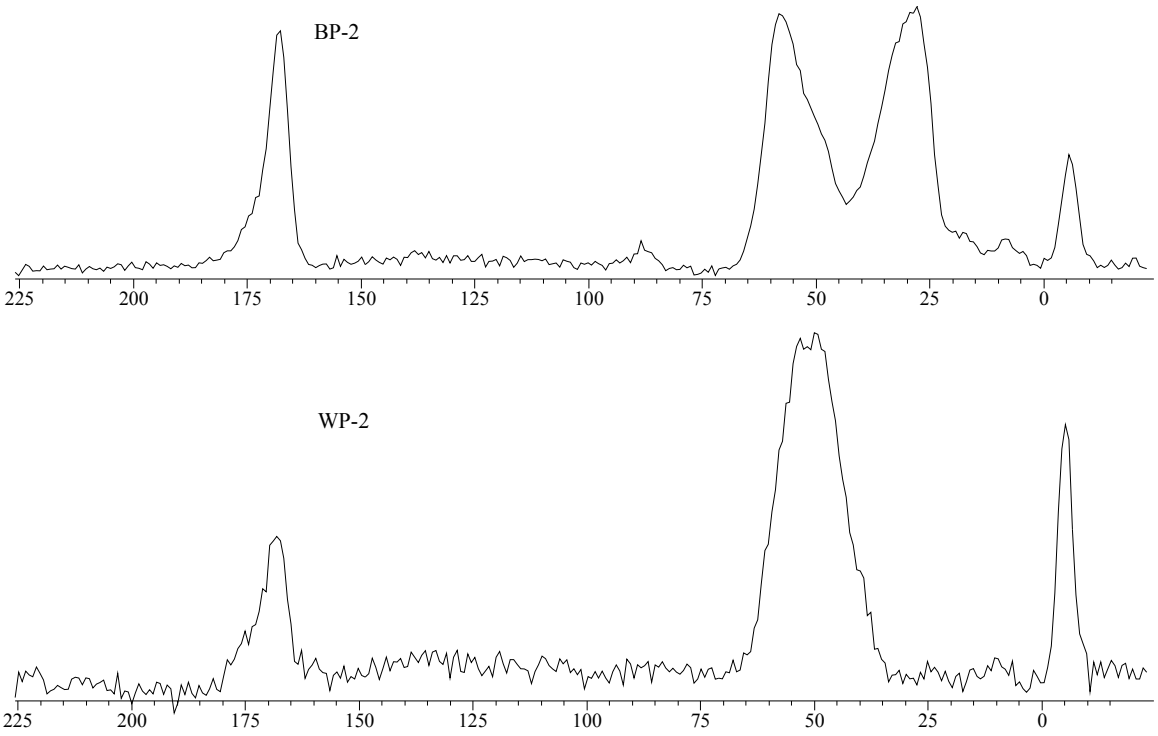

Figure 3.2. Both spectra in ppm. (Top) CP/MAS ^{13}C NMR at 126 MHz of BP-1 (7.5:1 MTCS:CPTCS) modified with sodium chloroacetate (BP-2). (Bottom) CP/MAS ^{13}C NMR at 126 MHz of WP-1 (12.5:1 MTCS:CPTCS) modified with sodium chloroacetate (WP-2).

The synthesis of WP-2 has been previously reported, however WP-2 has not been thoroughly characterized with regards to specific selectivity.[100] In general, little is known concerning BP-2. In addition, there has been no attempt to investigate the effect of the polyamine when two SPC materials prepared from different polymers are modified identically. Figure 3.1 illustrates the CP/MAS ^{13}C NMR for both BP-1 and WP-1. Figure 3.2 illustrates the CP/MAS ^{13}C NMR for both BP-2 and WP-2. Table 3.1 displays data derived from elemental analysis of BP-2 and WP-2. The acetate functional group is responsible for the broad peak at 170 ppm in both the BP-2 and WP-2 ^{13}C spectrum (-$\underline{C}O_2H$). Further evidence of the presence of pendant ligand is the broad peak due to the acetate methylene carbon at 58 ppm in the BP-2 spectrum (-NH$\underline{C}H_2CO_2H$).

Table 3.1. Data derived from elemental analysis for two acetate modified SPC materials. WP-2 is prepared from PEI. BP-2 is prepared from PAA.

SPC	Carbon (mmol/g)	Hydrogen (mmol/g)	Nitrogen (mmol/g)	C/N	Ligand Loading (mmol/g)	Ligand/Amine
WP-2	11.6	24.6	2.86	4.06	2.03	0.71
BP-2	13.4	27.7	1.92	6.98	2.75	1.43

The same peak is present for WP-2 however it overlaps with the broad PEI methylene signal (~51 ppm). The peaks most up-field (-5.6 ppm) are a result of the surface methyl groups (-Si-$\underline{C}H_3$). Table 3.1 presents elemental composition data derived from elemental analysis. Ligand loading and percent amine functionalized can be calculated using Equation 3.1.

$$\%\ \text{Amines Functionalized}\left(A_F\right) = \frac{\frac{C_2}{N_2} - \frac{C_1}{N_1}}{C_L} \times 100\% \qquad (3.1)$$

A_F is the percentage of amines that have been functionalized in the product. C_2 and N_2 represent the mmol/g carbon and nitrogen in the product respectively. C_1 and N_1 represent the mmol/g carbon and nitrogen in the precursor respectively. C_L represents the number of carbons in the appended ligand. It is evident that, although WP-2 contains substantially more polymer amine groups per gram, it is BP-2 that possesses the greater acetate loading per gram of SPC.

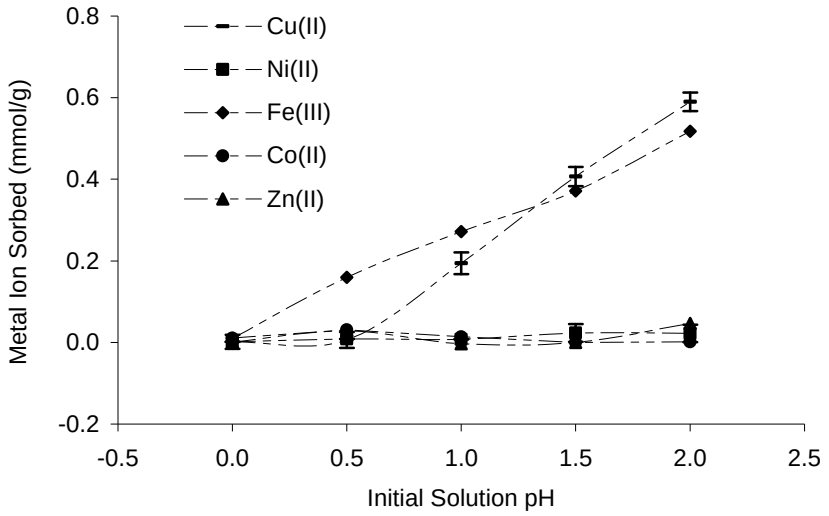

Figure 3.3. Batch pH profiles of divalent metal ions and the ferric ion for BP-2. Single metal ion solutions contained 1.5 g/L of each metal ion. 10 mL of solution was equilibrated with 0.10 g SPC for 24 hours.

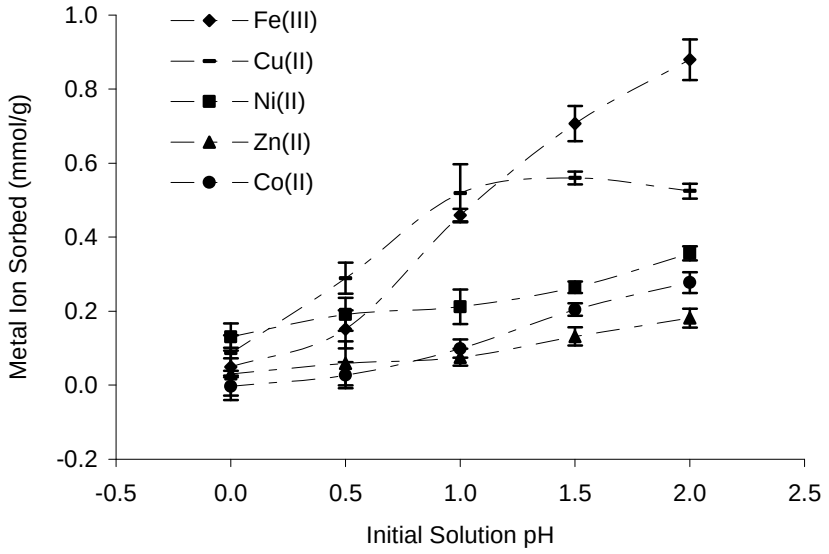

Figure 3.4. Batch pH profiles of divalent metal ions and the ferric ion for WP-2. Single metal ion solutions contained 1.5 g/L of each metal ion. 10 mL of solution was equilibrated with 0.10 g SPC for 24 hours.

WP-2 contains 25% less of the functional group relative to BP-2. The precursor WP-1 contains a large fraction of secondary and tertiary amines which may be hindered from functionalization by a complex steric environment and the more vigorous conditions

required for the alkylation of a tertiary amine. Single metal ion batch pH profiles were used as an initial characterization of the metal ion extraction properties of the SPC materials prepared. BP-2 and WP-2 batch pH profiles for several transition metals are presented in Figure 3.3 and Figure 3.4 respectively. Batch capacities are calculated using Equation 3.2. Q_{batch} represents the quantity of metal ion sorbed per gram of SPC. C_i is the initial concentration of metal ion (mmol/L), C_o is the concentration at equilibrium (mmol/L), m_{SPC} is the mass of SPC (g) and V is the volume of solution (L).

$$Q_{batch} = \frac{C_i - C_o}{m_{SPC}} \cdot V \tag{3.2}$$

For all metals, WP-2 removed greater quantities of metal ion per gram of SPC in the range pH 0 to pH 2 than did BP-2. It is clear that BP-2 extracts only Fe^{3+} and Cu^{2+} in the range pH 0 to pH 2. WP-2 also removes Fe^{3+} and Cu^{2+} in the same pH range however WP-2 extracts large amounts of Ni^{2+}, Co^{2+} and Zn^{2+} at low pH. Further, in the pH range pH 1 to pH 2 WP-2 shows a significant preference for Fe^{3+} over Cu^{2+} whereas BP-2 shows a similar affinity for both metal ions throughout. Table 3.2 provides the separation factors K_{Ni}^{Cu} for the batch sorption of Cu^{2+} and Ni^{2+} from a 10 mL solution that contains 1 g/L of both metal ions for 0.1 g all four SPCs considered. Separation factors were calculated using Equation 3.3.

$$K_{Ni}^{Cu} = \frac{\frac{Q_{Cu}}{C_{Cu}}}{\frac{Q_{Ni}}{C_{Ni}}} \tag{3.3}$$

Q_{Cu} is the concentration of Cu^{2+} loaded on the sorbent (mmol/g) and C_{Cu} is the concentration of Cu^{2+} remaining in solution (mmol/L). Q_{Ni} is the concentration of Ni^{2+} loaded on the sorbent (mmol/g) and C_{Ni} is the concentration of Ni^{2+} remaining in solution

(mmol/L). A greater selectivity factor indicates increased preference for Cu^{2+} over Ni^{2+}. Under these conditions copper is preferentially extracted throughout. At pH 1 the order of preference for copper over nickel is WP-2>BP-2. At pH 2 the order is BP-2>>WP-2 and at pH 3 BP-2>>WP-2.

Table 3.2. Data representing separation factors for two acetate modified SPC materials. WP-2 is prepared from PEI. BP-2 is prepared from PAA. Data was collected in the range of pH 1 to pH 3. Solutions contained 1 g/L of copper and 1 g/L nickel. 10 mL of solution was contacted with 0.10 g SPC for 24 hours. Experiment was replicated three times.

	Cu/Ni Separation Factor		
SPC	pH 1	pH 2	pH 3
BP-2	3.53	26.79	44.62
WP-2	6.21	9.38	10.54

Kinetic data is presented in Figure 3.4 for both BP-2 and WP-2. Figure 3.5 portrays the initial 200 minutes. Samples were taken at intervals from batch tests over a period of 24 hours. BP-2 and WP-2 both reach equilibrium between 200 and 400 minutes. There is no significant difference in mass transfer kinetics for the WP-2 when compared with the BP-2.

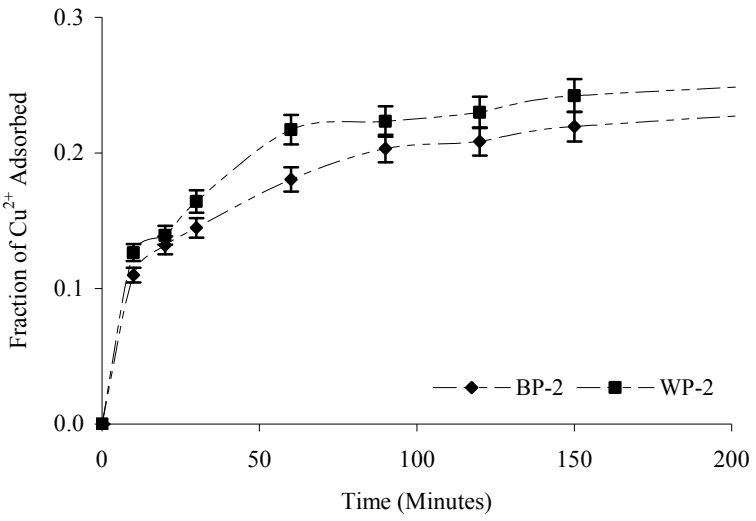

Figure 3.5. Initial 200 minutes of Cu^{2+} copper batch kinetic profiles for BP-2 and WP-2. Single metal Cu^{2+} solutions contained 1.5 g/L of copper ion. 10 mL of solution was equilibrated with 0.10 g of SPC and sampled at intervals over a 24 hour period.

Results of column breakthrough tests are located in Figure 3.6 to Figure 3.9 for BP-2 and WP-2 respectively. Slurry packed columns of BP-2 and WP-2 were supplied a solution containing both Cu^{2+} and Ni^{2+} at pH values of 1 and 3. The feed solution was fed from the top of the column and exited at the base of the column. The metal concentration for each metal ion was 1.5 g/L Cu^{2+} and 1.5 g/L Ni^{2+}. The breakthrough profiles for WP-2 across the pH range examined (pH 1 to pH 3) contrast with that of BP-2 over the same range. Cu^{2+} and Ni^{2+} can be entirely recovered from the column by a 2 mol/L sulfuric acid strip solution. In terms of Cu^{2+} purity in the recovered solution, WP-2 performed best at pH 1 at which point Cu^{2+} purity is 99%. At pH 2 the Cu^{2+} purity in the recovered solution is 87% and at pH 3 the Cu^{2+} purity in the recovered solution is 86%. The quantity of Ni^{2+} extracted increases from negligible at pH 1 to 4 mg/mL at pH 3. BP-2 does not remove significant amounts of Ni^{2+} in any of the experiments conducted.

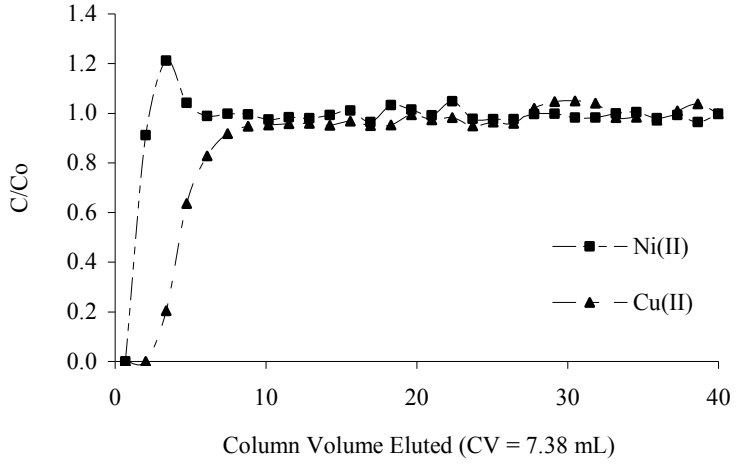

Figure 3.6. Dynamic separation of copper from nickel with BP-2 at pH 1. Column was packed with 7.4 mL of BP-2. Feed solution contained 1.5 g/L of both metal ions. Column experiments were run at a flow rate of 1 mL/min.

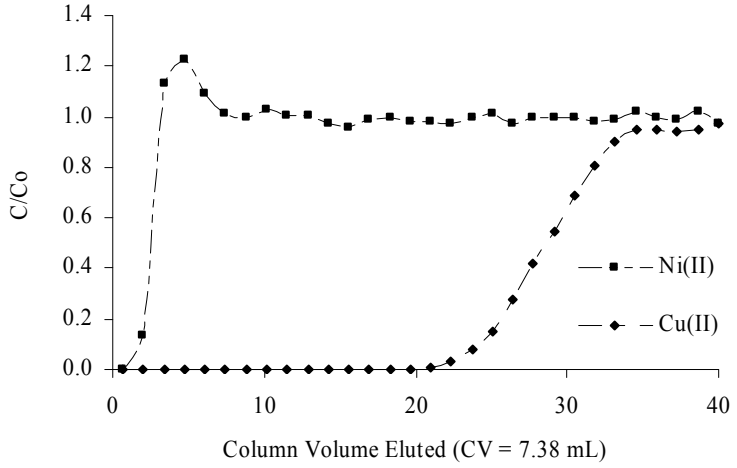

Figure 3.7. Dynamic separation of copper from nickel with BP-2 at pH 3. Column was packed with 7.4 mL of BP-2. Feed solution contained 1.5 g/L of both metal ions. Column experiments were run at a flow rate of 1 mL/min.

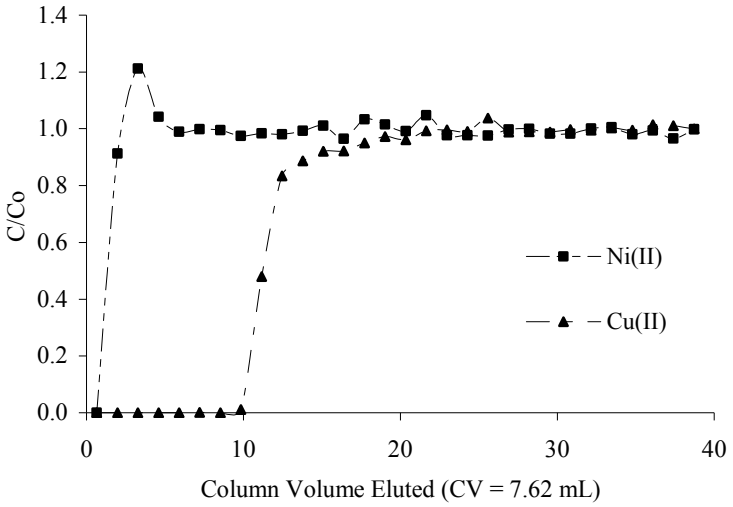

Figure 3.8. Dynamic separation of copper from nickel with WP-2 at pH 1. Column was packed with 7.6 mL of WP-2. Feed solution contained 1.5 g/L of both metal ions. Column experiments were run at a flow rate of 1 mL/min.

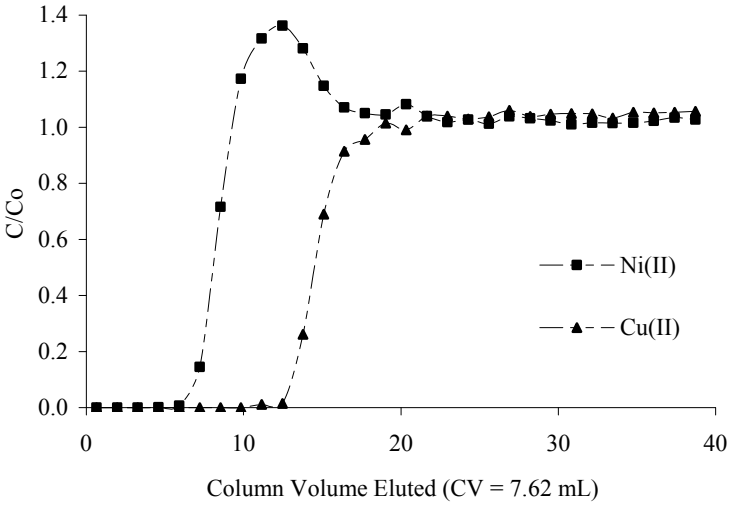

Figure 3.8. Dynamic separation of copper from nickel with WP-2 at pH 3. Column was packed with 7.6 mL of WP-2. Feed solution contained 1.5 g/L of both metal ions. Column experiments were run at a flow rate of 1 mL/min.

The Cu^{2+} purity in the recovered solution after application of the sulfuric acid strip was >99% for each pH studied. It is apparent that WP-2 performs best at pH 1. In

comparison, BP-2 performs best at pH 2 and pH 3. This is consistent with the pH profile and separation factor data. The degree of utilization for BP-2 for Cu^{2+} was 0.74 at pH 3. The degree of utilization for WP-2 for Cu^{2+} was 0.85 and 0.94 at pH 1 and pH 3 respectively. In order to probe the issue of polyamine structure, further concentration dependent iostherms were acquired for Cu^{2+} and Ni^{2+}. Equilibria are described by standard isotherm equations, such as those described by Freundlich, Langmuir, Brunauer Emmett and Teller and others. A preliminary study of curves and equations suggests that the Freundlich model and Langmuir model fit better the experimental data. These models have been used for IX materials previously.[105]

The Langmuir sorption model for the relationship between the concentration of metal ion adsorbed onto a material and the concentration of a metal ion remaining in solution at equilibrium assumes that sorption occurs as a monolayer on a homogenous surface without interactions between metal ions.[106] The Langmuir model provides an estimate of the theoretical quantity of surface sites available for sorption, Q_{max} (mmol/g), and the driving force for the sorption process (K_{ads}) for the coordination of a metal ion onto the chelating surface. The full derivation of the Langmuir equation can be found elsewhere.[106] The rearranged Langmuir equation as shown in Equation 3.4.

$$\frac{C_e}{Q_e} = \frac{C_e}{Q_{max}} + \frac{1}{Q_{max} K_{ads}} \tag{3.4}$$

C_e represents the concentration of metal ions in solution at equilibrium (mmol/L) and Q_e is the concentration of metal ions adsorbed onto the composite (mmol/g). Q_m can be calculated from the slope of the straight line for a plot of C_e/Q_e vs. C_e. The constant *b* can be derived from the y intercept of the same straight line ($1/K_{max}K_{ads}$). The Freundlich sorption model is an empirically derived model that describes the relationship between

concentration of metal ions in solution at equilibrium (C_e) and concentration of metal ions adsorbed onto the composite (Q_e) at low metal ion concentrations.[107] The equation is exponential in nature as shown in Equation 3.5.

$$Q_e = AC_e^{\frac{1}{n}} \tag{3.5}$$

The constant A is defined as the sorption coefficient representing the quantity of metal adsorbed ($mmol^{1-1/n}g^{-1}L^{1/n}$) at unit equilibrium concentration. The value 1/n (dimensionless) is a measure of the surface heterogeneity. Values of 1/n above one indicate cooperative sorption where as a value below one indicates normal Langmuir (monolayer and non-cooperative) sorption. A plot of log Q_e vs. log C_e allows the calculation of the parameters A and 1/n from the y intercept and slope of the linear regression, respectively.

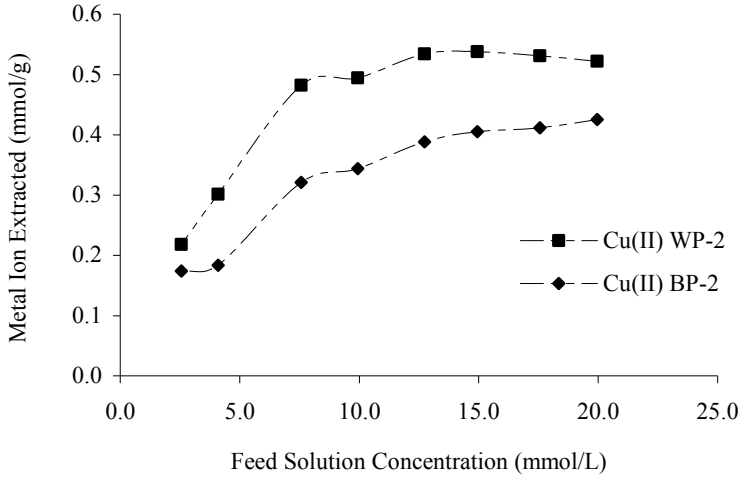

Figure 3.10. Concentration dependent sorption isotherms for Cu^{2+} onto BP-1 and WP-1 at pH 2. Equilibration time was 24 hours. 0.10 g of SPC was challenged with 10 mL of feed solution.

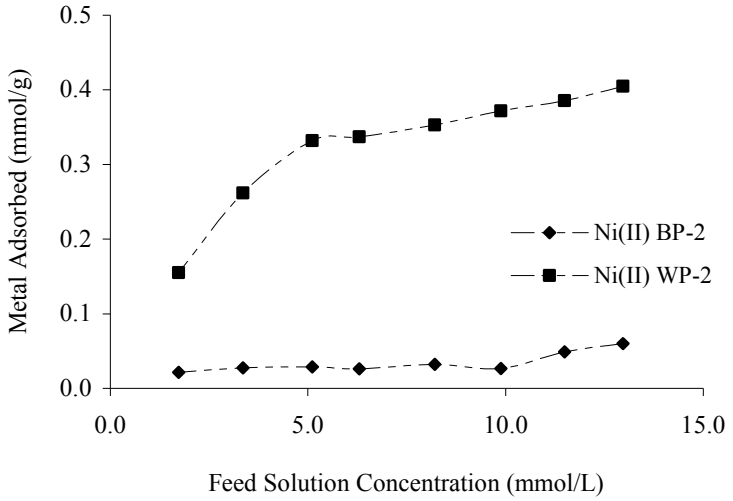

Figure 3.11. Concentration dependent sorption isotherms for Ni^{+2} onto BP-1 and WP-1 at pH 2. Equilibration time was 24 hours. 0.10 g of SPC was challenged with 10 mL of feed solution.

Figure 3.10 and Figure 3.11 illustrate concentration isotherms for BP-2 and WP-2 with Cu^{2+} and Ni^{2+}, respectively. It is immediately clear that for all concentrations WP-2 removes more Cu^{2+} than BP-2. Furthermore, it is apparent that BP-2 removes only negligible amounts of Ni^{2+} whereas WP-2 removes substantial amounts of Ni^{2+}.

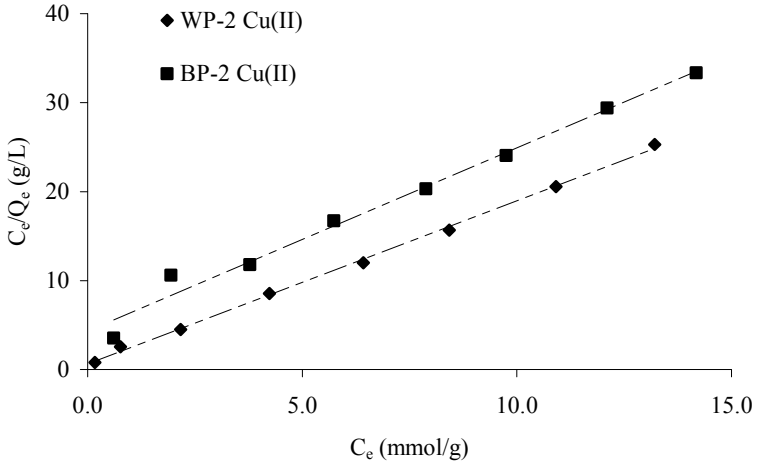

Figure 3.12. Langmuir plot for Cu^{2+} for BP-2 and WP-2

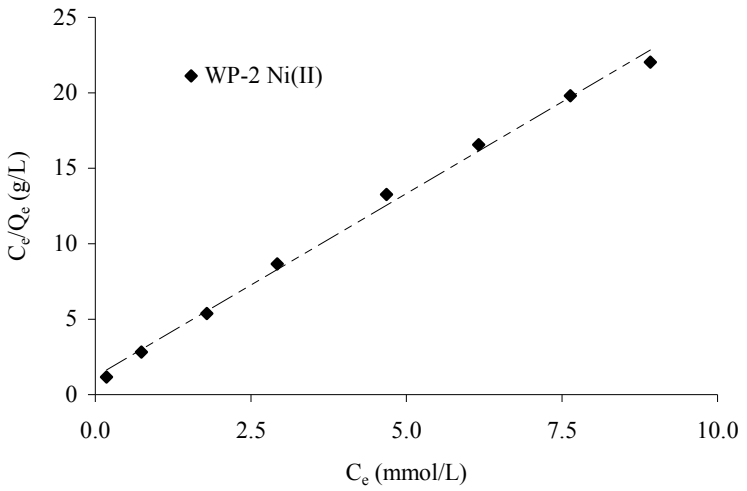

Figure 3.13. Langmuir plot for Ni^{2+} for WP-2. Langmuir model did not fit Ni^{2+} sorption.

Langmuir plots were constructed (Figure 3.12 and Figure 3.13) from the concentration isotherms by using Equation 3.3. Freundlich plots were also constructed (Figure 3.14 and 3.15) from the concentration isotherms using Equation 3.4. Table 3.3 lists the Langmuir and Freundlich parameters derived from these plots. This data was derived according to the descriptions provided above. The Langmuir and Freundlich models did not simulate the sorption of nickel by BP-2 very well. This is evident from analysis of the R^2 values for both models for the sorption of Ni^{2+} using BP-ED. In contrast the R^2 (Table 3.3) values arrived at for nickel sorption onto WP-2 indicate that both the Langmuir and Freundlich models are applicable to this process.

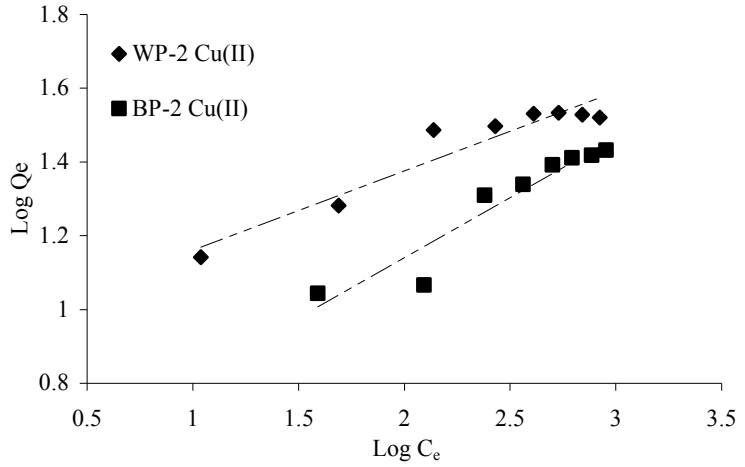

Figure 3.14. Freundlich plot for Cu^{2+} for BP-2 and WP-2

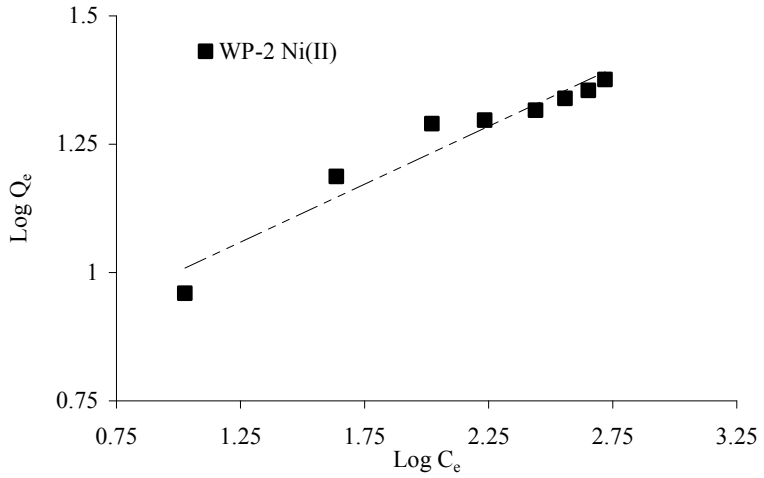

Figure 3.15. Freundlich plot for Ni^{2+} for WP-2

Also, both models are adequate for the sorption of copper onto both BP-2 and WP-2. It is notable that the R^2 values for the Langmuir model are significantly better than the empirical Freundlich model. A good correlation with the Langmuir model indicates monolayer and non-cooperative sorption. Moreover, the model provides information regarding the intensity of the sorption process (K_{ads}) as well as an approximation of the theoretical number of sorption sites on the surface (Q_m). Due to the poor correlation

between both sorption models and sorption of Ni^{2+} onto BP-2, parameters for this process could not be derived reliably. Q_m is greater for Cu^{2+} with both BP-2 and WP-2 than Ni^{2+} with WP-2. K_{ads} is significantly higher for WP-2 with Cu^{2+} and Ni^{2+}, thus indicating a sizably more intense adsorption process for WP-2. The Freundlich parameter 1/n is less than 1 in all cases, which again confirms non-cooperative sorption.

Table 3.3. Langmuir and Freundlich parameters for BP-2 and WP-2 as calculated from concentration isotherms. R2 values included for Ni^{2+} to demonstrate the poor fit of the models.

BP-2	LANGMUIR			FREUNDLICH		
Metal ion	Q_m (mmol/g)	K_{ads} (mmol/L)$^{-1}$	R^2	A (mmol$^{1-1/n}$g^{-1}L$^{1/n}$)	1/n	R^2
Cu^{2+}	0.48	0.48	0.99	3.08	0.33	0.91
Ni^{2+}	-	-	0.48	-	-	0.55
WP-2						
Metal ion	Q_m (mmol/g)	K_{ads} (mmol/L)$^{-1}$	R^2	A (mmol$^{1-1/n}$g^{-1}L$^{1/n}$)	1/n	R^2
Cu^{2+}	0.54	2.92	0.99	8.81	0.22	0.91
Ni^{2+}	0.41	2.03	0.99	5.99	0.23	0.93

3.2.2 Discussion. The functionalization with acetate groups of BP-1 and WP-1 to yield BP-2 and WP-2 respectively has been confirmed by solid state ^{13}C NMR. Selectivity is a function of structural factors that favor certain coordination geometries. It is also a function of the denticity of the coordination sites and the hard/soft nature of the donor atoms present. Elemental analysis (Table 2.4) indicates that the PEI SPC (WP-1) contains a greater quantity of amine groups per gram (3.9 mmol/g) than the PAA SPC (BP-1) (2.8 mmol/g). However, elemental analysis (Table 3.1) of BP-2 and WP-2 indicate that the quantity of acetate functionality per polymer amine groups is 1.45 for BP-2 and 0.71 for WP-2.

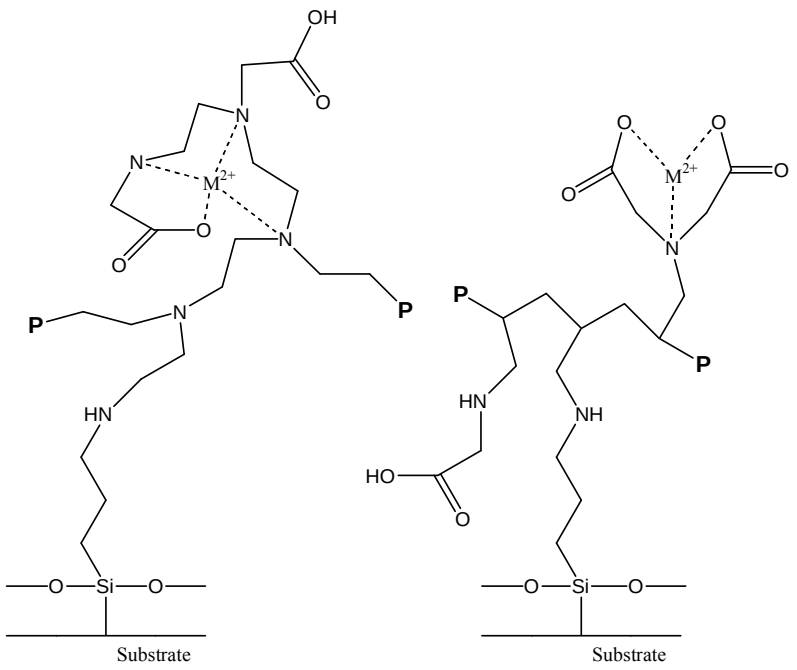

Figure 3.16. The approximate structure of WP-2 (left) and BP-2 (right) based on elemental analysis as well as the results of metal ion sorption characterization. P represents the polymer backbone. M^{2+} represents a sequestered divalent metal ion.

Twice functionalized amine groups must be present to a minimum of 45% of all amines for BP-2. Therefore BP-2 must contain a large fraction of IDA (iminodiacetic acid) functional groups thus generating an SPC similar to the polymeric resin IRC-748 which contains solely IDA groups. [44;45;81] The PEI polymer of WP-2 contains primary, secondary and tertiary amines in the ratio 35:35:30. The acetate loading per polymer amine of WP-2 is approximately half that of BP-2. Thus, functionalization of secondary and tertiary amines must be sterically hindered and also require more vigorous conditions for alkylation. Hence, it can be concluded that a greater fraction of mono amino-acetate groups and a smaller fraction of IDA functional groups is present in WP-2. The amino-acetate functional groups of WP-2 are separated by only two carbons. Therefore, relative

to BP-2 the WP-2 amino-acetate groups are proximal to amino-acetate groups of adjacent branches in the entangled PEI polymer. We therefore hypothesize that the structures illustrated in Figure 3.16 are representative of both BP-2 and WP-2.

The close proximity of functional groups and higher density of possible donor atoms will most likely allow cooperative coordination by more than one amino acetate group and perhaps other un-functionalized amines also. Thus coordination sites within WP-2 are of a higher denticity (more available donor atoms) relative to BP-2. In contrast, the BP-2 SPC is constructed from a linear polyamine (PAA) containing a large fraction of (IDA) iminodiacetic acid groups separated by five carbon atoms. Cooperation between atoms within a single IDA ligand ($-NH(CH_2OOH)_2$) facilitates metal ion coordination for BP-2. The maximum denticity of the IDA ligand is 3. The higher denticity of the WP-2 sorption sites must invoke a greater formation constant especially for those ions that prefer to form higher coordinate complexes such as Fe^{3+} and Ni^{2+} (typically octahedral). The lower denticity of the BP-2 coordination sites favors metal ions that prefer low coordination complexes such as Cu^{2+} (typically square planar). This explains the increased affinity for $Fe^{3+}$and Ni^{2+} for WP-2 and the preference for Cu^{2+} of BP-2. The parameters derived from the Langmuir and Freundlich models also indicate a significantly stronger sorption process for WP-2 relative to BP-2. A larger equilibrium constant indicates a more stable complex. A more stable complex results from the formation of a chelate of larger denticity, as described for WP-2. This is the well known chelate effect. Also a more stable complex can also result when a smaller conformational change (less reorganization) is required for complex formation. Thus WP-2 must be relatively tailored for the sorption of Ni^{2+} on the bases of the number of coordinating

ligands and the inherent conformation of the PEI ligand system. These factors contribute to a more positive entropy change for complex formation.

The ruthenium complex $Ru(CO)_3(TFA)_3^-K^+$ was used to further investigate the differences between BP-2 and WP-2. This complex has been shown to be highly reactive. A systematic substitution of the ligands with phosphines has already been accomplished. When a methanol solution of $Ru(CO)_3(TFA)_3^-K^+$ is contacted with 0.1 g of SPC the ligands are displaced by the electron donating groups of the SPC. In the case of WP-1 and BP-1 the amine functional groups can displace the triflouroacetic acid (TFA) or carbonyl groups of the ruthenium complex. The TFA groups are the more labile groups, thus it would be expected that the TFA groups would be first to be displaced by the polymer amines. As a result of the complexity of the immobilized polymer layer it is reasonable to expect that several distinct surface bound complexes will result. It is also possible that different isomers of a particular complex will dominate. The resulting Ru-SPC complex will display a unique carbonyl pattern in the ^{13}C solid state NMR spectrum (Figure 3.17). This pattern is dependent on the quantity and types of ligand displaced from the original complex. The pattern provides information with regards to coordination environment for each material assessed. Figure 3.16 displays the CPMAS ^{13}C solid state NMR for the ruthenium complex, and also for WP-1, WP-2, BP-1 and BP-2 loaded with the complex. The sharp peak located at approximately 170 ppm in the Ru complex spectrum is assigned to the TFA ligands. The peaks in the range 180 ppm to 215 ppm are assigned to the carbonyl ligands. The peaks in this range are attributed to isomers that posess non-equivalent carbonyls. From the carbonyl peaks in the region 190 ppm to 210

ppm, it is clear, in the case of BP-1 and WP-1, that the ruthenium complex has been loaded.

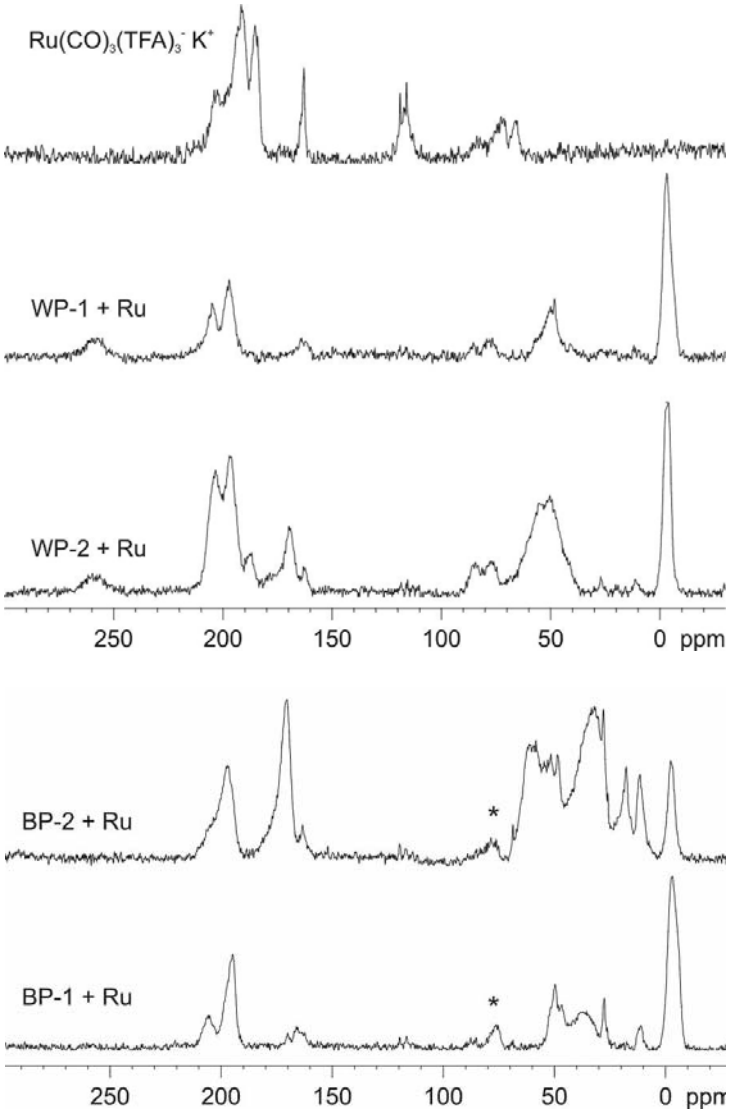

Figure 3.17. (Top) Solid state ^{13}C NMR of $Ru(CO)_3(TFA)_3^-K^+$ complex and of WP-1 and WP-2 loaded with Ru complex. (Bottom) Solid state ^{13}C NMR of BP-1 and BP-2 loaded with a Ru complex.

It is also noteworthy that in the case of the loaded BP-1 and WP-1 the peak attributed to the TFA groups has diminished which indicates the displacement of TFA groups by the amine groups of BP-1 and WP-1. BP-1 and WP-1 both show two carbonyl

peaks due to the formation of isomers of the Ru complex on the SPC. BP-2 and WP-2 both show a diminished TFA peak next to a peak at 170 ppm which is due to the acetate functional group of both SPCs. Again there is a carbonyl pattern that is dependent on the formation of isomers on the surface of BP-2 and WP-2. With regards to the effect of the polyamine it is worth noting the peak at approximately 260 ppm present in the spectra for both WP-1 and WP-2 loaded with the ruthenium complex. These peaks are not present for both BP-1 and BP-2. A peak in this region can generally be attributed to bridging carbonyl groups. This infers that the surface structure of the polyamine in WP-1 and WP-2 permits the coordination of two ruthenium atoms in close enough proximity to allow for the formation of one or more bridging carbonyls.[108] This bridging carbonyl peak is not found in the ^{13}C NMR spectrum for either BP-1 or BP-2 suggesting that the coordination sites are far enough apart to prevent the formation of bridging carbonyl complexes on the surface. The formation of bridging carbonyl ruthenium complexes ties in well with the arguments set forth previously regarding the nature of coordination in WP-2 in comparison to BP-2.

3.3 EDTA modified SPCs

Ethylenediamine tetraacetic (EDTA) acid is a well known chelator.[109] This amino acid is widely used to sequester both trivalent and divalent metal ions. EDTA bonds to metal ions through two tertiary amine groups as well as via four carboxylate groups (Figure 3.18). EDTA is insoluble in acidic medium. EDTA can be used for the purpose of solid phase ion exchange by reacting immobilized amine groups with EDTA dianhydride.

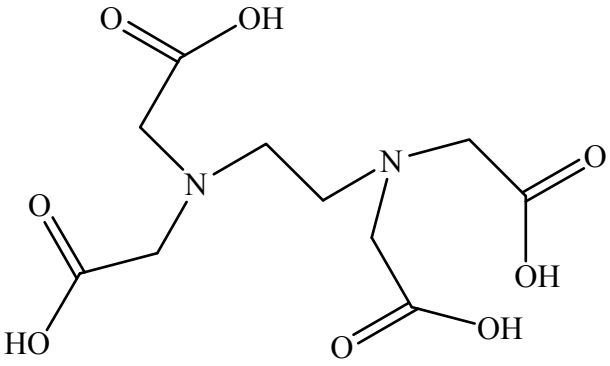

Figure 3.18. Ethylenediamine tetraacetic acid (EDTA)

Materials modified with EDTA dianhydride have shown promise for the selective separation and recovery of divalent transition metals such as Ni^{2+} from Co^{2+}, Zn^{2+} and Mn^{2+}. Such separations are based on the differences in the formation constants for metal ions with EDTA as shown in Table 3.4. If the immobilized EDTA derivative maintains a specific selectivity profile similar to free EDTA the resulting materials may be useful for certain metal ion separations. For instance this Table indicates that EDTA will selectively extract Fe^{3+} in preference to Fe^{2+}.

Table 3.4. Binding constants (K_{MY}) of the divalent metals and ferric iron with EDTA at neutral pH.

Metal Ion	K_{MY}
Fe^{3+}	1.3×10^{25}
Cu^{2+}	6.3×10^{18}
Ni^{2+}	4.2×10^{18}
Zn^{2+}	3.2×10^{16}
Co^{2+}	2.0×10^{16}
Fe^{2+}	2.1×10^{14}

The natural polysaccharide chitosan has been successfully modified with EDTA anhydride.[110] At pH 2, Cu^{2+} sorption capacities per gram of the resulting material were reported to be approximately 2 mmol/g. However, to the best of our knowledge dynamic testing was carried out at reported flow rates no faster than 7.7 cm^3 hr^{-1} using columns requiring a large quantity of glass beads. Non-immobilized polyallylamine (PAA) has previously been modified with EDTA dianhydride also, although metal selectivity in this form was reported to be poor.[111] EDTA dianhydride has also been reacted with functionalized silica gel through the use of aminopropyl silane.[112] For this work this material will be termed Silica-ED. Silica-ED displayed only modest ligand loading per gram sorbent (~0.3mmol/g), hence only modest metal ion sorption capacities (~22.3 mg/g Cu^{2+} and ~6.3 mg/g Ni^{2+} at pH 1).[112] Further, although it is well known that the chelating ability of non-immobilized EDTA is improved at higher pH, metal ion capacities for Silica-ED decrease as the challenge solution pH increases.[112] The surface charge of silica gel becomes increasingly negative as pH increases, thus the electrostatic attraction between acetate groups of the immobilized ligand and surface hydroxyl groups becomes greater in magnitude. This micro-environmental effect suppresses the ability of the acetate ligands to complex metal ions as pH increases. SPCs make use of a polyamine layer, which may shield a pendant ligand from the charged surface allowing increased

capacities at increased pH. Also, immobilized polyamines contain a large quantity of amine sites per gram of composite (2 ~ 4 mmol/g) which may promote increased ligand loading and therefore increased metal ion sorption capacity. Thus BP-1 and WP-1 (prepared from CPTCS only silica gel) were modified with EDTA dianhydride by way of an acid catalyzed aminolysis as shown in Figure 3.19. A third material was also prepared from BP-ED 7.5:1 MTCS:CPTCS for comparison. EDTA dianhydride is commercially available. However, it can be prepared in high yield from the condensation of EDTA in pyridine and acetic anhydride.[113] The resulting materials are termed BP-ED and WP-ED, respectively.

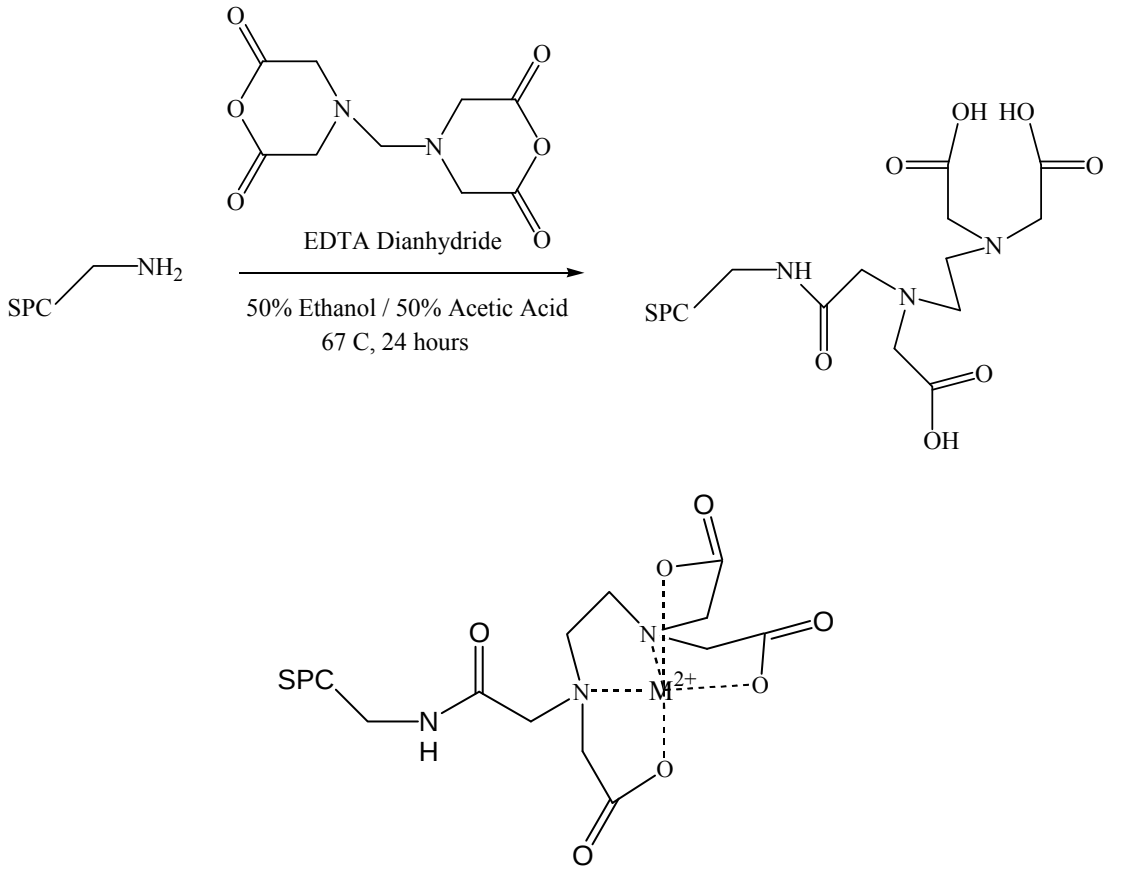

Figure 3.19. (Top) Synthetic pathway to BP-ED and WP-ED. (Bottom) The resulting ligand is an immobilized ethylenediamine triacetic acetamide chelating functional group shown while chelating a divalent metal ion (M^2+).

Table 3.5. Data derived from elemental analysis for two amido-aminoacetate modified SPC materials. WP-ED is prepared from WP-1 (PEI). BP-ED is prepared from BP-1 (PAA).

SPC	C (mmol/g)	H (mmol/g)	N (mmol/g)	C/N	Ligand loaded (mmol/g)
BP-1	11.25	29.6	2.75	3.93	-
BP-ED	16.49	32.70	3.73	4.29	0.68
WP-1	10.75	26.7	3.11	3.46	-
WP-ED	14.55	29.4	3.66	3.98	0.62

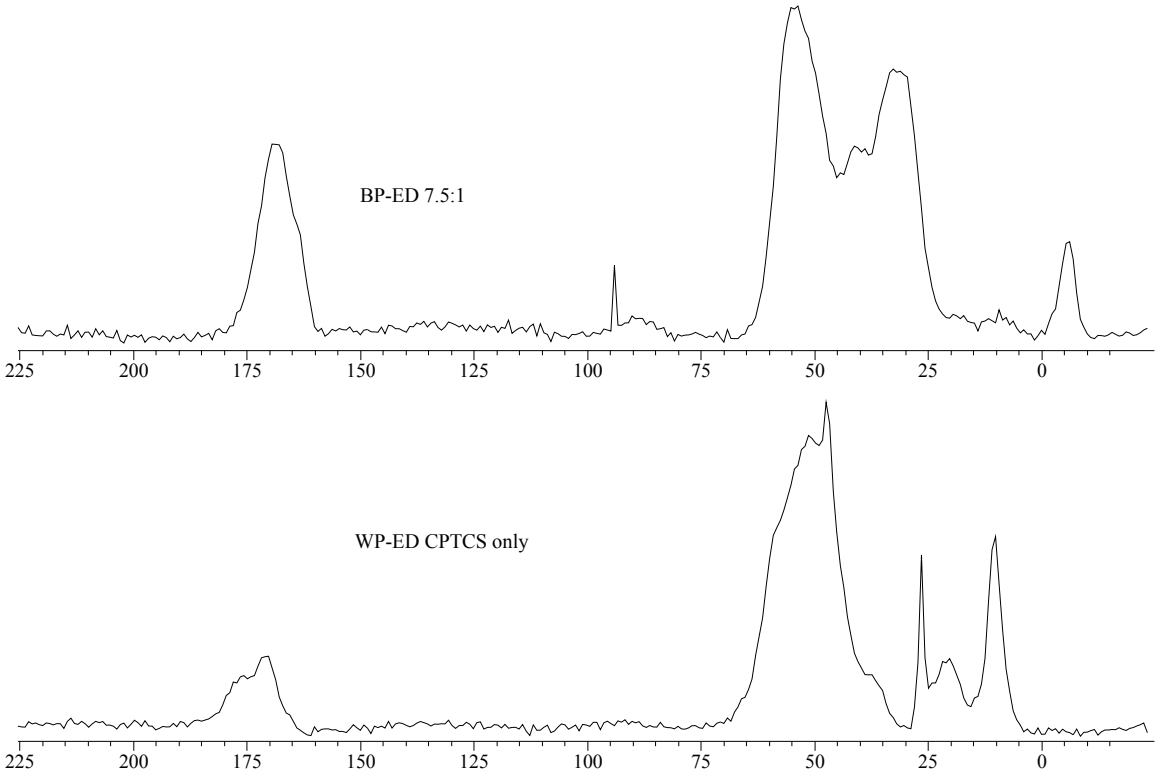

Figure 3.20. (Top) CP/MAS ^{13}C NMR at 126 MHz of BP-ED (7.5:1 MTCS:CPTCS). (Bottom) CP/MAS ^{13}C NMR at 126 MHz of WBP-ED (CPTCS only).

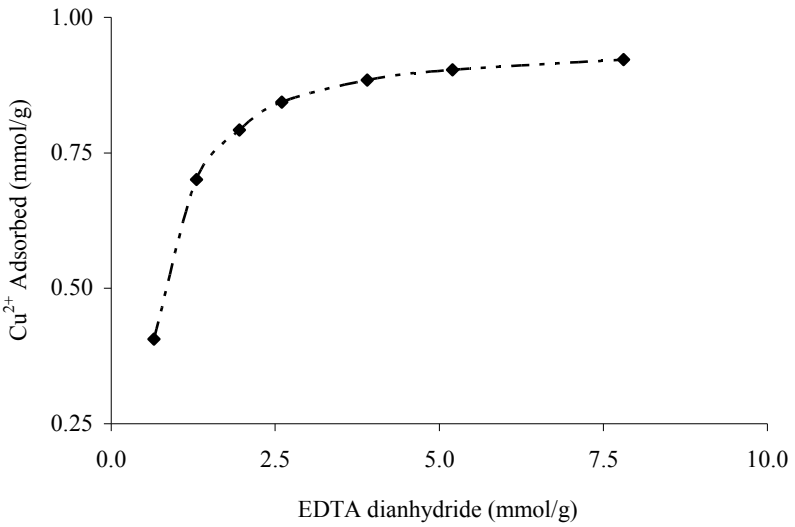

Figure 3.21. Reagent optimization. Cu^{2+} sorption capacity as a function of the mmol of EDTA dianhydride used per gram of BP-1 (7.5:1 MTCS:CPTCS) in the synthesis of BP-ED (7.5:1 MTCS:CPTCS).

Figure 3.20 presents the solid state CP/MAS ^{13}C NMR spectrim for BP-ED (7.5:1 CPTCS:MTCS) and WP-ED (CPTCS only). The broad envelope at approximately 170 ppm located in both spectra is due to the carboxylic acid groups (-$\underline{C}O_2H$). The carboxylic peak in the BP-ED spectra is more intense that the equivalent peak in the WP-ED spectra. This points to greater ligand loading. It is likely that a peak representing the amide functional group (-N$\underline{C}OCH_2$-) is also located in this envelope. The broad peak at ~53 ppm in both spectra are due to the acetate methylene carbon atoms (-$\underline{C}H_2COOH$). Figure 3.21 represents the optimization of BP-ED 7.5:1 MTCS:CPTCS synthesis. Initially, increasing the quantity of EDTA dianhydride per gram of 7.5:1 BP-1 has a dramatic effect on the resulting materials ability to extract Cu^{2+}. Eventually a period of diminishing returns is reached. In this regime a large increase in mmol/g EDTA dianhydride results in modest gains in sorption capacity. A reasonable compromise

between the quantity of EDTA dianhydride and adsorption capacity is 3 mmol EDTA dianhydride per gram of 7.5:1 BP-1.

Elemental analysis indicates a loading of 0.68 mmol/g of EDTA dianhydride for CPTCS only BP-ED and 0.62 mmol/g EDTA dianhydride for CPTCS only WP-ED. This was calculated using Equation 3.6.

$$\%\ \text{Amines Functionalized}\left(A_F\right) = \frac{\frac{C_2}{N_2} - \frac{C_1}{N_1}}{C_L - \left(N_L \times \frac{C_1}{N_1}\right)} \times 100\% \tag{3.6}$$

A_F is the percentage of amines that have been functionalized in the product. C_2 and N_2 represent the mmol/g carbon and nitrogen in the product respectively. C_1 and N_1 represent the mmol/g carbon and nitrogen in the precursor respectively. C_L and N_L represent the number of carbon and nitrogen in each individual ligand appended. This represents the functionalization of 28% of all CPTCS only BP-ED PAA amines for and 16% of all CPTCS only WP-ED PEI amines. The modest functionalization is most likely a result of large ligand size.

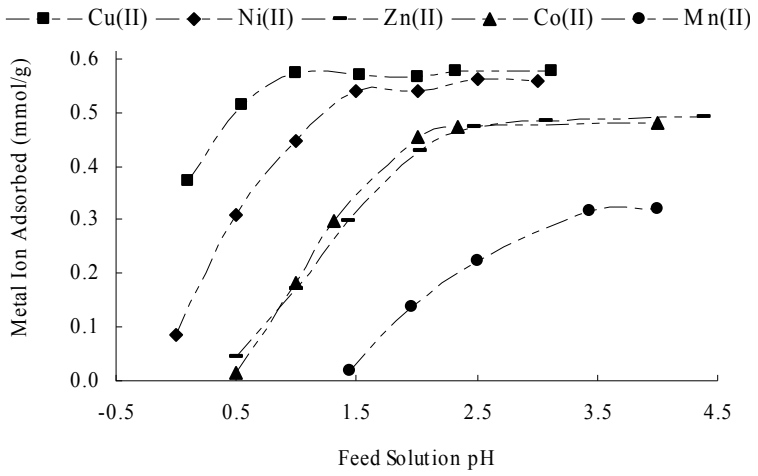

Figure 3.22. Batch pH profiles of divalent metal ions for BP-ED. Single metal ion solutions contained 1.5 g/L of each metal ion. 10 mL of solution was equilibrated with 0.10 g SPC for 24 hours.

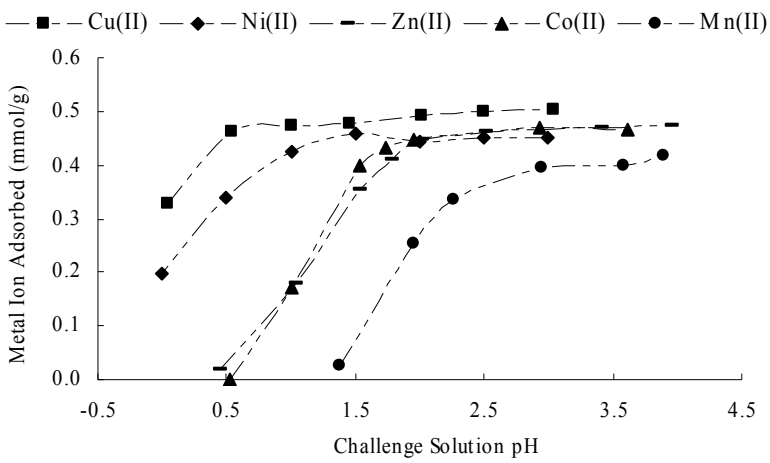

Figure 3.23. Batch pH profiles of divalent metal ions for WP-ED. Single metal ion solutions contained 1.5 g/L of each metal ion. 10 mL of solution was equilibrated with 0.10 g SPC for 24 hours.

The pH profiles for BP-ED and WP-ED for both divalent and trivalent metals are displayed Figure 3.22 and Figure 3.23 respectively. The dependence of metal ion sorption on pH is clearly illustrated. It is evident that BP-ED and WP-ED behave similarly with regard to pH. However, in most cases BP-ED has higher sorption capacities. This is in agreement with the elemental analysis data. Over the pH range studied (pH 0.0 to pH 4.0) the divalent metal ion sorption capacity (mmol/g) of BP-ED and WP-ED increases with increasing pH until a point is reached after which sorption capacity is constant. This is a trend in sorption capacity that is in agreement with chitosan modified with EDTA anhydride but not with that found for Silica-ED.[110-112] The profiles for Silica-ED decline with increased pH in the range investigated.[112] This leads to the conclusion that the polyamine matrix must create a great enough distance between immobilized ligands and surface silanols so that there is no suppression of metal ion capacity by surface-ligand interactions for either BP-ED or WP-ED. Further, this demonstrates an advantage of silica polyamine composites over chelating materials prepared with functionalized silica

gel but without the use of a polyamine (e.g. Silica-ED). Also, metal ion sorption capacities per gram of chelating material are substantially higher for BP-ED than for Silica-ED. The Cu^{2+} capacity at pH 1 is 36.5 mg/g for BP-ED compared with ~22.3 mg/g for Silica-ED. The Ni^{2+} capacity at pH 1 is 26.8 mg/g compared with 6.3 mg/g for Silica-ED. Based on the batch pH profile data the order of selectivity for both BP-ED and WP-ED for divalent metal ions is: $Cu^{2+}>Ni^{2+}>>Zn^{2+},Co^{2+}>>Mn^{2+}$, which is in agreement with that reported for both Silica-ED and chitosan EDTA chelating materials. This trend is also in good agreement with the formation constants (K_{MY}) for EDTA-metal ion complexes, indicating that the pendant ligand closely models EDTA behavior in solution. It is apparent from Figure 3.22 and Figure 3.23 that each divalent metal pH profile has two distinct regions:

1. A lower pH range in which solution acidity is great enough for protons to compete with metal ions for sorption sites thus preventing maximum metal uptake capacities.

2. A higher pH range in which metal uptake is limited by the extent of ligand loading per gram and the stability of the resulting EDTA metal complex.

For both BP-ED and WP-ED the highest metal ion sorption capacity for Zn^{2+}, Co^{2+} and Mn^{2+} over the pH range studied are not as large as the capacity for either Cu^{2+} or Ni^{2+}. This is due to lower formation constants of the complexes formed between these metal ions and the pendant ligands (Table 3.5). Calculations based upon elemental analysis yield a ligand loading of ~0.68 mmol/g for BP-ED and ~0.62 mmol/g for WP-ED (Table 3.3). The highest metal ion capacities for Cu^{2+} for BP-ED and WP-ED are 0.58 and 0.56 mmol/g respectively indicating that a small fraction of the

ethylenediaminetriacetic acid acetamide ligands are unavailable for coordination. It is possible that some ligands have attached to two polymer amine sites through two acetamide linkers leaving only two acetate groups available for coordination per ligand. Interestingly, elemental analysis of the precursors BP-1 and WP-1 indicates a larger quantity of polymer amines per gram for WP-1 than for BP-1. However BP-1 has a greater ligand loading, thus the PAA polymer must have more accessible amines. 30% of all PEI amines are tertiary and cannot be modified with EDTA. Also 35% of PEI amines are secondary and the steric bulk of two alkyl groups may hinder modification by the large EDTA ligand. PAA contains all primary amines that are not obstructed during subsequent functionalization hence higher ligand loading. Most importantly, the differences in the sorption of Ni^{2+} and Co^{2+}, Zn^{2+} at approximately pH 1, support the possibility of a column chromatography style separation of Ni^{2+} from Co^{2+} and/or Zn^{2+} with either BP-ED or WP-ED. Further, since Ni^{2+} is not appreciably chelated at very low pH (pH<0.5) the recovery of sequestered Ni^{2+} from BP-ED/WP-ED may be possible using an acidic strip solution.

Chapter 2 illustrates the benefits resulting from the use of MTCS. As such BP-ED was also prepared from 7.5:1 MTCS:CTPCS BP-1. Figure 3.20 (Top) illustrates the solid state ^{13}C NMR spectrum for the product. The lone peak at -5.6 ppm demonstrates the presence of the methyl silane ($-Si(O_2)-\underline{C}H_3$). pH profiles were determined for three divalent metal ions as well as for ferric ion for comparison with similar data for BP-ED prepared from CPTCS only BP-1. pH profiles for 7.5:1 BP-ED are located in Figure 3.24. The relative affinity for each metal is similar in both cases however the metal ion sorption capacity for each metal has increased dramatically in the case of BP-ED 7.5:1.

For example copper sorption has increased from less than 0.6 mmol/g to less than 1.0 mmol/g. Elemental analysis indicates that the ligand loading has increased to a value of 1.03 mmol/g (Equation 3.6). This corresponds to the functionalization of 57% (up from 28% for CPTCs only BP-ED) of all BP-ED PAA amines. Thus BP-ED also responds favorably when MTCS is used for the preparation of the BP-1 precursor.

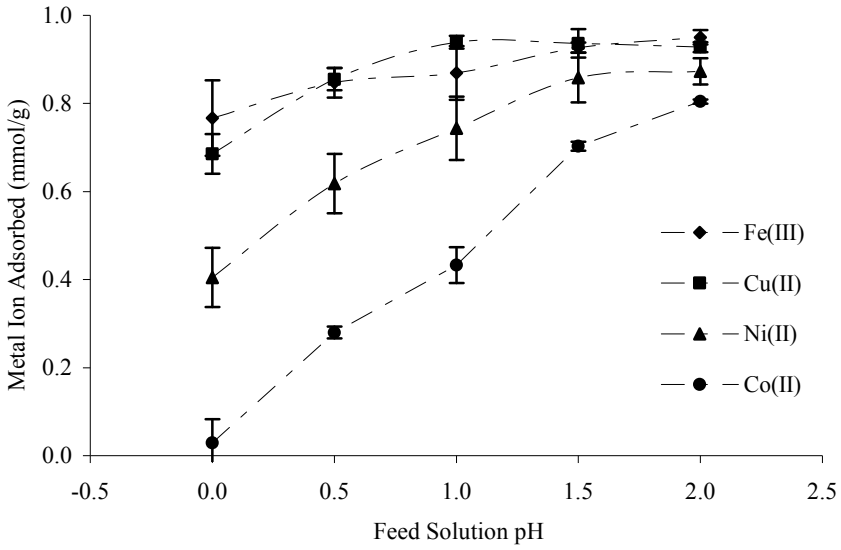

Figure 3.24. Batch pH profiles of divalent metal ions for BP-ED 7.5:1. Single metal ion solutions contained 1.5 g/L of each metal ion. 10 mL of solution was equilibrated with 0.10 g SPC for 24 hours.

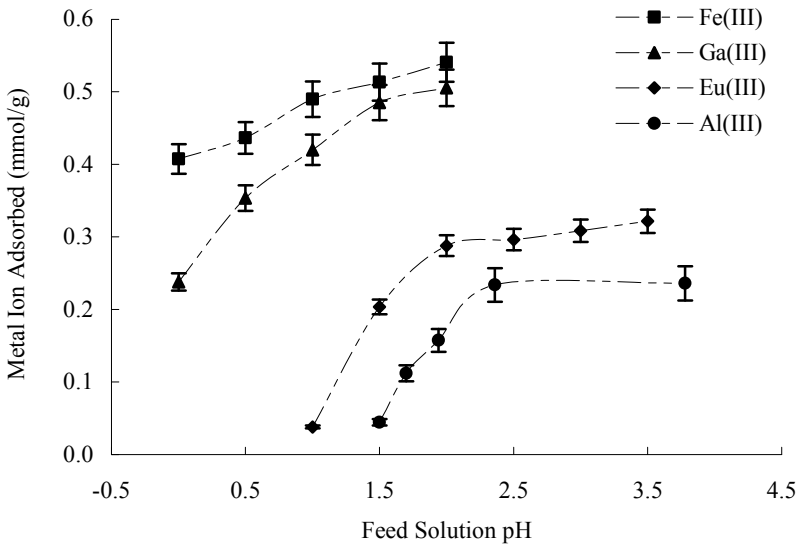

Figure 3.25. Batch pH profiles of trivalent metal ions for BP-ED. Single metal ion solutions contained 1.5 g/L of each metal ion. 10 mL of solution was equilibrated with 0.10 g SPC for 24 hours.

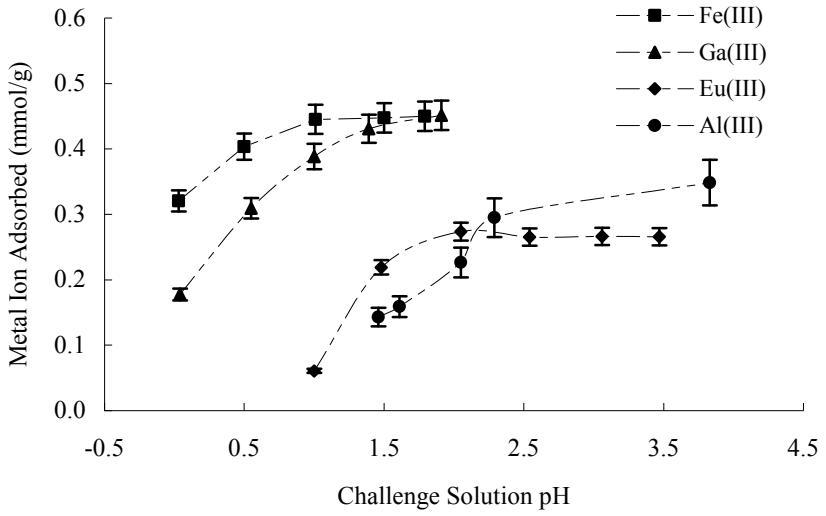

Figure 3.26. Batch pH profiles of trivalent metal ions for WP-ED. Single metal ion solutions contained 1.5 g/L of each metal ion. 10 mL of solution was equilibrated with 0.10 g SPC for 24 hours.

Figure 3.25 and Figure 3.26 display pH profiles for four trivalent metal ions. Based on these data the order of selectivity for both BP-ED (CPTCS only) and WP-ED (CPTCS only) for trivalent ions is: Fe^{3+}>Ga^{3+}>>Eu^{3+}>Al^{3+}. This is also in agreement with the K_{MY} values for the soluble EDTA-metal ion complexes. Similar to the divalent metal ion profiles, there are two regions for each profile as described previously. Fe^{3+} and Ga^{3+} both reach a maximum metal uptake value of 0.54 and 0.51 mmol/g respectively for BP-ED and 0.45 mmol/g for both metals for WP-ED. Sorption by WP-ED utilizes a larger fraction of the pendant ligands again indicating that a relatively large portion of BP-ED ligands may not participating in metal ion coordination. Both BP-ED and WP-ED composites have a relatively low affinity for Al^{3+} at low pH (negligible below pH 1.25), therefore selective complexation of Ga^{3+} or Fe^{3+} from a pH 1 solution containing high

Al^{3+} concentrations was proposed. Dynamic column experiments demonstrated successful sorption of Ga^{3+} in the presence of Al^{3+} (99.9% purity on the column, Figure 3.27), however because Ga^{3+} is readily adsorbed from solutions at pH less than 1 it was not possible to recover all of the adsorbed metal and regenerate the material even with highly acidic (4.5 mol/L H_2SO_4) strip solutions (92% recovery, Figure 3.28).

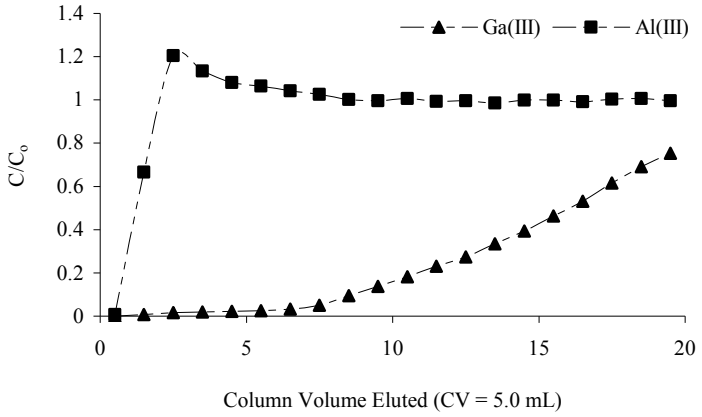

Figure 3.27. Dynamic separation of gallium from aluminum with BP-ED at pH 1. Column packed with 5.0 mL of BP-ED. Feed solution contains 1.0 g/L of gallium and 1.0 g/L of aluminum. Column experiments were run at a flow rate of 0.5 mL/min. Q_{tot} = 28 mg gallium per gram of SPC (99% purity).

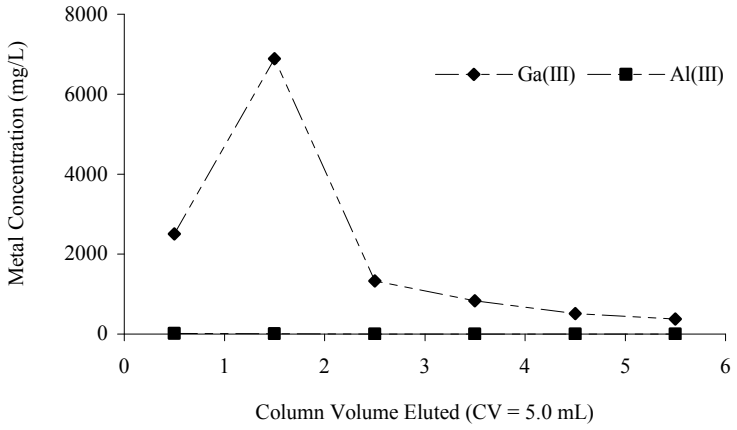

Figure 3.28. Strip profile for the separation of gallium from aluminum with BP-ED at pH 1. 4.5 mol/L H_2SO_4. Column packed with 5.0 mL of BP-ED. Column experiments were run at a flow rate of 0.5 mL/min. 99% gallium purity. 92% stripped.

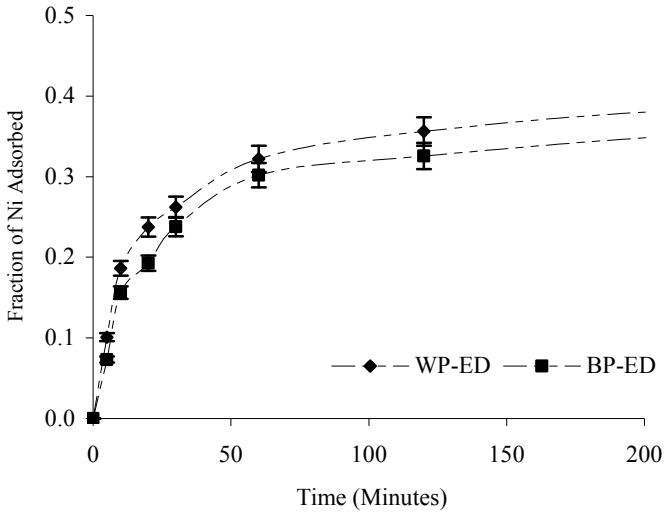

Figure 3.29. Batch kinetics profiles of Ni^{2+} for BP-ED. Cu^{2+} feed solution contains 1.5 g/L. 10 mL of solution was added to 0.10 g SPC. The solution was sampled and analyzed until equilibrium had been reached.

To reduce processing time and to increase efficiency in industrial applications a chelating material with improved mass transfer kinetics is necessary. Figure 3.29 compares the time required to reach equilibrium for both BP-ED (CPTCS only) and WP-ED (CPTCS only). The initial 200 minutes of each profile are shown. Equilibrium for each material is reached at ~800 minutes. Although both materials have very similar equilibrium capacities WP-ED adsorbs Ni^{2+} faster than BP-ED at pH 1. After 2 hours WP-ED has adsorbed ~92% of that adsorbed at 24 hours. At the same time BP-ED had adsorbed ~86% of that adsorbed at 24hrs. It has already been established here that BP-ED has greater capacities in general than WP-ED. However, since most industrial dynamic extraction applications are terminated at 10% breakthrough capacity to improve

efficiency, WP-ED may have equal or greater metal ion sorption capacity (mmol/g) than BP-ED at this point. Improvements in mass transfer kinetics, all other factors being equal, are primarily due to a larger equilibrium constant for the sorption process.

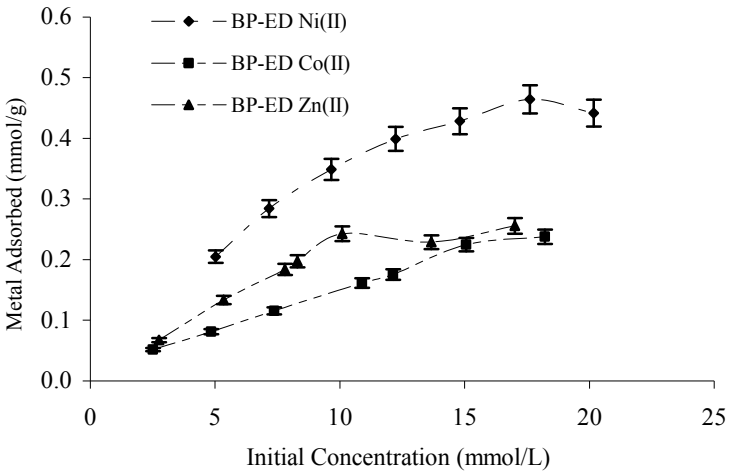

Figure 3.30. Concentration dependent sorption isotherms for Ni^{2+}, Zn^{2+} and Co^{2+} onto BP-ED at pH 1. Equilibration time was 48 hours. 0.1 g of composite was challenged with 10 mL of feed solution.

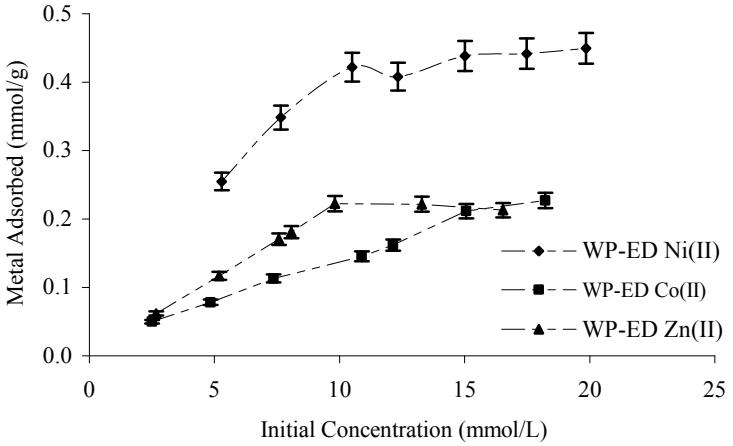

Figure 3.31. Concentration dependent sorption isotherms for Ni^{2+}, Zn^{2+} and Co^{2+} onto WP-ED at pH 1. Equilibration time was 48 hours. 0.1 g of composite was challenged with 10 mL of feed solution.

To explore, in greater detail, differences between BP-ED and WP-ED concentration dependant isotherms for BP-ED (CPTCS only) and WP-ED (CPTCS only)

are reported in Figure 3.30 and Figure 3.31 respectively. These data reconfirm that at pH 1 BP-ED and WP-ED have greater affinity for Ni^{2+} relative to Zn^{2+} and Co^{2+}. These plots also show that the metal ion sorption characteristics of BP-ED and WP-ED at pH 1 are quite similar. Interestingly, there are differences in the sorption capacities of Zn^{2+} and Co^{2+} at low concentrations. To further investigate the sorption of these three metals at pH 1 onto BP-ED and WP-ED, the concentration dependent data were fitted to the theoretical Langmuir and empirical Freundlich models.[16;105;107] Figure 3.32 and Figure 3.33 provide the Langmuir and Freundlich plots respectively for WP-ED.

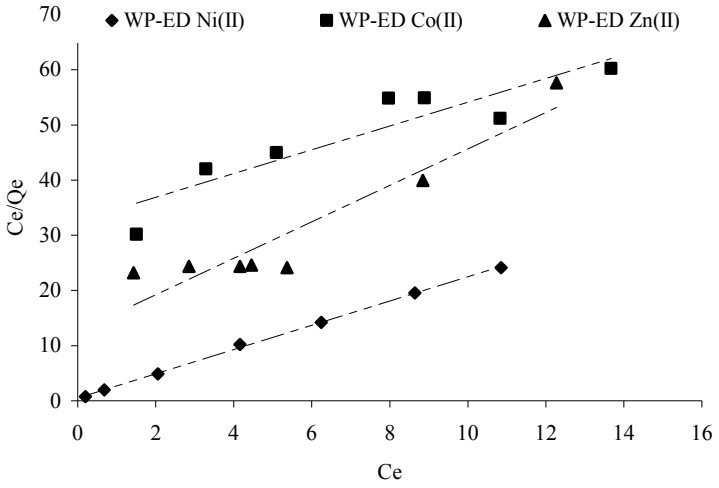

Figure 3.32. Langmuir plot for Ni^{2+}, Zn^{2+} and Co^{2+} for WP-ED.

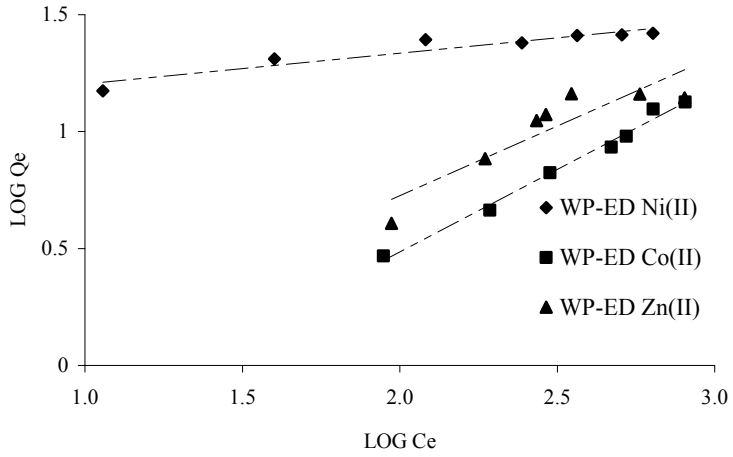

Figure 3.33. Freundlich plot for Ni^{2+}, Zn^{2+} and Co^{2+} for WP-ED

The plots for BP-ED and WP-ED were very similar therefore the BP-ED plots have been omitted to save space. Table 3.6 summarizes the Langmuir and Freundlich constants for BP-ED and WP-ED for Ni^{2+}, Zn^{2+} and Co^{2+}. The applicability of these models can be determined by analysis of the R^2 values for the Langmuir and Freundlich plots seen in Figure 3.32 and Figure 3.33. It is evident that, although both the theoretical Langmuir and Freundlich empirical models adequately describe the sorption of these divalent metals on both chelating materials, the Langmuir model better fits the data. The 1/n Freundlich parameter for all cases is between 0 and 1. This confirms Langmuir type sorption throughout. Q_{max} is a measure of the maximum theoretical number of coordination sites available. The data indicates that, in general, BP-ED has more sites for sorption than WP-ED. This is in agreement with the elemental analysis data and explains why Ni^{2+} sorption is higher for BP-ED than for WP-ED.

Table 3.6. Sorption model parameters of Ni^{2+}, Zn^{2+} and Co^{2+} for BP-ED and WP-ED. Solution pH 1, equilibration time was 48 hours and sample (g) to solution (mL) ratio was 1:10.

BP-ED	LANGMUIR			FREUNDLICH		
Metal ion	Q_m (mmol/g)	K_{ads} $(mmol/L)^{-1}$	R^2	A $(mmol^{1-1/n}g^{-1}L^{1/n})$	1/n	R^2
Ni(II)	0.50	0.88	0.99	4.06	0.30	0.91
Zn(II)	0.30	0.25	0.91	0.35	0.59	0.82
Co(II)	0.48	0.06	0.86	0.10	0.74	0.99
WP-ED						
Metal ion	Q_m (mmol/g)	K_{ads} $(mmol/L)^{-1}$	R^2	A $(mmol^{1-1/n}g^{-1}L^{1/n})$	1/n	R^2
Ni(II)	0.45	4.31	0.99	11.83	0.13	0.99
Zn(II)	0.30	0.26	0.89	0.59	0.59	0.81
Co(II)	0.46	0.07	0.84	0.12	0.71	0.89

The Langmuir constant K_{ads} describes the driving force for the sorption process. It is evident that the order of intensity is: $Ni^{2+}>>Zn^{2+}>Co^{2+}$ for both chelating materials. This indicates a higher K_{MY} for the immobilized EDTA-Ni^{2+} complex supporting the possibility of the separation of Ni^{2+} from a mixture of the three metal ions with either SPC. The Langmuir and Freundlich parameters indicate that, in comparison with BP-ED, WP-ED has consistently a greater affinity (K_{ads}) for Ni^{2+} at pH 1. This can only be a function of the polyamine. Therefore, although the polyamine does not impact the specific selectivity to the same degree as for BP-2 and WP-2, the polyamine structure does affect the stability of BP-ED and WP-ED Ni^{2+} complexes.

Results to this point clearly demonstrate the possibility of separating Ni^{2+} from Co^{2+} by a chromatographic column separation in which a column of the BP-ED or WP-ED material is fed with a solution containing 1.0 g/L of both metals in a sulfate matrix at pH 1. Figure 3.34 displays the column breakthrough profiles of nickel and cobalt. BP-ED was chosen for separation experiments because of its greater capacities relative to WP-ED. It has been established that BP-ED has a preference for nickel over cobalt. Therefore, although BP-ED loads cobalt in the initial stages of the breakthrough the nickel displaces almost all of the cobalt by the conclusion of the experiment. This is in agreement with the information derived from the Langmuir plots and the K_{MY} values for the free EDTA-Ni^{2+} ($K_{MY} = 4.2 \times 10^{18}$) and EDTA-$Co^{2+}$ ($K_{MY} = 2.0 \times 10^{16}$) complexes.

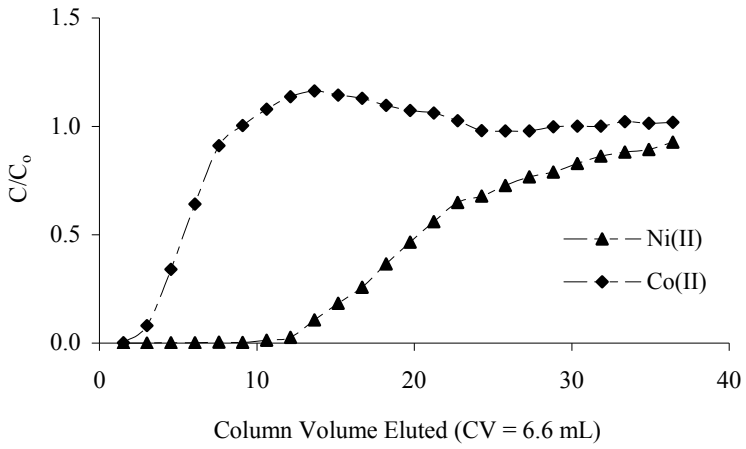

Figure 3.34. Dynamic separation of nickel from cobalt with BP-ED at pH 1. Column packed with 5.0 mL of BP-ED. Feed solution contains 1.0 g/L of nickel and 1.0 g/L of cobalt. Column experiments were run at a flow rate of 0.5 mL/min. Q_{tot} = 25 mg nickel per gram of SPC (98% purity).

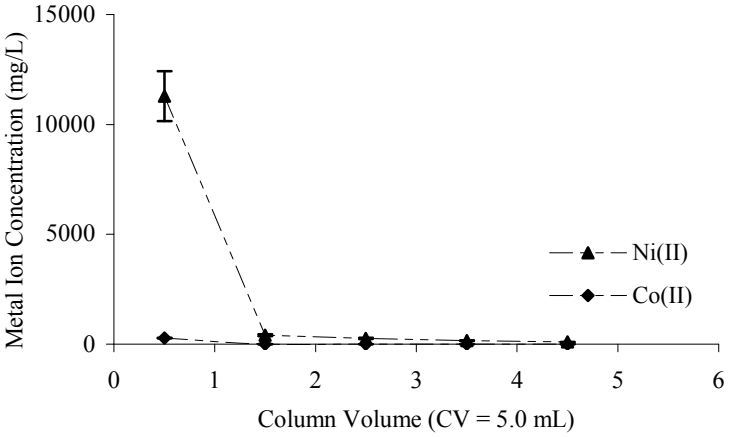

Figure 3.35. Strip profile for the separation of nickel from cobalt with BP-ED at pH 1. 4.5 mol/L H_2SO_4. Column packed with 5.0 mL of BP-ED. Column experiments were run at a flow rate of 0.5 mL/min. 98% nickel purity. 100% stripped.

The Co^{2+} concentration in the eluent quickly exceeds the cobalt concentration of the challenge solution ($C/C_o>1$) then slowly decreases until it is almost at the feed concentration of 1.0 g/L ($C/C_o=1$). This is indicative of a metal that has an affinity for the ligand but cannot remain on the material due to the presence of a competing metal (Ni^{2+})

whose coordination has greater stability. The column color was initially pink but gradually turned to green as the cobalt is replaced with nickel. After 20 column volumes (100 mL) the purity of nickel on the column was ~97%. At this point the Co^{2+} eluent concentration had not yet decreased to the Co^{2+} concentration in the challenge solution and the Ni^{2+} concentration in the eluent had not increased to the concentration of Ni^{2+} in the challenge solution. Therefore increasing the length of the experiment to 25 to 30 column volumes (125 mL to150 mL of feed solution) should increase the purity of Ni^{2+} on the column. Figure 3.35 shows the strip profile for both nickel and cobalt. 100% stripping was achieved with strong acid (4.5 mol/L H_2SO_4) at a flow rate of 0.5 mL/min resulting in an acidic strip solution of ~97% nickel purity.

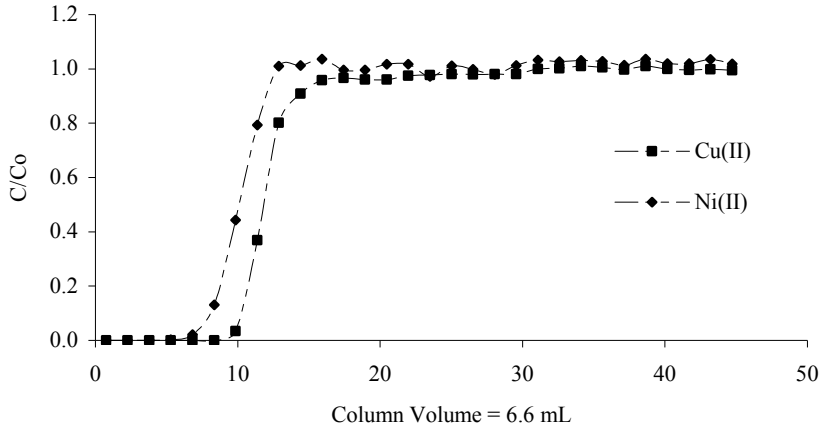

Figure 3.36. Dynamic separation of copper from nickel with BP-ED 7.5:1 MTCS:CPTCS at pH 1. Column packed with 6.6 mL of BP-ED. Feed solution contains 1.5 g/L of nickel and 1.5 g/L of cobalt. Column experiments were run at a flow rate of 0.5 mL/min. Q_{tot} = 18 mg copper per mL of SPC (65% purity). Degree of utilization was 0.85 for Cu^{2+}.

A second separation of interest is Cu^{2+}/Ni^{2+}. Analysis of this separation will allow a comparison of BP-ED with both BP-2 and WP-2. A column of BP-ED 7.5:1

MTCS:CPTCS was fed a solution containing 1.5 g/L of both Ni^{2+} and Cu^{2+}. Figure 3.36 displays the column breakthrough profiles of copper and nickel. BP-ED was also chosen for this separation experiments because of its greater copper sorption capacity compared to WP-ED.

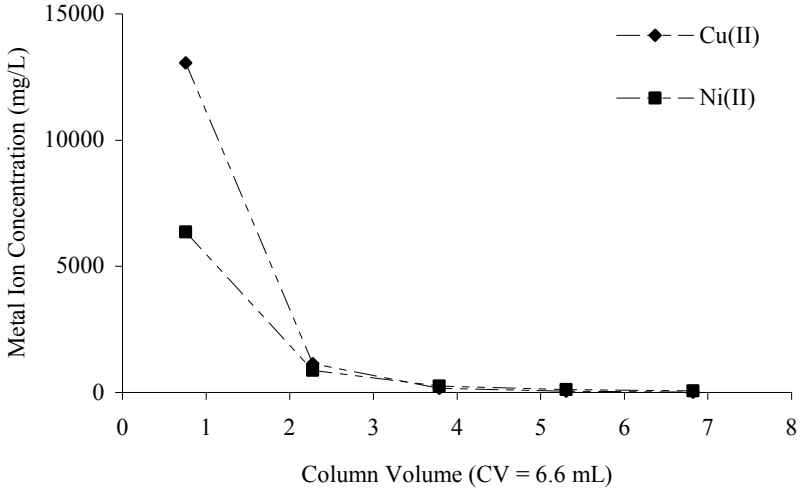

Figure 3.37. Strip profile for the separation of copper from nickel with BP-ED 7.5:1 MTCS:CPTCS at pH 1. 4.5 mol/L H_2SO_4. Column packed with 6.6 mL of BP-ED. Column experiments were run at a flow rate of 0.5 mL/min. 64% copper purity. 100% stripped.

Whereas it was possible to separate nickel from cobalt with BP-ED the column break through profiles indicate that it is not possible to separate copper from nickel (Figure 3.37). The purity of copper in the strip solution is approximately 64% which is much lower than the Cu^{2+} purity in any of the strip solutions for BP-2 and WP-2. BP-ED cannot separate these metals because the complex formation constants are relatively close. The formation constants for the free ligand EDTA-Cu^{2+} and EDTA-Ni^{2+} are 6.3 x 10^{18} and 4.2 x 10^{18} respectively. In conclusion, copper cannot displace nickel from BP-ED sorption sites to the same extent that Ni^{2+} can displace Co^{2+}. BP-ED coordinating groups favor Ni^{2+} sorption relative to WP-2 and especially BP-2. The increase in the

stability of the Ni^{2+} complex must be a result of the polydentate nature of each BP-ED site. As a consequence of these findings BP-ED and WP-ED can be described as a nickel selective chelating IX materials in the absence of copper. Of further interest is the flow rate used in these experiments (0.5mL/min through a 5mL column). The reported flow rates in the literature for chitosan modified with EDTA anhydride for a Ni^{2+}/Co^{2+} separation (3.92 mL/hr through a 20 mL to 30 mL column) is much slower. The porous nature of the silica gel, the hydrophilicity of the polymer matrix and the fact that the chelating sites are on the surface and highly accessible conspire to allow BP-ED to effectively operate at 0.1CV/min.

Out of all SPC materials reported, BP-ED and WP-ED posess the highest sorption capacity for Cu^{2+} and Ni^{2+} in acidic media. The specific selectivity profile of BP-ED suggests that this material could be used to remove nickel from complex mixtures. This material may eventually be commercially viable. However, for a material to be commercially viable it must have a long lifetime (durability). For example, BP-ED must be able to selectively remove Ni^{2+} from Co^{2+} and then release Ni^{2+} over thousands of cycles. The sorption capacity must not decrease and there should be no deterioration in the mass transfer kinetics as reflected by the degree of utilization. In order for a material to do this it must be mechanically and chemically stable. Previous reports of SPC materials have demonstrated material integrity for thousands of load strip cycles. However, all previous investigations were of materials for which the pendant ligand was attached by way of a robust C-N bond. In contrast BP-ED and WP-ED are attached to the matrix by an amide linker. As a result of resonance stabilization, amides are relatively unreactive under neutral conditions. However, amide bonds are subject to hydrolysis

under very acidic conditions, and when heated under basic conditions. This uusually takes place through attack by a nucleophile on the carbonyl carbon. This serves to break the carbonyl double bond and forms a tetrahedral intermediate. Under very acidic conditions the carbonyl oxygen can be protonated, although the pK_a is usually way above 15. Acidic conditions yield the carboxylic acid and the ammonium ion while basic hydrolysis yields the carboxylate ion and ammonia. Therefore the long term stability of BP-ED and WP-ED was an issue. In order to address this concern a 5 mL column of BP-ED 7.5:1 MTCS:CTPCS was subjected to 1001 load strip cycles. For each load cycle the column was fed 200 mL of a solution containing 1.5 g/L Cu^{2+} at pH 1. The column was then rinsed with deionized water and stripped with 4.5 mol/L sulfuric acid. Figure 3.38 represents the breakthrough profiles for column experiments. The three profiles shown are for the initial cycle, for cycle 101 and for cycle 1001.

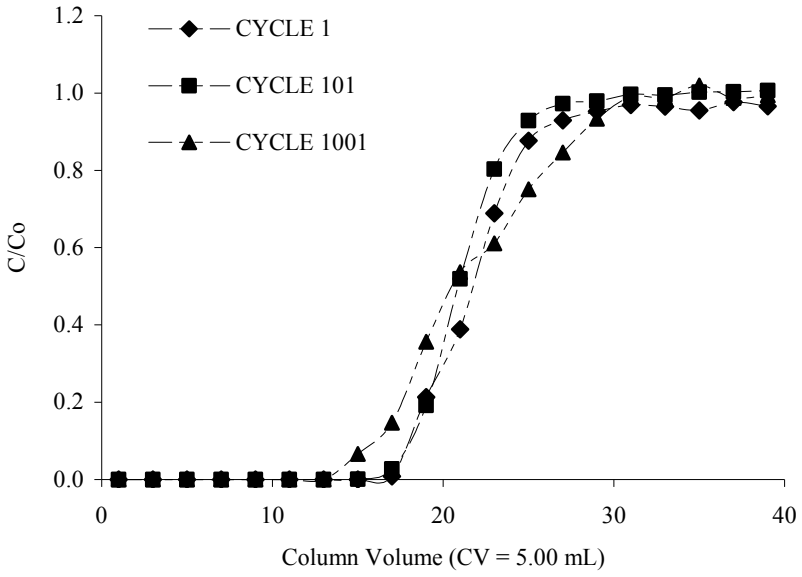

Figure 3.38. Dynamic extraction of copper for BP-ED 7.5:1 MTCS:CPTCS at pH 1. Column packed with 5.0 mL of BP-ED. Feed solution contains 1.5 g/L copper. Flow rate was 1 mL/min.

Visual examination of the three curves shows that there are small variations between the three profiles. However the full breakthrough sorption capacity for the three cycles tested were all in the range 29 to 30 mg of Cu^{2+} extracted per mL of BP-ED. These variations are statistically insignificant. If acid hydrolysis of the pendant EDTA derivative had occurred the sorption capacity would have dropped. As a result it can be concluded that BP-ED is stable in terms of amide hydrolysis for a minimum of 1001 load and strip cycles. SPC materials are not used under basic conditions because of the increased solubility of the bulk silica gel. As a result testing the stability of the amide bond under basic cycling was unwarranted.

3.4 DTPA modified SPCs

Diethylene triamine pentaacetic acid (DTPA) is an elongated version of EDTA.[109] DTPA contains one extra ethylamine group as well as one more acetate group (Figure 3.39).

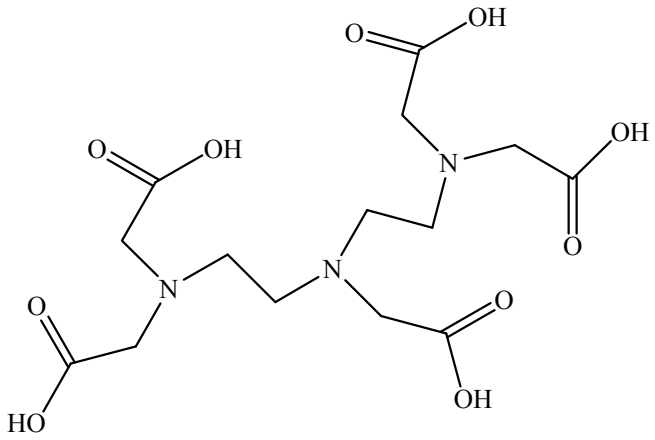

Figure 3.39. Diethylene diamine pentaacetic acid (DTPA)

DTPA is typically used in the medical field for chelation therapy. It is effective at removing radioactive metal ions such as plutonium or americium from the human body and for complexing Gd for use as an MRI contrast agent in humans. Similar to EDTA, DTPA can be attached to a solid support by reaction of immobilized amines with DTPA dianhydride. Silica gel functionalized with aminopropyl trichlorosilane has been reacted successfully with DTPA dianhydride (producing Silica-DT). [112] DTPA dianhydride is prepared from the dehydration of DTPA in pyridine with acetic anhydride.[114] Investigations of Silica-DT indicate good loading of the chelating ligand. Elemental analysis of Silica-DT estimated a ligand loading of approximately 1.29 mmol/g. Which is significantly higher than that reported for Silica-ED (0.30 mmol/g). However when Silica-DT was treated with Cu^{2+} solution the loading was significantly lower than for

Silica-ED. This is inconsistent with reported equilibrium constants for free DTPA, which are in general, higher relative to free EDTA. Thus immobilizing DTPA on SPC materials was of interest. The abundance of amines in SPC materials as well as large pores may result in greater loading. Further, the resulting material (SPC-DT) may show differences in selectivity relative to BP-ED. Such differences, if any, must be the result of the small structural differences between the two similar materials. Thus BP-DT was prepared by the acid catalyzed aminolysis of DTPA dianhydride by the amine groups of 7.5:1 MTCS:CPTCS BP-1 (Figure 3.40).

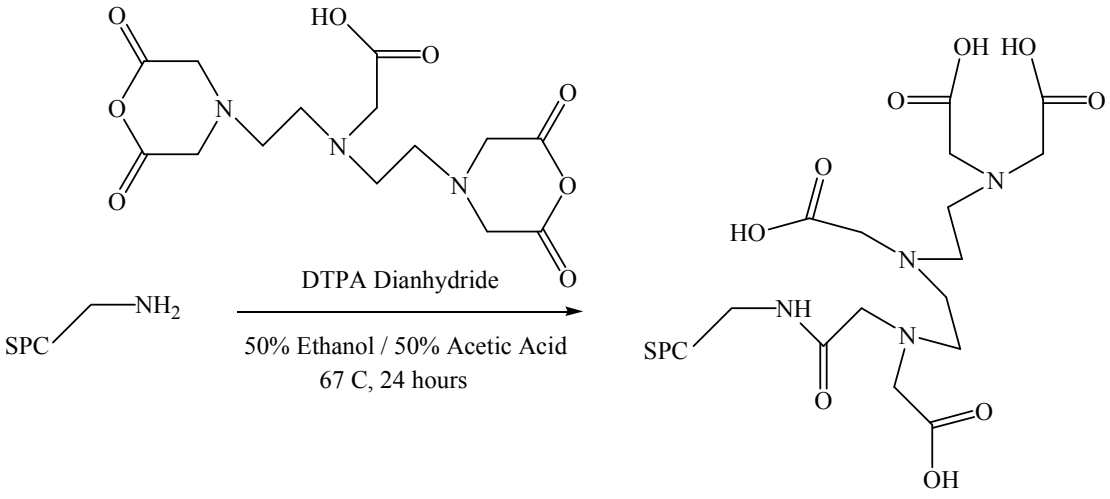

Figure 3.40. Synthetic pathway to DTPA functionalized SPCs.

Figure 3.41 confirms the presence of an immobilized DTPA derivative in BP-DT. The peak at approximately 168 ppm is attributed to the carboxylic groups of the ligand (-CO_2H). The acetate methylene produces the peak found at approximately 51 ppm (-N($\underline{C}H_2COOH$). These signals are not present for the precursor, BP-1. Table 3.7 displays the data derived from the elemental analysis of BP-DT. It is clear that the ligand loading is poor (0.23 mmol/g) in comparison to that for BP-ED and WP-ED. This is inconsistent

with reported data for Silica-DT as well as ligand loading data for DTPA loaded on molecular sieves (1.67 mmol/g) and on aluminum oxide (1.22 mmol/g). It is known that the pore volume of SPC materials decrease once the polyamine layer has been attached. DTPA is somewhat larger than EDTA. Thus, the large molecule in combination with the decreased pore volume may conspire to limit the ligand loading for DTPA on BP-1.

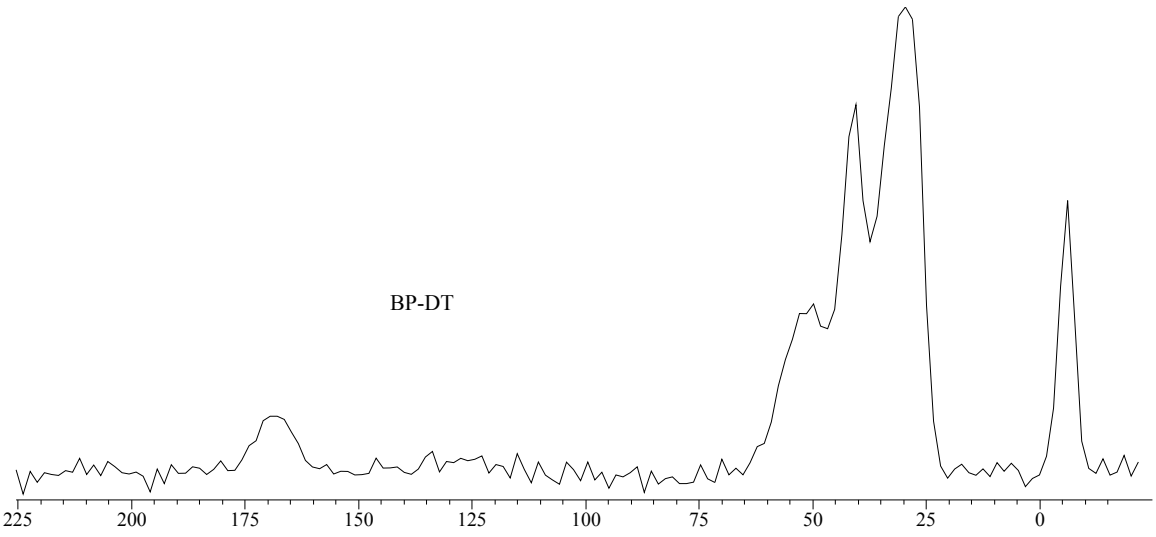

Figure 3.40. Units for spectrum ppm. CP/MAS ^{13}C NMR at 126 MHz of BP-DT (7.5:1 MTCS:CPTCS).

Table 3.7 Data derived from elemental analysis for a novel amido-aminoacetate modified SPC materials. BP-ED is prepared from BP-1 (PAA).

SPC	C (mmol/g)	H (mmol/g)	N (mmol/g)	C/N	Ligand loaded (mmol/g)
BP-1	10.68	25.30	2.67	4.00	-
BP-DT	11.03	34.00	2.64	4.17	0.23

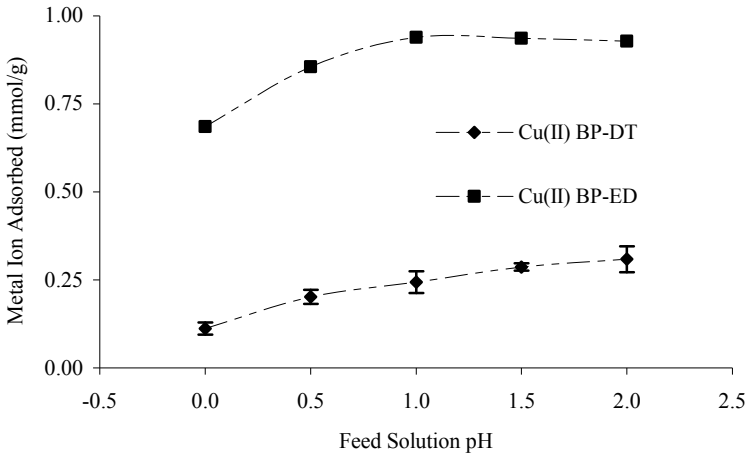

Figure 3.42. Batch pH profiles of Cu^{2+} for BP-DT. Single metal ion solution contained 1.5 g/L of Cu^{2+}. 10 mL of solution was equilibrated with 0.10 g BP-DT for 24 hours.

Figure 3.42 displays the pH profile of BP-DT 7.5:1 for Cu^{2+} in the range pH 0.0 to pH 2.0. For comparison the pH profile of BP-ED 7.5:1 for Cu^{2+} has been overlaid. From this data it is clear that copper sorption is significantly lower for BP-DT relative to BP-ED. This is consistent with the differences in ligand loading for each material. It should be noted that at pH 2 the quantity of metal ion adsorbed per gram absorbent is almost equivalent to the calculated number of functional groups per gram. This indicates a one to one complex formation. This points toward a strong sorption process since the sorption equilibrium must be heavily in favor of BP-DT-Cu^{2+} complex formation. A column separation of Cu^{2+}/Ni^{2+} yields very different results to that for BP-ED. BP-ED was unable to separate copper from nickel because the affinity of BP-ED for nickel is relatively high. In the case of BP-DT copper is selectively removed from a solution containing both copper and nickel (1.5 g/L each). The column breakthrough profile presented in Figure 3.43 shows that although Ni^{2+} is extracted early in the experiment,

Ni^{2+} is rapidly removed from the sites by Cu^{2+} ions. Thus Cu^{2+} must have a significantly higher formation constant with BP-DT in comparison with Ni^{2+}.

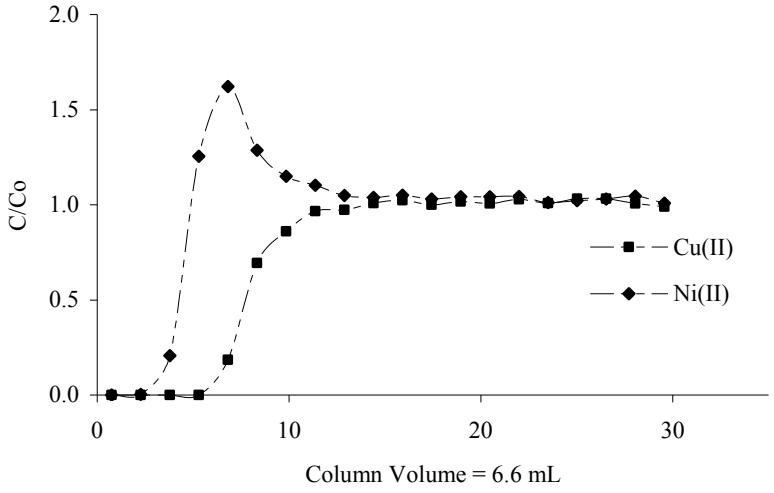

Figure 3.43. Dynamic separation of copper from nickel with BP-DT 7.5:1 MTCS:CPTCS at pH 1. Column packed with 6.6 mL of BP-DT. Feed solution contains 1.5 g/L of nickel and 1.5 g/L of cobalt. Column experiments were run at a flow rate of 0.5 mL/min. Q_{tot} = 18 mg copper per mL of SPC (65% purity).

Although DTPA is only a small extension of EDTA, the immobilized ligand in BP-DT must be significantly different to that for BP-ED. Therefore, a small change in the ligand can result in large differences in specific selectivity. It is known that for every metal ion the formation constant with DTPA is greater than that for EDTA. However, the formation constant for BP-DT with Cu^{2+} is not large enough to prevent complete stripping of the column with 4.5 mol/L H_2SO_4. Copper is recovered with a purity of 99.9% (Figure 3.44). Despite the high purity, the sorption capacity for Cu^{2+} from solutions at low pH remains significantly lower than any of the materials tested thus far. In conclusion, based on the data for acquired for BP-DT it seems reasonable to propose that DTPA binds to the surface with more than one amide bond. DTPA anhydride can

span the distance between two polymer amine groups. As a result one end of the anhydride may react with one amine group whilst the other end reacts with another amine group. This accounts for the lower ligand loading as it requires two amines for one ligand attachment. Also, if this is the case the selectivity of Cu over Ni will be the result of a ligand of lower denticity and hindered conformation freedom.

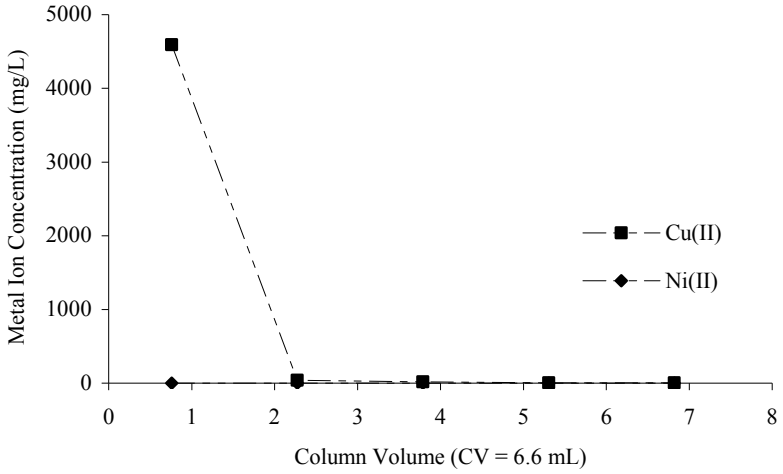

Figure 3.44. Strip profile for the separation of copper from nickel with BP-DT 7.5:1 MTCS:CPTCS at pH 1. 4.5 mol/L H_2SO_4. Column packed with 6.6 mL of BP-DT. Column experiments were run at a flow rate of 0.5 mL/min. 64% copper purity. 100% stripped.

No further metal ion sorption experiments were carried out using BP-DT. WP-DT was not prepared.

3.5 NTA modified SPCs

Nitrilotriacetic acid (NTA) is a third chelating compound in the series of amino acids (Figure 3.45). The uses of NTA are similar to that of EDTA, however NTA is biodegradable.

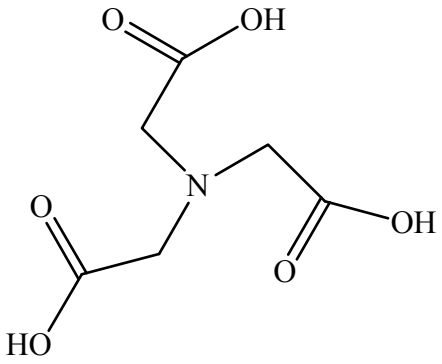

Figure 3.45. Nitrilotriacetic acid (NTA)

To the best of our knowledge there have been no reports in the literature of NTA anhydride as a reagent for the preparation of a chelating IX material the selective removal of heavy metal ions. NTA anhydride is prepared in only moderate yield by dehydration of NTA in pyridine or dimethylacetamide (DMA) with acetic anhydride.[115] The product is much more difficult to isolate relative to isolate relative to EDTA and DTPA. EDTA anhydride and DTPA anhydride are insoluble in pyridine. As a result the recovery of the final product is only a matter of filtration and washing. NTA anhydride is soluble in both pyridine and DMA. Consequently it must be concentrated before the addition of chloroform which forces precipitation. Although this is not a major concern for bench scale production, it will present extra expense and complexity for commercial production. Also, the yield is poor and is very sensitive to the molar ratios of the reagents. Despite

this a third amide linked SPC was prepared from nitrilotriacetic anhydride. The resulting materials displayed excellent metal ion extraction characteristics.

NTA anhydride was reacted with both BP-1 7.5:1 and WP-1 7.5:1 by way of an acid catalyzed aminolysis in a 50:50 ethanol/acetic acid solvent (Figure 3.46). The resulting materials from precursors BP-1 and WP-1 have been dubbed BP-NT and WP-NT respectively. Table 3.8 displays composition data for BP-NT and WP-NT. This data was derived from elemental analysis. In keeping with all of the other materials analyzed BP-NT has a greater ligand loading per gram of sorbent in comparison with WP-NT. Again this must be a result of the presence of secondary and tertiary amines in PEI, the polymer used in WP-NT production.

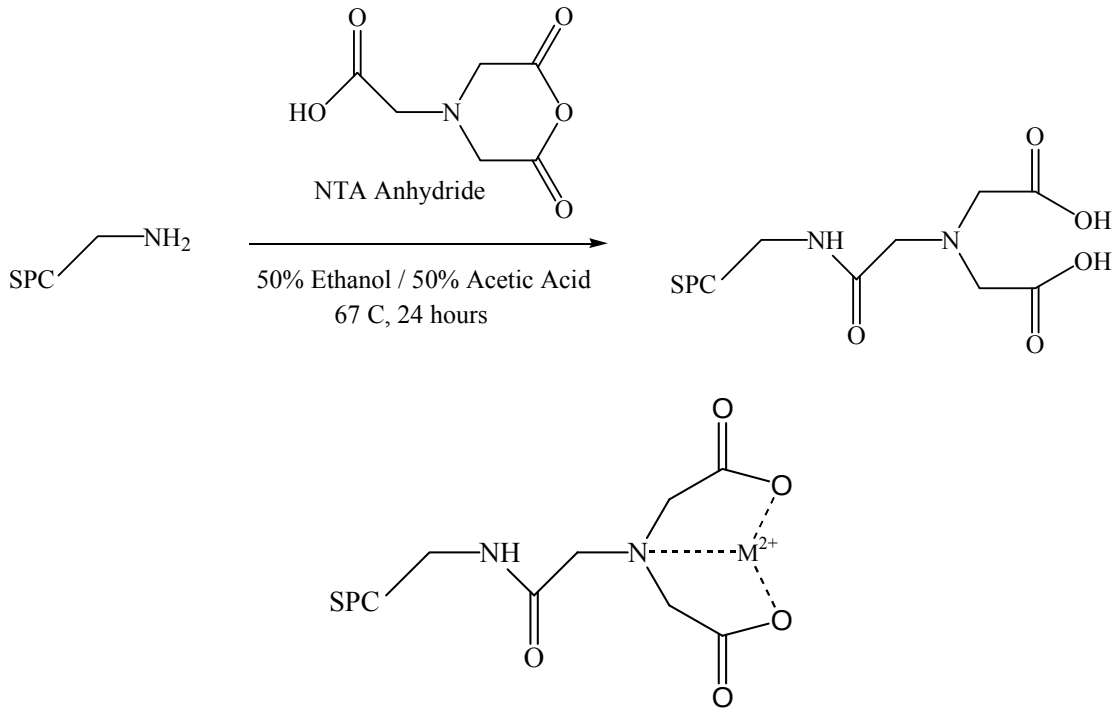

Figure 3.46. (Top) Synthetic pathway from BP-1 and WP-1 to BP-NT and WP-NT. (Bottom) Resulting ligand chelating a (M^{2+}) divalent metal ion.

Also, the ligand loading per gram of BP-NT (1.36 mmol/g) is greater than the corresponding ligand loading for BP-ED (1.03 mmol/g). Ligand loading was calculated using Equation 3.6. Thus, decreasing the size of the amino acid is reflected in greater loading of the chelating molecule. As a result of the large degree of functionalization BP-NT and WP-NT were characterized in a detailed manner. Figure 3.47 displays the solid state ^{13}C NMR for BP-NT (bottom) and WP-NT (top). The presence of the NTA functionality is evident by the large broad peak at approximately 170 ppm. This signal is a result of the two acetate and single amide in each pendant ligand (-CO_2H, -NH-$\underline{C}$(O)-CH_2-). The acetate methylene groups create the signal at approximately 55 ppm (-$\underline{C}H_2COOH$).

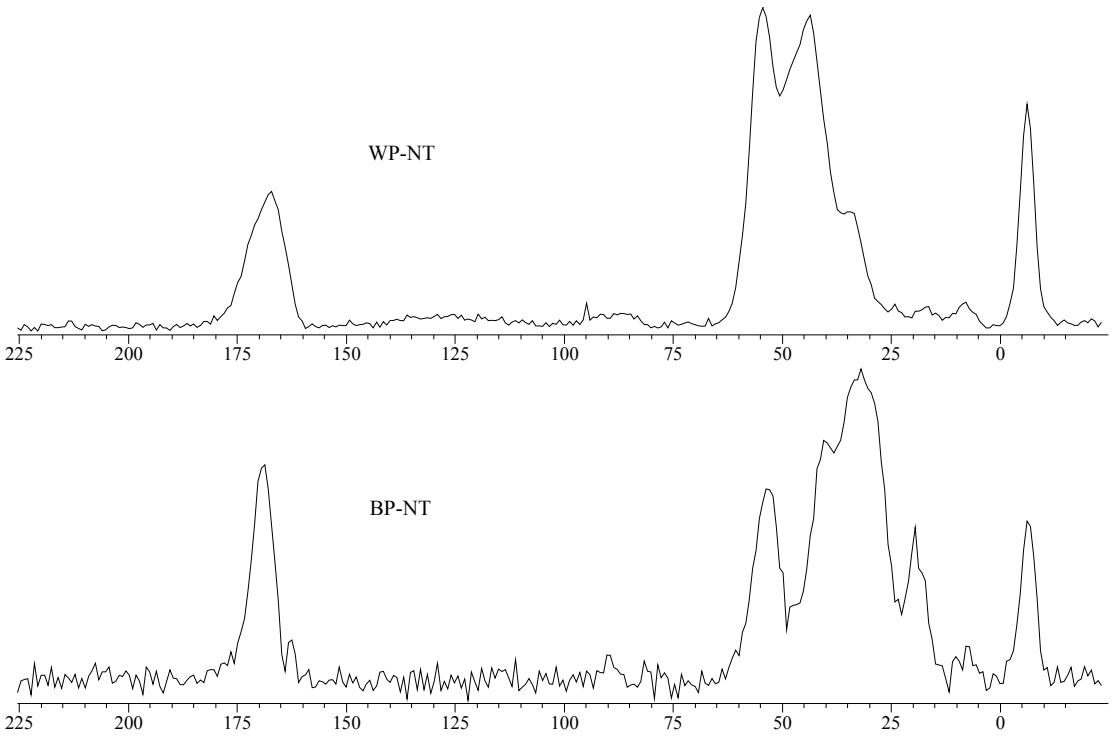

Figure 3.47. Units for both spectrum ppm. (Top) CP/MAS ^{13}C NMR at 126 MHz of WP-NT (12.5:1 MTCS:CPTCS). (Bottom) CP/MAS ^{13}C NMR at 126 MHz of BP-NT (7.5:1 MTCS:CPTCS).

Table 3.8. Data derived from elemental analysis for two amido-aminoacetate modified SPC materials. WP-NT is prepared from WP-1 (PEI). BP-NT is prepared from BP-1 (PAA).

SPC	C (mmol/g)	H (mmol/g)	N (mmol/g)	C/N	Ligand loaded (mmol/g)
BP-1	11.51	25.80	2.70	4.26	-
BP-NT	16.33	29.50	3.27	4.99	1.36
WP-1	10.51	27.40	3.79	2.77	-
WP-NT	13.93	30.10	4.10	3.40	0.79

Figure 3.48 and Figure 3.49 display the divalent and trivalent batch pH profiles respectively for BP-NT. Figure 3.50 and Figure 3.51 display the divalent and trivalent batch pH profiles respectively for WP-NT. 10 mL of a single metal ion solution containing approximately 1.5 g/L of metal ion was contacted with 0.10 g of SPC for 24 hours. It is clear from the pH profiles that for divalent ions the order of preference for both BP-NT and WP-NT is Cu^{2+}>Ni^{2+}>Zn^{2+}, Co^{2+}. Further it is evident that the specific selectivity for trivalent metal ions tested is Ga^{3+}>Fe^{3+}>Eu^{3+}>Al^{3+}. The Cu^{2+} sorption capacity of BP-NT and WP-NT rival those of BP-ED and WP-ED. However the sorption capacity for Ni^{2+} is lower than that for BP-ED and WP-ED. This is true for Zn^{2+} and Co^{2+} also. Thus although the order of preference for the divalent metal ions is similar to BP-ED the separation between the metals is much larger in the case of BP-NT and WP-NT.

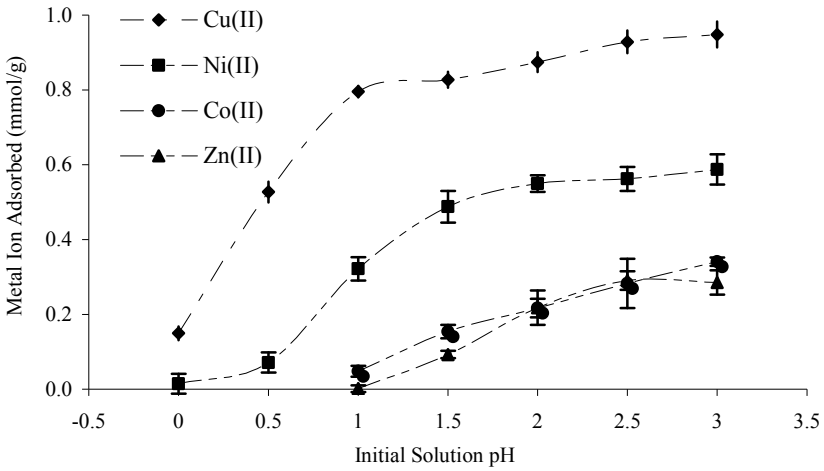

Figure 3.48. Batch pH profiles of divalent metal ions for BP-NT. Single metal ion solutions contained 1.5 g/L of each metal ion. 10 mL of solution was equilibrated with 0.10 g SPC for 24 hours.

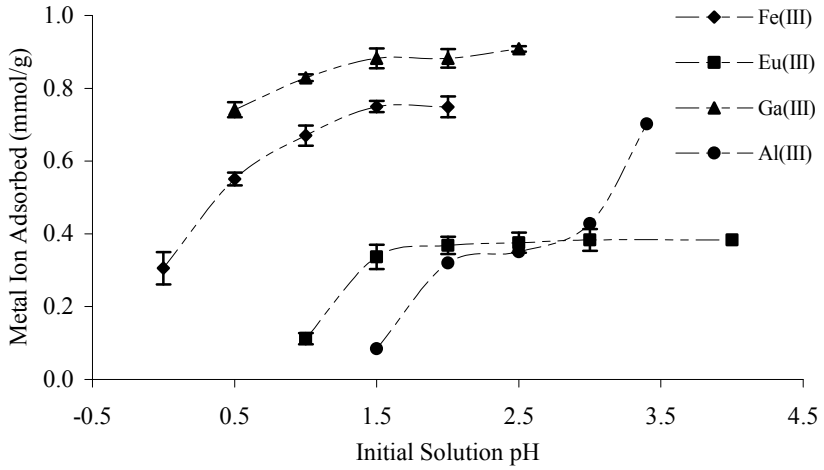

Figure 3.49. Batch pH profiles of trivalent metal ions for BP-NT. Single metal ion solutions contained 1.5 g/L of each metal ion. 10 mL of solution was equilibrated with 0.10 g SPC for 24 hours.

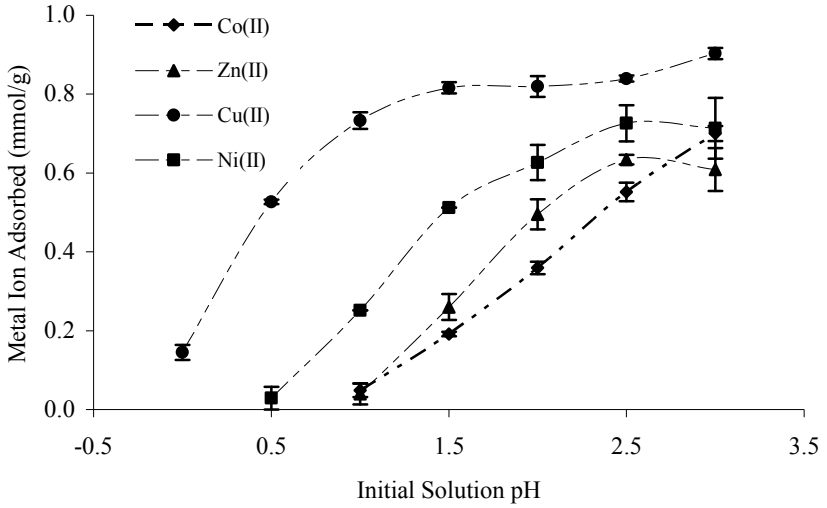

Figure 3.50. Batch pH profiles of divalent metal ions for WP-NT. Single metal ion solutions contained 1.5 g/L of each metal ion. 10 mL of solution was equilibrated with 0.10 g SPC.

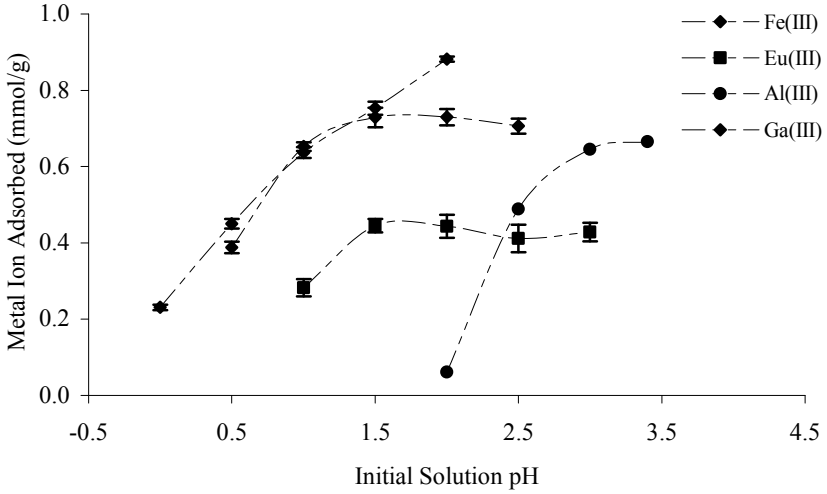

Figure 3.51. Batch pH profiles of trivalent metal ions for WP-NT. Single metal ion solutions contained 1.5 g/L of each metal ion. 10 mL of solution was equilibrated with 0.10 g SPC.

The batch pH profiles for BP-NT and WP-NT are similar, however above pH 2 the profiles for WP-NT merge somewhat. In contrast the profiles for BP-NT remain separated. A similar trend is present for WP-ED and BP-ED. This suggests large K_{ads} constants for sorption on WP-ED relative to sorption on BP-ED. To study the differences

between BP-NT and WP-NT further, concentration isotherms were determined for both materials for Cu^{2+} at pH 1 (Figure 3.52). It is clear from the Figure that at all copper concentration values BP-NT is a more effective extractant. Langmuir and Freundlich models were used to aid the analysis (Figure 3.53 and Figure 3.54).[86;105]

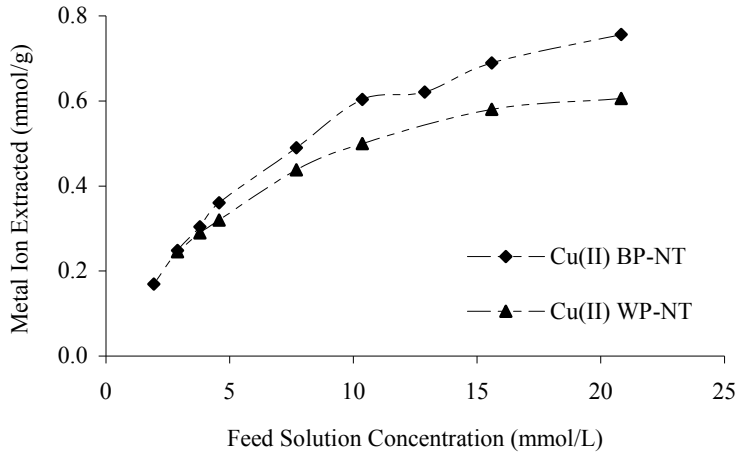

Figure 3.52. Batch concentration isotherms of Cu^{2+} for BP-NT and WP-NT. Single metal ion solutions contained 1.5 g/L of each metal ion. 10 mL of solution was equilibrated with 0.10 g SPC.

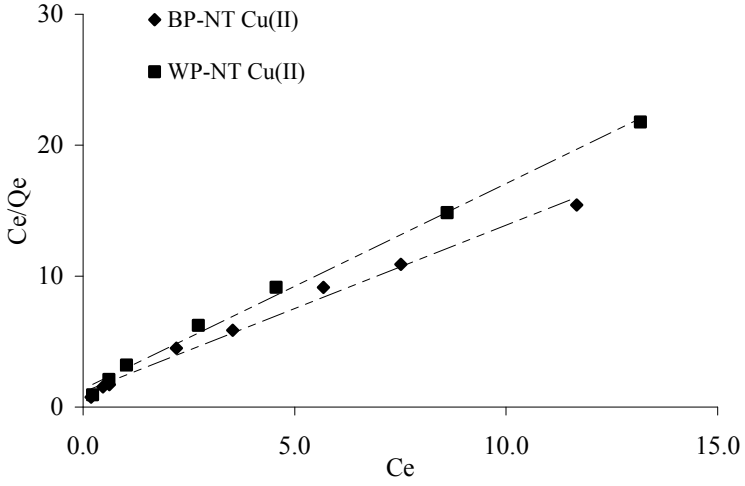

Figure 3.53. Langmuir isotherm for Cu^{2+} for WP-NT and BP-NT.

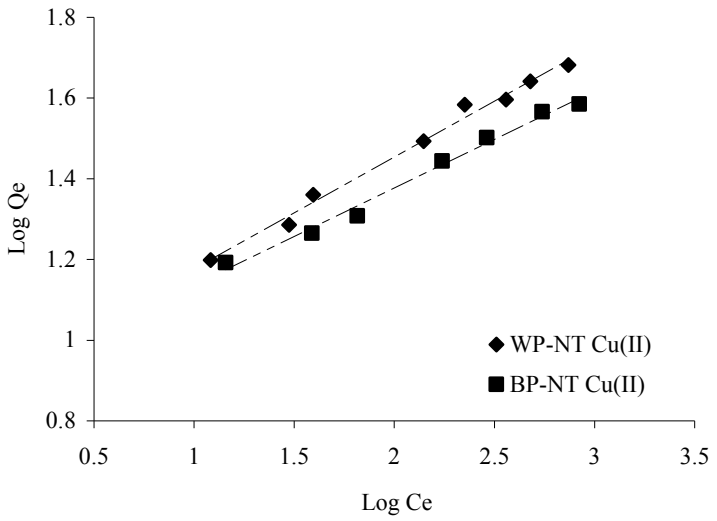

Figure 3.54. Freundlich isotherm for Cu^{2+} for WP-NT and BP-NT.

The parameters derived from each model were collected and are displayed in Table 3.9. The R^2 values for both models indicate that both models fit the data excellently. As expected the 1/n Freundlich parameter indicates non-cooperative metal binding in a monolayer arrangement. Therefore it can be assumed that sorption is monolayer and non-cooperative. The maximum number of theoretical sorption sites is great for BP-NT than for WP-NT which again fits both the ligand loading and metal ion sorption pH profile data. Interestingly, the Langmuir equilibrium parameter (K_{ads}) for both BP-NT and WP-NT with copper are very similar (1.11 mmol/L^{-1} and 1.13 mmol/L^{-1}) respectively. Hence the sorption of Cu^{2+} on BP-NT and WP-NT must have similar formation constants. This is in stark contrast to BP-2 and WP-2 as well as BP-ED and WP-ED. Thus it can be concluded that, for Cu^{2+} at pH 2, there is no significant effect of the polyamine on sorption. This presents the possibility that Cu^{2+} sorption is similar for both BP-NT and WP-NT because the low preferred coordination geometry is satisfied

solely by the tetra-dentate ligand. It is possible that metals preferring octahedral geometry will show very different Langmuir equilibrium parameters for BP-NT and WP-NT.

Table 3.9. Sorption model parameters of Cu^{2+} for BP-NT and WP-NT. Solution pH 1, equilibration time was 48 hours and sample to solution ratio was 1:10.

BP-2	LANGMUIR			FREUNDLICH		
Metal ion	Q_m (mmol/g)	K_{ads} (mmol/L)$^{-1}$	R^2	A (mmol$^{1-1/n}$g^{-1}L$^{1/n}$)	1/n	R^2
Cu^{2+}	0.78	1.11	0.99	7.88	0.24	0.99
WP-2						
Metal ion	Q_m (mmol/g)	K_{ads} (mmol/L)$^{-1}$	R^2	A (mmol$^{1-1/n}$g^{-1}L$^{1/n}$)	1/n	R^2
Cu^{2+}	0.64	1.13	0.99	7.96	0.28	0.99

From analysis of the data presented to this point, the separation for which BP-NT and WP-NT appear most suited is Cu^{2+} from Ni^{2+}. Also BP-ED was not able to conduct this separation and to this point BP-NT is the only material to rival BP-ED in terms of sorption capacity at low pH, out of all SPCs including those described in Chapter 2. The data suggests that the separation of Cu^{2+} and Ni^{2+} will be possible at pH 1. Hence, Figure 3.55 and Figure 3.56 represent the breakthrough profiles resulting from the column separation of Cu^{2+} from Ni^{2+} using BP-NT and WP-NT respectively.

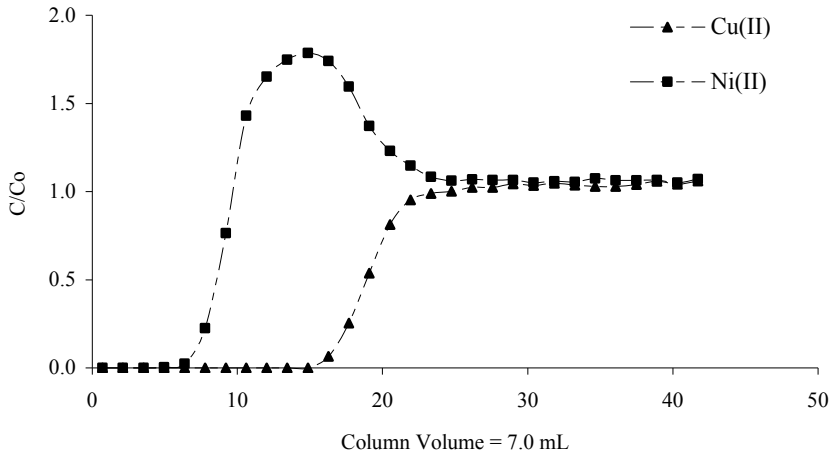

Figure 3.55. Dynamic separation of copper from nickel with BP-NT 7.5:1 MTCS:CPTCS at pH 1. Column packed with 7.0 mL of BP-NT. Feed solution contains 1.5 g/L of nickel and 1.5 g/L of cobalt. Column experiments were run at a flow rate of 0.5 mL/min. Q_{tot} = 26 mg copper per mL of SPC (99 % purity).

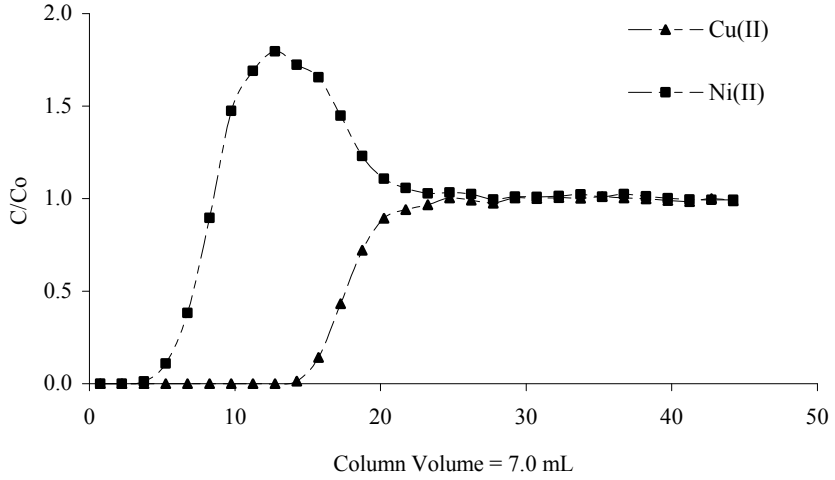

Figure 3.56. Dynamic separation of copper from nickel with WP-NT 7.5:1 MTCS:CPTCS at pH 1. Column packed with 7.0 mL of WP-NT. Feed solution contains 1.5 g/L of nickel and 1.5 g/L of cobalt. Column experiments were run at a flow rate of 0.5 mL/min. Q_{tot} = 23 mg copper per mL of SPC (99 % purity).

BP-NT and WP-NT both accomplish the task of removing Cu^{2+} from Ni^{2+} in a solution at pH 1. BP-NT extracts 26 mg of Cu^{2+} per mL of absorbent. WP-NT extracts 23 mg of Cu^{2+} per mL of sorbent. BP-NT and WP-NT did not adsorb any Ni^{2+}. The copper was 100% recovered from both materials using 4.5 mol/L H_2SO_4. It should be noted that BP-ED was unable to perform this separation and that BP-2 and WP-2 show very different characteristics when challenged with a similar separation. As a result it can be concluded that the immobilized amido-aminoacetate chelating group (NTA derivative) is not influenced by the nature of the polyamine to the same extent as for BP-2 and WP-2. Also, BP-NT does not show the same affinity for nickel, relative to copper, that BP-ED does, most likely as a result of the decreased denticity of the pendant ligand.

Table 3.10. Acid and base stability study. Amide linked composites, BP-NT and WP-NT, were treated with 4 mol/L H_2SO_4 and 4 mol/L NH_4OH solutions for 3 days. Cu^{2+} uptake was recorded for no treatment and after treatment. BP-2 (no amide linker) was used as a control. Sorption model parameters of Cu^{2+} for BP-NT and WP-NT. Solution pH 1, equilibration time was 48 hours and sample to solution ratio was 1:10.

SPC	Cu^{2+} Adsorbed (mg/g)		
	No Treatment	72 hrs Acid	72 hrs Base
BP-2	24	29	31
BP-NT	60	61	69
WP-NT	53	53	55

Like BP-ED and WP-ED, BP-NT and WP-NT are very promising materials. Nevertheless, the same concern regarding amide hydrolysis is appropriate for the BP-NT and WP-NT. To determine the stability of these materials 1 g of BP-NT and WP-NT, as well as 1 g of BP-2 as a control, was added to 100 mL of 4.5 mol/L H_2SO_4 as well as to 100 mL of 4M NH_4OH. After 72 hours each material was washed, dried and batch tested

for copper sorption. Table 3.10 summarizes the results. After contact with acidic and basic medium there was no decrease in copper sorption. For the amido SPCs this indicates the stability of the amide bond to these conditions. In general, there were significant increases in Cu^{2+} sorption capacity upon contact with base. This must have been caused either by cleaning of the material or by residual base after washing which can positively impact chelation by aiding in deprotonation of the ligand. This is a second set of experiments that have validated the stability of amido-SPC materials.

3.5 IDA modified SPCs

The final amino acid considered was iminodiacetic acid (IDA). IDA or diglycine is also a chelating molecule. IDA has one less acetate group than NTA. IDA has three coordinating groups (Figure 3.57).

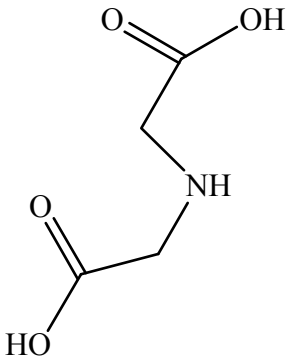

Figure 3.57. Iminodiacetic acid (IDA)

IDA has been immobilized on many solid supports to yield an array of commercially available chelating materials (e.g. Amberlite IRC-748 from Rohm and Haas).[44] Typical uses of these materials include the separation of first row transition metal ions from aqueous media. However, most often the attachment of IDA to a solid support involves the alkylation of the IDA group.[116] For example Figure 3.58 shows the attachment of IDA to iodopropylsilane functionalized silica gel.

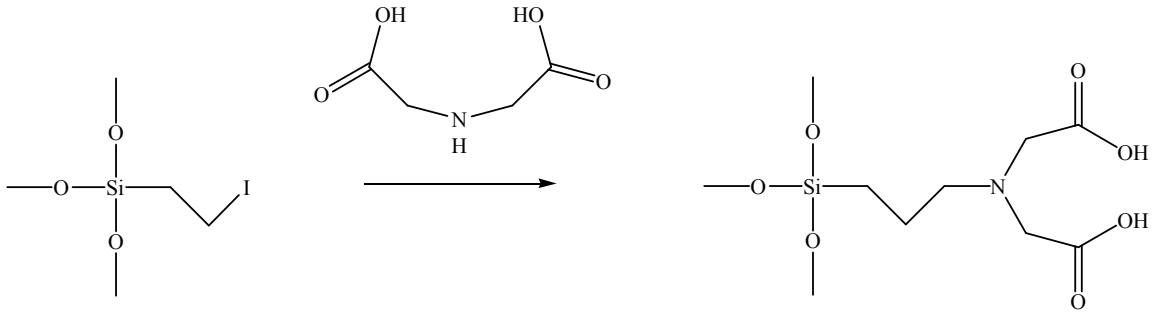

Figure 3.58. Synthesis of iminodiacetic acid (IDA) functionalized silica gel.

As a result the tridentate nature of the IDA chelator is kept intact with the exception that the secondary amine is converted to the tertiary amine (Figure 1.7). BP-2 is the SPC most similar to these commercially available IDA materials (Figure 3.16). However, in this work the attachment will proceed by the formation of an amide bond between one of the IDA acetate groups and a SPC amine group. This will yield an amido-amino-monoacetate immobilized ligand. This is one less acetate than that of BP-NT and WP-NT. However, to proceed with this pathway requires the protection of the secondary amine. This prevents polymerization of the ligand prior to reaction with the SPC substrate.

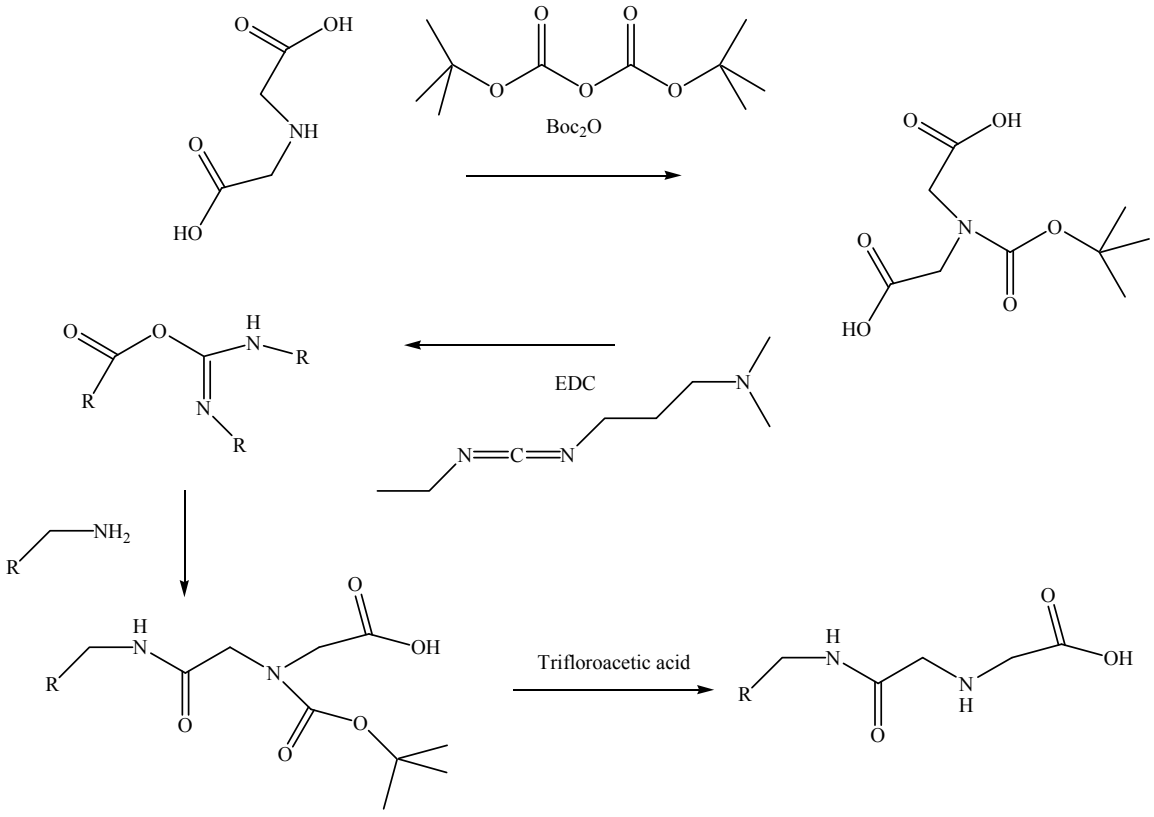

Figure 3.59. Synthesis of iminodiacetic acid (IDA) functionalized SPC.

Thus a reaction scheme has been used that is commonly used for peptide preparation.[117] First the secondary amine is protected with di-tert-butyl dicarbonate (Boc_2O). Next the water soluble 1-ethyl-3-(3-dimethylaminopropyl) carbodiimide (EDC) activates the carboxylic acid towards amide formation with BP-1 amine groups. This proceeds through O-acylisourea intermediate which can react with the amine to give the desired product. However rearrangement of O-acylisourea can take place to form an N-acylurea.[117]

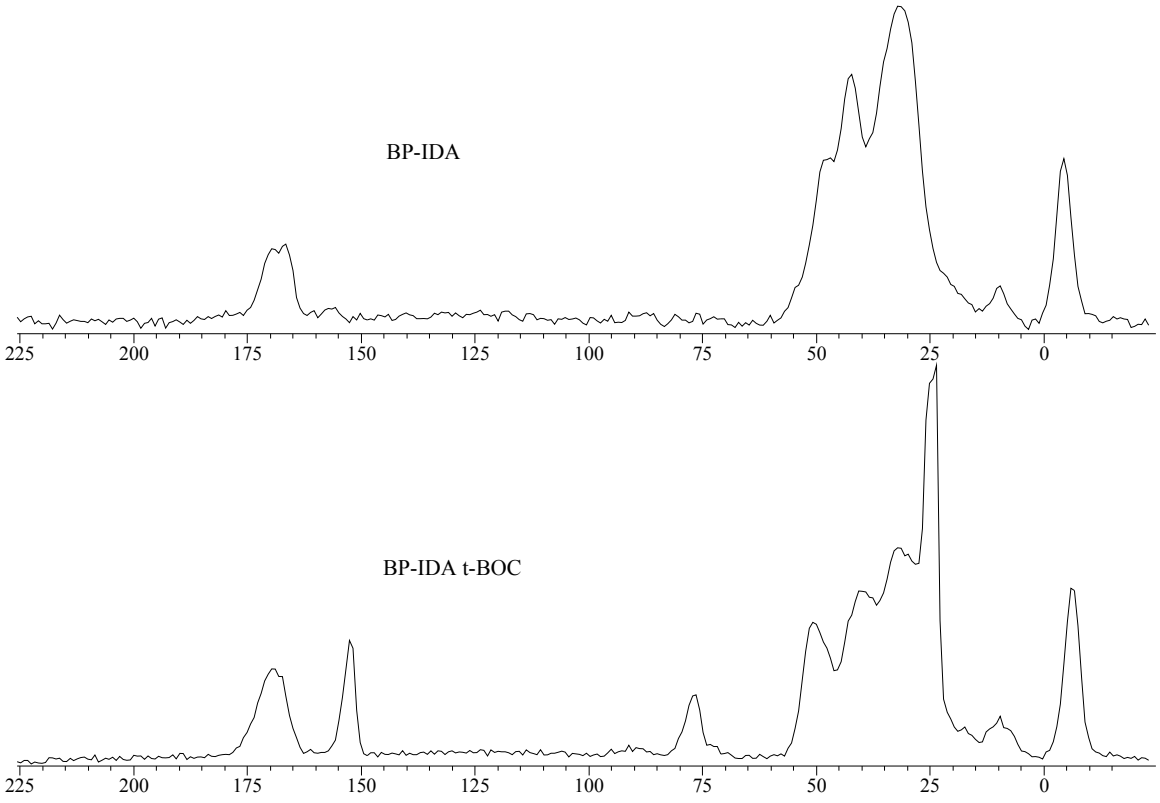

Figure 3.60. Both spectrum ppm. (Top) CP/MAS ^{13}C NMR at 126 MHz of t-Boc protected BP-IDA (7.5:1 MTCS:CPTCS). (Bottom) CP/MAS ^{13}C NMR at 126 MHz of BP-IDA after deprotection (7.5:1 MTCS:CPTCS).

Figure 3.59 shows the synthetic pathway to BP-ID. IDA was boc protected before attachment to the amine groups of BP-1 7.5:1 MTCS:CPTCS by EDC activation. The

resulting material possessed a large weight increase indicating the addition of the boc protected IDA to the SPC. The attachment was confirmed with CP/MAS ^{13}C solid state NMR (Figure 3.60 (bottom)). The ^{13}C NMR shows the carbamate carbon signal at 154 ppm (-N-C(O)-O-)as well as the tertiary carbon of the protecting group at approximately 77 ppm(-OC$(CH_3)_3$). The three methyl carbons of each boc group have a signal at approximately 24 ppm (-C(C$H_3)_3$). At this point the material was tested for Cu^{2+} sorption by way of batch analysis. The Cu^{2+} sorption was negligible (0.04 mmol/g). To remove the boc protecting group a 10% triflouroacetic acid (TFA) solution in dichloromethane (DCM) was used. The resulting material was dubbed BP-ID. After deprotecting for 4 hrs the Cu^{2+} sorption capacity at pH 2 had increased to 0.19 mmol per gram sorbent. After 24 hours in contact with the same solution the Cu^{2+} sorption capacity increased slightly to a value of 0.22 mmol Cu^{2+} per gram BP-ID at pH 2. However, this represents the functionalization of only a small fraction of BP-ID amines. Despite modest functionalization, deprotection was confirmed by CP/MAS ^{13}C NMR (Figure 3.60 top). The disappearance of the broad peaks at 154 ppm, 77 ppm and 24 ppm indicate the absence of the boc group. The broad peak at 170 ppm is attributed to the acetate and amide groups (-NC(O)-CH_2, -CH_2CO_2H). In both spectra there appears to be some resolution of these groups. Again, the peak at 52 ppm is attributed to the acetate methylene groups on the ligand (-N-CH_2-COOH). The peak at 43 ppm may be attributed to the amide methylene groups (-N-C(O)-CH_2-N-). Table 3.11 represents data derived from elemental analysis of BP-ID and the precursor BP-1. The increased carbon and nitrogen are indicative of ligand loading however the C/N ratio for BP-ID is unusual. The C/N ratio of the BP-1 prceursor is approximately 4. The C/N ratio of the ligand after

deprotection is also 4. Therefore addition of the ligand should have no effect on the C/N ratio. However, data from elemental analysis indicates an increase in the C/N ratio for the BP-ID protect. For this to occur one of three things could occur. 1. A side reaction whose product is rich in carbon. EDC can react with amines to form a guanadine type product. However the guanidine product would be rich in nitrogen relative to carbon (7C:3N). As a result the C/N ratio would decrease. 2. The deprotection is incomplete. The pendant ligand is rich in carbon prior to deprotection (9C:1N). However, the 13C NMR of BP-ID shows no signs of the boc group. 3. Excess triflouroacetic acid or methylene dichloride. Deprotecting group or solvent may remain in the pores of the SPC. This would greatly enrich the carbon content of BP-ID.

Table 3.11. Data derived from elemental analysis for BP-ID aminoacetate modified SPC material. BP-ID is prepared from BP-1 (PAA).

SPC	C (mmol/g)	H (mmol/g)	N (mmol/g)	C/N
BP-1	10.68	25.30	2.67	4.00
BP-NT	14.63	42.50	3.24	4.52

A Cu^{2+} pH profile for BP-ID (Figure 3.61) shows only a slight increase in sorption capacity at pH 3 relative to pH 2. The affinity for Cu^{2+} drops off dramatically at pH 1. The capacity for copper drops off sharply at pH 1. This is due to a lower formation constant for the BP-ID-Cu^{2+} complex relative to BP-DT, BP-ED or BP-NT. This drop off is similar to that for BP-2. The weaker sorption for BP-ID can be explained in terms of the decrease in coordinating groups in the ligand. At most BP-ID is a tridentate ligand. It contains one amide, a secondary amine and a carboxylate group. The amide group will

only coordinate weakly to Cu^{2+} because of amide resonance stability. Thus, only the amine and carboxylate remain as relatively good coordinating ligands.

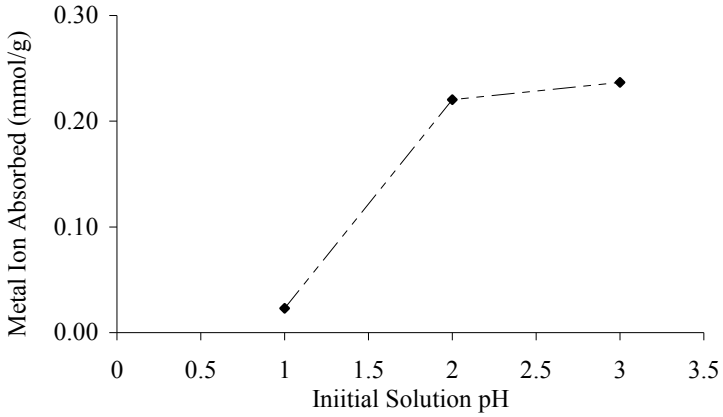

Figure 3.61. Batch Cu^{2+} pH profiles for BP-ID. Single metal ion solutions contained 1.5 g/L of Cu^{2+}. 10 mL of solution was equilibrated with 0.10 g BP-ID.

In conclusion, BP-ID represents an interesting route to an SPC sorbent material. This is the first time a relatively complex synthetic route has been used to successfully prepare a chelating SPC. Thus this material stands as proof of concept for the production of interesting materials through this route. However, as a result of the relative synthetic complexity and the problems associated with the deprotection process it is unlikely that this material has any potential as a commercial material. Therefore, any future investigations of this material will address differences in selectivity relative to the amido-SPC materials described in this chapter.

CHAPTER 4: Applications

4.1. Acid Mine Drainage (AMD)

4.1.1 Introduction. The issue of acid mine drainage was expressed in detail in section 1.2.2. In the current section, novel SPC materials have been applied to the remediation of water polluted as a result of AMD in western Montana. A consequence of the mining legacy is that large portions of western Montana are now subject to the menace of acid mine drainage (AMD). There are numerous abandoned mining sites, large and small, throughout the region. One such region is the Colorado district. The Colorado district was the original name for what is known as the Wickes mining district. The Colorado/Wickes district is 20 miles south of Helena, MT. The lode ores of the Colorado/Wickes district were composed of a combination of silver, gold, lead, copper and zinc in the correct proportion for smelting the ore. Consequently, the area was mined heavily between 1869 and 1957. In total the Alta mine and its sister mines in the district produced over $47 million in gold, silver, lead and copper. However, since abandonment, the streams and creeks in the region have become heavily polluted with metal ions. Alta Creek is one such polluted stream located by Helena, Montana. Researchers from the Department of Chemistry at Caroll College, Helena, have identified this stream and other near by streams (e.g. Corbin Creek) as a concern. Samples were taken from Alta Creek at various points along its flow. The metal ion content of one of the samples, taken at a point where contamination levels are typical, is displayed in Table 4.1. The creek at this point is contaminated with approximately 1400 mg/L of several metal ions.

Table 4.1. Table showing the concentrations of several metal ions in the water sample collected by workers from Carroll College, Helena, MT.

	Metal	As	Cd	Pb	Zn	Mn	Fe	Cu	Mg	Ca	Co	Al
Feed conc.	mg/L	1.40	0.26	0.31	28.8	512	373	0.48	73.7	365	0.22	34.1
Total feed	mg	0.28	0.052	0.062	5.76	102.4	74.6	0.096	14.74	73	0.044	6.82

The sample is rich in manganese, iron (Fe^{3+}), magnesium, calcium and aluminum. The sample also contains As, Cd, and Pb, which are well documented toxins.[11;12;18] The goal was the removal of all toxic metals from the stream sample. The sorption of manganese from aqueous solution can be a challenge. In general, most complexing agents form weak coordination compounds with Mn^{2+}. There is no solid phase chelating IX material, to the best of our knowledge, which can selectively remove manganese in the presence of other transition metal ions. Manganese is of value, therefore for commercial operations isolation of Mn^{2+} is typically achieved by removing all other metals from solution. However, since the water in Alta creek scenario is part of an ecosystem, all of the potentially toxic metals including manganese must be removed. The treated water must be free of metal ion pollutants. BP-ED removes a broad spectrum of metal ions thus may be of use for this application. BP-ED has shown excellent metal ion sequestration characteristics and a modest affinity for manganese has been confirmed (Figure 3.21). It was noted, that BP-ED is not selective for manganese in the presence of other metal 1st row transition metal ions. This heavily polluted solution provided an opportunity to determine the potential of BP-ED for real world applications.

4.1.2 Treatment 1: BP-ED. A 5 mL column was packed with BP-ED and fed, under flow conditions, with a 200 mL portion of the feed. The breakthrough profiles resulting from this experiment can be found in Figure 4.1 and Figure 4.2.

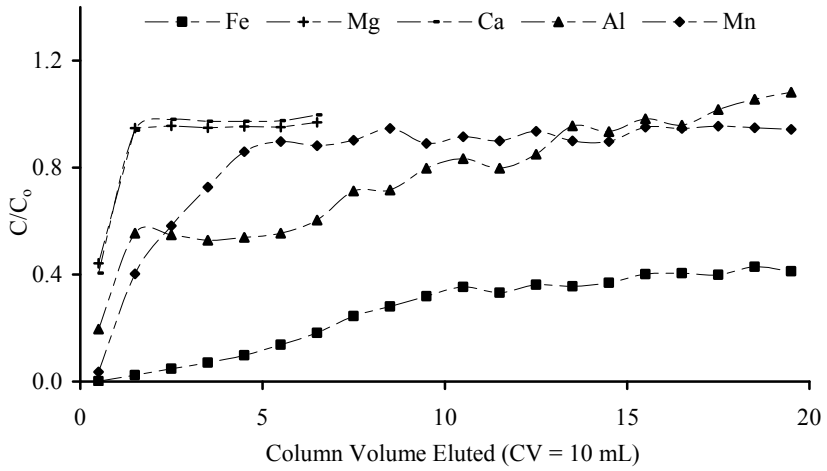

Figure 4.1. Breakthrough profiles for Fe, Mg, Ca, Al and Mn using BP-ED (CPTCS only). Flow rate was 0.5 mL/min. Column volume was 5 mL. Feed solution composition found in Table 4.1.

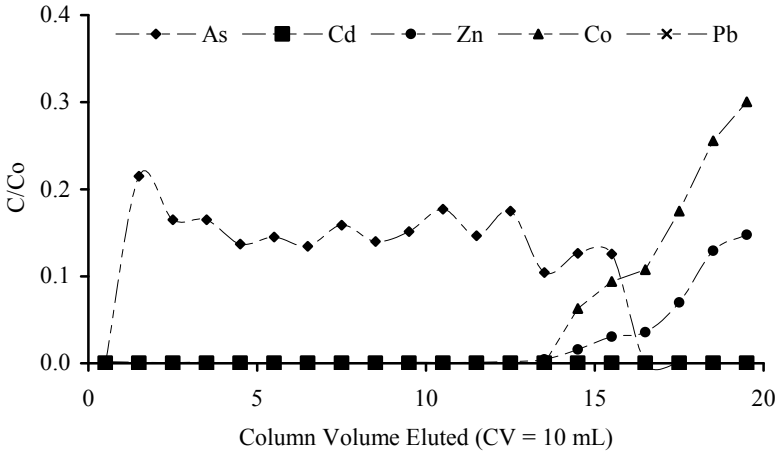

Figure 4.2. Breakthrough profiles for As, Cd, Zn, Co and Pb using BP-ED (CPTCS only). Flow rate was 0.5 mL/min. Column volume was 5 mL. Feed solution composition found in table 4.1.

It is clear from the figures shown above that BP-ED has an affinity for Fe and Al and a slight affinity for Mn. BP-ED does not extract magnesium or calcium to any

appreciable extent. This is in agreement with the data presented for BP-ED in section 3.3. BP-ED removes all of the Cd, Zn, Co and Pb from approximately 120 mL of the feed solution. Appreciable levels of each metal are detected from this point on. Interestingly, BP-ED removes ~80% of the As in the initial stage of the experiment. 100% of As is removed towards the end of the experiment. BP-ED contains a large portion of amine groups that are protonated at low pH and therefore positively charged. As a result, arsenate (As(V)), the dominant species in this pH regime, is extracted by the quaternized amines. As the experiment proceeds metal ions such as Fe^{3+} form coordination complexes with the BP-ED ligands. If the complex formed is positively charged, then it will also have the capacity to extract arsenate. There is much precedent for the use of quaternary amine IX materials and Fe loaded IX materials for arsenic removal.[118;119] Once the 200 mL feed solution was treated, the column was eluted with 30 mL of 4.5 mol/L H_2SO_4 (Figure 4.3 and Figure 4.4).

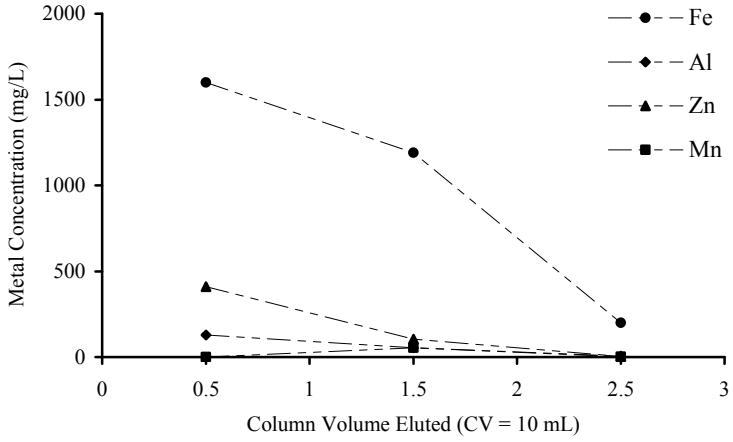

Figure 4.3. Strip profiles for Fe, Zn, Al and Mn from BP-ED (CPTCS only). The flow rate was 0.5 mL/min. Column volume was 5 mL. The strip solution was 30 mL of 4.5 mol/L H_2SO_4.

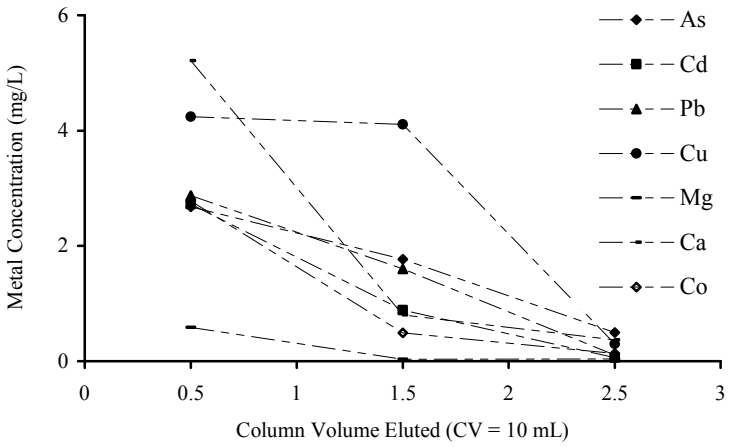

Figure 4.4. Strip profiles for As, Cd, Cu, Co, Pb, Ca and Mg using BP-ED (CPTCS only). The flow rate was 0.5 mL/min. Column volume was 5 mL. The strip solution was 30 mL of 4.5 mol/L H_2SO_4.

Table 4.2 provides the concentration of each metal ion, in the final 10 mL column fraction of feed solution, after passing through the BP-ED column. Table 4.2 also includes the concentration of each metal ion in the 30 mL of 4.5 mol/L H_2SO_4 strip solution after elution of the metal ions.

Table 4.2. Table showing the levels of several metal ions in the final 10 mL column volume treated and in the 30 mL of 4.5 mol/L strip solution.

	Metal	As	Cd	Pb	Zn	Mn	Fe	Cu	Mg	Ca	Co	Al
Col. 20	mg/L	0	0	0	4.3	483	154	0	79.7	374	0.07	36.9
Strip	mg/L	1.64	1.22	1.52	172	28.8	996	2.88	0.22	2.12	1.13	62.4

It is clear that although BP-ED does not remove all of the metal ions present in the feed solution it does remove most of the toxic metal ions to very low levels. For example Co^{2+}, Cd^{2+} and Pb^{2+} have all been removed from the feed solution, and continue to be removed to negligible levels, after treatment of 200 mL feed solution with the 5 mL of BP-ED SPC. The strip data indicates that, as expected, BP-ED preferentially removes

Fe^{3+} over Mn^{2+} despite the larger concentrations of Mn^{2+} in the feed. In conclusion, BP-ED can remove a significant amount of metal ions from the feed solution. Despite this, arsenic in the flow through is a concern, as well as the high levels of Fe, Mn and Al. To address these issues BP-ED was used in tandem with another SPC material.

4.1.2 Treatment 2: Zr-BP-AP followed by BP-ED

It was demonstrated in the previous section (section 4.1.1) that BP-ED alone was unable to remove the arsenic to negligible levels for the entirety of the breakthrough experiment, but showed promise for the extraction of many of the low level toxic metal ions. Thus, a strategy was employed in which a pre-treatment with Zr-BP-AP SPC was used. [100]BP-AP is a phosphonic acid modified SPC. BP-AP selectively removes tri- and tetra-valent metal ions in the presence of divalent metal ions. BP-AP has a very strong affinity for zirconium. The formation constant is large enough to prevent removal of Zr^{4+} from BP-AP when treated with a 4.5 mol/L H_2SO_4 strip solution. When zirconium is loaded onto BP-AP the resulting material is termed Zr-BP-AP. Previous work indicates that Zr^{4+} bonds to BP-AP in a 1:1 mode of complexation with the BP-AP phosphonic acid ligands (Figure 4.5).[100]

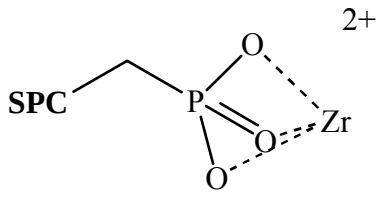

Figure 4.5. A Zr^{4+} ion chelated by a phosphonate ligand of Zr-BP-AP. SPC represents the remainder of the material. Residual charge is 2+.

Phosphonic acid when fully deprotonated has a -2 charge. Hence, when Zr^{4+} is captured in a 1:1 fashion each complex created will have a residual charge of +2. The positively charged Zr-BP-AP SPC material can remove the arsenate anion across a wide range of pH. Pre-treating the feed solution described in the previous section with Zr-BP-AP should remove the arsenic thus alleviating the issue of arsenic in the flow through when the solution is subsequently treated with BP-ED. Thus, a 5 mL column was packed with BP-AP and challenged under flow conditions with a 200 mL portion of the same feed solution used in the previous experiment. The breakthrough profiles resulting from this experiment can be found in Figure 4.6 and Figure 4.7.

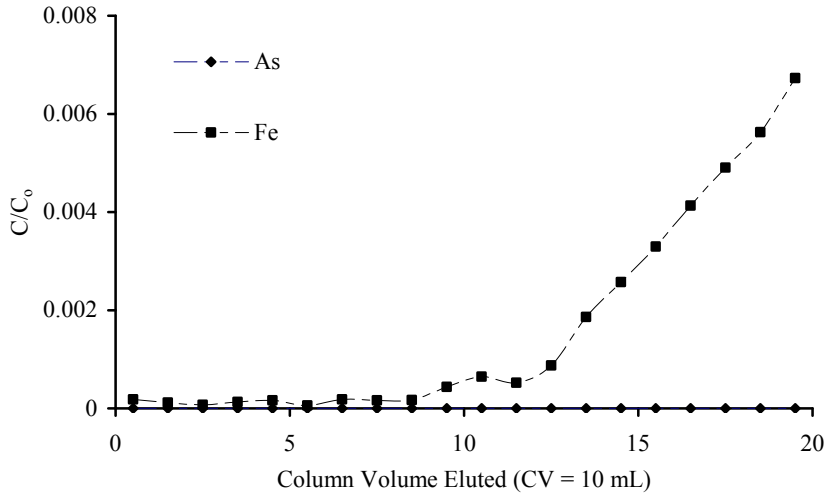

Figure 4.6. Breakthrough profiles for As and Fe using Zr-BP-AP. Flow rate was 0.5 mL/min. Column volume was 5 mL.

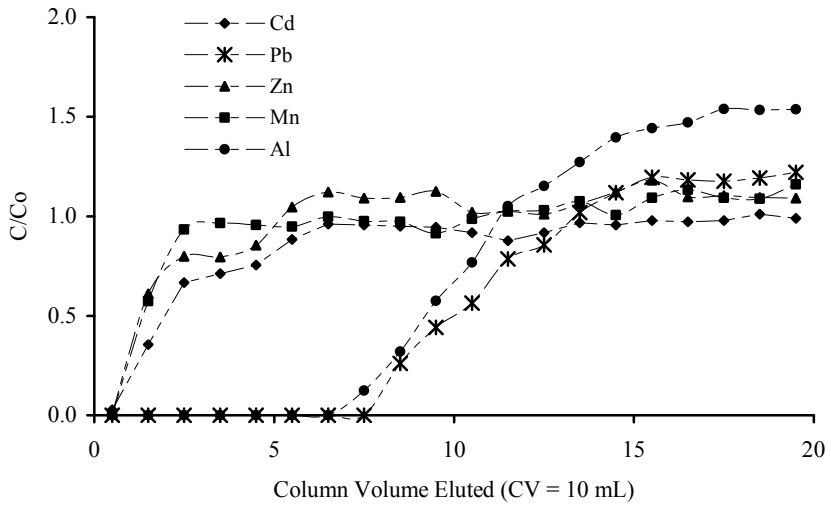

Figure 4.7. Breakthrough profiles for Cd, Pb, Zn, Mn and Al using Zr-BP-AP. Flow rate was 0.5 mL/min. Column volume was 5 mL.

Figure 4.6 shows the breakthrough profiles for iron and arsenic when the solution is treated with Zr-BP-AP. It is apparent that the BP-AP SPC does remove the arsenic to concentrations below detection. In addition the Zr-BP-AP sequestered a large amount of Fe^{3+}. Hence, both Fe and As are removed by the BP-AP pretreatment. Aluminum is also removed from the solution by the Zr-BP-AP column. However, the concentration of aluminum in the eluent is greater than the feed concentration ($C/C_o>1$) shortly after aluminum is detected in the eluent. This is indicative of aluminum displacement by Fe^{3+}. Zr-BP-AP also removes a significant amount of several of the divalent metal ions from the feed solution (Figure 4.8).

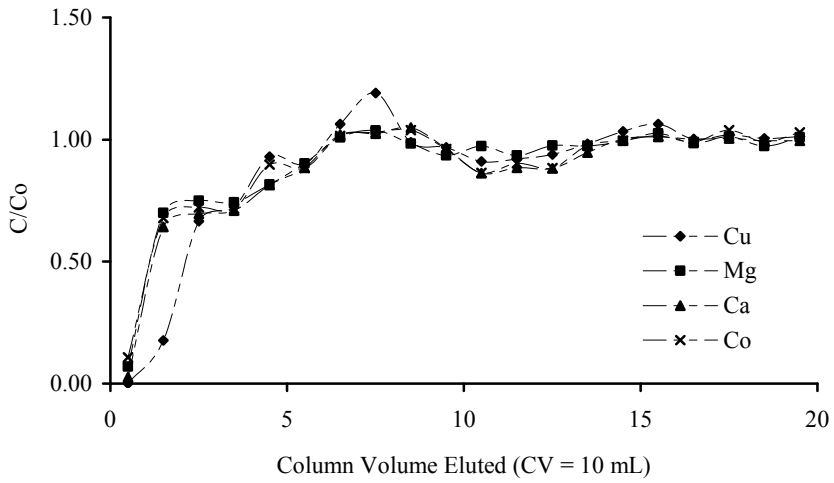

Figure 4.8. Breakthrough profiles for Cu, Mg, Ca and Co using BP-ED (CPTCS only). Flow rate was 0.5 mL/min. Column volume was 5 mL. Feed solution composition found in Table 4.1.

There are several possibilities for the observed removal of cations by Zr-BP-AP. Some physical sorption of ions to the silica gel surface may be possible. Cations such as Fe^{3+} can form associations with the oxy anions of arsenic. As a result immobilized arsenate or arsenite may remove cations from solution. Polymer amine groups may be responsible for capturing the cations. Further, the negative charge of the phosphonic acid groups may not have been neutralized by Zr^{4+}. Residual negative charge may be responsible for the capture of cations. Elemental analysis calculations show that the ratio of Zr^{4+} to P in the Zr-BP-AP material is roughly 1:1. Therefore, there should be no vacant phosphonic acid sites. This issue will not be addressed in this work. Table 4.3 provides the concentrations of the metal ions in the final column volume of treated feed solution. Table 4.3 also provides the concentrations of the metal ions in 30 mL of a 4.5 mol/L strip solution.

Table 4.3. Table showing the concentrations of all metal ions in the final 10 mL column volume treated after pretreatment with Zr-BP-AP. Concenrations in the 30 mL of 4.5 mol/L strip solution also provided.

	Metal	As	Cd	Pb	Zn	Mn	Fe	Cu	Mg	Ca	Co	Al
Col. 20	mg/L	0.00	0.19	0.38	31.4	594	2.51	0.57	90.9	448	0.21	52.4
Strip	mg/L	1.6	1.2	1.5	172.4	28.8	996.3	2.9	0.2	2.1	1.1	62.5

It is clear that the goal of removing the arsenic from the solution has been accomplished. However, it would appear that the material has also sequestered large amounts of other metal ions. The 200 mL of treated feed solution was then treated with a 5 mL column of BP-ED in the same manner as that described for experiment 1. Table 4.4 provides a summary of the results.

Table 4.4. Table showing the concentrations of all metal ions in the final 10 mL column volume treated after treatment with BP-ED. Concenrations in the 30 mL of 4.5 mol/L strip solution also provided.

	Metal	As	Cd	Pb	Zn	Mn	Fe	Cu	Mg	Ca	Co	Al
Col. 20	mg/L	0	0	0	0.003	481	0.029	0	74.9	359	0	25.3
Strip	mg/L	0.0	0.0	0.2	4.2	1.2	20.9	3.5	0.2	1.2	0.0	11.3

In the final 10 mL of pretreated solution passed through the BP-ED column there are negligible amounts of As, Cd, Pb, Cu and Co. There are also only very small amounts of Zn and Fe. Metals that have not been fully extracted from the 200 mL solution include Mn and Al as well as Mg and Ca. Thus, with the exception of Mn and Al the treatment strategy was very successful in removing many of the toxic heavy metal ions from solution. It is expected that Mn and Al have not been sequestered. The pH profile data from section 2.3 indicate that BP-ED shows the lowest affinity for these two metals out of all the metals tested. In conclusion BP-ED shows promise as a tool for the remediation

of waters affected by AMD. However, the use of an anion removal SPC material prior to BP-ED is required.

4.2 Laterite HPAL Treatment.

4.2.1 Introduction. The issue of processing mine solutions and in particular Laterite leach solutions was discussed in detail in section 1.2.4. In the current section two of the novel SPC materials discussed in chapter 3 have been applied to a synthetic Laterite type solution. Quite often Laterite leach solutions contain high levels of nickel.[45] However, such solutions also contain high levels of trivalent iron as well as appreciable levels of copper, zinc and cobalt. A solution such as this can be passed over elemental iron to cement out the copper. This is an efficient and profitable process as copper cement is of reasonable value. As a consequence of the cementation process the iron is reduced to the ferrous form. Once this is accomplished the goal is to remove the Ni^{2+} from the Co^{2+}, Zn^{2+} and Fe^{2+}. After reviewing the data presented in chapter 3, it became clear that BP-ED and BP-NT are two novel SPC materials that may be appropriate for this application.

4.2.2 BP-ED. In order to test the ability of BP-ED to separate Fe^{2+}, Zn^{2+} and Co^{2+} from Ni^{2+} in an aqueous solution containing these metals in ratios similar to those found in a Laterite acid leach, a solution containing 2g/L Fe^{2+}, 0.8g/L Ni^{2+}, 0.1 g/L Zn^{2+} and 0.1 g/L Co^{2+} in a sulfate matrix at pH 1 was prepared. Laterite leach solutions are typically in this pH range (pH~1). This solution was fed to a packed column of BP-ED at 0.5 mL/min in order to selectively capture Ni^{2+}. The breakthrough profiles for all four metal ions are presented in Figure 4.9.

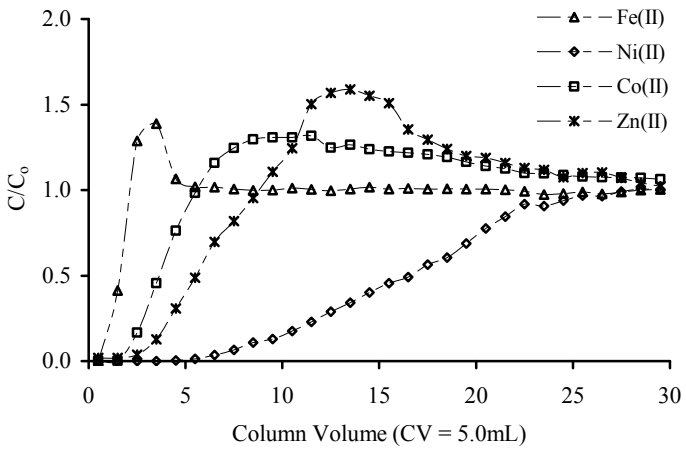

Figure 4.9. Breakthrough profiles for Ni, Zn, Co and Fe using BP-ED (CPTCS only). Flow rate was 0.5 mL/min. Column volume was 5 mL.

The first experiment used BP-ED prepared from CPTCS only functionalized silica gel. Clearly the BP-ED column (Figure 4.9) has only a slight affinity for Fe^{2+}, $Zn^{2+}$and Co^{2+} relative to Ni^{2+} which is extracted selectively. The eluent concentrations of Fe^{2+}, Zn^{2+} and Co^{2+} quickly exceed the feed solution concentration (C/Co>1), as Ni^{2+} effectively competes with all three metals for sorption sites. The eluent concentration of each then returns to the concentration of the feed solution indicating that the separation is complete. However, as the extraction proceeds a small portion of composite turns slightly brown non-uniformly at the entrance to the column. This is indicative of the oxidation of Fe^{2+} to Fe^{3+}. Ferric iron is chelated readily by the BP-ED. The formation complex for an EDTA-Fe^{3+} complex (K_{MY} = 1.3 x 10^{25}) in solution is much greater than that of Ni^{2+}. Thus Fe^{3+} should successfully compete for BP-ED sorption sites. Figure 4.10 illustrates the strip profile of BP-ED when the fully loaded column is fed with 30 mL of a 4.5 mol/L H_2SO_4 strip solution.

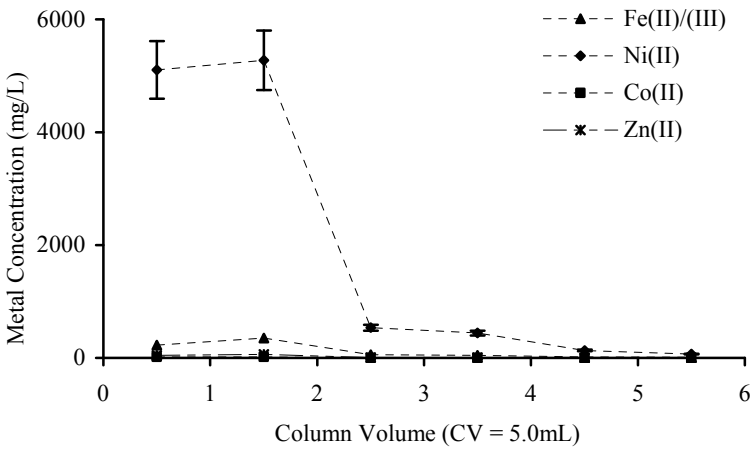

Figure 4.10. Breakthrough profiles for Ni, Zn, Co and Fe using BP-ED (CPTCS only). Flow rate was 0.5 mL/min. Column volume was 5 mL.

The purity of nickel in the strip is greater than 90% (Table 4.5). The contaminant metal is most likely trivalent iron. Ferrous iron was easily displaced from the column sorption sites by Ni^{2+} in the early stages of the experiment.

Table 4.5. Table showing the concentrations of all metal ions in the 30 mL 4.5 mol/L strip solution.

CYCLE	$Fe^{2+/3+}$ (mmol/g)	Zn^{2+} (mmol/g)	Co^{2+} (mmol/g)	Ni^{2+} (mmol/g)	Ni^{2+} Purity %	C_f	TOTAL (mmol/g)
1	0.025	0.0044	0.0012	0.39	92.8	2.30	0.42
2	0.034	0.0022	0.0010	0.37	90.8	2.19	0.41
3	0.038	0.0017	0.0011	0.37	90.2	2.16	0.41
4	0.043	0.0019	0.0009	0.37	89.1	2.24	0.42

Isolated oxidation is most likely due to imperfections in the frit material, non-uniform composite packing or surface catalyzed oxidation by adsorbed oxygen. This may allow air pockets to form in areas close to the inlet thus promoting the likelihood of oxidation in these locations. The multi-element experiment was repeated four times (Table 4.7). The brown composite appears in the same position in all four cycles

reinforcing the conclusion that oxidation is caused by imperfections in the column rather than by the BP-ED material. Slurry packing, the use of a pulse-less pump, degassing of the challenge solution, re-engineering of the column and the introduction of a reducing agent into the challenge solution are all options for alleviating the problem of oxidation. In this way Ni^{2+} purity should approach 99.9%. Table 4.7 provides data for each of four consecutive load strip cycles. It appears that the Ni^{2+} strip solution purity decreases slightly by strip cycle 4. In contrast the small amount of Fe in the strip solution increases. This indicates that the problem of Fe oxidation may be gradually increasing with each load/strip cycle. Figure 4.11 presents the breakthrough profiles for a similar experiment using BP-ED 10:1 MTCS:CPTCS as opposed to CPTCS only BP-ED. The profiles are similar to that for the BP-ED CPTCS only experiment.

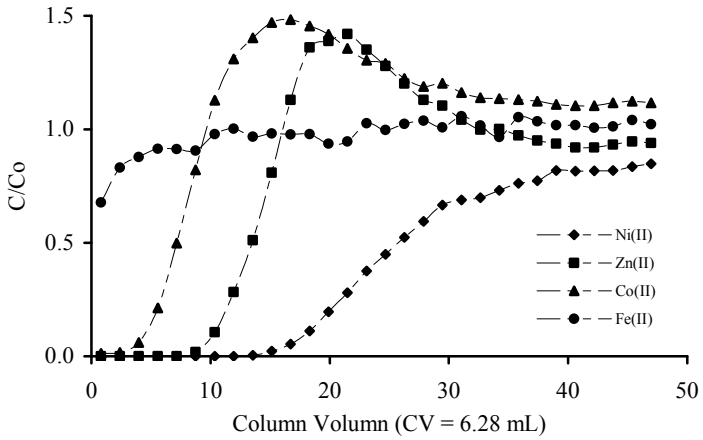

Figure 4.11. Breakthrough profiles for Ni, Zn, Co and Fe using BP-ED (10:1 MTCS:CTPCS). Flow rate was 0.5 mL/min. Column volume was 5 mL. Feed solution pH 1.

The concentrations of each metal ion in the 4.5 mol/L sulfuric acid strip solution for 10:1 BP-ED are shown in Table 4.5. The quantity of Ni^{2+} sequestered per mL of SPC has increased substantially from a value of 0.19 mmol/mL to 0.31 mmol/mL at pH 1. The

Ni^{2+} purity has increased only slightly as the concentrations of Fe, Zn and Co have also increased. A third experiment was conducted to determine the effect of pH. The same feed solution at pH 2 was fed to a column of 10:1 BP-ED. The breakthrough profiles are presented in Figure 4.12.

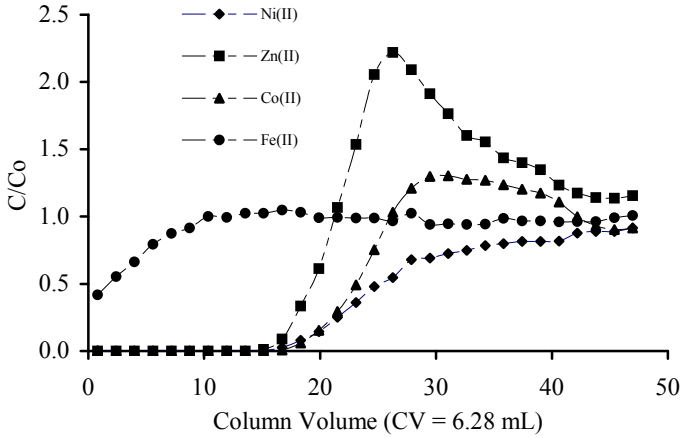

Figure 4.12. Breakthrough profiles for Ni, Zn, Co and Fe using BP-ED (10:1 MTCS:CTPCS). Flow rate was 0.5 mL/min. Column volume was 5 mL. Feed solution pH 2.

The order of preference for the metal ions at pH 2 mimics that of the order of preference for the metal ions at pH 1. However, the breakthrough profiles at pH 2 appear substantially different from that at pH 1. In particular Co, Zn and Ni are 100% extracted for the majority of the experiment. After approximately 18 column volumes of feed solution have passed through the column, all three metals begin to show appreciable concentrations in the flow through. However Ni^{2+} quickly displaces Co^{2+} followed by Zn^{2+} from BP-ED sorption sites. This is caused by the relative formation constants of these metals with the sorbent. In the acidic strip solution the concentration of Ni^{2+} indicates an increased loading relative to pH 1 (0.35 mmol/mL). However, because a greater quantity of Zn and Fe were found in the strip the Ni^{2+} purity was modest at 88%.

Oxalic acid (Figure 4.13) is a reducing agent. Oxalic acid is a relatively strong acid and is also a chelator.

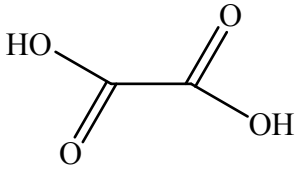

Figure 4.13. Oxalic acid.

The addition of oxalic acid to the feed solution was hypothesized to reduce any Fe^{3+} to Fe^{2+} according to Equation 4.1.

$$(COOH)_2 + 2Fe^{3+} \rightarrow 2Fe^{2+} + 2CO_2 + 2H^+ \quad (4.1)$$

If oxidation could be prevented then Ni^{2+} purity should increase. Oxalic acid was added to the pH 1 feed solution so that the concentration of oxalic acid in the feed was 0.2 g/L. A column of BP-ED was then fed the oxalic acid modified feed solution. The breakthrough profiles for this experiment can be found in Figure 4.14.

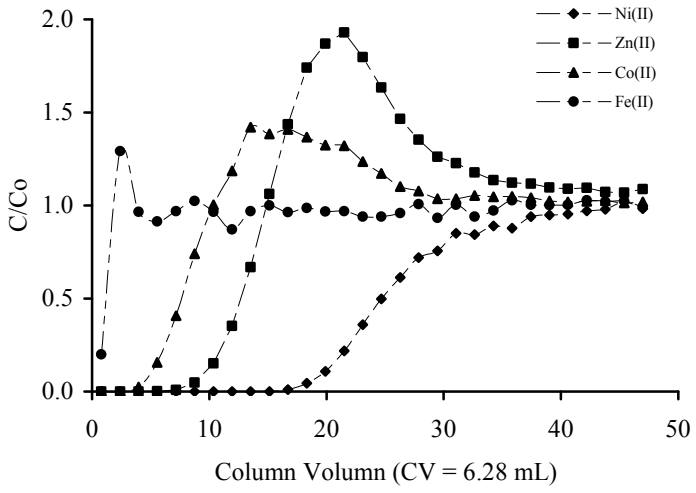

Figure 4.14. Breakthrough profiles for Ni, Zn, Co and Fe using BP-ED (10:1 MTCS:CTPCS). Flow rate was 0.5 mL/min. Column volume was 5 mL. Feed solution pH 1. Oxalic acid included.

The order of preference is the same as for the same experiment conducted without oxalic acid. The data in Table 4.6 indicates that the oxalic acid addition, led to no improvement in the purity of Ni^{2+} in the strip solution. In a further experiment, the addition of 0.4 g/L oxalic acid led to the formation of an insoluble iron oxalate complex. In conclusion, BP-ED prepared with MTCS (as opposed to CPTCS only) is able to selectively remove Ni^{2+} from other divalent transition metal ions. However the BP-ED has an affinity for Zn, Co and Fe also. Thus Ni^{2+} must displace these metal ions from their sorption sites in order to achieve high purity. As a result small amounts of each metal ion relative to the feed concentration of each are detected in the acidic strip solution. The addition of a reducing agent did not increase the purity of Ni^{2+} in the strip. As a consequence it can be concluded that either the oxalic acid is not present in great enough quantities to prevent oxidation or that oxidation was not occurring. Oxidation may not occur at this pH because the equilibrium constant for the reduction process (Equation 4.1) decreases with pH.

Table 4.6. The table shows the concentrations (mmol/mL) of all four metal ions (Fe, Zn, Co and Ni) in the 30 mL 4.5 mol/L strip solution for each of the four experiments.

BP-ED	pH	Oxalic Acid (g/L)	$Fe^{2+/3+}$ (mmol/mL)	Zn^{2+} (mmol/mL)	Co^{2+} (mmol/mL)	Ni^{2+} (mmol/mL)	Ni^{2+} Purity %	C_f	TOTAL (mmol/mL)
CTPCS only	1.0	n/a	0.0129	0.0023	0.0006	0.200	92.7	2.30	0.22
10:1	1.0	n/a	0.0154	0.0041	0.0019	0.307	93.5	5.26	0.33
10:1	2.0	n/a	0.0265	0.0128	0.0080	0.350	88.1	5.44	0.40
10:1	1.0	0.2	0.0199	0.0025	0.0009	0.310	93.1	5.78	0.33

4.2.3 BP-NT. In order to test the ability of BP-NT to separate Fe^{2+}, Zn^{2+} and Co^{2+} from Ni^{2+} in an aqueous solution containing these metal in ratios similar to those found in a Laterite acid leach, a solution containing 2g/L Fe^{2+}, 0.8g/L Ni^{2+}, 0.1 g/L Zn^{2+} and 0.1 g/L Co^{2+} in a sulfate matrix at pH 1.5 was prepared. Laterite leach solutions are typically in a lower pH range (pH ~1). However, the pH profile data in section 2.5 suggest that BP-NT will have only a slight affinity for Ni^{2+} in this pH regime. Therefore two experiments were undertaken at higher pH (pH 1.5 and pH 2.5). The synthetic solution at pH 1.5 was fed to a packed column of BP-NT at 0.5 mL/min in order to selectively capture Ni^{2+}. The breakthrough profiles for all four metal ions are presented in Figure 4.15. These experiments employed BP-NT prepared from 7.5:1 MTCS:CPTCS functionalized silica gel.

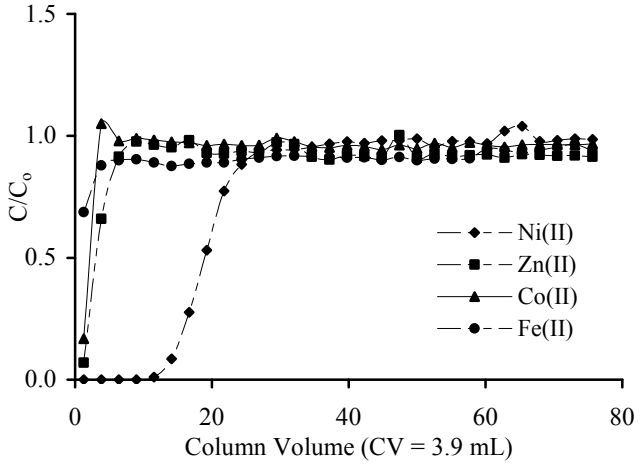

Figure 4.15. Breakthrough profiles for Ni, Zn, Co and Fe using BP-NT (7.5:1 MTCS:CTPCS). Flow rate was 0.5 mL/min. Column volume was 5 mL. Feed solution pH 1.5.

The data represented by the curves in Figure 4.15 indicates that at pH 1.5 BP-NT selectively removes Ni^{2+} in a manner different to that for BP-ED. BP-NT has no affinity for Fe, Zn or Co at pH 1.5. However, BP-NT only captures 0.22 mmol of Ni^{2+} per mL of

SPC (0.31 mmol/mL Ni^{2+} for BP-ED at pH 1). After applying the same 4.5 mol/L strip solution as before, the Ni^{2+} purity in the strip is displayed in Table 4.7. The purity of Ni^{2+} was 83 %, which is much lower than that for any of the BP-ED experiments described previously. This lower purity is due to a higher ratio of Fe^{3+}/Ni^{2+} for BP-NT relative to a higher ratio of Fe^{3+}/Ni^{2+} for BP-NT relative to BP-ED (0.2 and 0.05, respectively).

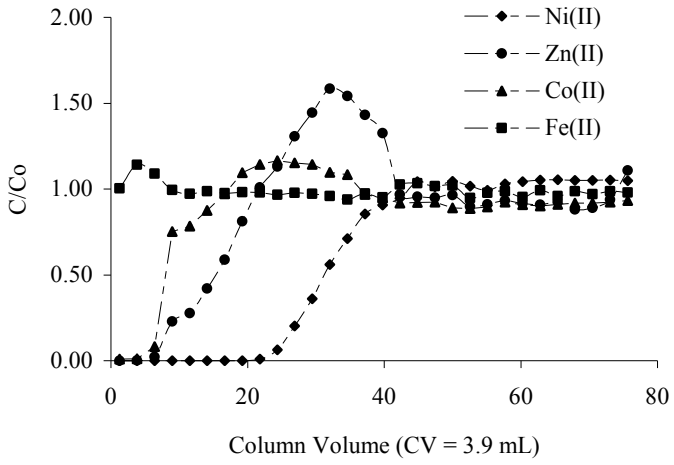

Figure 4.16. Breakthrough profiles for Ni, Zn, Co and Fe using BP-NT (7.5:1 MTCS:CTPCS). Flow rate was 0.5 mL/min. Column volume was 5 mL. Feed solution pH 2.5

A second experiment was conducted with the same feed solution but at a pH of 2.5. The breakthrough profiles for this experiment can be found in Figure 4.16. It is clear that the material maintains an affinity for Ni^{2+}. However, BP-NT also shows a significant affinity for Co and Zn at this pH. After the application of the 4.5 mol/L strip solution, it is clear that the amount of Ni^{2+} loaded has increased substantially (0.43 mmol/mL, Table 4.9). The Ni^{2+} purity has also increased substantially to 96.6%, which is the highest purity achieved thus far and the ratio of Fe^{3+} to Ni^{2+} is 0.02. This suggests that O_2 is the oxidant ($4H^+ + O_2 + 4e^- \rightarrow 2H_2O$).

Table 4.7. The table shows the concentrations (mmol/mL) of all four metal ions (Fe, Zn, Co and Ni) in the 30 mL 4.5 mol/L strip solution for each of the two BP-NT experiments.

BP-NT	pH	Oxalic Acid (g/L)	$Fe^{2+/3+}$ (mmol/mL)	Zn^{2+} (mmol/mL)	Co^{2+} (mmol/mL)	Ni^{2+} (mmol/mL)	Ni^{2+} Purity %	C_f	TOTAL (mmol/mL)
7.5:1	1.5	n/a	0.044	0.0012	0.0001	0.22	82.9	2.25	0.27
7.5:1	2.5	n/a	0.007	0.0077	0.0003	0.43	96.6	3.84	0.45

In conclusion, the extraction of Ni^{2+} from the synthetic leach solution with BP-NT is heavily dependent on pH. At pH 1.5 the data indicates an extraction of lower purity and lower sorption capacity than for any of the BP-ED experiments attempted. In contrast at pH 2.5 BP-NT yields the highest Ni^{2+} sorption capacity as well as the highest purity. The pH dependency noted for BP-NT is in agreement with the data presented in section 2.5. With regards to Ni^{2+} extraction from synthetic Laterite HPAL solutions these experiments provide incentive for the continued development and characterization of this novel class of SPC materials.

CHAPTER 5: Conclusions and Future Work

5.1 Mixed Silane SPCs

SPC materials have many advantages over crosslinked polystyrene resins. These include superior mass transfer kinetics and no shrink/swell characteristics. However, to this point polystyrene resins have, in general, had superior metal ion sorption capacities relative to SPC materials. The work presented in chapter 2 clearly demonstrated that this gap in sorption capacity can be overcome by the incorporation of MTCS into the synthetic pathway for SPC preparation. The use of MTCS in the production of SPC materials has greatly improved the SPC technology. The following lists the general conclusions for the study of mixed silane SPCs:

- MTCS can be successfully incorporated into the synthetic pathway as a mole fraction of the reagent silane mixture.
- The use of MTCS positively impacts the surface silane coverage by as much as 1 mmol/g. This is a relative increase of ~ 66 %.
- MTCS:CPTCS modified silica gel can be further modified with three distinct polyamines (PAA, PEI and PVA).
- Modifying MTCS:CPTCS silica gels with low molecular weight (MW ~ 1000) polyamines leads to decreased polymer loading and free amines relative to CPTCS only silica gel.
- Modifying MTCS:CPTCS silica gels with high molecular weight (MW > 10,000) polyamines leads to increased mmol/g quantities of free amines relative to CPTCS only silica gel.

- An optimum MTCS:CPTCS ratio has been determined for each of three polyamines. All optimum ratios contain more than 70% MTCS.
- Modifying these optimized SPC materials with metal selective ligands can lead to significant increases in ligand loading and 30% to 50% increases in metal ion sorption capacity.
- Materials modified with MTCS as well as CPTCS show elevated silica leaching relative to the CPTCS only materials. However, the silica leaching observed was negligible relative to the initial mass of SPC.

5.2 Acetate modified SPCs

There are fewer ligand modified SPC materials in comparison to ligand modified crosslinked polystyrene resins.[66;80]To remedy this, this work presents four novel SPC materials. These materials have been characterized in detail. In addition, the structural features of acetate modified SPCs have been investigated. It has been found that the nature of the polyamine can have profound impacts on specific metal ion selectivity. It has also been shown that slight variations in the ligand structure can significantly impact loading, sorption capacity and selectivity. The following lists some of the major conclusions drawn from the work presented in chapter 3.

- BP-2 shows negligible affinity for Ni^{2+} in acidic media. In contrast WP-2 shows appreciable affinity for Ni^{2+} in acidic media. The nature of the polyamine has been shown to impact the selectivity of these materials by governing the denticity and geometry of the sorption sites.

- BP-2 is a useful extractant for Cu^{2+} from Ni^{2+} at pH > 2. WP-2 is a useful extractant for Cu^{2+} at pH < 2 and may be a useful extractant for Ni^{2+} from Co^{2+} and Zn^{2+} at pH > 1.
- BP-1 and WP-1 can be modified with EDTA dianhydride to produce the amido-amino-acid SPCs BP-ED and WP-ED respectively. This has been confimed by CP/MAS ^{13}C NMR as well as elemental analysis. BP-ED displays greater ligand loading and sorption capacity relative to WP-ED.
- BP-ED is unable to separate Cu^{2+} from Ni^{2+} at acidic pH. However BP-ED can remove Ni^{2+} from Co^{2+} with high sorption capacity. BP-ED and WP-ED may be extremely useful Ni^{2+} selective materials.
- BP-1 can be modified with DTPA dianhydride to produce the amido-amino-acid SPC BP-DT. This has been confimed by CP/MAS ^{13}C NMR as well as elemental analysis.
- Elemental analysis indicates substantially lower ligand loading for DTPA relative to EDTA. As a result the Cu^{2+} sorption capacity for BP-DT is significantly lower than for BP-ED. Reduced loading may be due to increased ligand size or due to two attachment sites to the surface for each ligand.
- BP-1 and WP-1 can be modified with NTA dianhydride to produce the amido-amino-acid SPCs BP-NT and WP-NT respectively. This has been confimed by CP/MAS ^{13}C NMR as well as elemental analysis. BP-NT displays greater ligand loading and sorption capacity relative to WP-NT.

- BP-NT rivals BP-ED in terms of sorption capacity per gram for Cu^{2+}. In contrast to BP-ED, BP-NT can separate Cu^{2+} from Ni^{2+}. However pH profiles indicate that BP-NT may also be a Ni^{2+} selective material.
- BP-1 can be modified with boc-protected IDA using a carbodiimide (EDC) activating agent to produce the amido-amino-acid SPC BP-ID. This has been confirmed by CP/MAS ^{13}C NMR.
- BP-ID possesses inferior ligand loading relative to BP-ED and BP-NT. As a result Cu^{2+} sorption capacities are low. A Cu^{2+} pH profile indicates a heavy dependence of sorption on pH. BP-ID represents a novel path to a SPC IX material.
- In general the stability of the amide attachment has been shown to be robust. BP-ED maintained excellent sorption capacities over 1001 cycles. BP-NT and WP-NT withstood harsh acidic and moderate basic conditions for 72 hours with no loss in sorption capacity.
- The use of MTCS in the production BP-ED led to substantial increases in ligand loading and as a result significant increases in divalent metal sorption capacities were detected. MTCS is now used in commercial production.

5.3 Applications

Two of the major target applications for SPCs have been AMD and mine process solutions. Chapter 4 demonstrated that BP-ED and BP-NT have potential for treating such solutions. A polluted stream near Helena, Montana was treated with BP-ED in combination with an anion exchange SPC to remove much of the metal ion pollution. In

addition a synthetic Laterite HPAL solution was treated by BP-ED and BP-NT under a range of conditions. Both materials show great promise as tools for the selective removal of Ni2+. In general the following conclusions can be listed.

- A sample of water from Alta Creek near Helena, MT was heavily polluted by heavy metal ions from AMD. These metals include As, Cd, Co, Cu, Fe, Mn and Al.
- With the exception of As BP-ED removed all of the low level toxic metal ions and much of the Fe and Al. BP-ED did not remove Mg, Ca and Mn to any appreciable extent.
- Pretreatment with Zr-BP-AP removed all of the arsenic, as well as much of the Fe and Al. Some divalent metal ions were removed in appreciable amounts also.
- Following pretreatment BP-ED removed all of the remaining metal ions with the exception of Mg, Ca, Mn and some aluminum.
- BP-ED and BP-NT both selectively removed Ni^{2+} from a solution containing high levels of Fe^{2+} as well as low level Zn^{2+} and Co^{2+}. In general the order of selectivity was $Ni^{2+}>>Zn^{2+}>Co^{2+}>Fe^{2+}$ for both materials.
- The Ni^{2+} purity in the strip was generally greater than 90% for BP-ED. Impurities were thought to be a result of Fe^{2+} oxidation to Fe^{3+}. However the addition of a reducing chelator to the feed solution did not improve the purity. Varying the pH also had no effect on purity.
- The Ni^{2+} purity in the strip and Ni^{2+} sorption capacity was heavily pH dependent for BP-NT. At pH 1.5 the sorption capacity and purity of Ni^{2+} were much less

than that of BP-ED however elevating the pH to pH 2.5 brought about the highest sorption capacity and highest purity found to date.

- In general both materials show great promise for this application.

5.4 Future Work

SPC materials are remarkable tools for selective metal extraction from aqueous media. Outside of this work SPCs are being investigated for catalysis, anion removal, bacterial elimination and CO_2 sorption applications. The work presented here was an attempt to bring about a more detailed understanding of the technology by investigating structural features of the materials. As a result, MTCS is now utilized in the synthetic procedure for commercial production. Several novel materials have been produced and potential applications have been assessed. However, there remains much to explore with regards to this technology. Future experiments will lead to improvements in existing materials and the materials introduced in this work.

There are many trifunctional silanes that can be incorporated onto a silica gel surface. In this work CPTCS with MTCS and CPTCS with PTCS have been investigated. Polymer addition has not been attempted with CPTCS:PTCS modified silica gels. Experiments similar to those in chapter 2 will provide insight to the effect of the 'dummy' chain length i.e. methyl versus propyl. In future work CTPCS can be used in combination with other silanes such as phenyltrichlorosilane (PHTCS). This silane is much larger than the silane previously investigated. The effect on silane coverage, free amines and subsequent functionalization with metal selective groups can be assessed. The use of a bulky hydrophobic group may force the polyamine away from the surface and

into solution. This may positively impact mass transfer kinetics. A second silane combination of interest will be MTCS with chloromethylphenyltrichlorosilane (CMPTCS). This combination is unique given that the polyamine will now attach at the methyl phenyl silane as opposed to the propyl silane. Again, the extended distance from the surface and the variation in electrostatic properties of the surface are of interest. Extending the range of silanes used in the production of SPCs will allow for tailoring of these materials to specific applications. This includes applications outside of cation removal.

The work here has identified for the first time the importance of the type of polyamine i.e. PAA versus PEI. Molecular weight and polymer structure can greatly impact performance characteristics. In particular the polyamine impacts the site of sorption by influencing denticity and inherent geometry. This has been shown for WP-2 and BP-2. This study will be expanded to incorporate other existing materials such as WP-4 and CuWRAM. It will be of great interest to determine how each polymer affects the sorption of various metal ions. In addition ^{15}N labeling of polyamines will allow the acquisition of ^{15}N solid state NMR spectra that may provide more information regarding the groups that participate in coordination of Ni^{2+} and Cu^{2+} for WP-2 and BP-2. Variable temperature ^{13}C NMR experiments may also yield further insight into these materials. Through this technique it may be possible to resolve the amide and carboxylic functional groups for the amido-amino-acid SPCs. This study will extend the characterization of these materials.

With regards to the promising new class of amido-amino-acid modified SPCs their remains much to be studied. BP-ED has been characterized in detail. However,

extended investigations of potential applications are required. In addition, for this product to be commercially viable a process of scaling production will be necessary. BP-ED and BP-DT may have use in the selective sequestration of actinides and lanthanides for applications as discussed in chapter 1. EDTA and in particular DTPA have been used previously for the extraction of f-element cations. BP-DT possesses only modest metal ion sorption capacities. As a result methods towards increasing this capacity must be investigated if BP-DT is to be useful. To increase ligand loading, thus sorption capacity, optimization of synthetic conditions will be required. BP-NT is another promising material. Similar to BP-ED it has already been characterized in detail. BP-ID is currently a proof of concept material. However, it is envisioned that, with continued development, all four of these materials may be used in combination to develop a process for the selective removal of metal ions sequentially from aqueous solution.

To further investigate the properties of SPC materials variable temperature experiments will be conducted. Often metal laden waters are at elevated temperature. As a result the sorption equilibrium will differ from that at standard conditions. The performance characteristics of SPCs at high temperature may differ from that presented in this work. In order to test the temperature effect batch pH profiles will be conducted at varying temperatures. Using the equation: $-RT\ln K = \Delta H - T\Delta S$ it will be possible to calculate the change in enthalpy and entropy for each material. This will provide further information regarding the mode of sorption.

Laterite HPAL solutions are a potential application for which SPC materials may useful. Chapter 5 identified the potential of BP-ED and BP-NT for the selective removal of Ni^{2+} from other divalent 1st row transition metal ions. It was assumed that the solution

would have undergone copper cementation. Using an array of specifically tailored SPC materials it may be possible to develop a stepwise process, in which each metal is removed one at a time. For example the removal of Cu^{2+} from the solution can be carried out using CuWRAM. Fe^{3+} may be removed by BP-2, WP-4 or BP-NT depending on pH and relative concentrations. Ni^{2+} can then be removed by BP-ED, BP-NT or WP-2. This leaves a solution rich in Zn^{2+} and Co^{2+}. Currently investigations are underway to produce an SPC that can separate these metals. In particular phosphinic and phosphonic acid modified SPCs BP-5 and BP-AP are under investigation for this purpose.

CHAPTER 6: Experimental

6.1 Materials. Silica gel (267Å pore diameter, 2.82mL/g pore volume, 84.7% porosity, 422m^2/g surface area) was obtained from INEOS enterprises Ltd., UK (previously Crosfield UK). EDTA dianhydride and DTPA dianhydride were purchased from Aldrich Co. Sodium chloroacetate, NTA and IDA were also purchased from Aldrich. All other reagents were purchased from Aldrich Co. or VWR. Metal solutions were prepared by dissolving the appropriate quantity of the sulfate salt in deionized (DI) water. The solution pH was adjusted from intrinsic with 0.05 mol/L, 2.0 mol/L or 4.5 mol/L H_2SO_4. Stripping was conducted using 4.5 mol/L H_2SO_4. Base regeneration was conducted with 4 mol/L NH_4OH. Metal standards for FAA (flame atomic adsorption) analysis were also obtained from Aldrich Co. Poly(vinylamine)s (PVA, 1000 MW, 50,000 MW) were obtained from BASF, Germany. Poly(ethyleneimine)s (PEI, 1200 MW, 25,000 MW) were obtained from Aldrich Chemicals. Poly(allylamine) (PAA, 15,000 MW) was obtained from Summit Chemicals Inc., NJ, USA.. All polymers were in the free base form and were used as received. Chloropropyltrichlorosilane (CPTCS), methyltrichlorosilane (MTCS), propyltrichlorosilane (PTCS) and chlorotrimethylsilane (CTMS) were used as received from the Aldrich Chemicals Co. The synthesis of all SPCs was repeated several times to ensure reproducibility.

6.2 Equipment. Elevated temperature pH measurements were recorded using a Thermo Orion 250Aplus pH meter with a Thermo Orion Triode electrode. Ambient pH measurements were made with a VWR SympHony SB20 meter with a VWR SympHony

Posi-pHlo electrode. Reactions were mixed by the overhead method using an overhead tallboy laboratory stirrer, Model 134-1, Troemner, LLC. Reaction flasks were heated using a GLAS-COL heating mantle controlled via a STACO Inc. variable autotransformer. Elemental analysis (Carbon, Hydrogen, Nitrogen, Chlorine) was conducted at Schwarzkopf Microanalytical Laboratory, N.Y. The error in elemental analysis was reported as no more than 0.3% absolute for CHN analysis. Chlorine was detimined by the ion elective electrode method was a relative error of 0.3%. Batch experiments were conducted in a Precision Scientific 360 shaker bath (Precision Scientific, Inc., Chicago, IL. Dynamic experiments were conducted with a 5 mL column fashioned from a disposable syringe fitted with frits at both ends. 10 mL adjustable volume OMNIFIT columns were also used for breakthrough experiments. Columns were slurry packed and fed challenge solution by a variable-flow FMI Lab Pump model QG150 (Fluid Metering Inc., Syosset, N.Y.). Metal ion concentrations were determined via a Flame Atomic Sorption (FAA) method using a S2 FAA Spectrometer from SOLAR, UK.

6.3 Spectroscopic Characterization. The CP/MAS (cross polarization magic angle spinning) ^{13}C NMR spectra were recorded on a Varian NMR SYSTEMS 500 MHz NMR. The CPMAS data at 125 MHz were measured using ramped cross polarization and SPINAL64 and TPPM decoupling techniques with sample spinning speeds of 10 kHz. SPC CP/MAS. FTIR (KBr pellet method) experiments were conducted using a Thermo-niclet 633 spectrometer.

6.4 Preparation of Hydrated Silica Gels. Silica gels were sieved to ensure particle diameters are in the desired range (90 μm to 105 μm and 150 μm to 250 μm for raw INEOS silica gel). 200 g of sieved silica gel was added to 800 mL of 1.0 mol/L HCl in a 2 L three neck round bottom flask. The flask was equipped with an overhead stirrer and a condenser. During mixing the flask was degassed by an applied vacuum (30 mm Hg). The reaction flask was restored to atmospheric pressure. The mixture was then brought to reflux (98°C) for six hours. Upon cooling the product was filtered and washed successively with three 800 mL water washes and two 800 mL methanol washes. The resulting gel was dried at 120 °C to a constant mass. Air was forced over a bed of water and through a 2 L column containing 200 g of acid washed silica gel for 72 hours creating a monolayer of water on the silica gel surface. The percent weight gain (W) is used to quantify the increase in mass associated with modifying silica gel. W is calculated using equation 6.1.

$$W\ \% = (M_f - M_i)/M_i \times 100\ \% \qquad (6.1)$$

In which M_f is the mass of the modified silica gel and M_i is the mass prior to modification. For the hydration of acid washed silica gel W ~ 6 %.

6.5 Preparation of CPTCS only Functionalized Silica Gel (CP-Gel). For the preparation of CPTCS only functionalized INEOS silica gel, a 30 g quantity of hydrated silica gel was placed in a 250 mL three neck round bottom flask equipped with an overhead stirrer. 120 mL of hexanes was added to the reaction flask and the resulting mixture was stirred under a constant flow of dry N_2. 90 mmol (3 mmol/g of silica gel) of CPTCS and MTCS in the desired ratio was dissolved in 30 mL of dry hexanes. The silane

solution was then added drop-wise to the reaction mixture. As the reaction proceeded, HCl gas was evolved and was forced out of the reaction flask by dry N_2 flow. The reaction flask was degassed with an applied vacuum (30 mm Hg) for 15 minutes and allowed to react for 24 hours. The product was filtered and washed three times with 120 mL of dry hexanes and two times with 120 mL of methanol. The product was filtered and then dried at 110°C until there is a negligible mass decrease. For the modification of hydrated silica gel with CPTCS only W = 20 %.

6.6 Preparation of MTCS:CPTCS Functionalized Silica Gels. MTCS:CPTCS functionalized silica gels are silica gels functionalized with MTCS and CPTCS in a specified molar ratio. In keeping with CPTCS only silica gel, a total of 3 mmol of silanes for each gram silica gel was employed. The silane solution of the requisite molar ratio was prepared in 30 mL of hexanes. From this point the procedure described for CPTCS only gels (Section 6.4) was adhered to. The percent weight gains for hydrated silica gel functionalized with both MTCS and CPTCS in the molar reagent ratios specified above are in the range W = 7 % to W = 20 %. Elemental analysis data shown in table 6.1.

Table 6.1. Elemental analysis raw data for CPTCS:MTCS modified silica gel.

Sample	C %	Cl %
0:1	4.94	4.69
1:1	4.54	3.05
2.5:1	4.31	1.67
5:1	3.94	1.37
7.5:1	3.5	0.98
10:1	3.38	0.74
12.5:1	3.74	0.63

6.7 Preparation of PTCS:CPTCS Functionalized Silica Gels. PTCS:CPTCS functionalized silica gels are silica gels functionalized with PTCS and CPTCS in a specified molar ratio. In keeping with CPTCS only silica gel, a total of 3 mmol of silanes for each gram silica gel was employed. The silane solution of the requisite molar ratio was prepared in 30 mL of hexanes. From this point the procedure described for CPTCS only gels (Section 6.4) was adhered to. The percent weight gains for hydrated silica gel functionalized with both PTCS and CPTCS in the molar reagent ratios specified above are in the range W = 10.6 % to W = 20 %. Elemental analysis can be found in table 6.2.

Table 6.2. Elemental analysis raw data for CPTCS:PTCS modified silica gel.

% PTCS	C %	Cl %
0	7.14	6.67
25	6.68	5.23
50	4.60	2.03
75	3.94	1.37
100	3.05	-

6.8 Preparation of 'CTMS only' Silica Gels. The preparation of CTMS only functionalized INEOS silica gel is the same as the preparation of CPTCS only silica gel (Section 6.4) with the exceptions that CTMS is substituted for all CPTCS and there is no hydration step in the preparation of the raw INEOS silica gel. For silica gel functionalized with CTMS only W = 10 %. Elemental analysis: Carbon = 3.02%.

6.9 Preparation of SPCs BP-1, WP-1 and VP-1. In a 100 mL three neck round bottom flask equipped with a condenser and overhead stirrer 5 g of CP-Gel or MTCS:CPTCS INEOS type silica gel was added to a 25 mL aqueous polyamine solution containing 2

mL of methanol as an antifoaming agent. The resulting mixture was stirred for 15 minutes and degassed by an applied vacuum (30 mm Hg). The mixture was continuously stirred at a temperature of 65°C for 48 hours. The mixture was then cooled, allowed to settle and then carefully decanted. The resulting composite was washed five times with 20 mL portions of water, one 20 mL portion of a 4 mol/L ammonia solution, three 20 mL portions of water and two 20 mL methanol. The resulting composites were then dried to constant mass at 60°C. A sample of each composite underwent elemental analysis (CHN). Polyamines and concentration used include: polyallylamine (15,000 MW) in a 10% aqueous solution, polyvinylamine)(<1000 and 50,000 MW) in an aqueous solution containing a mass fraction of 10% polymer and polyethyleneimine (1,200 and 25,000 MW) in an aqueous solution containing a mass fraction of 18% polymer. For the addition of polyamines to functionalized silica gels the percent weight gains are in the range W = 8 % to W = 18 %. Elemental analysis can be found in table 6.3.

Table 6.3. Elemental analysis raw data for CPTCS:MTCS modified silica gel further modified with PVA, PAA and PEI.

COMPOSITE	%Carbon	%Nitrogen
PVA 50 000 MW		
0:1	15.26	4.76
2.5:1	11.33	3.97
5:1	12.71	4.77
7.5:1	11.77	4.33
10:1	11.31	4.13
12.5:1	7.18	2.25
PAA 15 000 MW		
0:1	14.0	3.40
1:1	13.3	3.40
2.5:1	12.1	3.20
7.5:1	13.8	3.90
12.5:1	11.0	3.00
PEI 25 000 MW		

0:1	13.7	5.51
5:1	11.4	4.80
12.5:1	11.8	4.90

6.10 Preparation of Modified SPCs. The preparation of BP-AP, WP-4 and CuWRAM can be found in detail elsewhere.[120] For the preparation of the 7.5:1 MTCS:CPTCS derivatives of these materials the pathway is identical to the previously reported procedure with the exception that 7.5:1 BP-1 was employed. W for 7.5:1 BP-AP was ~23%. W for 7.5:1 WP-4 was ~48%. W for 7.5:1 CuWRAM was ~18%. Weight gains all relative to the 7.5:1 BP-1 precursor.

6.11 Preparation of WP-2 and BP-2. In a 100 mL three neck round bottom flask equipped with an overhead stirrer and condenser, 5 g of CPTCS only PEI (25,000 MW) composite was added to 6 g of sodium chloroacetate in 25 mL of water. The resulting mixture was stirred for 15 minutes and degassed by an applied vacuum (30 mm Hg). The contents of the flask were heated to a temperature of 70°C for 24 hours. After 1 hour 1 mL of 8 mol/L NaOH was added drop wise to the reaction mixture whilst monitoring pH. The pH was maintained above 9. A further 1 mL of 8 mol/L NaOH was added similarly after 18 hours. The maximum recorded pH of the reaction mixture was 10.5. The flask was then allowed to cool and filtered. The resulting composite was washed 3 times with 20 mL of water, once with 2 mol/L H_2SO_4, a further 3 times with 20 mL of water, twice with 20 mL of methanol, then dried at 70°C for 24 hours. The same procedure was used to produce a 12.5:1 MTCS:CPTCS acetate modified PEI composite (WP-2) using 5 g 12.5:1 MTCS:CPTCS PEI composite (WP-1). Each WP-2 synthesis was repeated three times (a total of six were prepared) to test for reproducibility. The weight gain for

addition of acetate groups to PEI composites prepared from silica gel functionalized with CPTCS only, and MTCS:CPTCS in the ratio 12.5:1, were W = 11% and W = 14% respectively. For the synthesis of BP-2 a procedure identical to WP-2 was used with the exception that BP-1 is the precursor. The weight gain for BP-2 CPTCS only and BP-2 7.5:1 MTCS:CTPCS were W = 11% and W = 13% respectively. WP-2 CPTCS only elemental analysis: carbon = 15.22 %, nitrogen = 4.13 %. WP-2 12.5:1 elemental analysis: carbon = 13.58 %, nitrogen = 3.39. BP-2 7.5:1 elemental analysis: carbon =16.03 %, nitrogen = 2.69 %. FTIR analysis of BP-2 and WP-2 show carboxylic peaks at 1737 cm^{-1} and 1639 cm^{-1}. ^{13}C NMR (CP/MAS) WP-2: -10 to 0 ppm $–Si(O_2)-\underline{\mathbf{C}}H_3$, 5 to 15 ppm $-Si(O_2)(\underline{\mathbf{C}}H_2)_3NH-$, 30 to 65 ppm PEI $\underline{\mathbf{C}}H_2$, $–NH\underline{\mathbf{C}}H_2COOH$, 165 to 175 $-CH_2\underline{\mathbf{C}}OOH$. ^{13}C NMR (CP/MAS) BP-2: -10 to 0 ppm $–Si(O_2)-\underline{\mathbf{C}}H_3$, 5 to 15 ppm $-Si(O_2)(\underline{\mathbf{C}}H_2)_3NH-$, 20 to 45 ppm PAA $\underline{\mathbf{C}}H_2$, PAA $\underline{\mathbf{C}}H$, 45 to 65 ppm $–\underline{\mathbf{C}}H_2COOH$, 165 to 180 $-CH_2\underline{\mathbf{C}}OOH$.

6.12. Synthesis of EDTA SPCs: BP-ED and WP-ED. The synthesis of BP-1 (polyallylamine grafted onto chloro-propyl functionalized amorphous silica gel) and WP-1 (polyethyleneimine grafted onto chloro-propyl functionalized amorphous silica gel) have been reported in section 6.9. For the modification of BP-1 and WP-1 with EDTA anhydride 25 g of BP-1/WP-1 (containing 75 mmoles of amines) was mixed with 50 g (195 mmoles) of EDTA anhydride in 250 mL of 50% acetic acid/ethanol solution in a 500 mL flask equipped with an overhead stirrer. The reaction mixture was heated to 70°C for 24 hours. The flask was cooled and the product was filtered. The resulting composite

was washed once with 75 mL of water, once with 75 mL of 4 mol/L NH_4OH, three times with 75 mL of water, once with 75 mL of 50% acetic acid/ethanol, three more times with 75 mL of water, twice with 75 mL of methanol and dried to a constant mass at 70°C. BP-ED was prepared using CTPCS only BP-1 and 7.5:1 MTCS:CPTCS BP-1 Weight gain after 24 hours drying: BP-ED CPTCS only = 20.2%, WP-ED CPTCS only = 14.6% and BP-ED 7.5:1 = 32.3%. WP-ED (CPTCS only) elemental analysis: carbon 17.46 %, nitrogen 4.94 %. BP-ED (CPTCS only) elemental analysis: carbon 21.16%, nitrogen 4.70 %. BP-ED (7.5:1 MTCS:CPTCS) elemental analysis: carbon 21.01%, nitrogen 5.31 %. FTIR spectra of BP-ED and WP-ED show amide and carboxylic adsorptions at 1638 cm^{-1} and 1747 cm^{-1} for the resultant ethylenediaminetriacetic acid acetamide ligand. ^{13}C NMR (CP/MAS) WP-ED (CPTCS only) 5 to 15 ppm -$Si(O_2)$**C**$H_2CH_2CH_2NH$-, -$Si(O_2)CH_2$**C**H_2CH_2NH-, 25 ppm -$Si(O_2)CH_2CH_2$**C**H_2NH-, 30 to 65 ppm PEI **C**H_2, -NH**C**H_2COOH, -NH(CO)**C**H_2NH-, 165 to 185 ppm -CH_2**C**OOH, -NH(**C**$O)CH_2NH$-. ^{13}C NMR (CP/MAS) BP-ED (10:1): -10 to 0 ppm -$Si(O_2)$-**C**H_3, 5 to 15 ppm -$Si(O_2)$(**C**$H_2)_3NH$-, 30 to 70 ppm PAA **C**H_2, PAA **C**H, -NH**C**H_2COOH, -NH(CO)**C**H_2NH-, 160 to 180 -CH_2**C**OOH, -NH(**C**$O)CH_2NH$-.

6.13. Synthesis of DTPA SPC: BP-DT. The synthesis of BP-1 (polyallylamine grafted onto chloro-propyl functionalized amorphous silica gel) was reported in section 6.9. For the modification of BP-1 DTPA anhydride 25 g of BP-1 (containing ~ 75 mmoles of amines) was mixed with 50 g (195 mmoles) of DTPA anhydride in 250 mL of 50% acetic acid/ethanol solution in a 500 mL flask equipped with an overhead stirrer. The reaction mixture was heated to 70°C for 24 hours. The flask was cooled and the product was

filtered. The resulting composite was washed once with 75 mL of water, once with 75 mL of 4 mol/L NH_4OH, three times with 75 mL of water, once with 75 mL of 50% acetic acid/ethanol, three more times with 75 mL of water, twice with 75 mL of methanol and dried to a constant mass at 70°C. Weight gain after 24 hours drying: BP-DT = 20.1%. BP-DT (7.5:1 MTCS:CPTCS) elemental analysis: carbon 13.23 %, nitrogen 3.70 %. ^{13}C NMR (CP/MAS) BP-DT (7.5:1): -10 to 0 ppm $–Si(O_2)$-**C**H_3, 20 to 45 ppm PAA **C**H_2, PAA **C**H, 30 to 50 ppm -NH(CO)**C**H_2NH-, 40 to 65 ppm -NH**C**H_2COOH, 160 to 175 -CH_2**C**OOH, -NH(**C**O)CH_2NH-.

6.14 Synthesis of NTA SPCs: BP-NT and WP-NT. The synthesis of NTA anhydride was preformed according to a patented procedure Hindersinn et al.[115] 19.1 g of NTA (nitrilotriacetic acid), 34.8 mL of DMA (N,N-dimethyl acetamide) and 30.6 mL of acetic anhydride were placed in a 250 mL three neck round bottom flask equipped with a reflux condenser, thermometer, nitrogen inlet, overhead stirrer and heat source. The vessel was heated to 80°C for 24 hours. Unreacted acetic anhydride and acetic acid side product and DMA solvent were removed at 80°C under reduced pressure. 100 mL of chloroform was added to the vessel. The NTA anhydride precipitate was filtered and washed with 150 mL of chloroform. The white powder was then dried under vacuum. (Yield = 30%) For this work BP-1 was prepared from silica gel functionalized with CPTCS and MTCS in a molar ratio of 7.5:1 (Section 6.9) WP-1 was prepared from silica gel functionalized with CPTCS and MTCS in a molar ratio of 12.5:1. For the modification of BP-1 with NTA anhydride 25 g of BP-1 (containing 75 mmoles of amines) was mixed with 25 g (100

mmoles) of NTA anhydride in 250 mL of 50% acetic acid/ethanol solution in a 500 mL flask equipped with an overhead stirrer. The reaction mixture was heated to 67°C for 24hrs. The flask was cooled and the product was filtered. The resulting composite was washed once with 75 mL of 4 mol/L NH_4OH, three times with 75 mL of water, once with 75 mL of 50% acetic acid/ethanol, three more times with 75 mL of water, twice with 75 mL of methanol and dried to a constant mass at 70 °C. The weight gain (W) after 24hrs drying at 70°C were W = 24.4% and W = 23.6% for BP-NT and WP-NT respectively. Weight gains are relative to the BP-1 7.5:1 and WP-1 12.5:1 precursor respectively. BP-NT (7.5:1 MTCS:CPTCS) elemental analysis: carbon 19.59 %, nitrogen 4.58 %. BP-NT (12.5:1 MTCS:CPTCS) elemental analysis: carbon 16.71 %, nitrogen 5.74 %. FTIR analysis of BP-NT and WP-NT show an amide and carboxylic envelope at 1652 cm^{-1}. An aliphatic carbon (C-C) stretch is evident and broad at 2980 cm^{-1} and the presence of the polymer and ligand amines is confirmed by another broad signal at 3100 cm^{-1}. ^{13}C NMR (CP/MAS) WP-NT (12.5:1) -10 to 0 -$Si(O_2)$-**C**H_3, 5 to 15 ppm -$Si(O_2)$(**C**H_2)$_3$NH-, 25 to 50 ppm PEI **C**H_2, -NH(CO)**C**H_2NH-, 40 to 60 ppm –NH**C**H_2COOH, 160 to 180 ppm -CH_2**C**OOH, -NH(**C**O)CH_2NH-. ^{13}C NMR (CP/MAS) BP-NT (7.5:1): -10 to 0 ppm -$Si(O_2)$-**C**H_3, 5 to 15 ppm -$Si(O_2)$(**C**H_2)$_3$NH-, 15 to 50 ppm PAA **C**H_2, PAA **C**H, -NH(CO)**C**H_2NH-, 50 to 60 ppm -NH**C**H_2COOH, 160 to 180 -CH_2**C**OOH, -NH(**C**O)CH_2NH-.

6.15. Synthesis of IDA SPC: BP-ID. To protect the secondary amine of IDA 13.3 g (100 mmol) of the amino acid were placed in a 1 L flask to which 200 mL of dioxane were added. 8 g (200 mmol) of NaOH was dissolved in 200 mL of DI H_2O and added to the

reaction flask. The solution was mixed until all solids had dissolved. To the solution 23.75 g of di-t-butylcarbonate was added. The reaction mixture was allowed to mix for 72 hours. The product solution was extracted twice with 2 x 100 mL of diethyl ether. The mixture was then acidified with 100 mL of a 10% HCl solution. This was then extracted four times with 150 mL of ethyl acetate and washed three times with a saturated NaCl solution. The product was then dried using sodium sulfate overnight. Crystals of the the t-boc-IDA were recovered by evaporation of the solvent. Mass of product was 13.5 g. (Yield ~ 90%) For the attachment to 7.5:1 MTCS:CPTCS BP-1 4.9 g of the boc protected IDA was added to 60 mL of DMF. To this solution 3.8g (4.33 mL) of EDC was added and allowed to mix for 1 hour at room temperature. After 1 hour of mixing, 5.0 g of BP-1 was added to the solution. The reaction was mixed at room temperature for 24 hours. The orange reaction product mixture was filtered and the yellow product was washed with 20 mL of DMF, 3 times with 20 mL of DI H_2O, 20 mL of a 4 mol/L H_2SO_4, 3 more times with DI H_2O, and washed once with 20 mL of MeOH. The product was dried overnight and the weight gain for the boc-protected product was W = 27%. Deprotection was carried out by stirring in a 10% TFA solution in CH_2Cl_2 for 24 hours. The mixture was then filtered and washed with 20 mL of CH_2Cl_2, three times with 20 mL of DI H_2O, once with 20 mL of 4 mol/L H_2SO_4, 3 more times with 20 mL of DI H_2O, and once with 20 mL of MeOH. The product was dried overnight at 70°C. W = -8%. BP-NT (7.5:1 MTCS:CPTCS) elemental analysis: carbon 17.56 %, nitrogen 4.53 %. FTIR analysis of deprotected BP-ID shows a broad amide and carboxylic envelope at 1657 cm^{-1}. An aliphatic carbon (C-C) stretch is evident and broad at 2960 cm^{-1}. ^{13}C NMR (CP/MAS) BP-ID-BOC (7.5:1): -10 to 0 ppm -Si(O_2)-**C**H_3, 5 to 15 ppm -Si(O_2)(**C**H_2)$_3$NH-, 20 to 25

ppm -O-C-(**C**H_3)$_3$, 25 to 50 ppm PAA **C**H_2, PAA **C**H, 35 to 45 ppm -NH(CO)**C**H_2NH-, 45 to 55 ppm -NH**C**H_2COOH, 75 to 160 ppm -(CO)O**C**$(CH_3)_3$, 150-155 -N(**C**O)O$C(CH_3)_3$, to 165 to 180 ppm -CH_2**C**OOH, -NH(**C**O)CH_2NH-. ^{13}C NMR (CP/MAS) BP-ID (7.5:1): -10 to 0 ppm -Si(O_2)-**C**H_3, 5 to 15 ppm -Si(O_2)(**C**$H_2)_3$NH-, 25 to 50 ppm PAA **C**H_2, PAA **C**H, 35 to 45 ppm -NH(CO)**C**H_2NH-, 45 to 55 ppm -NH**C**H_2COOH, 165 to 180 ppm -CH_2**C**OOH, -NH(**C**O)CH_2NH-.

6.16. pH Profiles. pH profiles were acquired for several divalent and trivalent metals. The pH of the challenge solutions was adjusted with sulfuric acid. Metal concentrations in feed solutions were typically 1.5 g/L. Batch extraction tests were conducted by adding 0.1 g of SPC to 10 mL of metal solution at selected pH values. To ensure equilibrium, the metal ion and SPC mixtures were placed in a shaker bath. After 24 hours the mixtures were allowed to settle. Each supernatant was extracted and diluted with 2% nitric acid for analysis using the FAA method. All pH profile experiments performed in triplicate.

6.17. Mass Transfer Kinetics. Sorption isotherms were obtained for SPCs as a function of time. Using the batch method described previously samples of each composite were fed with a 1.5 g/L metal ion (typically Cu^{2+} or Ni^{2+}) solution at the requisite pH. The supernatant was sampled several times over the following 24 hours. Samples were diluted and preserved in 2% HNO_3 solution before FAA analysis. All mass transfer kinetics experiments performed in triplicate.

6.18. Concentration Dependent Isotherms. In order to assess the applicability of the Langmuir and Freundlich models for SPC metal ion sorption, concentration dependant isotherms were acquired. Isotherms were obtained by batch experiments as described in Section 6.15. Metals investigated included Cu^{2+}, Ni^{2+}, Zn^{2+} and $Co^{2+.}$ Metal ion concentration was varied, pH was held constant and each sample was shaken for 24 hours to ensure equilibrium. Langmuir and Freundlich parameters were obtained from the appropriate linear regressions. The details of these models are described in Section 3.2. All concentration isotherm experiments performed in triplicate.

6.19. Breakthrough Testing. Column breakthrough experiments were carried out using a 5 mL (120 mm diameter x 440 mm length) column fritted at both ends. Flow was in the bottom to top for these columns. Column experiments were also carried out using a 10 mL adjustable Ominifit glass column. Flow was top to bottom for these columns. The columns received flow from a variable flow FMI Lab Pump, Model QG150 from Fluid Metering Inc., NJ, and USA. The flow rate was typically in the range of 0.1 to 0.5 column volume/min. Each column was slurry packed with the necessary SPC. Columns were then conditioned for metal ion extraction by passing through the column the following solutions: 20 mL DI H2O, 30 mL 4.5 mol/L H_2SO_4, 100 mL DI H_2O. For SPC materials such as BP-1 and WP-1 that require base regeneration a further 30 mL of 4 mol/L ammonia solution and 100 mL DI H_2O were passed through the column. Acid is used to remove impurities from the packed composite and the ammonia is used to deprotonate the polymer amines to facilitate sorption. Columns packed with SPC were conditioned for use by passing the following solutions through the column: 20 mL water,

30 mL 4.5 mol/L H_2SO_4 and 100 mL water. Columns were then treated with a metal ion contaminated feed solution adjusted to the necessary pH. All columns were then rinsed with 20 mL DI water, stripped with 30 mL 4.5 mol/L H_2SO_4 and rinsed again with 100 mL DI water. Effluent fractions were collected in 5 mL or 10 mL aliquots beginning with the first 5 mL or 10 mL of the feed solution passes through the column. The fractions were preserved with one drop of concentrated HNO_3. All breakthrough experiments were run once only unless otherwise stated. Also, the acid solutions used were all adequate for complete removal of the metal ions off the column unless otherwise stated.

6.20 Cycle Testing. 1001 load strip cycles were carried out on BP-ED for longevity analysis. A 5 mL fritted column was loaded with BP-ED 7.5:1 MTCS:CPTCS. The column was then subjected to the following procedure. The 5 mL column attached to a six way manifold equipped with a solenoid valve (Cole-Parmer Instrument Co., Vernon Hills, IL) wired to a computer containing the operational software (An MS-DOS cycling program written by Dr. Bruce King). Teflon tubing connects each solution to the valve and from the valve to the column. The feed solution contained 3g/L Cu^{2+} at pH 1.5. 16 mL of feed solution was added in 48 seconds. This was followed by a 5 second wash with DI H_2O. The Cu^{2+} was stripped with 10 mL of 33% v/v H_2SO_4, which lasted 30 seconds. Finally the column was rinsed with 30 mL of DI H_2O, which last 90 seconds. A regular breakthrough analysis, as described in section 6.18, was performed for the 1st cycle. The process was stopped so that a breakthrough could be recorded (as for cycle 1) for cycle 101. The final cycle (cycle 1001) was also performed by the regular breakthrough method.

6.21 Acid and Base Stability. To analyze the stability of the amide bond for the amido-amino-acid SPCs, 1 g of BP-NT, WP-NT and BP-2 were placed in 100 mL of 4.5 mol/L H2SO4 and also in 100 mL of 4 mol/L NH_4OH for 72 hours. The SPC material was then filtered and washed with 20 mL of DI H_2O three times followed by 20 mL of 4M H_2SO4, 20 mL of DI H_2O three times and once with MeOH before drying overnight at 70°C. Batch tests were performed on the resulting SPCs as described in section 6.16. Stability tests were performed in triplicate.

BIBLIOGRAPHY

1. Clarke, P. The decorative uses of metals. Met. Mark. Place, Met. Congr. Paper No. 10, 8 pp. 78.

2. Page, Bev, Edwards, Mike, and May, Nick. Metal cans. Food Packaging Technology. 120-151. 2003.

3. Allan, Rod. Introduction: Mining and metals in the environment. Journal of Geochemical Exploration 58(2-3), 95-100. 97.

4. Lichti, G. and Mulcahy, J. Acid mine drainage-environmental nightmare or asset? Chemistry in Australia 65(1), 10-13. 98.

5. Mohammed, Ali and Najar, P. A. Mohamed. Treatment methods for the removal of heavy metal pollutants from water and wastewaters. Journal of Industrial Pollution Control 13(2), 85-106. 97.

6. Kwolek, J. K. Aspects of geo-legal mitigation of environmental impact from mining and associated waste in the UK. Journal of Geochemical Exploration 66(1-2), 327-332. 99.

7. Nguta, C. M. and Guma, J. Lead and cadmium concentrations in cattle tissue: the effect of industrial pollution from Nakuru town. Journal of the Kenya Chemical Society 2(1), 19-24. 2004.

8. Moleux, Peter. Designing a new PCB facility for successful pollution prevention & waste minimization. Plating and Surface Finishing 81(4), 44-7. 94.

9. Somers, E. Toxic potential of trace metals in foods. Review. Journal of Food Science 39(2), 215-17. 74.

10. Vukovic, Z. Environmental impact of radioactive silver released from nuclear power plant. Journal of Radioanalytical and Nuclear Chemistry 254(3), 637-639. 2002.

11. Swaine, Dalway J. Trace elements in coal and their dispersal during combustion. Fuel Processing Technology 39(1-3), 121-37. 94.

12. Meharg, Andrew A. and Rahman, Md. Mazibur. Arsenic Contamination of Bangladesh Paddy Field Soils: Implications for Rice Contribution to Arsenic Consumption. Environmental Science and Technology 37(2), 229-234. 2003.

13. Wiener, J. G., Knights, B. C., Sandheinrich, M. B., Jeremiason, J. D., Brigham, M. E., Engstrom, D. R., Woodruff, L. G., Cannon, W. F., and Balogh, S. J. Mercury in Soils, Lakes, and Fish in Voyageurs National Park (Minnesota): Importance of Atmospheric Deposition and Ecosystem Factors. Environmental

Science & Technology 40(20), 6261-6268. 2006.

14. Tavakoli Omid and Yoshida Hiroyuki. Effective recovery of harmful metal ions from squid wastes using subcritical and supercritical water treatments. Environ Sci Technol 39(7), 2357-63.

15. Forzani, Erica S., Zhang, Haiqian, Chen, Wilfred, and Tao, Nongjian. Detection of Heavy Metal Ions in Drinking Water Using a High-Resolution Differential Surface Plasmon Resonance Sensor. Environmental Science and Technology 39(5), 1257-1262. 2005.

16. Boddu, Veera M., Abburi, Krishnaiah, Talbott, Jonathan L., and Smith, Edgar D. Removal of Hexavalent Chromium from Wastewater Using a New Composite Chitosan Biosorbent. Environmental Science and Technology 37(19), 4449-4456. 2003.

17. Vijver, Martina G., van Gestel, Cornelis A. M., Lanno, Roman P., van Straalen, Nico M., and Peijnenburg, Willie J. G. M. Internal Metal Sequestration and Its Ecotoxicological Relevance: A Review. Environmental Science and Technology 38(18), 4705-4712. 2004.

18. Kawata, Koji, Yokoo, Hiroyuki, Shimazaki, Ryuhei, and Okabe, Satoshi. Classification of Heavy-Metal Toxicity by Human DNA Microarray Analysis. Environmental Science & Technology 41(10), 3769-3774. 2007.

19. Dillard C J and Tappel A L. Mercury, silver, and gold inhibition of selenium-accelerated cysteine oxidation. J Inorg Biochem 28(1), 13-20.

20. Tinggi, Ujang. Selenium toxicity and its adverse health effects. Reviews in Food and Nutrition Toxicity 4, 29-55. 2005.

21. Johnson, D. Barrie and Hallberg, Kevin B. Acid mine drainage remediation options: a review. Science of the Total Environment 338(1-2), 3-14. 2005.

22. Castro, J. M. and Moore, J. N. Pit lakes: Their characteristics and the potential for their remediation. Environmental Geology (Berlin) 39(11), 1254-1260. 2000.

23. Mccarty, Douglas K., Moore, Johnnie N., and Marcus, W. Andrew. Mineralogy and trace element association in an acid mine drainage iron oxide precipitate; comparison of selective extractions. Applied Geochemistry 13(2), 165-176. 98.

24. Pagnanelli, Francesca, Luigi, Marta, Mainelli, Sara, and Toro, Luigi. Use of natural materials for the inhibition of iron oxidizing bacteria involved in the generation of acid mine drainage. Hydrometallurgy 87(1-2), 27-35. 2007.

25. Nordstrom, Darrell Kirk, Alpers, Charles N., Ptacek, Carol J., and Blowes, David W. Negative pH and Extremely Acidic Mine Waters from Iron Mountain, California. Environmental Science and Technology 34(2), 254-258. 2000.

26. McIntyre, Ruluff D. Some current uses for metals in, on, and around your body. Materials Engineering (Cleveland) 96(3), 40-7. 82.

27. Tabak, Henry H., Scharp, Richard, Burckle, John, Kawahara, Fred K., and Govind, Rakesh. Advances in biotreatment of acid mine drainage and biorecovery of metals: 1. Metal precipitation for recovery and recycle. Biodegradation 14(6), 423-436. 2003.

28. Deorkar, N. V. and Tavlarides, L. L. An adsorption process for metal recovery from acid mine waste: The Berkeley Pit problem. Environmental Progress 17(2), 120-125. 98.

29. Yang, K., Misra, M., and Mehta, R. Removal of heavy metal ions from Noranda tailings water and Berkeley pit water by ferrite coprecipitation process. Waste Processing and Recycling in Mineral and Metallurgical Industries II, Proceedings of the International Symposium on Waste Processing and Recycling in Mineral and Metallurgical Industries, 2nd, Vancouver, B. C., Aug. 20-24, 1995. 425-38. 95.

30. Huang, Hsin Hsiung and Liu, Qi. Bench-scale chemical treatability study of the Berkeley Pit water. ACS Symposium Series 607(Emerging Technologies in Hazardous Waste Management 5), 196-209. 95.

31. Karathanasis, A. D. and Johnson, C. M. Metal removal potential by three aquatic plants in an acid mine drainage wetland. Mine Water and the Environment 22(1), 22-30. 2003.

32. Marcinowski Frank and Tonkay Douglas W. Low-activity radioactive materials management at the U.S. Department of Energy. Health Phys 91(5), 498-501.

33. Thorne, M. C. and Vennart, J. The toxicity of strontium-90, radium-226, and plutonium-239. Nature (London, United Kingdom) 263(5578), 555-8. 76.

34. Foust, Henry, Holton, Langdon, and Demick, Larry. Maximizing production capacity from an ultrafiltration process at the Hanford Department of Energy Waste Treatment Facility. Separation Science and Technology 40(16), 3323-3337. 2005.

35. Fryxell, Glen E., Lin, Yuehe, Fiskum, Sandy, Birnbaum, Jerome C., Wu, Hong, Kemner, Ken, and Kelly, Shelley. Actinide Sequestration Using Self-Assembled Monolayers on Mesoporous Supports. Environmental Science and Technology 39(5), 1324-1331. 2005.

36. Manchanda, V. K. and Pathak, P. N. Amides and diamides as promising extractants in the back end of the nuclear fuel cycle: an overview. Separation and Purification Technology 35(2), 85-103. 2004.

37. Madic, Charles, Hudson, Michael J., Liljenzin, Jan-Olov, Glatz, Jean-Paul,

Nannicini, Roberto, Facchini, Alessandro, Kolarik, Zdenek, and Odoj, Reinhardt. Recent achievements in the development of partitioning processes of minor actinides from nuclear wastes obtained in the frame of the NEWPART European program (1996-1999). Progress in Nuclear Energy 40(3-4), 523-526. 2002.

38. Balu, K. and Wattal, P. K. Indian experiences in management of radioactive waste from nuclear fuel cycle. Proceedings of the International Topical Meeting on Nuclear and Hazardous Waste Management, SPECTRUM '96, 6th, Seattle, Aug. 18-23, 1996. 3, 2072-2075. 96.

39. Ozawa, Masaki. Novel partitioning technologies for minor actinides in high level liquid wastes. Radioisotopes 45(8), 527-530. 96.

40. Y. Morita, S. Tani, T. Kobayashi, M. Kubota, "Present status of research and development on the partitioning of minor actinides at Japan Atomic Energy Research Institute" *Report No. EUR 13347, Proc. Workshop Partitioning Transmutat. Minor Actinides, 1989* 1991).

41. Schapira, J. P. Long-term nuclear waste management: present status and alternatives. Nuclear Instruments & Methods in Physics Research, Section A: Accelerators, Spectrometers, Detectors, and Associated Equipment A280(2-3), 568-82. 89.

42. Alexandratos, Spiro D. and Zhu, Xiaoping. High-affinity ion-complexing polymer-supported reagents: Immobilized phosphate ligands and their affinity for the uranyl ion. Reactive & Functional Polymers 67(5), 375-382. 2007.

43. Kordosky, Gary A. Copper solvent extraction: the state of the art. JOM 44(5), 40-5. 92.

44. Mendes, F. D. and Martins, A. H. Selective nickel and cobalt uptake from pressure sulfuric acid leach solutions using column resin sorption. International Journal of Mineral Processing 77(1), 53-63. 2005.

45. Mendes, F. D. and Martins, A. H. Recovery of nickel and cobalt from acid leach pulp by ion exchange using chelating resin. Minerals Engineering 18(9), 945-954. 2005.

46. Cheng, C. Y. Purification of synthetic laterite leach solution by solvent extraction using D2EHPA. Hydrometallurgy 56(3), 369-386. 2000.

47. Meyer, Kurt and Krueger, Joachim. Raw materials for the production of nickel and processes used for it. Stahl und Eisen 92(3), 113-20. 72.

48. Wilson, Forbes. The Moa Bay-Port Nickel project. Mining Engineering (Littleton, CO, United States) 10, 563-5. 58.

49. De Graaf, J. E. The treatment of lateritic nickel ores - a further study of the caron

process and other possible improvements. Part I. Effect of reduction conditions. Hydrometallurgy 5(1), 47-65. 79.

50. Reddy, B. Ramachandra and Park, Kyung Ho. Process for the Recovery of Cobalt and Nickel from Sulphate Leach Liquors with Saponified Cyanex 272 and D2EHPA. Separation Science and Technology 42(9), 2067-2080. 2007.

51. Beauvais, Robert A. and Alexandratos, Spiro D. Polymer-supported reagents for the selective complexation of metal ions: an overview. Reactive & Functional Polymers 36(2), 113-123. 98.

52. Szymanowski, J. Kinetics and interfacial phenomena in solvent extraction of metals. Mineral Processing and Extractive Metallurgy Review 18(1), 1-66. 98.

53. McGarvey, F. X. and Tamaki, D. Selective ion exchange resins for toxic metal removal. Official Proceedings - International Water Conference 52nd, 228-33. 91.

54. Geckeler, Kurt E. and Volchek, Konstantin. Removal of Hazardous Substances from Water Using Ultrafiltration in Conjunction with Soluble Polymers. Environmental Science and Technology 30(3), 725-34. 96.

55. Matheickal, Jose T. and Yu, Qiming. Biosorption of lead(II) and copper(II) from aqueous solutions by pre-treated biomass of Australian marine algae. Bioresource Technology 69(3), 223-229. 99.

56. Jay, W. H. Application of ion exchange polymers in copper cyanide and acid mine drainage. Hydrometallurgy 2003, Proceedings of the International Symposium honoring Professor Ian M. Ritchie, 5th, Vancouver, BC, Canada, Aug. 24-27, 2003. 1, 717-728. 2003.

57. Garcia Liranza, E., Moreno Daudinot, A. M., Viera Martinez, R., and Rosales Barzaga, B. Solvent extraction studies for cobalt and nickel separation from the processing of ammonium carbonate mixed sulfides. Solvent Extraction for the 21st Century, Proceedings of ISEC '99, Barcelona, Spain, July 11-16, 1999. 1, 735-740. 2001.

58. Hurst, Fred J. Separation of cobalt from nickel in ammonia-ammonium carbonate solutions using pressurized ion exchange. Hydrometallurgy 1(4), 319-38. 76.

59. Irving, Harry M. N. H. William Skey (1835-1900). Centenary in the history of solvent extraction. Chemistry & Industry (London, United Kingdom) (42), 1780-1. 67.

60. Guedes de Carvalho, R. A. and Sampaio, M. N. M. Solvent extraction of tungsten by alkylamines-hydrochloric acid and alkylamines-sulfuric acid systems. Hydrometallurgy 26(2), 137-50. 91.

61. Guibal, E., Guzman, J., Navarro, R., and Revilla, J. Vanadium extraction from fly

ash - Preliminary study of leaching, solvent extraction, and sorption on chitosan. Separation Science and Technology 38(12 & 13), 2881-2899. 2003.

62. Habashi, Fathi. Cementation of copper - the end of an era. CIM Magazine 1(4), 99-101. 2006.

63. Power, K. L. Operation of the first commercial liquid ion-exchange and electrowinning plant. Solvent Extr., Proc. Int. Solvent Extr. Conf. 2, 1409-15. 71.

64. Grinstead, Robert R. Copper-selective ion-exchange resin with improved iron rejection. Journal of Metals 31(3), 13-16. 79.

65. Diniz, Claudia V., Ciminelli, Virginia S. T., and Doyle, Fiona M. The use of the chelating resin Dowex M-4195 in the adsorption of selected heavy metal ions from manganese solutions. Hydrometallurgy 78(3-4), 147-155. 2005.

66. Geckeler, Kurt E., Rosenberg, Edward, and Editors. Functional Nanomaterials. 488 pp. 2006.

67. Hall, Dorothy W., Sandrin, Joseph A., and McBride, Rhonda E. An overview of solvent extraction treatment technologies. Environmental Progress 9(2), 98-105. 90.

68. Pereira, Daniel Dayrell, Rocha, Sonia Denise Ferreira, and Mansur, Marcelo Borges. Recovery of zinc sulphate from industrial effluents by liquid-liquid extraction using D2EHPA (di-2-ethylhexyl phosphoric acid). Separation and Purification Technology 53(1), 89-96. 2007.

69. Kekesi, Tamas. Gallium extraction from synthetic Bayer liquors using Kelex 100-kerosene, the effect of loading and stripping conditions on selectivity. Hydrometallurgy 88(1-4), 170-179. 2007.

70. Ren, Zhongqi, Zhang, Weidong, Meng, Huilin, Liu, YiMing, and Dai, Yuan. Extraction Equilibria of Copper(II) with D2EHPA in Kerosene from Aqueous Solutions in Acetate Buffer Media. Journal of Chemical & Engineering Data 52(2), 438-441. 2007.

71. Rosenberg, Edward, Nielsen, Dan, Miranda, Paul, and Hart, Carolyn. Silica polyamine composites: advanced materials for ion recovery and remediation. Official Proceedings - International Water Conference 66th, IWC.05.40/1-IWC.05.40/12. 2005.

72. Geckeler, K. E., Shkinev, V. M., and Spivakov, B. Ya. Liquid-phase polymer-based retention (LPR) - a new method for selective ion separation. Separation and Purification Methods 17(2), 105-40. 88.

73. Geckeler, K. E., Bayer, E., Shkinev, V. M., and Spivakov, B. Ya. A new method for anion exchange using soluble polymers. Naturwissenschaften 75(4), 198-9.

88.

74. Geckeler, Kurt, Pillai, V. N. Rajasekharan, and Mutter, Manfred. Applications of soluble polymeric supports. Advances in Polymer Science 39, 65-94. 81.

75. Novikov, A. P., Shkinev, V. M., Spivakov, B. Ya., Myasoedov, B. F., Geckeler, K. E., and Bayer, E. Separation and preconcentration of actinides by a water-soluble oxine polymer using membrane filtration. Radiochimica Acta 46(1), 35-7. 89.

76. Geckeler, K. E., Bayer, E., Vorob'eva, G. A., and Spivakov, B. Ya. Water-soluble quinolin-8-ol polymer for liquid-phase separation of elements. Analytica Chimica Acta 230(1), 171-4. 90.

77. Alexandratos, Spiro D. and Crick, Darrell W. Polymer-Supported Reagents: Application to Separation Science. Industrial & Engineering Chemistry Research 35(3), 635-44. 96.

78. Alexandratos, Spiro D., Grady, Corinne E., Crick, Darrell W., and Beauvais, Robert. Bifunctional interpenetrating polymer networks. Advances in Chemistry Series 239(Interpenetrating Polymer Networks), 197-203. 94.

79. Soper, B., Haward, R. N., and White, E. F. T. Intramolecular cyclization of styrene-p-divinylbenzene copolymers. Journal of Polymer Science, Polymer Chemistry Edition 10(9), 2545-64. 72.

80. Alexandratos, Spiro D. New polymer-supported ion-complexing agents: Design, preparation and metal ion affinities of immobilized ligands. Journal of Hazardous Materials 139(3), 467-470. 2007.

81. Seggiani, Maurizia, Vitolo, Sandra, and D'Antone, Salvatore. Recovery of nickel from Orimulsion fly ash by iminodiacetic acid chelating resin. Hydrometallurgy 81(1), 9-14. 2006.

82. Hughes, Mark A., Wood, Jessica, Wong, Onn, Sardot, Tova, and Rosenberg, Edward. Comparisons of silica polyamine composites and crosslinked polystyrene resins. Abstracts of Papers, 233rd ACS National Meeting, Chicago, IL, United States, March 25-29, 2007 , IEC-104. 2007.

83. Nielsen, Daniel John and Rosenberg, Edward. Continued development of modified silica polyamine composite materials and reclamation of acid mine drainage. Abstracts, 58th Northwest Regional Meeting of the American Chemical Society, Bozeman, MT, United States, June 12-14. 10. 2003.

84. Rosenberg, Edward, Fischer, Robert J., Deming, John, Hart, Carolyn, Miranda, Paul, and Allen, Ben. Silica polyamine composites: Advanced materials for heavy metal recovery, recycling and removal. PMSE Preprints 86, 79-80. 2002.

85. Beatty, Susan T., Fischer, Robert J., Hagers, Dana L., and Rosenberg, Edward. A Comparative Study of the Removal of Heavy Metal Ions from Water Using a Silica-Polyamine Composite and a Polystyrene Chelator Resin. Industrial & Engineering Chemistry Research 38(11), 4402-4408. 99.

86. Hughes, Mark A. and Rosenberg, Edward. Characterization and applications of poly-acetate modified silica polyamine composites. Separation Science and Technology 42(2), 261-283. 2007.

87. Fatunmbi, H. O. and Wirth, M. J. Horizontally polymerized chromatographic stationary phases. Special Publication - Royal Society of Chemistry 173(Chemically Modified Surfaces: Recent Developments), 61-65. 96.

88. Beatty, Susan T., Fischer, Robert J., Rosenberg, Edward, and Pang, David. Comparison of novel and patented silica-polyamine composite materials as aqueous heavy metal ion recovery materials. Separation Science and Technology 34(14), 2723-2739. 99.

89. Fan, Zhong-Lei, Li, Dian-Qing, and Rosenberg, Edward. Synthesis and adsorption property of poly(allylamine)-silica composite. Yingyong Huaxue 20(9), 867-870. 2003.

90. Arasawa, Hiroko, Odawara, Chiharu, Yokoyama, Ruriko, Saitoh, Hiroshi, Yamauchi, Takeshi, and Tsubokawa, Norio. Grafting of zwitterion-type polymers onto silica gel surface and their properties. Reactive & Functional Polymers 61(2), 153-161. 2004.

91. Watanabe, K., Chow, W. S., and Royer, G. P. Column chromatography on polyethylenimine-silica: rapid resolution of nucleotides and proteins with short columns and low pressures. Analytical Biochemistry 127(1), 155-8. 82.

92. Rosenberg, Edward and Pang, David. System for extracting soluble heavy metals from liquid solutions, especially aqueous solutions. (The University of Montana, USA. 48 pp. 19990514. PCT Int. Appl. 97.

93. Anderson, Corby, Rosenberg, Edward, Cao, Yuchen, Ratz, Lisa, and Hart, Carolyn. Single step separation and recovery of palladium using nitrogen species catalyzed pressure leaching and silica polyamine composites. Hydrometallurgy 2003, Proceedings of the International Symposium honoring Professor Ian M. Ritchie, 5th, Vancouver, BC, Canada, Aug. 24-27, 2003. 1, 393-403. 2003.

94. Alexandratos, Spiro D. and Hong, Min-Jeong. Enhanced metal ion affinities by supported ligand synergistic interaction in bifunctional polymer-supported aminomethylphosphonates. Separation Science and Technology 37(11), 2587-2605. 2002.

95. Chinn, A. F., McAndrew, R. T., Hummel, R. L., and Mouland, J. E. Application of short bed reciprocating flow ion exchange to copper/zinc separation from

concentrated leach solutions. Hydrometallurgy 30(1-3), 431-44. 92.

96. Bandosz, Teresa J., Seredych, Mykola, Allen, Jesse, Wood, Jessica, and Rosenberg, Edward. Silica-Polyamine-Based Carbon Composite Adsorbents as Media for Effective Hydrogen Sulfide Adsorption/Oxidation. Chemistry of Materials 19(10), 2500-2511. 2007.

97. Cox, G. B., Loscombe, C. R., Slucutt, M. J., Sugden, K., and Upfield, J. A. The preparation, properties and some applications of bonded ion-exchange packings based on microparticulate silica gel for high-performance liquid chromatography. Journal of Chromatography 117(2), 269-78. 76.

98. Chow, Francis K. and Grushka, Eli. Separation of aromatic amine isomers by high pressure liquid chromatography with a copper(II)-bonded phase. Analytical Chemistry 49(12), 1756-61. 77.

99. Bonn, G., Reiffenstuhl, S., and Jandik, P. Ion chromatography of transition metals on an iminodiacetic acid bonded stationary phase. Journal of Chromatography 499, 669-76. 90.

100. Hughes, Mark A., Nielsen, Dan, Rosenberg, Edward, Gobetto, Roberto, Viale, Alessandra, Burton, Sarah D., and Ferel, Joseph. Structural investigations of silica polyamine composites: surface coverage, metal ion coordination, and ligand modification. Industrial & Engineering Chemistry Research 45(19), 6538-6547. 2006.

101. Zhuravlev, L. T. The surface chemistry of amorphous silica. Zhuravlev model. Colloids and Surfaces, A: Physicochemical and Engineering Aspects 173(1-3), 1-38. 2000.

102. Hietala, S. L., Smith, D. M., Hietala, V. M., Frye, G. C., and Martin, S. J. Pore structure characterization of thin films using a surface acoustic wave/volumetric adsorption technique. Langmuir 9(1), 249-51. 93.

103. Zhuravlev, L. T. Concentration of hydroxyl groups on the surface of amorphous silicas. Langmuir 3(3), 316-18. 87.

104. Iler, R. K. The Chemistry of Silica: Solubility, Polymerization, Colloid and Surface Properties and Biochemistry. 892 pp. 79.

105. Deepatana, A. and Valix, M. Ion-exchange recovery of nickel and cobalt from metal-organic complexes generated in bioleaching of low-grade nickel laterite ores. Proceedings of the International Conference on Environmental Degradation of Materials in Nuclear Power Systems--Water Reactors, 12th, Salt Lake City, UT, United States, Aug. 14-18, 2005 , 1059-1068. 2005.

106. Adamson, Arthur W., Gast, Alice P., and Editors. Physical Chemistry of Surfaces, Sixth Edition. 784 pp. 97.

107. Wang, Wenming and Fthenakis, Vasilis. Kinetics study on separation of cadmium from tellurium in acidic solution media using ion-exchange resins. Journal of Hazardous Materials 125(1-3), 80-88. 2005.

108. Amevor, S. Francis, Hund, Hans-Ulrich, and Salzer, Albrecht. New heterodimetallic cyclopentadienyl carbonyl complexes: crystal structure of (C5Me4Et)W(m-CO)3Ru(C5Me5). Journal of Organometallic Chemistry 520(1-2), 79-84. 96.

109. Sillanpaa, Mika and Sihvonen, Marja-Liisa. Analysis of EDTA and DTPA. Talanta 44(8), 1487-1497. 97.

110. Shimizu, Yoshiaki, Izumi, Sinya, Saito, Yoshihiro, and Yamaoka, Hitoshi. Ethylenediamine tetraacetic acid modification of crosslinked chitosan designed for a novel metal-ion adsorbent. Journal of Applied Polymer Science 92(5), 2758-2764. 2004.

111. Inoue, Katsutoshi, Yoshizuka, Kazuharu, and Ohto, Keisuke. Adsorptive separation of some metal ions by complexing agent types of chemically modified chitosan. Analytica Chimica Acta 388(1-2), 209-218. 99.

112. Shiraishi, Yasuhiro, Nishimura, Go, Hirai, Takayuki, and Komasawa, Isao. Separation of transition metals using inorganic adsorbents modified with chelating ligands. Industrial & Engineering Chemistry Research 41(20), 5065-5070. 2002.

113. Capretta, Alfredo, Maharajh, Rabindranath B., and Bell, Russell A. Synthesis and characterization of cyclomaltoheptaose-based metal chelants as probes for intestinal permeability. Carbohydrate Research 267(1), 49-63. 95.

114. Prudencio, Miguel, Rohovec, Jan, Peters, Joop A., Tocheva, Elitza, Boulanger, Martin J., Murphy, Michael E. P., Hupkes, Hermen-Jan, Kosters, Walter, Impagliazzo, Antonietta, and Ubbink, Marcellus. A caged lanthanide complex as a paramagnetic shift agent for protein NMR. Chemistry--A European Journal 10(13), 3252-3260. 2004.

115. Hindersinn, Raymond R., Hopkins, George C., and Ilardo, Charles S. Compositions of epoxy resins with 2,6-dioxo-N-(carboxymethyl)morpholine. (Hooker Chemical Corp.). 2 pp. Division of U.S. 3,621,018 (CA 76;34269d). 19720905. U.S. 71.

116. El-Nahhal, Issa M., Zaggout, Farid R., Nassar, Mona A., El-Ashgar, Nizam M., Maquet, Jocelyne, Babonneau, Florence, and Chehimi, Mohamed M. Synthesis, Characterization and Applications of Immobilized Iminodiacetic Acid-Modified Silica. Journal of Sol-Gel Science and Technology 28(2), 255-265. 2003.

117. Boger, Dale L., Ducray, Pierre, Chai, Wenying, Jiang, Weiqin, and Goldberg, Joel. Higher order iminodiacetic acid libraries for probing protein-protein

interactions. Bioorganic & Medicinal Chemistry Letters 8(17), 2339-2344. 98.

118. Deng, S. and Ting, Y. P. Removal of As(V) and As(III) from water with a PEI-modified fungal biomass. Water Science and Technology 55(1-2, Wastewater Reclamation and Reuse for Sustainability), 177-185. 2007.

119. Roberts, Linda C., Hug, Stephan J., Ruettimann, Thomas, Billah, Md Morsaline, Khan, Abdul Wahab, and Rahman, Mohammad Tariqur. Arsenic Removal with Iron(II) and Iron(III) in Waters with High Silicate and Phosphate Concentrations. Environmental Science and Technology 38(1), 307-315. 2004.

120. Nielsen Dan. Synthesis and Reclamation of Novel Silica Polyamine Composites and their Application to the Reclamation of Hazardous Mining Wastewater and Tailings . PhD . 2006.